

HODGE-TYPE DECOMPOSITIONS FOR
PIECEWISE CONSTANT VECTOR FIELDS
ON SIMPLICIAL SURFACES AND SOLIDS
WITH BOUNDARY

KONSTANTIN POELKE

Dissertation zur Erlangung des Grades
eines Doktors der Naturwissenschaften (Dr. rer. nat.),
eingereicht am

FACHBEREICH MATHEMATIK UND INFORMATIK
FREIE UNIVERSITÄT BERLIN

Berlin 2016

Erstgutachter und Betreuer: Prof. Dr. Konrad Polthier (Freie Universität Berlin)
Zweitgutachter: Prof. Dr. Martin Rumpf (Universität Bonn)

Tag der Disputation: 20. März 2017

CONTENTS

1	INTRODUCTION	1
2	SMOOTH DECOMPOSITIONS	7
2.1	Cohomology	7
2.2	Differential Forms on Manifolds with Boundary	11
2.3	Hodge-Type Decompositions	14
2.4	Orthogonality of \mathcal{H}_N^k and \mathcal{H}_D^k	16
3	DISCRETE DECOMPOSITIONS	21
3.1	Function Spaces on Simplicial Manifolds	21
3.2	Decompositions on Simplicial Surfaces	30
3.3	Decompositions on Simplicial Solids	41
3.4	When is $\mathcal{H}_{h,N} \cap \mathcal{H}_{h,D} = \{0\}$? Obstructions	47
4	CONVERGENCE	59
4.1	Generalizing Dodziuk's Convergence Result	60
4.2	Convergence with Approximating Metrics	68
4.3	Approximation by PCVFs	75
5	APPLICATIONS	79
5.1	Cohomology Representatives on Simplicial Surfaces	79
5.2	Hodge Decompositions on Simplicial Surfaces	85
5.3	Cohomology Representatives on Simplicial Solids	91
5.4	Hodge Decompositions on Simplicial Solids	95
5.5	Numerical Aspects	98

INTRODUCTION

Piecewise constant vector fields (PCVFs) on simplicial geometries are indispensable objects for the discretization of smooth vector fields. Defined by one tangent vector per affine cell, they can be thought of as cell averages of a smooth field, coming from an L^2 -projection for instance, and therefore constitute a lowest order L^2 -approximation with respect to a given metric on a simplicial mesh. As such they provide an intuitive representation for velocity and force fields in fluid dynamics or computational electromagnetics, just to name a few examples. Furthermore, they appear naturally as weak gradient fields of linear Lagrange functions used in H^1 -conforming finite element methods for variational problems, or as piecewise defined gradient fields of Crouzeix-Raviart elements for discontinuous nonconforming methods.

But their application area does not restrict to approximation of smooth fields. In discrete differential geometry and geometry processing they are important objects in their own right, without the presence of a smooth field which is to be approximated. For instance, discrete differential geometry has coined notions of discrete curvature directions on simplicial surfaces, and several algorithms for surface parametrization and remeshing tasks make heavy use of so-called frame fields, usually represented by tuples of PCVFs. The simplicity of their definition, numerical representation and implementation seems particularly appealing for these kinds of problems. Furthermore, geometric models coming e.g. from high-resolution scan data or computer graphics frequently exhibit a huge number of cells, so with respect to performance there is a desire for low-order ansatz spaces defined by a low number of degrees of freedom.

However, in order to develop a rich vector calculus on the space \mathcal{X}_h of PCVFs one has to define notions of curl and divergence. It is clear that the piecewise application of smooth differential operators to PCVFs does not give a meaningful result. In two dimensions, a prominent solution is to define divergence and curl as L^2 -adjoint operators to the piecewise gradient and cogradient of Lagrange and Crouzeix-Raviart elements, respectively, forcing Green's formula to hold true. More precisely, for a PCVF $X \in \mathcal{X}_h$ on a closed simplicial surface, its divergence and curl shall be the functions $\operatorname{div}_{\mathcal{L}}(X) \in \mathcal{L}$ and $\operatorname{curl}_{\mathcal{F}}(X) \in \mathcal{F}$ satisfying

$$\begin{aligned} \langle \operatorname{div}_{\mathcal{L}}(X), \varphi \rangle_{L^2} &= -\langle X, \nabla \varphi \rangle_{L^2} \text{ for all } \varphi \in \mathcal{L} \\ \langle \operatorname{curl}_{\mathcal{F}}(X), \psi \rangle_{L^2} &= \langle X, J \nabla \psi \rangle_{L^2} \text{ for all } \psi \in \mathcal{F}, \end{aligned}$$

where \mathcal{L} and \mathcal{F} denote the ansatz spaces of linear Lagrange and Crouzeix-Raviart elements, respectively. A field $X \in \mathcal{X}_h$ is then said to be harmonic if its divergence and curl vanishes, and it turns out that the space \mathcal{H}_h of all harmonic PCVFs on a closed oriented simplicial surface M_h has dimension $2g$, where g denotes the genus of M_h . Moreover, on a closed surface, the space $\nabla \mathcal{L}$ of gradient fields of Lagrange elements is always L^2 -orthogonal to the space $J \nabla \mathcal{F}$ of cogradient fields of Crouzeix-Raviart elements, leading to the orthogonal decomposition

$$\mathcal{X}_h = \nabla \mathcal{L} \oplus J \nabla \mathcal{F} \oplus \mathcal{H}_h.$$

This result is in structural accordance with the smooth theory, where the classical Hodge decomposition on a closed oriented Riemannian manifold states that the space of smooth k -forms Ω^k can be L^2 -orthogonally decomposed as

$$\Omega^k = d\Omega^{k-1} \oplus \delta\Omega^{k+1} \oplus \mathcal{H}^k.$$

Here, the space of harmonic k -forms \mathcal{H}^k has dimension equal to the dimension of the k -th cohomology space $H^k(M)$ with real coefficients. Indeed, a basis for \mathcal{H}^k provides a set of concrete representatives for a basis of cohomology classes of $H^k(M)$. This latter fact is a consequence of de Rham's theorem, and it is due to the mixing of the ansatz spaces \mathcal{L} and \mathcal{F} in the definition of discrete curl and divergence that this remarkable linkage between smooth harmonic forms and the topology of the underlying geometry also holds in the discrete case.

In the presence of a boundary ∂M , the spaces of exact forms $d\Omega^{k-1}$ and coexact forms $\delta\Omega^{k+1}$ are no longer L^2 -orthogonal to each other, though, and the Hodge theory on M becomes drastically richer. To circumvent this problem one usually poses Dirichlet boundary conditions (the tangential part $\mathbf{t}(\omega)$ of a differential form has to vanish along the boundary ∂M) on the space Ω^{k-1} and Neumann boundary conditions (the normal part $\omega|_{\partial M} - \mathbf{t}(\omega)$ has to vanish along ∂M) on Ω^{k+1} to obtain a decomposition

$$\Omega^k = d\Omega_D^{k-1} \oplus \delta\Omega_N^{k+1} \oplus \mathcal{H}^k.$$

However, in this splitting the space of harmonic forms \mathcal{H}^k is now infinite-dimensional and has no topological significance any more. Still, it can be further split into subspaces \mathcal{H}_D^k and \mathcal{H}_N^k of so-called Dirichlet and Neumann fields, isomorphic to the k -th relative and absolute cohomology space. This leads to the two Hodge-Morrey-Friedrichs decompositions

$$\begin{aligned} \Omega^k &= d\Omega_D^{k-1} \oplus \delta\Omega_N^{k+1} \oplus \mathcal{H}^k \cap d\Omega^{k-1} \oplus \mathcal{H}_N^k \\ &= d\Omega_D^{k-1} \oplus \delta\Omega_N^{k+1} \oplus \mathcal{H}^k \cap \delta\Omega^{k+1} \oplus \mathcal{H}_D^k. \end{aligned}$$

A natural question that arises is whether both decompositions can be unified to a single orthogonal decomposition involving both the spaces of Neumann and Dirichlet fields at the same time. This is also stimulated by the fact that always

$$\mathcal{H}_N^k \cap \mathcal{H}_D^k = \{0\},$$

so that the spaces form at least a direct sum. However, it turns out that they are in general not orthogonal to each other. The reason for this is the presence of certain fields that represent cohomology classes which are not induced by the boundary components ∂M , but rather come from the ‘‘interior topology’’ of a manifold. This insight provides a further splitting of the spaces \mathcal{H}_N^k and \mathcal{H}_D^k into two subspaces each, one of them representing cohomology coming from the boundary and the other representing cohomology coming from the interior.

These subspaces provide refined decompositions which are interesting not only from a theoretical point of view, but also with respect to computational decompositions and the analysis of vector fields, as they distinguish harmonic fields intrinsic to a geometry from those induced by the boundary components. Furthermore, they give a simple criterion in which cases the spaces \mathcal{H}_N^k and \mathcal{H}_D^k are orthogonal to each other. In view of applications, this is in particular the case for surfaces homeomorphic to a sphere with several holes cut out (including two-dimensional flat domains in \mathbb{R}^2) as well as for three-dimensional domains embedded in \mathbb{R}^3 .

It is no longer the case, though, for oriented surfaces with boundary which exhibit interior cohomology, which are—by the classification of surfaces—exactly those homeomorphic to a surface of genus $g \geq 1$ with several boundary components.

On the discrete side, a similar development of a Hodge theory for PCVFs on surfaces and solids with boundary is missing, and the result on closed surfaces is so far state of the art.

CONTRIBUTIONS. The aim of this work is to transfer this evolution of smooth Hodge-type decomposition statements to corresponding structurally consistent decomposition statements for the space \mathcal{X}_h on simplicial surfaces with boundary and simplicial solids, i.e. bounded tetrahedral domains, in \mathbb{R}^3 . Here, *structurally consistent* is understood with respect to three aspects: first, the *geometric* orthogonality statements should be preserved by the corresponding discrete spaces. Second, the deep linkage to the cohomology of the shape, which is a purely *topological* invariant, needs to be reflected and manifested in the correct dimensions of the topologically significant subspaces $\mathcal{H}_{h,D}$ and $\mathcal{H}_{h,N}$ of discrete Dirichlet and Neumann fields, respectively, and their respective subspaces. Third, in the case that the discrete vector field on a discrete mesh approximates a smooth vector field on a smooth geometry, we require convergence for the components of a discrete decomposition to their respective counterparts in the smooth decomposition, assuming that the mesh converges metrically to the smooth geometry.

It turns out that the intricate interplay of geometry and topology in the smooth Hodge theory can be completely reflected by the discrete decomposition statements for PCVFs which we will derive in the following. In particular we obtain a complete characterization of the space \mathcal{X}_h in terms of its Hodge decompositions, which is in agreement with the smooth results, and various experimental results confirm the theory.

In detail, this work includes the following contributions:

- We derive discrete analogues of the Hodge-Morrey-Friedrichs decompositions for the space \mathcal{X}_h on simplicial surfaces with boundary and show that the corresponding spaces of discrete Dirichlet and Neumann fields have the correct dimensions.
- We define discrete spaces of exact and boundary-coexact Dirichlet fields, and coexact and boundary-exact Neumann fields. These subspaces provide a refined splitting and add the distinction between harmonic fields representing inner cohomology and boundary cohomology to the decompositions. In the absence of inner cohomology we obtain a complete orthogonal decomposition for surfaces with boundary, involving both the spaces $\mathcal{H}_{h,D}$ and $\mathcal{H}_{h,N}$ at the same time.
- In a similar spirit we derive decomposition statements for simplicial solids. In particular, the cohomology of such solids is always induced by the boundary and we obtain a complete five-term decomposition.
- On simplicial surfaces the equality $\mathcal{H}_{h,D} \cap \mathcal{H}_{h,N} = \{0\}$ is not always true. Surprisingly, it turns out that the discretization of the mesh, i.e. the combinatorial connectivity of the mesh, plays another important role in view towards a consistent discretization. We derive and prove a criterion on the mesh which guarantees the intersection to be trivial, and investigate a few exemplary cases which exhibit possible obstructions.

- We define refined decomposition statements for spaces of Whitney k -forms on manifolds with boundary and prove an extension of the seminal convergence result by Dodziuk [Dod76] to include these new decompositions. Incorporating a norm estimate by Stern [Ste13], we obtain convergence of these decompositions with respect to a sequence of approximating metrics. These results will be central to the convergence proof of our discrete vector field decompositions.
- We prove convergence of the decomposition statements for PCVFs for simplicial surfaces with boundary approximating a smooth surface, following the strategy by Wardetzky [War06]. Furthermore, we explain how to modify this approach in order to obtain the corresponding convergence statements on simplicial solids.
- We propose and explore a strategy for the computation of harmonic bases for the various topologically significant harmonic subspaces in our decompositions.
- Based on an iterated L^2 -projection, we provide algorithms to compute all decompositions for a given PCVF on a simplicial surface or solid. We evaluate this approach by comparing the components obtained by the discrete decompositions of PCVF interpolants of smooth stereotypical examples to their corresponding smooth components.

RELATED WORK. The discretization of vector fields or more generally differential forms is a vast and classical topic both on the applied side as well as from a theoretical point of view, and it is far too vast to provide a complete overview on all related concepts that have been developed in the last decades. We therefore focus on recent work that emphasizes geometrical and topological aspects for the discretization strategy.

On the smooth side, a comprehensive treatment of Hodge decompositions up to the four-term Hodge-Morrey-Friedrichs decomposition for differential forms is given by Schwarz in [Sch95]. A five-term decomposition for vector fields on domains in \mathbb{R}^3 is derived in the expository article [CDG02]. The distinction between fields representing inner and boundary cohomology and the question of orthogonality between the spaces of Neumann and Dirichlet fields is first published by Shonkwiler in [Sho09] and [Sho13], but is, according to him, based on previous work by Dennis DeTurck and Herman Gluck (cf. [Sho13, Sec. 1]).

The focus on PCVFs on simplicial surface meshes in modern geometry processing and their theoretical description goes back at least to Polthier and Preuss [PP03] who used them as a concept for analysis and decomposition of vector fields, with a convergence proof on closed surfaces given by Wardetzky in [War06]. An elementary extension to three-dimensional domains is given in [TLHD03]. A discrete Levi-Civita connection for PCVFs on simplicial surfaces is proposed in [AOCBC15]. Exemplary applications in geometry processing and modelling include field generation for interactive surface processing [XZCOX09], remeshing [DKG05, SZS08], deformation [KNP14], parametrization [KNP07] or visualization and analysis of vector fields [SZ12, PP03].

A different way to define discrete vector fields or more generally discrete k -forms is provided by the *discrete exterior calculus (DEC)* [Hir03], which defines discrete k -forms as a synonym for simplicial k -cochains. For numerical computations, though, these quantities assigned to k -cells usually need to be interpolated to the full-dimensional cells. The *elementary forms* suggested by Whitney in his classical book [Whi12] from 1957 can be considered a first discretization strategy for differential forms, since they provide interpolants of simplicial

cochains on a smooth triangulation. In the 1970s and 1980s, Raviart and Thomas [RT77] and Nédélec [Né80] developed families of finite elements for the computational treatment of Navier-Stokes- and Maxwell-type problems, and Bossavit [Bos88] later put these finite elements in the context of Whitney forms in two and three dimensions.

The *finite element exterior calculus* developed by Arnold et al. [AFW06, AFW10] provides a unifying framework for mixed problems involving more than one ansatz space. Therein, the Whitney form complex is generalized to complexes of polynomial differential forms of arbitrary degree, where at each stage there is a choice between a full polynomial ansatz space over each element or a reduced polynomial space, as is the case for Whitney forms. All complexes are subcomplexes of a Sobolev-de Rham complex and can be therefore considered a conforming discretization. In contrast, Holst and Stern [HS12] extend this theory to include complexes whose ansatz spaces are not subspaces of a Sobolev space on a smooth geometry, as is the case for ansatz spaces on simplicial surface meshes approximating a smooth surface in \mathbb{R}^3 , for instance.

The definition of a discrete curl and divergence for PCVFs as those elements that enforce Green’s formula to hold true is driven by a paradigm inherent to *mimetic discretization methods* [BH06]. Here, the definition of discrete operators and objects is primarily driven by the attempt to mimic properties from the smooth world such as conservation laws, Green’s formula or the complex property $\text{im}(T^{k-1}) \subseteq \ker(T^k)$ for a sequence $\{T^k\}$ of operators.

Notions of curl- and divergence-freeness also exist on the level of weightings on directed networks. An exposition is given by Lovász and Benjamini in [Lov04, BL03], with applications to random processes on networks embedded on a closed surface given in [BL02a, BL02b].

Of particular interest for geometric applications are *harmonic fields*, i.e. fields which are both curl- and divergence-free, as they constitute an even, steady flow in the interior of the domain. A subset of those arises as gradient fields of linear Lagrange potential functions which solve the Laplace-Beltrami problem $\Delta u = 0$ on a surface mesh. For instance, [DKG05] use such a gradient field to obtain an orthogonal frame field (X_1, X_2) by setting $X_1 := \nabla u$, $X_2 := JX_1$, where JX_1 denotes a piecewise 90-degree rotation in the tangent space of each triangle, and take this field as a guidance for quadrilateral remeshing applications. [XZCOX09] extend this approach by providing a fast update mechanism for the efficient computation of harmonic gradients under changing boundary constraints, possibly modified by user interaction. Relaxing the notion of harmonicity a bit, [SZS08] consider quasi-harmonic gradient fields, which can be thought of as minimizers of the Dirichlet energy on an inhomogeneous medium with varying permeability. But not all harmonic fields arise as potentials. [HKWW10] suggest a strategy for finding cochains that represent cohomology generators on a surface.

Finally, it should be noted that there are many different definitions and approaches for the computation of a discrete Hodge decomposition. For instance, [RHS16] discuss a decomposition in the spectral domain after Fourier transformation, and [PPL⁺10] propose a meshless decomposition on point set samples in \mathbb{R}^2 . See also [BNPB13] for a survey on various discrete Hodge decompositions.

OUTLINE. The next chapters are ordered as follows:

Chapter 2 reviews the necessary smooth theory and topological definitions, since all these notions are central for the following discretization. Section 2.1 summarizes simplicial cohomology on manifolds with boundary and provides cohomological computations for surfaces

and solids. With regard to a topologically consistent discretization, these quantities need to be preserved in the discrete theory. Section 2.2 lists the most important notions from the theory of differential forms on manifolds with boundary, with an emphasis on the boundary components of a differential form. Section 2.3 introduces the fundamental spaces \mathcal{H}_D^k and \mathcal{H}_N^k of harmonic Dirichlet and Neumann fields and concludes with the Hodge-Morrey-Friedrichs decomposition. Section 2.4 then reviews the recent results by Shonkwiler and provides a slightly modified proof for the orthogonal subsplittings of \mathcal{H}_D^k and \mathcal{H}_N^k , as this is not yet contained in the standard literature on differential forms.

Chapter 3 constitutes the heart of this work as it develops the discrete decompositions for simplicial surfaces and solids with boundary. The essential ansatz spaces are introduced in Section 3.1. Discrete decompositions on simplicial surfaces are derived in Section 3.2 and their geometric and topological consistency with the smooth analogues is proved. Similar results are proved for simplicial solids in Section 3.3. However, the spaces of discrete Dirichlet and Neumann fields on simplicial surfaces do not always intersect trivially, in contrast to the smooth world, and it is the objective of Section 3.4 to illustrate why and in which situations this is not the case. Finally, we prove a criterion on the mesh which guarantees a trivial intersection also for the discrete spaces.

Chapter 4 deals with the third pillar of structural consistency—approximation and convergence. To this end we first generalize an approximation result by Dodziuk for Whitney form spaces in Section 4.1. Next, we consider the case of an approximating mesh inducing a distorted metric on a smooth mesh and therefore a distorted orthogonal decomposition for Whitney forms in Section 4.2. Finally, in Section 4.3 we compare the discretizations from Chapter 3 with the distorted Whitney decompositions to obtain convergence.

Chapter 5 puts the discrete theory into practice and demonstrates its relevance for a few central applications. In Section 5.1 we propose a strategy for the computation of bases for harmonic fields on surfaces and illustrate some examples. Section 5.2 then provides an algorithm based on iterated L^2 -projections for the refined decompositions derived in Section 3.2. Sections 5.3 and 5.4 explain the analogue strategies for simplicial solids, stress the slight differences and evaluate the complete decomposition for stereotypical smooth fields which are interpolated on a discrete mesh. Finally, Section 5.5 concludes with a few remarks on the numerical solution of the problems in the previous sections.

PUBLICATIONS: Parts of this thesis have been published in

- Poelke, Konstantin and Polthier, Konrad: *Boundary-aware Hodge Decompositions for Piecewise Constant Vector Fields*, Computer-Aided Design, Volume 78, September 2016, Pages 126–136

SMOOTH DECOMPOSITIONS

2.1 COHOMOLOGY

This section provides a background on cohomology groups of compact manifolds with boundary since these algebraic-topological results will be essential to the remaining chapters. For practical computations, the long exact cohomology sequence is an indispensable tool, so is the Poincaré-Lefschetz duality theorem. Explicit computations are given for surfaces and volumes in \mathbb{R}^3 which are the interesting cases with regard to the discretization later on. All facts can be found in standard textbooks on algebraic topology, e.g. [Mun84], [Bre93] or [Hat02].

GENERAL FACTS. In all what follows let M be a compact, topological, orientable manifold with boundary ∂M . We are mostly interested in the case $\dim M = 2$ or $\dim M = 3$, but all results hold in arbitrary dimensions. In order to work with simplicial (co-)homology, we assume that M is triangulable, so that it carries the structure of a simplicial complex, i.e. there is a homeomorphism $|K| \xrightarrow{\simeq} M$ from a geometric realization of a simplicial complex K . Again, most results hold in much wider generality, using other flavours of homology theories such as singular, Čech or sheaf cohomology, but in view towards numerical applications, simplicial cohomology is the most tractable, so we briefly outline its construction. Furthermore, for dimensions two and three, topological manifolds with boundary are always triangulable, which is not the case for higher dimensions any more. It is, though, if M is smooth by Whitehead's triangulation theorem, see e.g. [Man14] and the literature referenced therein, and then the singular and simplicial (co-)homology theories yield isomorphic (co-)homology groups.

Let $C_k(M)$ and $C_k(\partial M)$ denote the groups of *simplicial k -chains* on M and ∂M with real coefficients. Since M is assumed to be compact, we can restrict to finite triangulations and then $C_k(M)$ and $C_k(\partial M)$ are finite-dimensional \mathbb{R} -vector spaces. The inclusion $\iota : \partial M \hookrightarrow M$ gives rise to a short exact sequence

$$0 \rightarrow C_k(\partial M) \xrightarrow{\iota_{\sharp}} C_k(M) \xrightarrow{\pi_{\sharp}} C_k(M)/C_k(\partial M) \rightarrow 0 \quad (2.1)$$

for each k . There is a *boundary operator* $\partial_k : C_k(M) \rightarrow C_{k-1}(M)$ commuting with the maps ι_{\sharp} and π_{\sharp} in (2.1), and we denote by $Z_k(M) := \ker(\partial_k)$ and $B_k := \text{im}(\partial_{k+1})$ the subspaces of *cycles* and *boundaries*, and similarly for the spaces $C_k(\partial M)$ and $C_k(M)/C_k(\partial M)$, where in the latter case we write $Z_k(M, \partial M)$ and $B_k(M, \partial M)$. The boundary map satisfies $\partial_k \circ \partial_{k+1} = 0$ and therefore forms a complex, i.e. at each stage it is $B_k(M) \subseteq Z_k(M)$. The corresponding quotient spaces $H_k(M) := Z_k(M)/B_k(M)$ and $H_k(\partial M) := Z_k(\partial M)/B_k(\partial M)$ are the *k -th homology spaces* for M and ∂M , respectively, and the space $H_k(M, \partial M) := Z_k(M, \partial M)/B_k(M, \partial M)$ is the *k -th relative homology space* of M . The maps ι_{\sharp} and π_{\sharp} in (2.1) induce maps $\iota_* : H_k(\partial M) \rightarrow H_k(M)$ and $\pi_* : H_k(M) \rightarrow H_k(M, \partial M)$, and there are connecting morphisms $\delta_* : H_k(M, \partial M) \rightarrow H_{k-1}(\partial M)$ such that all these maps fit into a *long exact sequence in homology*

$$\cdots \rightarrow H_{k+1}(M, \partial M) \xrightarrow{\delta_*} H_k(\partial M) \xrightarrow{\iota_*} H_k(M) \xrightarrow{\pi_*} H_k(M, \partial M) \xrightarrow{\delta_*} H_{k-1}(\partial M) \rightarrow \cdots$$

Dualizing these notions, one obtains the corresponding results for simplicial cohomology: Let $C^k(M)$, $C^k(\partial M)$ and $C^k(M, \partial M)$ denote the dual spaces of $C_k(M)$, $C_k(\partial M)$ and $C_k(M)/C_k(\partial M)$, respectively. The first two are the spaces of *simplicial k -cochains* on M and ∂M . The space $C^k(M, \partial M)$ is the space of *relative k -cochains* and can be naturally identified with all cochains of $C^k(M)$ that vanish on k -chains contained in the boundary ∂M . These spaces now form a short exact cochain sequence

$$0 \rightarrow C^k(M, \partial M) \xrightarrow{\pi^\sharp} C^k(M) \xrightarrow{\iota^\sharp} C^k(\partial M) \rightarrow 0.$$

In the following it will be helpful to think of $C^k(M, \partial M) \xrightarrow{\pi^\sharp} C^k(M)$ as a subspace inclusion. The map ι^\sharp is just the restriction of a k -cochain on M to the boundary ∂M .

Now there is a *coboundary operator* $d_\Delta^k : C^k(M) \rightarrow C^{k+1}(M)$ defined as the adjoint to ∂_k by $d_\Delta^k(w)(\sigma) := w(\partial_{k+1}\sigma)$ for any cochain $w \in C^k(M)$ and chain $\sigma \in C_{k+1}(M)$, and therefore $d_\Delta^{k+1} \circ d_\Delta^k = 0$. Again, we have spaces of *cocycles* $Z^k(M) := \ker(d_\Delta^k)$ and *coboundaries* $B^k(M) := \text{im}(d_\Delta^{k-1})$ and so on, and their respective quotient spaces are the *k -th cohomology spaces* $H^k(M) := Z^k(M)/B^k(M)$, $H^k(\partial M) := Z^k(\partial M)/B^k(\partial M)$ and the *relative cohomology spaces* $H^k(M, \partial M) := Z^k(M, \partial M)/B^k(M, \partial M)$.

As above, these spaces give rise to a *long exact sequence in cohomology*

$$\dots \rightarrow H^{k-1}(\partial M) \xrightarrow{\delta^*} H^k(M, \partial M) \xrightarrow{\pi^*} H^k(M) \xrightarrow{\iota^*} H^k(\partial M) \xrightarrow{\delta^*} H^{k+1}(M, \partial M) \rightarrow \dots \quad (2.2)$$

which will be of central importance in the following.

Since all the involved spaces are finite-dimensional and the coefficient ring is the field of real numbers, the k -th homology space and cohomology space are always isomorphic in all three cases, i.e. $H_k(M) \cong H^k(M)$, $H_k(\partial M) \cong H^k(\partial M)$ and $H_k(M, \partial M) \cong H^k(M, \partial M)$ ([Mun84, Cor. 53.6]). Furthermore, *Lefschetz-Poincaré duality* states that there are isomorphisms

$$H^k(M, \partial M) \xrightarrow{\sim} H_{n-k}(M). \quad (\cong H^{n-k}(M))$$

If $\partial M = \emptyset$ this reduces to the classical *Poincaré duality* $H^k(M) \xrightarrow{\sim} H_{n-k}(M)$ for closed manifolds.

Finally, we need the *Mayer-Vietoris sequence* stated in singular cohomology, which is the exact sequence

$$\dots \rightarrow H^{k-1}(A \cap B) \rightarrow H^k(M) \rightarrow H^k(A) \oplus H^k(B) \xrightarrow{\iota_A^* + \iota_B^*} H^k(A \cap B) \rightarrow H^{k+1}(M) \rightarrow \dots \quad (2.3)$$

for subsets $A, B \subseteq M$ such that $\overset{\circ}{A} \cup \overset{\circ}{B} = M$, and ι_A^* and ι_B^* come from the inclusions $\iota_A : A \cap B \hookrightarrow A$ and $\iota_B : A \cap B \hookrightarrow B$.

In the following we will omit the indices for ∂_k , d_Δ^k , if they are of no particular importance. Usually, they are clear from the context anyway. Furthermore, we shall write

$$\begin{aligned} h^k(M) &:= \dim H^k(M) \\ h_r^k(M) &:= \dim H^k(M, \partial M) \end{aligned}$$

for the dimensions of the absolute and relative k -th cohomology, and usually we will even just write h^k or h_r^k , if there is no confusion on the manifold under investigation.

COHOMOLOGY OF SURFACES WITH BOUNDARY. Let M be an orientable compact surface with boundary. It is a classical result that M is homeomorphic to a surface that is obtained by removing $m \geq 0$ disjoint open discs from a closed surface of genus $g \geq 0$, and furthermore that for a fixed pair (g, m) , all such surfaces obtained from a closed surface of genus g by removing m discs are topologically equivalent, see e.g. [Kin97, Thm. 4.17]. We will say that M is of type $\Sigma_{g,m}$ or M is homeomorphic to $\Sigma_{g,m}$, where $\Sigma_{g,m}$ is for each pair (g, m) a representative surface. The following result is a standard computation, but since we make heavy use of it, we give the short proof.

Lemma 2.1.1. *Let M be a surface of type $\Sigma_{g,m}$, $m \geq 1$. Then*

$$h^1(M) = 2g + m - 1.$$

Proof. Let \tilde{M} be a closed and connected surface of genus g , let $B := \bigcup_{j=1}^m D_{j,R}$ be the union of $m \geq 1$ closed, pairwise disjoint closed topological disks $D_{j,R}$, and let $D_{j,r}$ be a closed topological disk contained in the open interior of $D_{j,R}$ for each j , i.e. $D_{j,r} \subset \mathring{D}_{j,R}$. Set $A := \tilde{M} \setminus \left(\bigcup_{j=1}^m \mathring{D}_{j,r} \right)$. Then A is a surface of type $\Sigma_{g,m}$, so by the classification theorem, M is homeomorphic to A .

The result now follows from a direct computation of the Mayer-Vietoris sequence for this particular case: \tilde{M} and A are connected, so $H^0(\tilde{M}) \cong H^0(A) \cong \mathbb{R}$, B and $A \cap B$ are disjoint unions of m topological disks and annuli, respectively, so $H^0(B) \cong H^0(A \cap B) \cong \mathbb{R}^m$. Each disk in B is contractible whereas each annulus in $A \cap B$ deformation retracts to the one-dimensional sphere S^1 , so $H^1(B) = 0$ and $H^1(A \cap B) \cong \mathbb{R}^m$. Finally, we have $H^2(A) = H^2(A \cap B) = H^2(B) = 0$ since all these sets have non-empty boundary, and $H^2(\tilde{M}) \cong \mathbb{R}$ by Poincaré duality. Therefore, the Mayer-Vietoris sequence is isomorphic to an exact sequence

$$0 \rightarrow \mathbb{R} \xrightarrow{\alpha} \mathbb{R} \oplus \mathbb{R}^m \xrightarrow{\beta} \mathbb{R}^m \xrightarrow{\gamma} H^1(\tilde{M}) \xrightarrow{\delta} H^1(A) \oplus 0 \xrightarrow{\epsilon} \mathbb{R}^m \xrightarrow{\zeta} \mathbb{R} \rightarrow 0$$

and it follows by exactness that β is surjective, so $\gamma = 0$ and δ is an injection. Since $\dim \ker(\epsilon) = \dim \text{im}(\delta) = 2g$ and $\dim \text{im}(\epsilon) = m - 1$ this shows $h^1(M) = h^1(A) = 2g + m - 1$, as (co-)homology is a topological invariant. \square

A trivial consequence of Lemma 2.1.1 is that for surfaces of type $\Sigma_{0,m}$ with $m \geq 1$ it is $h^1(M) = m - 1$. This includes the common case of two-dimensional, bounded domains with holes embedded in \mathbb{R}^2 . Summarizing, for surfaces of type $\Sigma_{g,m}$ the cohomology sequence (2.2) is isomorphic to an exact sequence

$$0 \rightarrow \mathbb{R} \rightarrow \mathbb{R}^m \rightarrow \mathbb{R}^{2g+m-1} \rightarrow \mathbb{R}^{2g+m-1} \rightarrow \mathbb{R}^m \rightarrow \mathbb{R} \rightarrow 0. \quad (2.4)$$

COHOMOLOGY OF BOUNDED DOMAINS IN \mathbb{R}^3 . For compact, three-dimensional manifolds M with boundary which are embedded as compact subsets in \mathbb{R}^3 it is always $H^3(M) = 0$. More importantly, however, is the fact that the cohomology always comes from the boundary in the sense that the first and second cohomology spaces $H^1(M)$ and $H^2(M)$ inject in the cohomology spaces $H^1(\partial M)$ and $H^2(\partial M)$ of the boundary. This observation will be the cornerstone for the orthogonality result in Theorem 3.3.13 and provides a generalization of a discrete decomposition result by Monk [Mon91] which we will give in Corollary 3.3.6. We will refer to M as above as a *bounded domain* in the following.

Lemma 2.1.2. *Let M be a bounded domain in \mathbb{R}^3 . Then the maps $H^1(M) \rightarrow H^1(\partial M)$ and $H^2(M) \rightarrow H^2(\partial M)$ in the cohomology sequence (2.2) are injective.*

Proof. ∂M has a collar neighbourhood C homeomorphic to $\partial M \times [0, 1]$ in M (see e.g. [Hat02, Prop. 3.42]), and we set $A := M$ and $B := M^{\complement} \cup C$, where M^{\complement} denotes the complement of M in \mathbb{R}^3 . Then clearly $\mathring{A} \cup \mathring{B} = \mathring{M} \cup M^{\complement} \cup C = \mathbb{R}^3$ and $A \cap B = C$. Since the collar neighbourhood provides a deformation retraction of C onto ∂M and B onto $\overline{M^{\complement}}$, it is $H^k(A \cap B) = H^k(C) = H^k(\partial M)$ and $H^k(B) = H^k(\overline{M^{\complement}}) = H^k(M^{\complement})$ (see the proof of [Mun84, Thm. 70.7] for the last equality). Furthermore, since $H^k(A \cup B) = H^k(\mathbb{R}^3) = 0$ for $k \geq 1$, the Mayer-Vietoris sequence (2.3) becomes

$$\begin{aligned} 0 \rightarrow H^0(\mathbb{R}^3) \rightarrow H^0(M) \oplus H^0(M^{\complement}) &\rightarrow H^0(\partial M) \\ \rightarrow 0 \rightarrow H^1(M) \oplus H^1(M^{\complement}) &\xrightarrow{\iota_M^* + \iota_{M^{\complement}}^*} H^1(\partial M) \\ \rightarrow 0 \rightarrow H^2(M) \oplus H^2(M^{\complement}) &\xrightarrow{\iota_M^* + \iota_{M^{\complement}}^*} H^2(\partial M) \rightarrow 0. \end{aligned}$$

Therefore $\iota_M^* + \iota_{M^{\complement}}^*$ is an isomorphism for $k = 1, 2$, and ι_M^* must be injective. \square

As an immediate consequence of Lemma 2.1.2, the cohomology sequence for compact, connected three-dimensional domains with boundary in \mathbb{R}^3 reads

$$\begin{aligned} 0 \rightarrow H^0(M) \rightarrow H^0(\partial M) \rightarrow \\ H^1(M, \partial M) \xrightarrow{0} H^1(M) \rightarrow H^1(\partial M) \rightarrow \\ H^2(M, \partial M) \xrightarrow{0} H^2(M) \rightarrow H^2(\partial M) \rightarrow \\ H^3(M, \partial M) \rightarrow 0 \end{aligned} \tag{2.5}$$

where \rightarrow denotes an injective map and \twoheadrightarrow denotes a surjection. In particular, the maps $\iota^* : H^k(M) \rightarrow H^k(\partial M)$ induced by the inclusion $\iota : \partial M \hookrightarrow M$ are inclusions on the level of cohomology, too, the maps π^* map everything to zero and consequently the connecting homomorphisms $\delta^* : H^k(\partial M) \rightarrow H^{k+1}(M, \partial M)$ are surjective.

Let ∂M have m connected components, i.e. $\dim H^0(\partial M) = m$, then from (2.5) it follows that $\dim H^1(M, \partial M) = m - 1$. Let $\dim H^1(M) = h^1$, then by Poincaré-Lefschetz duality the sequence (2.5) yields the isomorphic sequence

$$0 \rightarrow \mathbb{R} \rightarrow \mathbb{R}^m \rightarrow \mathbb{R}^{m-1} \xrightarrow{0} \mathbb{R}^{h^1} \rightarrow \mathbb{R}^{2h^1} \rightarrow \mathbb{R}^{h^1} \xrightarrow{0} \mathbb{R}^{m-1} \rightarrow \mathbb{R}^m \rightarrow \mathbb{R} \rightarrow 0. \tag{2.6}$$

We explicitly mention the following obvious, but important situation:

Corollary 2.1.3. *Let M be a bounded domain in \mathbb{R}^3 with a connected boundary ∂M . Then $H^2(M) = 0$.*

Proof. This follows immediately from (2.6) with $m = 1$. \square

The intuition behind Corollary 2.1.3 is clear: if M has just a single boundary component, there can be no cavities inside M , as each cavity would add another boundary component. This insight shall give a simple proof for Corollary 3.3.6 later on.

2.2 DIFFERENTIAL FORMS ON MANIFOLDS WITH BOUNDARY

We give a short overview on differential forms on manifolds with boundary, most importantly Green's formula, tangential and normal boundary components and how they relate to tangential and normal components of representing vector proxy fields. All these results can be found in detail in [Sch95], further references are [Lee03] or [AFW06].

Let (M, g) be an n -dimensional oriented Riemannian manifold with boundary ∂M and let $\iota : \partial M \hookrightarrow M$ denote the inclusion. A smooth differential k -form on M is given by an assignment

$$p \mapsto \omega_p \in \text{Alt}^k(T_p M), \quad p \in M$$

where ω_p is an alternating k -form on the tangent space $T_p M$, such that for any family of smooth vector fields $\{X_1, \dots, X_k\}$ the function $p \mapsto \omega_p(X_1, \dots, X_k)$ is a smooth function on M , and we denote by $\Omega^k(M)$ the space of smooth differential k -forms on M . The metric g defines an inner product on each $T_p M$ and induces an inner product on $\text{Alt}^k(T_p M)$ by

$$\langle \omega_p, \eta_p \rangle_p := \sum_{1 \leq i_1 < i_2 < \dots < i_k \leq n} \omega_p(E_{p, i_1}, \dots, E_{p, i_k}) \cdot \eta_p(E_{p, i_1}, \dots, E_{p, i_k}) \quad (2.7)$$

for $\omega_p, \eta_p \in \text{Alt}^k(T_p M)$ and an arbitrary oriented g -orthonormal basis $\{E_{p, 1}, \dots, E_{p, n}\}$ of $T_p M$. These inner products define the L^2 -product on $\Omega^k(M)$ by

$$\langle \omega, \eta \rangle_{L^2} := \int_M \langle \omega_p, \eta_p \rangle_p \mu(p),$$

where $\mu \in \Omega^n(M)$ is the Riemannian volume form on M , satisfying $\langle \mu_p, \mu_p \rangle_p = 1$ for all $p \in M$.

For elements $\omega_p \in \text{Alt}^k(T_p M)$ and $\eta_p \in \text{Alt}^l(T_p M)$, their wedge product is defined as the element $\omega_p \wedge \eta_p \in \text{Alt}^{k+l}(T_p M)$ with

$$\omega_p \wedge \eta_p(X_{p, 1}, \dots, X_{p, k+l}) := \sum_{\sigma \in S_k^{k+l}} \text{sgn}(\sigma) \omega_p(X_{p, \sigma(1)}, \dots, X_{p, \sigma(k)}) \eta_p(X_{p, \sigma(k+1)}, \dots, X_{p, \sigma(k+l)})$$

where S_k^{k+l} denotes the set of all permutations σ of the numbers $\{1, \dots, k+l\}$ such that $\sigma(1) < \dots < \sigma(k)$ and $\sigma(k+1) < \dots < \sigma(k+l)$. The Hodge star operator \star combines the algebraic structure of alternating forms on $T_p M$ with the metric properties of M . It is an isomorphism $\star : \text{Alt}^k(T_p M) \rightarrow \text{Alt}^{n-k}(T_p M)$, $\eta_p \mapsto \star \eta_p$, where $\star \eta_p$ is the unique element in $\text{Alt}^{n-k}(T_p M)$ satisfying

$$\omega_p \wedge \star \eta_p = \langle \omega_p, \eta_p \rangle_p \mu_p \quad \text{for all } \omega_p \in \text{Alt}^k(T_p M),$$

and satisfies $\star \star = (-1)^{k(n-k)} \cdot \text{Id}$. Both definitions extend to maps $\wedge : \Omega^k(M) \times \Omega^l(M) \rightarrow \Omega^{k+l}(M)$ and $\star : \Omega^k(M) \rightarrow \Omega^{n-k}(M)$, defined in each fibre by the definitions given above.

For each k , there is a map $d^k : \Omega^k(M) \rightarrow \Omega^{k+1}(M)$ such that $d^{k+1} \circ d^k = 0$. It is uniquely defined by the additional assumptions that d^0 shall be the ordinary differential for any function $f \in \Omega^0(M)$ and that the *Leibniz rule* $d(\omega \wedge \eta) = d\omega \wedge \eta + (-1)^k \omega \wedge d\eta$ shall hold for any $\omega \in \Omega^k(M)$, $\eta \in \Omega^1(M)$. This unique map is the *exterior derivative* and turns the sequence of spaces $\Omega^k(M)$ into the *de Rham complex*

$$0 \rightarrow \mathcal{C}^\infty(M) \xrightarrow{d^0} \Omega^1(M) \xrightarrow{d^1} \dots \xrightarrow{d^{n-1}} \Omega^n(M) \xrightarrow{d^n} 0.$$

Moreover, for each k it defines the *coderivative* $\delta^k : \Omega^k(M) \rightarrow \Omega^{k-1}(M)$ by the relation $\delta^k \omega := (-1)^{n(k+1)+1} \star d^{n-k}(\star \omega)$, and both are related by *Green's formula*

$$\langle d\omega, \eta \rangle_{L^2} = \langle \omega, \delta\eta \rangle_{L^2} + \int_{\partial M} \iota^* \omega \wedge \iota^*(\star \eta) \quad \text{for } \omega \in \Omega^k(M), \eta \in \Omega^{k+1}(M), \quad (2.8)$$

where ι^* denotes the pullback along the inclusion $\iota : \partial M \hookrightarrow M$. This pullback commutes with wedge product and exterior derivative so that

$$\iota^*(\omega \wedge \eta) = \iota^* \omega \wedge \iota^* \eta \quad \text{and} \quad \iota^*(d\omega) = d(\iota^* \omega), \quad (2.9)$$

the latter derivative being the restriction to the boundary manifold ∂M . Green's formula (2.8) itself appears as a special case of *Stokes' theorem* which states that for any $(n-1)$ -form $\omega \in \Omega^{n-1}(M)$ it is

$$\int_M d\omega = \int_{\partial M} \iota^* \omega. \quad (2.10)$$

BOUNDARY COMPONENTS OF A DIFFERENTIAL FORM. Of particular interest to us is the boundary behaviour of vector fields and differential forms. At each point $p \in \partial M$, the tangent space $T_p \partial M$ of the boundary manifold ∂M can be identified as a subspace of codimension one of the tangent space $T_p M$ via the differential $D\iota_p$ of the inclusion ι . A *unit normal field* of M is then a smooth assignment

$$p \mapsto \nu_p \in T_p M \quad \text{for all } p \in \partial M$$

over ∂M such that $g(\nu_p, \nu_p) = 1$ and $g(\nu_p, X_p) = 0$ for all $p \in \partial M$ and $X_p \in T_p \partial M$. Since M is oriented, there is a unique unit normal field ν which we call the *outer unit normal field*. If $\varphi : U \subseteq M \rightarrow \mathbb{R}_{x_n \geq 0}^n$ is a chart in a neighbourhood of a boundary point $p \in \partial M$, it can be described as the unit normal field whose pushforward $(D\varphi)\nu$ has a negative coordinate $x_n < 0$, and since M has an oriented atlas, this convention is globally consistent.

The outer unit normal field ν allows us to decompose a vector field X on M restricted to the boundary into its *normal component* $\vec{\mathbf{n}}(X|_{\partial M}) := g(\nu, X|_{\partial M})\nu$ and its *tangential component* $\vec{\mathbf{t}}(X|_{\partial M}) := X|_{\partial M} - \vec{\mathbf{n}}(X|_{\partial M})$. This in turn defines the tangential and normal component of a differential form $\omega \in \Omega^k(M)$ over the boundary by

$$\mathbf{t}(\omega|_{\partial M})(X_1, \dots, X_k) := \omega|_{\partial M}(\vec{\mathbf{t}}(X_1), \dots, \vec{\mathbf{t}}(X_k)) \quad \text{and} \quad \mathbf{n}(\omega|_{\partial M}) := \omega|_{\partial M} - \mathbf{t}(\omega|_{\partial M}).$$

In the following we omit the explicit restriction $\omega|_{\partial M}$ in the operators \mathbf{t} and \mathbf{n} as this will be clear from the context. The tangential part $\mathbf{t}(\omega)$ only acts on the tangential components of

the input vector fields X_i and is therefore uniquely defined by a k -form in $\Omega^k(\partial M)$, thus one can identify $\mathbf{t}(\omega)$ with its pullback $\iota^*\omega$ to $\Omega^k(\partial M)$.

The tangential and normal component are related by the Hodge star operator in the following sense: for $\omega \in \Omega^k(M)$ it is

$$\star \mathbf{n}(\omega) = \mathbf{t}(\star \omega) \quad \text{and} \quad \star \mathbf{t}(\omega) = \mathbf{n}(\star \omega). \quad (2.11)$$

where the star operator in $\star \mathbf{n}(\omega)$ and $\star \mathbf{t}(\omega)$ is applied to a smooth extension of $\mathbf{n}(\omega)$ and $\mathbf{t}(\omega)$ and then restricted to ∂M . Furthermore, they are compatible with the exterior derivative and coderivative:

$$\mathbf{t}(d\omega) = d(\mathbf{t}(\omega)) \quad \text{and} \quad \mathbf{n}(\delta\omega) = \delta(\mathbf{n}(\omega)). \quad (2.12)$$

Green's formula then reads

$$\langle d\omega, \eta \rangle_{L^2} = \langle \omega, \delta\eta \rangle_{L^2} + \int_{\partial M} \mathbf{t}(\omega) \wedge \star \mathbf{n}(\eta)$$

which is the form we shall use in the following.

VECTOR FIELD PROXIES. In two and three dimensions, the theory of differential forms is classically formulated in terms of functions and vector fields only, with the classical vector calculus operators representing the exterior derivative and coderivative on the level of vector fields. The Riemannian metric induces a natural isomorphism between each tangent space $T_p M$ and its dual space $T_p^* M$: given an element $X_p \in T_p M$, there is a corresponding linear map $X_p^\flat := g(X_p, -) \in T_p^* M$, and conversely every element $X_p^* \in T_p^* M$ defines an element X_p^\sharp via Riesz representation. These *musical isomorphisms* extend to isomorphisms $\sharp : \Omega^1(M) \xrightarrow{\sim} \mathcal{X}(M)$ and $\flat : \mathcal{X}(M) \xrightarrow{\sim} \Omega^1(M)$ between the space of 1-forms and the space $\mathcal{X}(M)$ of smooth vector fields on M . A 2-form $\omega \in \Omega^2(M)$ is then represented by the vector field $(\star \omega)^\sharp$. Via these notions, the fibre metric (2.7) for two k -forms can be rewritten as

$$\langle \omega_{p,i_1} \wedge \cdots \wedge \omega_{p,i_k}, \omega_{p,j_1} \wedge \cdots \wedge \omega_{p,j_k} \rangle_p = \det \left(g(\omega_{p,i_s}^\sharp, \omega_{p,j_t}^\sharp) \right)_{1 \leq s, t \leq k}$$

for basis elements of the type $\omega_{p,i_1} \wedge \cdots \wedge \omega_{p,i_k} \in \text{Alt}^k(T_p M)$ and extended bilinearly.

In two dimensions, define the *curl* of a vector field $X \in \mathcal{X}(M)$ by $\text{curl}(X) := \star d^1 X^\flat$. This makes the following diagram commutative

$$\begin{array}{ccccc} \Omega^0(M) & \xrightarrow{d^0} & \Omega^1(M) & \xrightarrow{d^1} & \Omega^2(M) \\ \parallel & & \downarrow \# & & \downarrow \star \\ \mathcal{C}^\infty(M) & \xrightarrow{\nabla} & \mathcal{X}(M) & \xrightarrow{\text{curl}} & \mathcal{C}^\infty(M) \end{array}$$

In three dimensions, define the vector-valued *curl* of X as $\text{curl}(X) := (\star d^1 X^\flat)^\sharp$ and its *divergence* as $\text{div}(X) := \star d^2(\sharp \circ \star)^{-1} X = \star d^2 \star X^\flat$. This makes the diagram

$$\begin{array}{ccccccc} \Omega^0(M) & \xrightarrow{d^0} & \Omega^1(M) & \xrightarrow{d^1} & \Omega^2(M) & \xrightarrow{d^2} & \Omega^3 \\ \parallel & & \downarrow \# & & \downarrow \# \circ \star & & \downarrow \star \\ \mathcal{C}^\infty(M) & \xrightarrow{\nabla} & \mathcal{X}(M) & \xrightarrow{\text{curl}} & \mathcal{X}(M) & \xrightarrow{\text{div}} & \mathcal{C}^\infty(M) \end{array}$$

commutative. In Euclidean coordinates, these operators become the familiar expressions in terms of partial derivatives ∂_{x_i} . For instance, the two-dimensional curl is the operator $\text{curl} = \partial_{x_2} - \partial_{x_1}$ and the three-dimensional divergence is given by $\text{div} = \sum_i \partial_{x_i}$.

The boundary projections are compatible with the musical isomorphisms so that

$$\vec{\mathbf{n}}(\omega^\sharp) = \mathbf{n}(\omega)^\sharp \quad \text{and} \quad \vec{\mathbf{t}}(\omega^\sharp) = \mathbf{t}(\omega)^\sharp. \quad (2.13)$$

For many geometric applications these *vector proxies* are more intuitive to deal with, but they may also be misleading when the vector fields represent 2-forms in three dimensions. For instance, boundary conditions are swapped when 2-forms are represented by vector fields: a 2-form $\omega \in \Omega^2(M)$ with $\mathbf{t}(\omega) = 0$ is represented by the vector field $(\star\omega)^\sharp$ which now has vanishing normal component along the boundary, since

$$\vec{\mathbf{n}}((\star\omega)^\sharp) = \mathbf{n}(\star\omega)^\sharp = (\star\mathbf{t}(\omega))^\sharp \quad (2.14)$$

by (2.11) and (2.13). This will be important in Section 3.3.

2.3 HODGE-TYPE DECOMPOSITIONS

This section summarizes classical Hodge-type decomposition results on manifolds with boundary. Under appropriate boundary conditions every k -form can be decomposed into an exact, a coexact and a harmonic component. The Friedrichs decomposition identifies the spaces of so-called harmonic Neumann and Dirichlet fields as finite-dimensional subspaces of the infinite-dimensional space of harmonic k -forms, representing the k -th absolute and relative cohomology space, respectively. Both decomposition statements are combined in the four-term Hodge-Morrey-Friedrichs decomposition. The main reference is [Sch95], an introduction can also be found in [AMR88].

We define the spaces of *exact*, *coexact* and *harmonic* k -forms by

$$\begin{aligned} d\Omega^{k-1}(M) &:= \{d\omega : \omega \in \Omega^{k-1}(M)\} \\ \delta\Omega^{k+1}(M) &:= \{\delta\omega : \omega \in \Omega^{k+1}(M)\} \\ \mathcal{H}^k(M) &:= \{\omega \in \Omega^k(M) : d\omega = 0 \text{ and } \delta\omega = 0\}. \end{aligned}$$

Since the manifold M is fixed throughout the rest of this section, we will omit the reference to M in the definition and usage of subspaces of $\Omega^k(M)$, and simply write $d\Omega^{k-1}$, $\delta\Omega^{k+1}$, \mathcal{H}^k and so on.

On a manifold without boundary these three spaces constitute the ingredients of any k -form. More precisely:

Theorem 2.3.1 (Classical Hodge Decomposition, $\partial M = \emptyset$). *Let M be a smooth, compact manifold without boundary. Then there is an L^2 -orthogonal decomposition*

$$\Omega^k = d\Omega^{k-1} \oplus \delta\Omega^{k+1} \oplus \mathcal{H}^k.$$

A remarkable insight known as *de Rham's theorem* is that the space \mathcal{H}^k is in fact finite-dimensional and isomorphic to the k -th cohomology space $H^k(M)$, and therefore harmonic k -forms on a closed manifold represent the k -th cohomology classes.

However, in the presence of a boundary the spaces of exact forms $d\Omega^{k-1}$ and coexact forms $\delta\Omega^{k+1}$ are no longer L^2 -orthogonal to each other. Hence one has to pose appropriate boundary conditions on the (co-)potential spaces to retain orthogonality. A natural choice are *Dirichlet boundary conditions* on the space Ω^{k-1} and *Neumann boundary conditions* on Ω^{k+1} , as these types of boundary conditions are compatible with the exterior derivative and coderivative, respectively, see (2.12):

$$\begin{aligned}\Omega_D^{k-1} &:= \{\omega \in \Omega^{k-1} : \mathbf{t}(\omega) = 0\} \\ \Omega_N^{k+1} &:= \{\omega \in \Omega^{k+1} : \mathbf{n}(\omega) = 0\}\end{aligned}$$

Theorem 2.3.2 (Hodge Decomposition, $\partial M \neq \emptyset$). *Let M be a smooth, compact manifold with boundary. Then there is an L^2 -orthogonal decomposition*

$$\Omega^k = d\Omega_D^{k-1} \oplus \delta\Omega_N^{k+1} \oplus \mathcal{H}^k.$$

In this case, the resulting space \mathcal{H}^k of harmonic k -forms is infinite-dimensional and a priori the topological relation is lost. It is a result by Friedrichs ([Fri55, Ch. 9], [Sch95, Thm. 2.4.8, Thm. 2.6.1]) that \mathcal{H}^k can again be split in two different ways into two orthogonal subspaces, one of them being isomorphic to a cohomology space in each case. Define the spaces of *Neumann fields* and *Dirichlet fields* on M by

$$\begin{aligned}\mathcal{H}_N^k &:= \{\omega \in \mathcal{H}^k : \mathbf{n}(\omega) = 0\} \\ \mathcal{H}_D^k &:= \{\omega \in \mathcal{H}^k : \mathbf{t}(\omega) = 0\}.\end{aligned}$$

Theorem 2.3.3 (Friedrichs Decomposition). *On a manifold with boundary the space of harmonic fields \mathcal{H}^k has an L^2 -orthogonal splitting*

$$\begin{aligned}\mathcal{H}^k &= \mathcal{H}^k \cap d\Omega^{k-1} \oplus \mathcal{H}_N^k \\ &= \mathcal{H}^k \cap \delta\Omega^{k+1} \oplus \mathcal{H}_D^k.\end{aligned}$$

and it is $\mathcal{H}_N^k \cong H^k(M)$ and $\mathcal{H}_D^k \cong H^k(M, \partial M)$.

Writing

$$\begin{aligned}\mathcal{H}_{\text{ex}}^k &:= \mathcal{H}^k \cap d\Omega^{k-1} \\ \mathcal{H}_{\text{co}}^k &:= \mathcal{H}^k \cap \delta\Omega^{k+1}\end{aligned}$$

for the space of exact and coexact harmonic fields, this culminates in the *Hodge-Morrey-Friedrichs decomposition* ([Sch95, Thm. 2.4.8, Cor. 2.5.9]):

Theorem 2.3.4 (Hodge-Morrey-Friedrichs Decomposition). *On a manifold with boundary the space of k -forms admits the following L^2 -orthogonal decompositions:*

$$\begin{aligned}\Omega^k &= d\Omega_D^{k-1} \oplus \delta\Omega_N^{k+1} \oplus \mathcal{H}_{\text{ex}}^k \oplus \mathcal{H}_N^k \\ &= d\Omega_D^{k-1} \oplus \delta\Omega_N^{k+1} \oplus \mathcal{H}_{\text{co}}^k \oplus \mathcal{H}_D^k.\end{aligned}$$

The isomorphisms $\mathcal{H}_N^k \cong H^k(M)$ and $\mathcal{H}_D^k \cong H^k(M, \partial M)$ are induced by the *de Rham map* or *period map*

$$R^k : \Omega^k \rightarrow C^k(M), \quad \omega \mapsto \left(c_\omega : \sigma \mapsto \int_\sigma j^* \omega \right), \quad (2.15)$$

where σ is a k -simplex and $j : \sigma \hookrightarrow M$ denotes the inclusion. Let $H_{dR}^k(M)$ and $H_{dR}^k(M, \partial M)$ denote the k -th absolute and relative de Rham cohomology spaces, which are the k -th cohomology spaces of the complexes $(\Omega^k(M), d^k)_{k=0, \dots, n}$ and $(\Omega_D^k(M), d^k)_{k=0, \dots, n}$, respectively. Then de Rham's theorem states that R^k induces isomorphisms $\bar{R}_N^k : H_{dR}^k(M) \xrightarrow{\sim} H^k(M)$ and $\bar{R}_D^k : H_{dR}^k(M, \partial M) \xrightarrow{\sim} H^k(M, \partial M)$ on the level of cohomology. The Hodge-Morrey-Friedrichs decomposition in Theorem 2.3.4 now provides a concrete set of representatives for $H_{dR}^k(M)$ and $H_{dR}^k(M, \partial M)$, given by \mathcal{H}_N^k and \mathcal{H}_D^k . By abuse of notation we will denote the isomorphisms $\mathcal{H}_N^k \xrightarrow{\sim} H^k(M)$ and $\mathcal{H}_D^k \xrightarrow{\sim} H^k(M, \partial M)$ by \bar{R}_N^k and \bar{R}_D^k , too.

Remark 2.3.5. *The proofs for all these decomposition results rely on Hilbert space theory and properties of the Dirichlet energy $\mathcal{D}(\omega) := \langle d\omega, d\omega \rangle + \langle \delta\omega, \delta\omega \rangle$ on appropriate completions of the space Ω^k . Most common is the completion with respect to the L^2 -product which gives the space $L^2\Omega^k$, but the theory works even more generally for arbitrary Sobolev spaces of differential forms, too. For simplicity, here and in the following we shall restrict to splittings into spaces of smooth differential forms which appear as subspaces of their respective Sobolev completions. For a general treatment see [Sch95].*

2.4 ORTHOGONALITY OF \mathcal{H}_N^k AND \mathcal{H}_D^k

The spaces of harmonic Neumann and Dirichlet fields do not share a common non-trivial subspace. However, they are in general not L^2 -orthogonal to each other. Each space can be further decomposed into a space reflecting cohomology generated by boundary components, and a space reflecting interior cohomology, with the presence of the latter subspace being the reason for the non-orthogonality. For surfaces of type $\Sigma_{0,m}$ and bounded three-dimensional domains in \mathbb{R}^3 , this particular subspace is trivial though, and consequently there are orthogonal decompositions involving both the spaces of Neumann and Dirichlet fields at the same time.

A natural question to ask is whether there is a decomposition involving both the spaces \mathcal{H}_N^k and \mathcal{H}_D^k simultaneously. However, in general \mathcal{H}_N^k and \mathcal{H}_D^k are not necessarily orthogonal any more, see for instance the examples given in [Sho09]. At least their algebraic sum is still direct:

Theorem 2.4.1. *It is always $\mathcal{H}_N^k \cap \mathcal{H}_D^k = \{0\}$.*

Proof. [Sch95, Theorem 3.4.4] □

Combining this result with the Friedrichs decompositions Theorem 2.3.3 shows that $\mathcal{H}^k = \mathcal{H}_{\text{co}}^k + \mathcal{H}_{\text{ex}}^k$. In particular every k -form on a manifold with boundary is the sum of an exact form and a coexact form, although this sum is not unique:

$$\Omega^k = d\Omega^{k-1} + \delta\Omega^{k+1}.$$

As a consequence of Theorem 2.4.1, the Hodge-Morrey-Friedrichs decompositions can be merged into a single decomposition

$$\Omega^k = d\Omega_D^{k-1} \oplus \delta\Omega_N^{k+1} \oplus d\Omega^{k-1} \cap \delta\Omega^{k+1} \oplus (\mathcal{H}_N^k + \mathcal{H}_D^k), \quad (2.16)$$

where the sum $\mathcal{H}_N^k + \mathcal{H}_D^k$ is a direct, but in general not an L^2 -orthogonal sum.

The following theorem states a further decomposition of the spaces \mathcal{H}_N^k and \mathcal{H}_D^k into two orthogonal subspaces. This result seems to be first published by Shonkwiler in [Sho09, Thm. 2.1.2] and [Sho13], but is apparently due to Dennis DeTurck and Herman Gluck, cf. [Sho09, Introduction]. Since it does not appear in the standard literature we state the proof here, slightly modified and adjusted to our notation, as this result will be essential for the discrete decompositions in Sections 3.2 and 3.3. The following spaces will be relevant:

Definition 2.4.2. *The spaces*

$$\mathcal{H}_{N,\text{co}}^k := \mathcal{H}_N^k \cap \delta\Omega^{k+1} \quad (2.17)$$

$$\mathcal{H}_{N,\partial\text{ex}}^k := \{\omega \in \mathcal{H}_N^k : \iota^* \omega \in d\Omega^{k-1}(\partial M)\} \quad (2.18)$$

$$\mathcal{H}_{D,\text{ex}}^k := \mathcal{H}_D^k \cap d\Omega^{k-1} = \star \mathcal{H}_{N,\text{co}}^{n-k} \quad (2.19)$$

$$\mathcal{H}_{D,\partial\text{co}}^k := \{\omega \in \mathcal{H}_D^k : \iota^*(\star\omega) \in d\Omega^{n-k-1}(\partial M)\} = \star \mathcal{H}_{N,\partial\text{ex}}^{n-k} \quad (2.20)$$

are the spaces of coexact Neumann, boundary-exact Neumann, exact Dirichlet and boundary-coexact Dirichlet k -forms, respectively.

An immediate consequence of the Friedrichs decompositions in Theorem 2.3.3 are the orthogonalities $\mathcal{H}_{N,\text{co}}^k \perp \mathcal{H}_D^k$ and $\mathcal{H}_{D,\text{ex}}^k \perp \mathcal{H}_N^k$. Shonkwiler has proved that the subspaces of coexact and boundary-exact Neumann fields as well as the exact and boundary-exact Dirichlet fields constitute an orthogonal splitting of the spaces of Neumann and Dirichlet fields, respectively. Furthermore, the subspaces of coexact Neumann and exact Dirichlet fields are directly linked to the cohomology induced by the boundary components, whereas the other two subspaces reflect cohomology coming from the “interior” of the manifold, as will become clear from the proof.

Theorem 2.4.3 (Shonkwiler, DeTurck, Gluck). *The spaces \mathcal{H}_N^k and \mathcal{H}_D^k have the following L^2 -orthogonal decompositions:*

$$\begin{aligned}\mathcal{H}_N^k &= \mathcal{H}_{N,\text{co}}^k \oplus \mathcal{H}_{N,\partial\text{ex}}^k \\ \mathcal{H}_D^k &= \mathcal{H}_{D,\text{ex}}^k \oplus \mathcal{H}_{D,\partial\text{co}}^k.\end{aligned}$$

Proof. Following the strategy in [Sho09], we consider the first decomposition and start with proving orthogonality. Let $\eta = \delta\beta \in \mathcal{H}_{N,\text{co}}^k$ and $\xi \in \mathcal{H}_{N,\partial\text{ex}}^k$ with $\iota^*\xi = d\tau$ for some $\tau \in \Omega^{k-1}(\partial M)$. τ has a smooth extension to a form $\tilde{\tau} \in \Omega^{k-1}(M)$. By applying Green's formula (2.8), twice we obtain

$$\begin{aligned}\langle \eta, \xi \rangle &= \langle \delta\beta, \xi \rangle = \langle \beta, d\xi \rangle - \int_{\partial M} \mathbf{t}(\xi) \wedge \star \mathbf{n}(\beta) = - \int_{\partial M} \mathbf{t}(d\tilde{\tau}) \wedge \star \mathbf{n}(\beta) \\ &= \langle d\tilde{\tau}, \delta\beta \rangle - \langle dd\tilde{\tau}, \beta \rangle = \langle d\tilde{\tau}, \eta \rangle = \langle \tilde{\tau}, \delta\eta \rangle + \int_{\partial M} \mathbf{t}(\tilde{\tau}) \wedge \star \mathbf{n}(\eta) = 0\end{aligned}$$

because $\eta \in \mathcal{H}_N^k$ implies $\delta\eta = 0$ and $\mathbf{n}(\eta) = 0$.

To prove the existence of the splitting we proceed as follows: the inclusion $\iota : \partial M \hookrightarrow M$ induces a map $\iota_* : H_k(\partial M) \rightarrow H_k(M)$ on homology. Let $\mathcal{B}_{\partial,k} := \{\sigma_1^k, \dots, \sigma_{b_{\partial,k}}^k\}$ denote a basis of size $b_{\partial,k}$ for the subspace $\iota_*H_k(\partial M) \subseteq H_k(M)$, and extend it to a basis $\mathcal{B}_k := \{\sigma_1^k, \dots, \sigma_{b_{\partial,k}}^k, \sigma_{b_{\partial,k}+1}^k, \dots, \sigma_{b_k}^k\}$ for the whole space $H_k(M)$. Let $\mathcal{B}^{k,\vee} := \{c_i^k\}_{i=1,\dots,b_k}$ denote its Kronecker dual basis of $H^k(M)$.

We now show that $\dim \mathcal{H}_{N,\text{co}}^k = b_{\partial,k}$. Consider the commutative diagram

$$\begin{array}{ccccccc} & & & \mathcal{H}_D^{n-k} & & & \\ & & & \downarrow \bar{R}_D^{n-k} & & & \\ \dots & \longrightarrow & H^{n-k-1}(\partial M) & \longrightarrow & H^{n-k}(M, \partial M) & \xrightarrow{\pi^*} & H^{n-k}(M) \longrightarrow \dots \\ & & \downarrow & & \downarrow P^{n-k} & & \downarrow \\ \dots & \longrightarrow & H_k(\partial M) & \xrightarrow{\iota_*} & H_k(M) & \xrightarrow{\pi_*} & H_k(M, \partial M) \longrightarrow \dots\end{array}$$

with exact rows and Poincaré-Lefschetz isomorphisms as vertical arrows between the rows. The basis \mathcal{B}_k is mapped to a basis $\mathcal{B}^{n-k} := (P^{n-k})^{-1}(\mathcal{B}_k)$, and by exactness of the rows the subset $\mathcal{B}_{\partial}^{n-k} := (P^{n-k})^{-1}(\mathcal{B}_{\partial,k})$ is a basis for $\ker(\pi^*)$. But by commutativity of the diagram

$$\begin{array}{ccc} H_{dR}^{n-k}(M, \partial M) & \xrightarrow{\pi^*} & H_{dR}^{n-k}(M) \\ \bar{R}_D^{n-k} \downarrow & & \downarrow \bar{R}_N^{n-k} \\ H^{n-k}(M, \partial M) & \xrightarrow{\pi^*} & H^{n-k}(M) \end{array}$$

it is $c^{n-k} \in \ker(\pi^*)$ if and only if for the representative $\rho := (\bar{R}_D^{n-k})^{-1}(c^{n-k}) \in \mathcal{H}_D^{n-k}$ it is $\pi^*(\rho) = 0 \in H_{dR}^{n-k}(M)$, i.e. if and only if $\rho \in d\Omega^{n-k-1} \cap \mathcal{H}_D^{n-k} = \mathcal{H}_{D,\text{ex}}^{n-k}$. Since \star restricts to an isomorphism $\star : \mathcal{H}_{D,\text{ex}}^{n-k} \rightarrow \mathcal{H}_{N,\text{co}}^k$ it follows $\dim \mathcal{H}_{N,\text{co}}^k = \dim \mathcal{H}_{D,\text{ex}}^{n-k} = \dim \ker(\pi^*) = b_{\partial,k}$.

Next we prove that the map $\Pi_K \circ \bar{R}_N^k$ induces an isomorphism from $\mathcal{H}_{N,\text{co}}^k$ onto the subspace $K := \langle c_1^k, \dots, c_{b_{\partial,k}}^k \rangle_{\mathbb{R}} \subseteq H^k(M)$, where $\Pi_K : H^k(M) \rightarrow K$, $\sum_{i=1}^{b_k} a_i c_i^k \mapsto \sum_{i=1}^{b_{\partial,k}} a_i c_i^k$ denotes the algebraic projection onto K . By dimension counting it is enough to show injectivity. Assume there is an $\omega \in \mathcal{H}_{N,\text{co}}^k$ with $\Pi_K \circ \bar{R}_N^k(\omega) = 0$, i.e. $c^k := \bar{R}_N^k(\omega) = \sum_{i > b_{\partial,k}} a_i c_i^k$. Then for any $\sigma \in H_k(\partial M)$ it is $\iota^* c^k(\sigma) = c^k(\iota_* \sigma) = 0$ since by definition of the Kronecker dual basis only the cochains c_i^k with $i \leq b_{\partial,k}$, are non-vanishing on $\iota_* H_k(\partial M)$. Therefore $\iota^* c^k = 0 \in H^k(\partial M)$ and thus $\iota^* \omega = 0 \in H_{dR}^k(\partial M)$, i.e. $\iota^* \omega$ is exact on ∂M , so $\omega \in \mathcal{H}_{N,\partial\text{ex}}^k$. But by orthogonality of $\mathcal{H}_{N,\partial\text{ex}}^k$ and $\mathcal{H}_{N,\text{co}}^k$ it must be $\omega = 0$. This shows isomorphy.

Finally let $\omega \in \mathcal{H}_N^k$ and let $c := \Pi_K \circ \bar{R}_N^k(\omega) \in K \subseteq H^k(M)$. Then there is a unique $\eta \in \mathcal{H}_{N,\text{co}}^k$ with $\Pi_K \circ \bar{R}_N^k(\eta) = c$. Thus, for $\xi := \omega - \eta$ it is $\Pi_K \circ \bar{R}_N^k(\xi) = 0$, so $\xi \in \mathcal{H}_{N,\partial\text{ex}}^k$ by the above argument, and this gives the decomposition $\omega = \eta + \xi \in \mathcal{H}_{N,\text{co}}^k \oplus \mathcal{H}_{N,\partial\text{ex}}^k$.

The second decomposition follows from the first because $\star : \mathcal{H}_N^k \rightarrow \mathcal{H}_D^{n-k}$, being an isometry, respects the orthogonality and maps $\mathcal{H}_{N,\text{co}}^k$ to $\mathcal{H}_{D,\text{ex}}^{n-k}$ and $\mathcal{H}_{N,\partial\text{ex}}^k$ to $\mathcal{H}_{D,\partial\text{co}}^{n-k}$. \square

The dimension for the split spaces coming from the proof will be important in the following so we mention explicitly:

Corollary 2.4.4. *Let $b_{\partial,k} := \dim \iota_* H_k(\partial M) = \dim \ker(\pi^* : H^{n-k}(M, \partial M) \rightarrow H^{n-k}(M))$ and $b_k = \dim H_k(M) = \dim H^{n-k}(M, \partial M)$. Then*

$$\begin{aligned} \dim \mathcal{H}_{N,\text{co}}^k &= \dim \mathcal{H}_{D,\text{ex}}^{n-k} = b_{\partial,k} \\ \dim \mathcal{H}_{N,\partial\text{ex}}^k &= \dim \mathcal{H}_{D,\partial\text{co}}^{n-k} = b_k - b_{\partial,k}. \end{aligned}$$

Proof. This was shown in the proof of Theorem 2.4.3. \square

ORTHOGONALITY ON SURFACES AND VOLUMES. Theorem 2.4.3 gives an answer to the question whether there is an orthogonal decomposition of Hodge-Morrey-Friedrichs type involving both the spaces \mathcal{H}_D^k and \mathcal{H}_N^k at the same time for surfaces and volumes embedded in \mathbb{R}^3 as follows.

Lemma 2.4.5. *Let M be a surface of type $\Sigma_{0,m}$. Then there is an L^2 -orthogonal decomposition*

$$\Omega^1 = d\Omega_D^0 \oplus \delta\Omega_N^2 \oplus d\Omega^0 \cap \delta\Omega^2 \oplus \mathcal{H}_D^1 \oplus \mathcal{H}_N^1.$$

Proof. The sequence (2.4) shows that for genus $g = 0$ it is $\dim \ker(\pi^* : H^1(M, \partial M) \rightarrow H^1(M)) = m - 1 = \dim H^1(M, \partial M)$, so by Corollary 2.4.4 it is $\mathcal{H}_D^1 = \mathcal{H}_{D,\text{ex}}^1 \subset d\Omega^0$ and $\mathcal{H}_N^1 = \mathcal{H}_{N,\text{co}}^1 \subset \delta\Omega^2$, and the result follows from Theorem 2.3.4. \square

In particular, this decomposition applies to flat, two-dimensional domains in \mathbb{R}^2 . A similar statement holds for three-dimensional bounded domains in \mathbb{R}^3 .

Lemma 2.4.6. *Let M be a bounded domain in \mathbb{R}^3 . Then for $k = 1, 2$, there is an L^2 -orthogonal decomposition*

$$\Omega^k = d\Omega_D^{k-1} \oplus \delta\Omega_N^{k+1} \oplus d\Omega^{k-1} \cap \delta\Omega^{k+1} \oplus \mathcal{H}_D^k \oplus \mathcal{H}_N^k.$$

Proof. It follows from (2.5) that the maps $\pi^* : H^k(M, \partial M) \rightarrow H^k(M)$ are zero maps, so $\ker(\pi^*) = H^k(M, \partial M)$, $k = 1, 2$. Corollary 2.4.4 shows again that $\mathcal{H}_D^k \subset d\Omega^{k-1}$ and $\mathcal{H}_N^k \subset \delta\Omega^{k+1}$, and the result follows from Theorem 2.3.4. \square

Speaking in terms of vector proxies, Cantarella et al. [CDG02] have coined the following notions of the corresponding subspaces:

$$\begin{aligned} \text{GG} &:= \{\nabla\varphi \in \mathcal{C}^\infty : \varphi|_{\partial M} = 0\} \\ \text{FK} &:= \{\text{curl}(Y) : Y \in \mathcal{X}, \vec{\mathbf{t}}(Y) = 0\} \\ \text{CG} &:= \{X \in \mathcal{X} : \exists\varphi \in \mathcal{C}^\infty, Y \in \mathcal{X} \text{ such that } X = \nabla\varphi = \text{curl}(Y)\} \\ \text{HG} &:= \{X \in \mathcal{X} : \vec{\mathbf{t}}(X) = 0, \text{div}(X) = 0, \exists\varphi \in \mathcal{C}^\infty \text{ such that } X = \nabla\varphi\} \\ \text{HK} &:= \{X \in \mathcal{X} : \vec{\mathbf{n}}(X) = 0, \text{curl}(X) = 0, \exists Y \in \mathcal{X} \text{ such that } X = \text{curl}(Y)\} \end{aligned}$$

These spaces are called *grounded gradients*, *fluxless knots*, *curly gradients*, *harmonic gradients* and *harmonic knots*, and there is an orthogonal decomposition

$$\mathcal{X} = \text{GG} \oplus \text{FK} \oplus \text{CG} \oplus \text{HG} \oplus \text{HK} \tag{2.21}$$

which corresponds to the case $k = 1$ in Lemma 2.4.6. In particular, the spaces \mathcal{H}_D^1 and \mathcal{H}_N^1 correspond to HG and HK, respectively. See the examples in Section 5.4 for stereotypical vector fields in each of these spaces.

DISCRETE DECOMPOSITIONS

3.1 FUNCTION SPACES ON SIMPLICIAL MANIFOLDS

We introduce the space of piecewise constant vector fields \mathcal{X}_h on a simplicial manifold and the ansatz spaces used for the discrete decompositions which are derived in the following chapters. Of great importance are the notions of tangential and normal continuity of piecewise constant vector fields across inner facets. They relate subspaces of \mathcal{X}_h to subspaces of Whitney forms whose complex on the one hand encodes the cohomology of the mesh and on the other hand possesses enough interelement continuity to define an exterior derivative. Finally we define the corresponding spaces of vector field proxies classically known as Raviart-Thomas and Nédélec elements and tabulate dimensions of certain spaces which we shall need later on.

SIMPLICIAL MANIFOLDS. In the following we will consider manifolds of dimension two or three that are geometric realizations of finite simplicial complexes embedded in \mathbb{R}^3 . More precisely, we call $M_h \subset \mathbb{R}^3$ an *oriented, compact simplicial n -manifold with boundary*, $n = 2$ or $n = 3$, if M_h is an oriented, compact topological n -manifold with boundary ∂M_h such that there is a finite simplicial complex K whose geometric realization $|K|$ of affine n -simplices in \mathbb{R}^3 is as a set equal to M_h . The triangulation of the boundary ∂M_h is then a subcomplex of K . If $n = 2$, we also refer to M_h as a *simplicial surface*, and for $n = 3$ we say that M_h is a *simplicial solid*. In addition, we always assume that M_h is connected. In applications, M_h is often interpreted as a simplicial approximation of a smooth shape and we will attain this point of view in the convergence analysis in Chapter 4.

By abuse of notation we often identify M_h with its simplicial complex structure and write $M_h^{(i)}$ for the set of i -simplices in the triangulation on M_h . We denote by n_V , n_E , n_F and n_T the number of 0-, 1-, 2-, and 3-simplices which we call *vertices*, *edges*, *faces* or *triangles*, and *tetrahedra*, respectively. The simplices of highest dimension in M_h are also called *cells*. These are triangles for simplicial surfaces and tetrahedra for simplicial solids. The $(n - 1)$ -dimensional simplices forming the boundary of a cell σ are called the *facets* of σ . Furthermore, we write n_{bV} , n_{bE} and n_{bF} for the number of vertices, edges and triangles contained in the boundary subcomplex ∂M_h , and $n_{iV} := n_V - n_{bV}$, $n_{iE} := n_E - n_{bE}$, $n_{iF} := n_F - n_{bF}$ for the number of entities in the interior of M_h in the respective dimensions.

We shall need the following, simple combinatorial relations between these numbers: for a simplicial surface with boundary it is $n_{iE} = 3n_F - n_E$. Furthermore, its *Euler characteristic* is given by the formula

$$\chi(M_h) = n_V - n_E + n_F = 1 - h^1. \quad (3.1)$$

Similarly, a simplicial solid in \mathbb{R}^3 satisfies $n_{iF} = 4n_T - n_F$ and for its Euler characteristic, both in absolute and relative version, holds

$$\begin{aligned} \chi(M_h) &= n_V - n_E + n_F - n_T = 1 - h^1 + h^2 \\ \chi(M_h, \partial M_h) &= n_{iV} - n_{iE} + n_{iF} - n_T = -h_r^1 + h_r^2 - 1 = -\chi(M_h). \end{aligned} \quad (3.2)$$

For a simplicial surface M_h there is by definition an orientation on the triangulation and we can specify for each affine triangle a (constant) unit normal field N consistent with this

orientation. This orientation defines a complex structure J on every tangent space $T_p M_h$, where p is a point in the interior of a triangle f , which acts geometrically by an anti-clockwise rotation by $\pi/2$. More precisely, if we identify $T_p M_h$ with a plane through the origin in \mathbb{R}^3 parallel to f , and X_p is a vector in $T_p M_h$, then $JX_p := N_p \times X_p$, where \times denotes the Euclidean cross product in \mathbb{R}^3 .

PIECEWISE CONSTANT VECTOR FIELDS. Let M_h be a simplicial surface. If $f = [v_0, v_1, v_2]$ is a triangle of M_h , then the barycentric coordinates on f provide a chart $\lambda = (\lambda_1, \lambda_2)$ onto the unit triangle in \mathbb{R}^2 , spanned by $(0, 0)$, $(1, 0)$ and $(0, 1)$. We say that a tangent vector field $X \in \mathcal{X}(f)$ is a *constant tangent vector field* over f if it can be written as

$$X_p := \sum a_i \partial \lambda_i |_p \quad \text{for all } p \in f$$

for two coefficients $a_1, a_2 \in \mathbb{R}$ which do not depend on the point p . An analogous definition applies to constant tangent vector fields over a cell t of a simplicial solid in \mathbb{R}^3 .

Definition 3.1.1 (Piecewise Constant Vector Field). *Let M_h be a simplicial surface or a simplicial solid in \mathbb{R}^3 . A piecewise constant vector field (PCVF) on M_h is an element $X \in L^2(M_h, \mathbb{R}^3)$ such that $X|_\sigma$ is represented by a constant tangent vector field over each cell σ . The space of all PCVFs is denoted by $\mathcal{X}_h(M_h)$.*

If M_h is clear from the context, we usually just write \mathcal{X}_h . For a simplicial surface M_h , one can identify an element $X \in \mathcal{X}_h$ with a family $(X_f)_{f \in M_h^{(2)}}$ indexed by the triangles of M_h , where X_f is a vector in the plane through the origin parallel to f . The L^2 -product on \mathcal{X}_h then reduces to a sum of weighted Euclidean scalar products as

$$\langle X, Y \rangle_{L^2} = \sum_{f \in M_h^{(2)}} \langle X_f, Y_f \rangle \cdot \text{area}(f)$$

The same formula applies to simplicial volumes, summing over all tetrahedra $t \in M_h^{(3)}$ and replacing the area factor by the three-dimensional volumes $\text{vol}(t)$ of the tetrahedra.

By the very definition of a piecewise constant vector field X the only non-static information is captured by the transition across an edge between adjacent triangles in the case of surfaces or more generally across any $(n-1)$ -face which is the intersection between any two adjacent n -cells. This transition can be characterized by a *normal jump* $[X]_N$ and *tangential jump* $[X]_T$ as follows: for a simplicial surface M_h assign an arbitrary but fixed orientation to all edges $e \in M_h^{(1)}$. If e is such an oriented edge in the intersection of two adjacent triangles f_1 and f_2 , let ν_i denote the outward unit normal field of f_i at e . Then, define the normal and tangential jumps of X at e by

$$\begin{aligned} [X]_N(e) &:= \langle X_1, \nu_1 \rangle + \langle X_2, \nu_2 \rangle \\ [X]_T(e) &:= \langle X_1, J \nu_1 \rangle + \langle X_2, J \nu_2 \rangle. \end{aligned}$$

Equivalently, these quantities can be expressed by first unfolding the two triangles at e until they become coplanar, i.e. $\nu_1 = -\nu_2$. Then $[X]_N(e) = \langle X_1 - X_2, \nu_1 \rangle$ and $[X]_T(e) = \langle X_1 - X_2, e/\|e\| \rangle$, assuming e is oriented such that $e/\|e\| = J \nu_1$.

Similarly, if M_h is a simplicial solid in \mathbb{R}^3 , assign an arbitrary, but fixed unit normal direction ν to each face $f \in M_h^{(2)}$. For $f = t_1 \cap t_2$, define normal and tangential jump of X at f by

$$\begin{aligned} [X]_N(f) &:= \langle X_1 - X_2, \nu \rangle \\ [X]_T(f) &:= \nu \times (\nu \times (X_1 - X_2)). \end{aligned}$$

Note that the tangent spaces of the cells at f , identified as subspaces of $T_p\mathbb{R}^3$, are already coplanar for each point $p \in f$, since M_h is flat. In any case we say that X is *normally continuous* if all normal jumps vanish at inner facets, and *tangentially continuous* if all tangential jumps vanish at inner facets.

These two notions are essential in the analysis and formulation of finite element spaces, because the interelement continuity of piecewise smooth finite element functions determines the regularity of the Sobolev space the finite element space belongs to. For instance, if $M \subset \mathbb{R}^2$ is a triangulated domain then a piecewise smooth vector field is in $H(\text{curl}, M)$ (i.e. has a weak curl) if and only if it is tangentially continuous across inner edges, and it is in $H(\text{div}, M)$ if and only if it is normally continuous.

LINEAR ANSATZ SPACES FOR FUNCTIONS. We shall consider the following ansatz spaces of functions $M_h \rightarrow \mathbb{R}$, where M_h could be either a simplicial surface or a simplicial solid.

$$\mathcal{L} := \{\varphi : M_h \rightarrow \mathbb{R} : \varphi|_{\sigma} \text{ linear for each cell } \sigma \text{ and } \varphi \text{ globally continuous}\}$$

$$\mathcal{F} := \{\psi : M_h \rightarrow \mathbb{R} : \psi|_{\sigma} \text{ linear for each cell } \sigma \text{ and } \psi \text{ continuous at facet barycentres}\}$$

The space \mathcal{L} is the space of *linear Lagrange elements* on M_h . Its standard basis is given by the vertex basis functions φ_j with $\varphi_j(v_i) = \delta_{ij}$, where $v_i \in M_h^{(0)}$ is a vertex, and we say that their *degrees of freedom* lie at the vertices. An alternative interpretation of these basis functions is as *generalized barycentric coordinates*: over each triangle $f = [v_0, v_1, v_2]$ of a simplicial surface, the restrictions of the associated basis functions φ_j to f are the barycentric coordinates $\lambda_0, \lambda_1, \lambda_2$ on f . Consequently, φ_j can be interpreted as a generalized barycentric coordinate function, supported on the star of the vertex v_j , and by abuse of notation we shall also write $\lambda_j := \varphi_j$ whenever we want to emphasize that we think of φ_j as a piecewise barycentric coordinate function, and similarly for simplicial solids. We will attain this point of view later on to define Whitney forms.

The space \mathcal{F} is the space of *Crouzeix-Raviart elements*. Its standard basis is given by the facet basis functions ψ_j with $\psi_j(b_i) = \delta_{ij}$, where b_i is the barycentre of the $(n-1)$ -face with index i , and we say that their degrees of freedom lie at facet midpoints. Therefore, for $n=2$ these are all functions which are linear over each triangle and continuous at edge midpoints, whereas for $n=3$ they are linear over each tetrahedral cell and continuous at barycentres of the triangular faces.

The boundary-constrained subspaces $\mathcal{L}_0 \subset \mathcal{L}$ and $\mathcal{F}_0 \subset \mathcal{F}$ are defined by

$$\begin{aligned} \mathcal{L}_0 &:= \{\varphi \in \mathcal{L} : \varphi(v_b) = 0 \text{ for all } v_b \in \partial M_h^{(0)}\} \\ \mathcal{F}_0 &:= \{\psi \in \mathcal{F} : \psi(b) = 0 \text{ for all barycenters } b \text{ of facets in } \partial M_h^{(n-1)}\}. \end{aligned}$$

Note that elements in \mathcal{L}_0 vanish identically on boundary facets whereas elements in \mathcal{F}_0 in general only vanish at the barycentres of boundary facets.

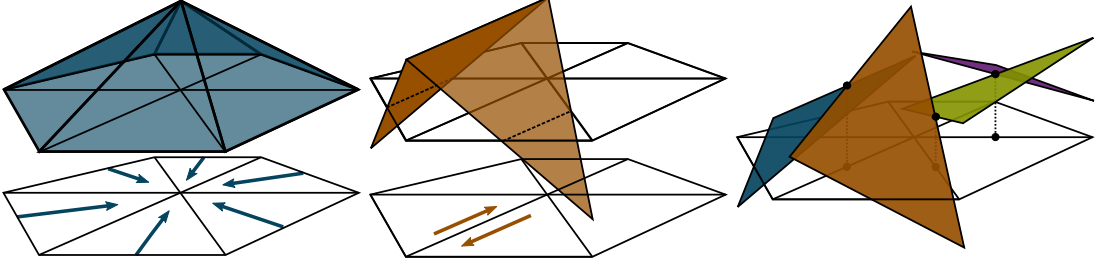


Figure 3.1: Left: Lagrange basis function on a simplicial surface associated to the middle vertex and its gradient field. Middle: Crouzeix-Raviart basis function associated to an edge and its cogradient field. Right: A general Crouzeix-Raviart function is only continuous at edge midpoints.

DISCRETE GRADIENTS. For any piecewise linear function ϕ on M_h the *gradient* is defined piecewise by

$$(\nabla\phi)|_{\sigma} := \nabla(\phi|_{\sigma}) \quad \text{for all cells } \sigma \in M_h^{(n)},$$

where the right-hand side is the restriction of the smooth gradient over the n -cell σ . The gradient maps the space of linear Lagrange elements \mathcal{L} as well as the space of Crouzeix-Raviart elements \mathcal{F} to subspaces of \mathcal{X}_h which we denote by $\nabla\mathcal{L}$ and $\nabla\mathcal{F}$, respectively, that is

$$\begin{aligned} \nabla\mathcal{L} &:= \{\nabla\varphi : \varphi \in \mathcal{L}\} \\ \nabla\mathcal{F} &:= \{\nabla\psi : \psi \in \mathcal{F}\}. \end{aligned}$$

If $\dim M_h = 2$ we shall also need the *cogradient space* of Crouzeix-Raviart elements defined by

$$J\nabla\mathcal{F} := \{J\nabla\psi : \psi \in \mathcal{F}\}.$$

The gradient and cogradient field for a linear Lagrange and a Crouzeix-Raviart basis function, respectively, are illustrated in Figure 3.1.

The gradients of linear Lagrange and Crouzeix-Raviart functions have the following intrinsic representations: if M_h is a simplicial surface and f a triangle, let e denote an edge of f , with its orientation induced from the boundary ∂f , and let v be the vertex of f opposite to e , see Figure 3.2. Then for the linear Lagrange basis function $\varphi_v \in \mathcal{L}$ associated to v and the Crouzeix-Raviart basis function $\psi_e \in \mathcal{F}$ associated to e it is

$$\nabla\varphi_v|_f = \frac{Je}{2 \cdot \text{area}(f)} \quad \text{and} \quad \nabla\psi_e|_f = \frac{-Je}{\text{area}(f)}. \quad (3.3)$$

Similarly, if M_h is a simplicial solid, let $f = [v_0, v_1, v_2]$ denote a facet of a tetrahedron t , and let v be the vertex of t opposite to f . Assume that the vertices v_i are ordered such that for the edges $e_1 := [v_0, v_1]$ and $e_2 := [v_0, v_2]$ their cross product $e_1 \times e_2$ points inside t . Then using $\|e_1 \times e_2\| = 2 \cdot \text{area}(f)$ and $\text{vol}(t) = \text{area}(f) \cdot \text{height}/3$, one obtains for $\varphi_v \in \mathcal{L}$ associated to v and $\psi_f \in \mathcal{F}$ associated to f :

$$\nabla\varphi_v|_t = \frac{e_1 \times e_2}{6 \cdot \text{vol}(t)} \quad \text{and} \quad \nabla\psi_f|_t = -\frac{e_1 \times e_2}{2 \cdot \text{vol}(t)}.$$

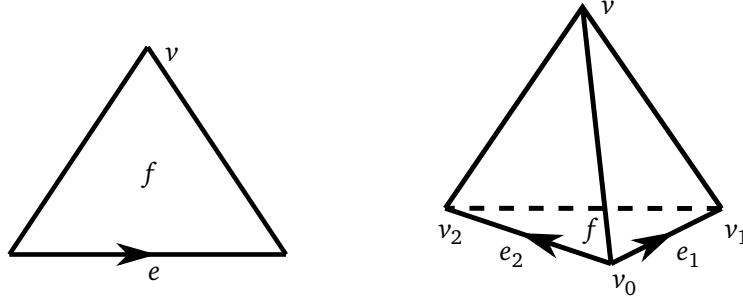


Figure 3.2: Notation used for the intrinsic representation of gradients on a triangle and a tetrahedron.

In order to use Green's formula for PCVFs on individual cells, we need to extend $X \in \mathcal{X}_h$ to facets. However, since $X \in L^2(M_h, \mathbb{R}^3)$, its trace on facets is not well-defined. Still, we can apply Green's formula locally, since for any cell σ , $X|_\sigma$ has by definition a smooth constant representative $\bar{X} \in \mathcal{C}^\infty(\sigma; \mathbb{R}^3)$. We will implicitly refer to this representative whenever we deal with boundary integrals over boundaries of individual cells to obtain a well-defined local trace of X .

Lemma 3.1.2. *Let M_h be a simplicial surface or simplicial solid in \mathbb{R}^3 and let $X \in \mathcal{X}_h$. Then*

$$\langle X, \nabla \psi \rangle_{L^2} = 0 \quad \text{for all } \psi \in \mathcal{F}_0$$

if and only if X is normally continuous. Furthermore,

$$\langle X, \nabla \psi \rangle_{L^2} = 0 \quad \text{for all } \psi \in \mathcal{F}$$

if and only if X is normally continuous and has vanishing normal component along the boundary.

Proof. First, let M_h be a simplicial surface, $e = f_1 \cap f_2 \in M_h^{(1)}$ an inner edge adjacent to triangles f_1 and f_2 , and $\psi_e \in \mathcal{F}_0$ the Crouzeix-Raviart basis function associated to e . Then, if ν_i denotes the piecewise constant outer normal field of f_i , by Green's formula over the individual triangles it is

$$\begin{aligned} \langle X, \nabla \psi_e \rangle_{L^2} &= \int_{f_1} \langle X_{f_1}, \nabla \psi_e \rangle + \int_{f_2} \langle X_{f_2}, \nabla \psi_e \rangle \\ &= - \int_{f_1} \operatorname{div}(X_{f_1}) \cdot \psi_e + \int_{\partial f_1} \langle X_{f_1}, \nu_1 \rangle \psi_e - \int_{f_2} \operatorname{div}(X_{f_2}) \cdot \psi_e + \int_{\partial f_2} \langle X_{f_2}, \nu_2 \rangle \psi_e \\ &= \int_{\partial f_1} \langle X_{f_1}, \nu_1 \rangle \psi_e + \int_{\partial f_2} \langle X_{f_2}, \nu_2 \rangle \psi_e \\ &= \pm \|e\| (\langle X_{f_1}, \nu_1 \rangle + \langle X_{f_2}, \nu_2 \rangle) = \pm \|e\| [X]_N(e), \end{aligned}$$

since the divergence of the smooth, constant vector fields X_{f_i} vanishes and $\int_{e'} \psi_e = 0$ for all other edges $e' \neq e$ of f_i , as ψ_e vanishes at the midpoints of each e' . Hence $\langle X, \nabla \psi_e \rangle_{L^2} = 0$ for all basis functions $\psi_e \in \mathcal{F}_0$ if and only if $[X]_N(e) = 0$ for all inner edges $e \in M_h^{(1)} \setminus \partial M_h^{(1)}$, i.e. if and only if X is normally continuous.

If in addition $\langle X, \nabla \psi_b \rangle_{L^2} = 0$ where $\psi_b \in \mathcal{F}$ is the basis function associated to the barycentre of an edge e contained in ∂M_h , let f denote the single adjacent triangle to e and ν its outer normal at e . Then again by Green's formula it is

$$\langle X, \nabla \psi_b \rangle_{L^2} = - \int_f \operatorname{div}(X) \cdot \psi_b + \int_{\partial f} \langle X, \nu \rangle \psi_b = \|e\| \langle X, \nu \rangle$$

and therefore $\langle X, \nabla \psi_b \rangle_{L^2} = 0$, if and only if the normal component of X along e vanishes.

If M_h is a simplicial solid, the very same proof shows that $\langle X, \nabla \psi_{b_f} \rangle_{L^2} = 0$ for a basis function associated to the barycentre b_f of a facet $f = t_1 \cap t_2$ if and only if $[X]_N(f) = 0$. We just need to check that $\int_{f'} \psi_{b_f} = 0$ for all other facets $f' \neq f$ of t_1 and t_2 . To this end, assume that $t_1 = [v_0, v_1, v_2, v_3]$ and $f = [v_0, v_1, v_2]$. Then since ψ_{b_f} vanishes at all barycentres of facets $f' \neq f$ of t_1 , it vanishes along the plane through these barycentres, which is parallel to f , and $\psi_{b_f}|_f \equiv 1$. Without loss of generality let $f' = [v_1, v_2, v_3]$, then its barycentre is given by $\lambda_1 = \lambda_2 = \lambda_3 = 1/3$. Therefore, over f' it is $\psi_{b_f}|_{f'} = 1 - 3\lambda_3$, and using the coordinate chart $\lambda := (\lambda_2, \lambda_3) : f' \rightarrow f_0 := [(0, 0), (1, 0), (0, 1)] \subset \mathbb{R}^2$ to the standard triangle in \mathbb{R}^2 , we find

$$\begin{aligned} \int_{f'} \psi_{b_f}|_{f'} &= \int_{f_0} \psi_{b_f}|_{f'} \circ \lambda^{-1} \cdot G \\ &= G \cdot \int_0^1 \int_0^{1-x} 1 - 3\lambda_3 \circ \lambda^{-1}(x, y) \, dy dx \\ &= G \cdot \int_0^1 \int_0^{1-x} 1 - 3y \, dy dx = 0, \end{aligned}$$

where G denotes the square root of the Gramian determinant of λ^{-1} , which is constant, as λ^{-1} is affine. The proof for the vanishing normal component along ∂M_h goes along the same lines as in the surface case. \square

Corollary 3.1.3. *Let M_h be a simplicial surface and $X \in \mathcal{X}_h$. Then X is tangentially continuous if and only if $\langle X, J\nabla \psi \rangle_{L^2} = 0$ for all $\psi \in \mathcal{F}_0$. If $\langle X, J\nabla \psi_b \rangle_{L^2} = 0$ for every basis function $\psi_b \in \mathcal{F}$ associated to the barycentre of an edge contained in the boundary ∂M_h , then X has a vanishing tangential component along ∂M_h .*

Proof. This follows immediately from Lemma 3.1.2 since X is tangentially continuous if and only if JX is normally continuous. \square

WHITNEY'S ELEMENTARY FORMS. In [Whi12, Ch. 4, §27], Whitney gives an explicit definition for a right-inverse to the de Rham map R (2.15) in terms of what is nowadays commonly referred to as *Whitney forms*. Each Whitney form is a linear combination of *elementary forms*, where each elementary k -form is associated to an oriented k -simplex $\sigma := [v_{i_0}, \dots, v_{i_k}]$ of a smooth triangulation of M and defined by

$$\omega_\sigma := k! \sum_{j=0}^k (-1)^j \lambda_{i_j} d\lambda_{i_0} \wedge \dots \wedge \widehat{d\lambda_{i_j}} \wedge \dots \wedge d\lambda_{i_k}$$

with the λ_{i_j} being generalized, smooth barycentric coordinates on M such that

$$\int_{\sigma'} \omega_\sigma = \begin{cases} 1 & \text{if } \sigma' = \sigma \\ 0 & \text{else} \end{cases}$$

for any k -simplex σ' , and $\widehat{d\lambda_{i_j}}$ means that the j -th entry in the wedge product is omitted. We write $\mathscr{W}^k(M)$ for the space of *Whitney k -forms*, spanned by all elementary k -forms. The *Whitney map* is then the interpolation map $W^k : C^k(M) \rightarrow \mathscr{W}^k(M) \subset \Omega^k(M)$ which maps the k -cochain which is 1 on σ and 0 on all other k -simplices to the differential k -form $\omega_\sigma \in \Omega^k(M)$, and extended linearly. Whitney has proved in [Whi12, Ch. 4, §27] that this interpolation map is a right-inverse to $R : \Omega^k(M) \rightarrow C^k(M)$ and that it commutes with the exterior derivative on the level of differential forms and simplicial cochains. Therefore the diagram

$$\begin{array}{ccc} \dots C^k(M) & \xrightarrow{d_\Delta} & C^{k+1}(M) \dots \\ \downarrow W^k & & \downarrow W^{k+1} \\ \dots \mathscr{W}^k(M) & \xrightarrow{d} & \mathscr{W}^{k+1}(M) \dots \end{array} \quad (3.4)$$

commutes for all k , and W^k descends to an isomorphism between simplicial cohomology and smooth de Rham cohomology [Whi12, Thm. 29A, Ch. 4, §29].

Whitney's interpolation construction carries over to simplicial manifolds triangulated by piecewise affine n -simplices and is well-established in the finite element community, though it has been reinvented a couple of times under different names, most prominently as *Raviart-Thomas elements* ([RT77]) or *Nédélec elements* ([Né80]), constituting vector proxy fields for (Hodge star transformed) Whitney 1-forms on triangular domains in \mathbb{R}^2 in the former case, and Whitney 1- and 2-forms on simplicial solids in \mathbb{R}^3 in the latter. In this case the function λ_i is the piecewise linear barycentric coordinate supported on every cell that contains the vertex v_i and extended by zero outside of the simplicial star of v_i as discussed above, and the very same definition of Whitney forms carries over to simplicial surfaces in \mathbb{R}^3 .

The resulting Whitney forms are not smooth any more, but they are still smooth when restricted to a single cell, and possess desired transition properties so that a discrete exterior derivative can be defined for them as the piecewise smooth exterior derivative. If M_h is embedded in \mathbb{R}^2 (i.e. a bounded polygonal domain in \mathbb{R}^2) or a simplicial solid in \mathbb{R}^3 , then $d\omega$ is the weak derivative in the Sobolev sense, see. [AFW06, Lemma 5.1]. Consequently they are well-suited for problems that require $H(\text{curl})$ - or $H(\text{div})$ -regularity, which frequently appear in numerical computations for Maxwell- or Navier-Stokes-type problems.

We will need the following two well-known characterizations of Whitney k -forms:

Lemma 3.1.4. *Let $\omega \in \mathscr{W}^k(M_h)$. Then the tangential trace over the intersection of two adjacent n -cells is well-defined.*

Proof. Let $\tau \subset \sigma_1 \cap \sigma_2$ be the $(n-1)$ -cell adjacent to σ_1 and σ_2 and let $\iota_i : \tau \hookrightarrow \sigma_i$ denote the inclusion. Since the generalized barycentric coordinates $\{\lambda_j\}$ over M_h are globally continuous, it follows from (2.9) that

$$\mathbf{t}(d(\lambda_j |_{\sigma_1})) = d(\mathbf{t}(\lambda_j |_{\sigma_1})) = d(\mathbf{t}(\lambda_j |_{\sigma_2})) = \mathbf{t}(d(\lambda_j |_{\sigma_2})),$$

so the tangential trace $\mathbf{t}(d\lambda_j)$ on τ is well-defined and does not depend on σ_1 or σ_2 . In particular, if v_j is not a vertex in τ , then $\lambda_j|_{\tau} \equiv 0$ and consequently $\mathbf{t}(d\lambda_j) = 0$. By (2.9) and linearity of the pullback, this also holds for every elementary form ω_{τ_k} and thereby for all $\omega \in \mathcal{W}^k(M_h)$. \square

Lemma 3.1.5. *Let $\omega \in \mathcal{W}^k(M_h)$. Then $d\omega = 0$ if and only if ω is constant on every cell.*

Proof. [AFW06, Thm. 4.1 and Thm. 3.4]. Note that the authors write $\mathcal{P}_1^- \Lambda^k$ for the space of Whitney k -forms $\mathcal{W}^k(M_h)$. \square

Due to the fact that Whitney forms have a well-defined tangential trace, they obey Green's formula when used as the component to which the exterior derivative is applied. More precisely, if $w \in \mathcal{W}^k(M)$ is a Whitney k -form with respect to continuous, piecewise smooth barycentric coordinates on M , then for any smooth $(k+1)$ -form $\eta \in \Omega^{k+1}(M)$ it is

$$\langle dw, \eta \rangle_{L^2} = \langle w, \delta \eta \rangle_{L^2} + \int_{\partial M} \mathbf{t}(w) \wedge \star \mathbf{n}(\eta) \quad (3.5)$$

VECTOR FIELD PROXIES FOR WHITNEY FORMS. We will be mostly interested in the case where $\dim M_h = 2$ or $\dim M_h = 3$ and $k = 1$ or $k = 2$. In this case, Whitney forms can be expressed in the classical notion of vector calculus as functions and (co-)vector fields on M_h . Again, we shall abbreviate $\mathcal{W}^k = \mathcal{W}^k(M_h)$ whenever the domain is clear from the context. By definition, $\mathcal{W}^0 = \mathcal{L}$. Moreover, \mathcal{W}^1 corresponds to the space

$$\mathcal{N} := \{\omega^\sharp : \omega \in \mathcal{W}^1\},$$

which is the classical space of *lowest order Nédélec edge elements* as defined in [Né80], spanned by all piecewise linear vector fields of the form $\lambda_i \nabla \lambda_j - \lambda_j \nabla \lambda_i$, where e_{ij} is an edge in M_h . See Figure 3.3 for an illustration.

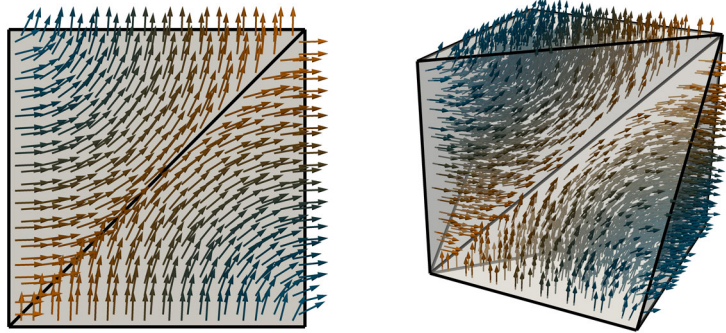


Figure 3.3: Nédélec basis function associated to the diagonal edge in two and three dimensions. The tangential component of the vector field along the diagonal integrates to one, but is zero along all other edges.

Furthermore, if $\dim M_h = 3$ we write $\mathcal{RT} := \{(\star \omega)^\sharp : \omega \in \mathcal{W}^2\}$ which is known as the space of *Raviart-Thomas elements*, defined in [RT77] and [Né80], and we denote by \mathcal{DG} the

space of *lowest order discontinuous Galerkin elements*, specified by a single constant value per cell. With these notions we obtain for simplicial surfaces the following correspondence

$$\begin{array}{ccccc}
 \mathcal{W}^0 & \xrightarrow{d} & \mathcal{W}^1 & \xrightarrow{d} & \mathcal{W}^2 \\
 \parallel & & \downarrow \# & & \downarrow * \\
 \mathcal{L} & \xrightarrow{\nabla} & \mathcal{N} & \xrightarrow{\text{curl}} & \mathcal{D}\mathcal{G}
 \end{array} \tag{3.6}$$

and for $\dim M_h = 3$, this diagram becomes

$$\begin{array}{ccccccc}
 \mathcal{W}^0 & \xrightarrow{d} & \mathcal{W}^1 & \xrightarrow{d} & \mathcal{W}^2 & \xrightarrow{d} & \mathcal{W}^3 \\
 \parallel & & \downarrow \# & & \downarrow \# \circ * & & \downarrow * \\
 \mathcal{L} & \xrightarrow{\nabla} & \mathcal{N} & \xrightarrow{\text{curl}} & \mathcal{R}\mathcal{T} & \xrightarrow{\text{div}} & \mathcal{D}\mathcal{G}
 \end{array} \tag{3.7}$$

To conclude this section, we list the dimensions of the function spaces involved in the decomposition results in the next sections. These results follow from straight-forward computations, making use of the combinatorial relations of the Euler characteristic (3.1) and (3.2) and the fact that the Whitney complexes (3.6) and (3.7) have cohomology spaces isomorphic to the simplicial cohomology spaces—a consequence of W^k being an isomorphism between the complex of Whitney forms and the complex of simplicial cochains.

$\dim M_h = 2$	Dimension	$\dim M_h = 3$	Dimension
$\nabla \mathcal{L}$	$n_V - 1$	$\nabla \mathcal{L}$	$n_V - 1$
$\nabla \mathcal{L}_0$	n_{iV}	$\nabla \mathcal{L}_0$	n_{iV}
$J\nabla \mathcal{F}$	$n_E - 1$	$J\nabla \mathcal{F}$	$n_F - 1$
$J\nabla \mathcal{F}_0$	$n_{iE} = 3n_F - n_E$	$J\nabla \mathcal{F}_0$	$n_{iF} = 4n_T - n_F$
		$\text{curl}(\mathcal{N})$	$n_E - n_V + 1 - h^1$
		$\text{curl}(\mathcal{N}_0)$	$n_{iE} - n_{iV} - h_r^1$

Table 3.1: Dimensions for certain subspaces of \mathcal{X}_h for simplicial surfaces (left) and simplicial solids (right) which appear in the decomposition results in Sections 3.2 and 3.3.

3.2 DECOMPOSITIONS ON SIMPLICIAL SURFACES

In this section we study discrete Hodge-type decompositions for simplicial surfaces with boundary. A discrete version of the Hodge-Morrey-Friedrichs decomposition is derived, using linear Lagrange elements as ansatz spaces for potentials and Crouzeix-Raviart elements for copotentials. The spaces $\mathcal{H}_{h,D}$ and $\mathcal{H}_{h,N}$ of discrete Dirichlet and Neumann fields have the same dimension as their smooth counterparts, equal to the dimension of the first cohomology space. Each of these two discrete spaces has subspaces reflecting non-trivial cohomology coming from boundary components and inner handles of the geometry, consistent with the smooth results obtained by Shonkwiler. Using these subspaces we answer the question whether $\mathcal{H}_{h,D}$ and $\mathcal{H}_{h,N}$ can simultaneously appear in a single decomposition and obtain such a decomposition for surfaces of type $\Sigma_{0,m}$. Finally we discuss how the choice of ansatz spaces affects the resulting decompositions and discretizations of harmonic fields.

In the following let M_h be a simplicial surface with non-empty boundary. Recall from Corollary 3.1.3 that $X \in (J\nabla\mathcal{F}_0)^\perp$ if and only if X is tangentially continuous across inner edges and moreover $X \in (J\nabla\mathcal{F})^\perp$ if and only if X is tangentially continuous across inner edges and has vanishing tangential component along the boundary. The following lemma relates these tangentially continuous subspaces of \mathcal{X}_h to closed Whitney 1-forms.

Lemma 3.2.1. *A PCVF X is in the space $J\nabla\mathcal{F}_0^\perp$ if and only if it represents a closed Whitney 1-form, and X is in the space $J\nabla\mathcal{F}^\perp$ if and only if it represents a closed Whitney 1-form with vanishing tangential component.*

Proof. Let $\omega \in \mathcal{W}^1$ be closed, i.e. $d\omega = 0$, then ω is constant over each cell by Lemma 3.1.5. Moreover, since each Whitney form is tangentially continuous, the representing proxy field $X := \omega^\sharp$ is tangentially continuous by (2.12), so $X \in J\nabla\mathcal{F}_0^\perp$ by Corollary 3.1.3.

Conversely, let $X \in J\nabla\mathcal{F}_0^\perp$. Pick an arbitrary, but fixed orientation for each edge $e \in M_h^{(1)}$, define $a_e := \int_e X^\flat$ and set $\omega := \sum_e a_e \omega_e \in \mathcal{W}^1$. Since X is tangentially continuous, a_e is well-defined. Then for every triangle $f \in M_h^{(2)}$ it is by Stokes' theorem

$$\int_f d\omega = \int_{\partial f} \omega = \sum_{e \in \partial f} a_e \int_e \omega_e = \sum_{e \in \partial f} a_e \epsilon_e$$

where each e now has the boundary orientation inherited from the triangle f . Therefore we have to multiply with $\epsilon_e = 1$ if this orientation agrees with the one we have fixed, and $\epsilon_e = -1$ otherwise. Let τ_e denote the oriented unit tangent of the triangle edge e , i.e. $\tau_e = e/\|e\|$. Then by writing this last sum in terms of line integrals of the vector field X along the edges e we conclude

$$\sum_{e \in \partial f} a_e \epsilon_e = \sum_{e \in \partial f} \int_e \langle X, \tau_e \rangle dS = \sum_{e \in \partial f} \|e\| \langle X, \tau_e \rangle = \langle X, \sum_{e \in \partial f} e \rangle = 0$$

since for any triangle the oriented boundary edges sum up to zero. Hence the assignment $R(d\omega) : f \mapsto \int_f d\omega$ is the zero element in $C^2(M_h)$, and since $R : \mathcal{W}^2 \xrightarrow{\sim} C^2(M_h)$ is an isomorphism, it follows $d\omega = 0$, i.e. ω is closed.

The addendum follows from the fact that for all boundary edges $e \in \partial M_h^{(1)}$ it is $a_e = 0$ if and only if $\mathbf{t}(X^\flat) = 0$ if and only if $\vec{\mathbf{t}}(X) = 0$. \square

Remark 3.2.2. *The construction in Lemma 3.2.1 provides isomorphisms $R : J\nabla\mathcal{F}_0^\perp \xrightarrow{\sim} Z^1(M_h)$ and $R_0 : J\nabla\mathcal{F}^\perp \xrightarrow{\sim} Z^1(M_h, \partial M_h)$ which are given by the assignment*

$$X \mapsto \left(c_X : e \mapsto \int_e \langle X, \tau_e \rangle = \langle X, e \rangle \right) \in Z^1(M_h) \quad (Z^1(M_h, \partial M_h)).$$

for any $X \in J\nabla\mathcal{F}_0^\perp$ ($X \in J\nabla\mathcal{F}^\perp$). We will come back to these maps below.

Lemma 3.2.3. *The following pairs of subspaces are L^2 -orthogonal:*

$$\begin{aligned} \nabla\mathcal{L} &\perp J\nabla\mathcal{F}_0 \\ \nabla\mathcal{L}_0 &\perp J\nabla\mathcal{F} \end{aligned}$$

Proof. With respect to the commutative diagram (3.6) this is a consequence of Lemma 3.2.1: since every exact form is closed, it follows for any $\varphi \in \mathcal{L}$ that $(\nabla\varphi)^\flat \in \ker(d_{\mathcal{W}}^1)$, where $d_{\mathcal{W}}^1 := d^1|_{\mathcal{W}^1}$, so indeed $\nabla\varphi \in J\nabla\mathcal{F}_0^\perp$.

If in addition $\varphi \in \mathcal{L}_0$, then φ vanishes along ∂M_h . Thus by (2.12), $d\varphi$ has vanishing tangential component, which in turn means that $\nabla\varphi$ has vanishing tangential component along ∂M_h , so $\nabla\varphi \in J\nabla\mathcal{F}^\perp$. □

Corollary 3.2.4. *If M_h is closed, then the spaces $\nabla\mathcal{F}$ and $J\nabla\mathcal{L}$ are L^2 -orthogonal.*

Proof. If $\partial M_h = \emptyset$, then $\mathcal{L}_0 = \mathcal{L}$ and $\mathcal{F}_0 = \mathcal{F}$, and the result follows from Lemma 3.2.3. □

In general, the direct sum of any two orthogonal spaces in Lemma 3.2.3 span a subspace \mathcal{V} that is strictly contained in the space \mathcal{X}_h . However, the complement \mathcal{V}^\perp will always be of a dimension independent of the triangulation and can therefore be seen as a topological invariant—it is nothing else but a concrete realization for the first cohomology group of M_h , either in its absolute or relative version. In analogy with the smooth situation we define:

Definition 3.2.5 (Discrete Harmonic, Neumann, Dirichlet (2d)). *The L^2 -orthogonal complements of the orthogonal sums $\nabla\mathcal{L}_0 \oplus J\nabla\mathcal{F}_0$, $\nabla\mathcal{L} \oplus J\nabla\mathcal{F}_0$ and $\nabla\mathcal{L}_0 \oplus J\nabla\mathcal{F}$ within \mathcal{X}_h are the spaces of discrete harmonic fields, discrete Neumann fields and discrete Dirichlet fields, and denoted by \mathcal{H}_h , $\mathcal{H}_{h,N}$ and $\mathcal{H}_{h,D}$, respectively.*

Since discrete Dirichlet fields are orthogonal to $J\nabla\mathcal{F}$, it follows that their tangential projection onto each boundary edge vanishes. In contrast, a discrete Neumann field has only weakly vanishing normal projection onto each boundary edge in the sense that it is orthogonal to gradients of linear Lagrange functions associated to boundary vertices. Since this is a condition over the star of each boundary vertex, it does in general not enforce the normal component to be strictly zero, see Figure 3.4 for an illustration.

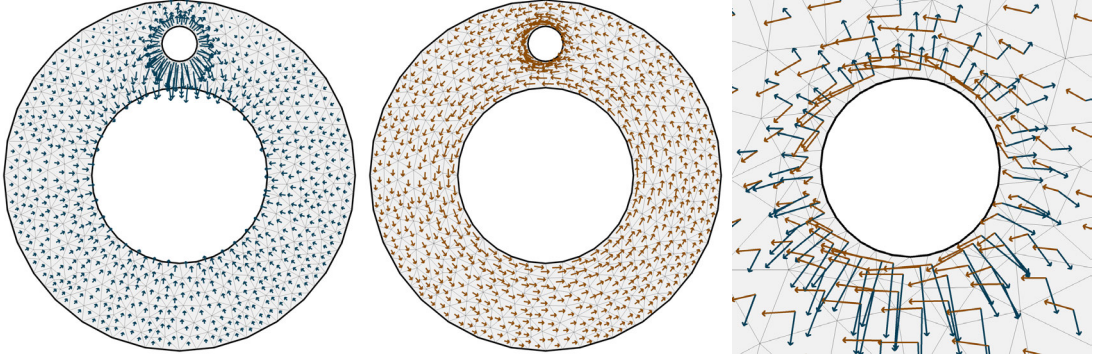


Figure 3.4: A discrete Dirichlet field (left) and Neumann field (middle) on a flat geometry of type $\Sigma_{0,2}$, each being one out of two basis fields for $\mathcal{H}_{h,D}$ and $\mathcal{H}_{h,N}$. The right image shows a close-up of both fields in a vicinity of the small boundary hole. The Dirichlet field (blue) is perpendicular to each boundary edge, whereas the Neumann field is only almost tangential. Both fields are L^2 -orthogonal to each other (see Lemma 3.2.17 later on), since all Dirichlet fields are exact on this geometry (and correspondingly, all Neumann fields are coexact).

Lemma 3.2.6 (Fundamental Decomposition (2d)). *The space \mathcal{X}_h admits the following L^2 -orthogonal decompositions*

$$\mathcal{X}_h = \nabla \mathcal{L} \oplus J \nabla \mathcal{F}_0 \oplus \mathcal{H}_{h,N} \quad (3.8)$$

$$= \nabla \mathcal{L}_0 \oplus J \nabla \mathcal{F} \oplus \mathcal{H}_{h,D} \quad (3.9)$$

and it is $\dim \mathcal{H}_{h,N} = \dim \mathcal{H}_{h,D} = h^1$.

Proof. The orthogonality for each decomposition follows from Lemma 3.2.3 and the definition of the spaces of discrete Neumann and Dirichlet fields. For the dimensions, one can perform a direct computation using the identity for the Euler characteristic (3.1). However, the following argument is more insightful since it directly identifies the spaces $\mathcal{H}_{h,N}$ and $\mathcal{H}_{h,D}$ as representatives for the absolute and relative first cohomology. Since $J \nabla \mathcal{F}_0^\perp \cong \{\omega^\sharp : \omega \in \ker(d_{\mathcal{W}}^1) \subset \mathcal{W}^1\}$ and $\nabla \mathcal{L} \subseteq J \nabla \mathcal{F}_0^\perp$ by Lemma 3.2.1 and Lemma 3.2.3, it follows that

$$\mathcal{H}_{h,N} \cong J \nabla \mathcal{F}_0^\perp / \nabla \mathcal{L} \cong \ker(d_{\mathcal{W}}^1) / \text{im}(d_{\mathcal{W}}^0) \cong Z^1(M_h) / B^1(M_h) = H^1(M_h).$$

Similarly, for the relative version it is

$$\mathcal{H}_{h,D} \cong J \nabla \mathcal{F}^\perp / \nabla \mathcal{L}_0 \cong \ker(d_{\mathcal{W}_0}^1) / \text{im}(d_{\mathcal{W}_0}^0) \cong Z^1(M_h, \partial M_h) / B^1(M_h, \partial M_h) = H^1(M_h, \partial M_h)$$

and by Lefschetz-Poincaré duality it is $H^1(M_h) \cong H^1(M_h, \partial M_h)$. \square

Remark 3.2.7. Lemma 3.2.6 shows that the isomorphisms in Remark 3.2.2 yield isomorphisms

$$\bar{R}_N : \mathcal{H}_{h,N} \xrightarrow{\cong} H^1(M_h)$$

$$\bar{R}_D : \mathcal{H}_{h,D} \xrightarrow{\cong} H^1(M_h, \partial M_h)$$

which can be thought of as discrete analogues of the de Rham isomorphism: \bar{R}_N maps an element $X \in \mathcal{H}_{h,N}$ to the equivalence class of the cocycle $R(X)$. Its inverse maps a cohomology class $[w]$ to the element $X := R^{-1}(w)$, decomposes X according to (3.8) as $X = \nabla\varphi + X_N$ with $\nabla\varphi \in \nabla\mathcal{L}$ and $X_N \in \mathcal{H}_{h,N}$, and drops the gradient part $\nabla\varphi$. Note that it does not depend on the representative w of $[w]$, and is therefore well-defined. A similar description applies to \bar{R}_D , using (3.9).

There is a third decomposition involving the space of all discrete harmonic fields by posing boundary conditions on both the potential as well as the copotential space:

$$\mathcal{X}_h = \nabla\mathcal{L}_0 \oplus J\nabla\mathcal{F}_0 \oplus \mathcal{H}_h \quad (3.10)$$

However, as in the smooth situation, \mathcal{H}_h has no topological significance any more in the presence of a boundary and moreover depends on the mesh: a simple calculation shows that

$$\dim \mathcal{H}_h = 2n_F - n_{iV} - n_{iE} = h^1(M) + n_{bE} - 1 \rightarrow \infty$$

under refinement of the boundary.

Remark 3.2.8. For the case that M_h is a closed surface (i.e. $\partial M = \emptyset$) the fundamental decompositions both become

$$\mathcal{X}_h(M_h) = \nabla\mathcal{L} \oplus J\nabla\mathcal{F} \oplus \mathcal{H}_h$$

with $\mathcal{H}_h \cong H^1(M_h)$ and thus $\dim \mathcal{H}_h = 2g$, where g is the genus of M_h . This special case is the situation considered in [War06].

The fundamental decompositions yield a discrete version of the Hodge-Morrey-Friedrichs decomposition in Theorem 2.3.4:

Theorem 3.2.9 (Discrete Hodge-Morrey-Friedrichs Decomposition (2d)). *The space \mathcal{X}_h admits the following L^2 -orthogonal decompositions:*

$$\mathcal{X}_h = \nabla\mathcal{L}_0 \oplus J\nabla\mathcal{F}_0 \oplus \mathcal{H}_h \cap \nabla\mathcal{L} \oplus \mathcal{H}_{h,N} \quad (3.11)$$

$$= \nabla\mathcal{L}_0 \oplus J\nabla\mathcal{F}_0 \oplus \mathcal{H}_h \cap J\nabla\mathcal{F} \oplus \mathcal{H}_{h,D}. \quad (3.12)$$

Proof. This is an immediate consequence of Lemma 3.2.6. □

INNER AND BOUNDARY COHOMOLOGY REPRESENTATIVES. These two discrete Hodge-Morrey-Friedrichs decompositions raise the question whether there is a single L^2 -orthogonal decomposition involving both the spaces of discrete Dirichlet and Neumann fields at the same time. A priori, the best one can get from Theorem 3.2.9 is a decomposition

$$\mathcal{X}_h = \nabla\mathcal{L}_0 \oplus J\nabla\mathcal{F}_0 \oplus \nabla\mathcal{L} \cap J\nabla\mathcal{F} \oplus (\mathcal{H}_{h,N} + \mathcal{H}_{h,D}), \quad (3.13)$$

but the latter sum is in general neither orthogonal, nor is it necessarily direct, as the obstructions in Section 3.4 will show.

Therefore we consider a further orthogonal decomposition into subspaces of the spaces $\mathcal{H}_{h,N}$ and $\mathcal{H}_{h,D}$ that correspond to cohomology classes coming from the inner topology and those coming from the boundary. The following definition is in accordance with Definition 2.4.2.

Definition 3.2.10. *The spaces of discrete coexact Neumann fields, boundary-exact Neumann fields, exact Dirichlet fields and boundary-coexact Dirichlet fields are defined as*

$$\begin{aligned}\mathcal{H}_{h,N,\text{co}} &:= \mathcal{H}_{h,N} \cap J\nabla\mathcal{F} \\ \mathcal{H}_{h,N,\partial\text{ex}} &:= (\mathcal{H}_{h,N,\text{co}})^\perp_{\mathcal{H}_{h,N}} \\ \mathcal{H}_{h,D,\text{ex}} &:= \mathcal{H}_{h,D} \cap \nabla\mathcal{L} \\ \mathcal{H}_{h,D,\partial\text{co}} &:= (\mathcal{H}_{h,D,\text{ex}})^\perp_{\mathcal{H}_{h,D}},\end{aligned}$$

where the orthogonal complement is taken inside $\mathcal{H}_{h,N}$ and $\mathcal{H}_{h,D}$, respectively.

Corollary 3.2.11. *It is $\mathcal{H}_{h,N,\text{co}} \perp \mathcal{H}_{h,D}$ and $\mathcal{H}_{h,D,\text{ex}} \perp \mathcal{H}_{h,N}$.*

Proof. This follows from Lemma 3.2.6. □

To establish a connection between the spaces defined in Definition 3.2.10 and the cohomological complexity introduced by boundary components and inner handles, we consider the projection map

$$\text{pr}_N : \mathcal{H}_{h,D} \rightarrow \mathcal{H}_{h,N}, \quad X_D \mapsto X_N$$

which takes an element $X_D \in \mathcal{H}_{h,D}$, decomposes it according to the fundamental decomposition in (3.8) as

$$X_D = \nabla\varphi + X_N$$

with $X_N \in \mathcal{H}_{h,N}$, and then drops the exact component $\nabla\varphi$.

Lemma 3.2.12. *It is $\ker(\text{pr}_N) = \mathcal{H}_{h,D,\text{ex}}$. Furthermore, if M_h is homeomorphic to $\Sigma_{g,m}$, then $\dim \mathcal{H}_{h,D,\text{ex}} = m - 1$.*

Proof. The definition of pr_N makes the diagram

$$\begin{array}{ccc} \mathcal{H}_{h,D} & \xrightarrow{\text{pr}_N} & \mathcal{H}_{h,N} \\ \downarrow \bar{R}_D & & \downarrow \bar{R}_N \\ H^1(M_h, \partial M_h) & \xrightarrow{\pi^*} & H^1(M_h) \end{array}$$

commutative, with the vertical arrows being the discrete de Rham isomorphisms from Remark 3.2.7. Indeed, if $\bar{R}_D(X_D) = [w] = w + B^1(M_h, \partial M_h) \in H^1(M_h, \partial M_h)$ is the relative cohomology class represented by $X_D \in \mathcal{H}_{h,D}$, then $\pi^*([w]) = w + B^1(M_h)$, as π^* is induced by the inclusion $C^1(M_h, \partial M_h) \hookrightarrow C^1(M_h)$ and is therefore an inclusion $Z^1(M_h, \partial M_h) \hookrightarrow Z^1(M_h)$ on the level of cocycles. But by Remark 3.2.7, the inverse of \bar{R}_N decomposes $R^{-1}(w)$ according to (3.8) and drops the exact component, and this is precisely how pr_N is defined.

Therefore, $\pi^*(\bar{R}_D(X_D)) = \bar{R}_N(\text{pr}_N(X_D)) = 0 \in H^1(M_h)$ if and only if $\text{pr}_N(X_D) \in \nabla\mathcal{L}$ is exact, which happens if and only if $X_D \in \mathcal{H}_{h,D,\text{ex}}$. In particular, it is $\dim \ker(\text{pr}_N) = \dim \ker(\pi^*)$ and from (2.4) it follows $\dim \ker(\pi^*) = m - 1$. □

Lemma 3.2.12 identifies the space $\mathcal{H}_{h,D,\text{ex}}$ as the space of representatives for the kernel of π^* in the cohomology sequence, that is, as the representatives for non-trivial relative cohomology classes that become exact when one includes the boundary for possible potential

functions. Since $\ker(\pi^*)$ is the image of the map $\delta^* : H^0(\partial M) \rightarrow H^1(M_h, \partial M_h)$ in the cohomology sequence (2.2), it is plausible to think of them as representing non-trivial *cohomology information coming from the boundary*, as coined in [Sho09], which is in accordance to the dimension $m-1$. The complementary space $\mathcal{H}_{h,D,\partial\text{co}}$ should therefore correspond to the *inner cohomology*, which is supported by the fact that its dimension is $2g$.

Lemma 3.2.13. pr_N restricts to an isomorphism $\text{pr}_N : \mathcal{H}_{h,D,\partial\text{co}} \xrightarrow{\sim} \mathcal{H}_{h,N,\partial\text{ex}}$. In particular, if M_h is of type $\Sigma_{g,m}$ it is

$$\begin{aligned} \dim \mathcal{H}_{h,D,\text{ex}} &= \dim \mathcal{H}_{h,N,\text{co}} = m-1 \\ \dim \mathcal{H}_{h,D,\partial\text{co}} &= \dim \mathcal{H}_{h,N,\partial\text{ex}} = 2g. \end{aligned}$$

Proof. We first check that pr_N indeed maps discrete boundary-coexact Dirichlet fields to boundary-exact Neumann fields. Since $\ker(\text{pr}_N) = \mathcal{H}_{h,D,\text{ex}}$, it follows that pr_N is injective on $\mathcal{H}_{h,D,\partial\text{co}}$. For a field $X_D \in \mathcal{H}_{h,D,\partial\text{co}}$ let $X_D = J\nabla\psi + Z + \nabla\varphi$ be its orthogonal decomposition in $\mathcal{H}_{h,N,\text{co}} \oplus \mathcal{H}_{h,N,\partial\text{ex}} \oplus \mathcal{H}_h \cap \nabla\mathcal{L}$. Then

$$0 = \langle X_D, J\nabla\psi \rangle_{L^2} = \langle J\nabla\psi, J\nabla\psi \rangle_{L^2} + \langle Z, J\nabla\psi \rangle_{L^2} + \langle \nabla\varphi, J\nabla\psi \rangle_{L^2}$$

where the last two summands vanish due to the orthogonality of the decomposition. It follows $J\nabla\psi = 0$, so indeed $\text{pr}_N(X_D) = Z \in \mathcal{H}_{h,N,\partial\text{ex}}$.

We now show that $\dim \mathcal{H}_{h,D,\text{ex}} = \dim \mathcal{H}_{h,N,\text{co}}$ which implies that the orthogonal complements are also of the same dimension. Then since pr_N is an injective map between spaces of the same dimension it must be an isomorphism. To this end, note that for $A := \mathcal{H}_h \cap J\nabla\mathcal{F}$ and $B := \mathcal{H}_h \cap \nabla\mathcal{L}$ we have $\mathcal{H}_{h,D,\text{ex}} = B \cap A^{\perp_{\mathcal{H}_h}}$ and $\mathcal{H}_{h,N,\text{co}} = A \cap B^{\perp_{\mathcal{H}_h}}$, where again $\perp_{\mathcal{H}_h}$ denotes the orthogonal complement inside \mathcal{H}_h . Then

$$\begin{aligned} \dim A \cap B^{\perp_{\mathcal{H}_h}} &= \dim \mathcal{H}_h - \dim (A \cap B^{\perp_{\mathcal{H}_h}})^{\perp_{\mathcal{H}_h}} \\ &= \dim \mathcal{H}_h - \dim (A^{\perp_{\mathcal{H}_h}} + B) \\ &= \dim \mathcal{H}_h - (\dim A^{\perp_{\mathcal{H}_h}} + \dim B - \dim (B \cap A^{\perp_{\mathcal{H}_h}})) \\ &= \dim \mathcal{H}_h - (\dim B^{\perp_{\mathcal{H}_h}} + \dim B) + \dim (B \cap A^{\perp_{\mathcal{H}_h}}) \\ &= \dim (B \cap A^{\perp_{\mathcal{H}_h}}), \end{aligned}$$

because $\dim A^{\perp_{\mathcal{H}_h}} = \dim \mathcal{H}_{h,D} = \dim \mathcal{H}_{h,N} = \dim B^{\perp_{\mathcal{H}_h}}$ by Lemma 3.2.6. \square

Considering again the cohomology sequence

$$\dots \rightarrow H^0(\partial M_h) \xrightarrow{\delta^*} H^1(M_h, \partial M_h) \xrightarrow{\pi^*} H^1(M_h) \xrightarrow{\iota^*} H^1(\partial M_h) \rightarrow \dots$$

we conclude:

Corollary 3.2.14. *The cohomology classes in $\ker(\iota^*)$ are represented by $\mathcal{H}_{h,N,\partial\text{ex}}$.*

Proof. By exactness of the sequence, $\ker(\iota^*) = \text{im}(\pi^*)$, and by Lemma 3.2.13, $\text{im}(\pi^*)$ is represented by $\mathcal{H}_{h,N,\partial\text{ex}}$. \square

In the case of smooth differential forms, we have first defined the space $\mathcal{H}_{N,\partial\text{ex}}^k$ explicitly as

$$\mathcal{H}_{N,\partial\text{ex}}^k = \{\omega \in \mathcal{H}_N^k : \iota^* \omega \in d\Omega^{k-1}(\partial M)\}$$

and only then proved in Theorem 2.4.3 that it is actually orthogonal to the space $\mathcal{H}_{N,\text{co}}^k$ of coexact Neumann fields. In contrast, in the discrete setting we have explicitly defined the space $\mathcal{H}_{h,N,\text{co}}$ as the intersection of discrete Neumann fields with the cogradient space $J\nabla\mathcal{F}$, and then defined $\mathcal{H}_{h,N,\partial\text{ex}}$ as its orthogonal complement within $\mathcal{H}_{h,N}$. Of course, this establishes the orthogonality of these two spaces by definition. We will now deduce that $\mathcal{H}_{h,N,\partial\text{ex}}$ can also be defined in analogy to its smooth counterpart. To this end, we define for a PCVF $X \in \mathcal{X}_h$ its *restriction to the boundary* as the piecewise constant, one-dimensional vector field on the one-dimensional boundary polygons ∂M_h to be

$$(X|_{\partial M_h})_e := \langle X_{f_e}, e \rangle = R(X)(e)$$

for each boundary edge $e \in \partial M_h$ with its adjacent face f_e .

Lemma 3.2.15. *Let $X \in \mathcal{H}_{h,N,\partial\text{ex}}$ be a discrete boundary-exact Neumann field. Then there is a function $\varphi \in \mathcal{L}(\partial M_h)$ such that $X|_{\partial M_h} = \nabla\varphi$ and therefore*

$$\mathcal{H}_{h,N,\partial\text{ex}} = \mathcal{H}_{h,N,\text{co}}^{\perp_{\mathcal{H}_{h,N}}} = \{X \in \mathcal{H}_{h,N} : X|_{\partial M_h} \in \nabla\mathcal{L}(\partial M_h)\}.$$

Proof. By Corollary 3.2.14, the space $\mathcal{H}_{h,N,\partial\text{ex}}$ represents cohomology classes in $\ker(\iota^*) \subset H^1(M_h)$. But since $\iota^\sharp : C^1(M_h) \rightarrow C^1(\partial M_h)$ is the restriction to ∂M_h , it follows $\iota^*(\bar{R}_N(X)) = 0$ in $H^1(\partial M_h)$ if and only if $X|_{\partial M_h} = \iota^\sharp(R(X))$ is in $B^1(\partial M_h)$, i.e. exact on ∂M_h . \square

Combining these results with the discrete Hodge-Morrey-Friedrichs decompositions in Theorem 3.2.9, we obtain:

Theorem 3.2.16. *The discrete Hodge-Morrey-Friedrichs decompositions have the following refinements into boundary and inner cohomology-representing subspaces:*

$$\mathcal{X}_h = \nabla\mathcal{L}_0 \oplus J\nabla\mathcal{F}_0 \oplus \mathcal{H}_h \cap \nabla\mathcal{L} \oplus \mathcal{H}_{h,N,\text{co}} \oplus \mathcal{H}_{h,N,\partial\text{ex}} \quad (3.14)$$

$$= \nabla\mathcal{L}_0 \oplus J\nabla\mathcal{F}_0 \oplus \mathcal{H}_h \cap J\nabla\mathcal{F} \oplus \mathcal{H}_{h,D,\text{ex}} \oplus \mathcal{H}_{h,D,\partial\text{co}} \quad (3.15)$$

As mentioned before, in general there is no hope for L^2 -orthogonality between $\mathcal{H}_{h,N}$ and $\mathcal{H}_{h,D}$ due to the presence of the spaces $\mathcal{H}_{h,N,\partial\text{ex}}$ and $\mathcal{H}_{h,D,\partial\text{co}}$. Roughly speaking, these fields concentrate on non-trivial paths that generate the homology for handle regions and the influence of the boundary constraints can be marginal in such a case, depending on the geometry. We will provide a few examples in Section 5.1. With regard to Corollary 3.2.11, the situation can be summarized as shown in Figure 3.5.

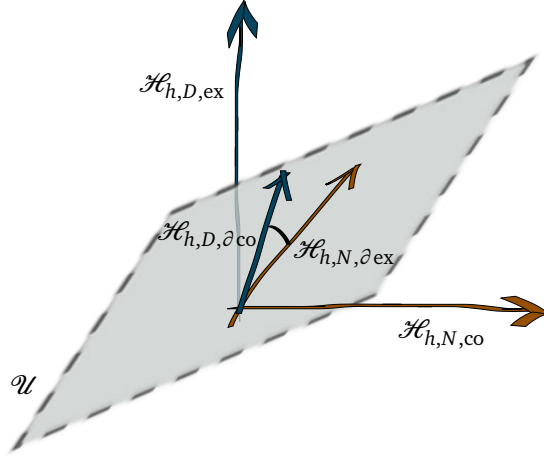


Figure 3.5: Schematic, low-dimensional alignment of the spaces $\mathcal{H}_{h,D}$ and $\mathcal{H}_{h,N}$. Both subspaces $\mathcal{H}_{h,N,\partial\text{ex}}$ and $\mathcal{H}_{h,D,\partial\text{co}}$ lie in a common subspace \mathcal{U} (dashed plane) that is orthogonal to both $\mathcal{H}_{h,D,\text{ex}}$ and $\mathcal{H}_{h,N,\text{co}}$. However, $\mathcal{H}_{h,N,\partial\text{ex}}$ and $\mathcal{H}_{h,D,\partial\text{co}}$ are not orthogonal to each other in \mathcal{U} , destroying the orthogonality of $\mathcal{H}_{h,D}$ and $\mathcal{H}_{h,N}$.

SURFACES COMING FROM A SPHERE. We now consider surfaces “coming from a sphere”, i.e. surfaces of type $\Sigma_{0,m}$. This includes all connected open, bounded domains in \mathbb{R}^2 with various holes cut out, for instance. Here the situation is much simpler.

Lemma 3.2.17. *Let M_h be of type $\Sigma_{0,m}$. Then it is $\mathcal{H}_{h,D} = \mathcal{H}_{h,D,\text{ex}}$ and $\mathcal{H}_{h,N} = \mathcal{H}_{h,N,\text{co}}$. In particular $\mathcal{H}_{h,D} \perp \mathcal{H}_{h,N}$.*

Proof. If $g = 0$, then by Lemma 3.2.13 it is $\dim \mathcal{H}_{h,D,\partial\text{co}} = \dim \mathcal{H}_{h,N,\partial\text{ex}} = 0$. The orthogonality $\mathcal{H}_{h,D} \perp \mathcal{H}_{h,N}$ now follows from Corollary 3.2.11. \square

Speaking geometrically, this says that in the case where M_h is of type $\Sigma_{0,m}$ every discrete harmonic vector field with vanishing tangential projection along the boundary is integrable, and a similar result holds for discrete Neumann fields. A remarkable consequence for surfaces of type $\Sigma_{0,m}$ is that always $\mathcal{H}_{h,D} \cap \mathcal{H}_{h,N} = \{0\}$, which can be considered a discrete version of Theorem 2.4.1. With respect to Lemma 3.2.6 this can be equivalently expressed by

$$\mathcal{X}_h = \nabla \mathcal{L} + J \nabla \mathcal{F}$$

and therefore, every PCVF is the (not unique) sum of a gradient field and a cogradient field. The same question for general surfaces turns out to be much harder and will be discussed in Section 3.4.

Coming back to the original question whether there is a single decomposition involving both the spaces at the same time, we have the following positive result for surfaces homeomorphic to $\Sigma_{0,m}$.

Theorem 3.2.18 (Complete Decomposition for Surfaces of Type $\Sigma_{0,m}$). *Let M_h be of type $\Sigma_{0,m}$. Then the space \mathcal{X}_h admits the following complete L^2 -orthogonal decomposition:*

$$\mathcal{X}_h = \nabla \mathcal{L}_0 \oplus J \nabla \mathcal{F}_0 \oplus \nabla \mathcal{L} \cap J \nabla \mathcal{F} \oplus \mathcal{H}_{h,D} \oplus \mathcal{H}_{h,N}.$$

Proof. By Lemma 3.2.17, it is $\mathcal{H}_{h,D} \perp \mathcal{H}_{h,N}$ and from the fundamental decompositions in Lemma 3.2.6 it follows

$$(\mathcal{H}_{h,D} \oplus \mathcal{H}_{h,N})^{\perp_{\mathcal{H}_h}} = \mathcal{H}_{h,D}^{\perp} \cap \mathcal{H}_{h,N}^{\perp} \cap \mathcal{H}_h = (\nabla \mathcal{L} \cap J \nabla \mathcal{F}) \cap \mathcal{H}_h = \nabla \mathcal{L} \cap J \nabla \mathcal{F}.$$

□

SWAPPING THE ANSATZ SPACES. Exchanging the roles of the ansatz spaces for potential functions and copotential functions amounts to applying the rotation operator J to each of the spaces in the decomposition. For instance, the analogues of the discrete Hodge-Morrey-Friedrichs decompositions Theorem 3.2.9 become

$$\begin{aligned} \mathcal{X}_h &= J \mathcal{X}_h = \nabla \mathcal{F}_0 \oplus J \nabla \mathcal{L}_0 \oplus J \mathcal{H}_h \cap J \nabla \mathcal{L} \oplus J \mathcal{H}_{h,N} \\ &= \nabla \mathcal{F}_0 \oplus J \nabla \mathcal{L}_0 \oplus J \mathcal{H}_h \cap \nabla \mathcal{F} \oplus J \mathcal{H}_{h,D}. \end{aligned}$$

For these decompositions, the space of Crouzeix-Raviart elements \mathcal{F} now plays the part of the space of potential functions whereas the Lagrange elements are used as copotential functions. Setting

$$\begin{aligned} \mathcal{H}_{h,N}^{\dagger} &:= J \mathcal{H}_{h,D} \\ \mathcal{H}_{h,D}^{\dagger} &:= J \mathcal{H}_{h,N}, \end{aligned}$$

it is now the discrete Neumann fields in $\mathcal{H}_{h,N}^{\dagger}$ which have strictly vanishing normal component at each boundary edge, whereas discrete Dirichlet fields have only weakly vanishing tangential component. Therefore, for the rest of this section we will call the spaces $\mathcal{H}_{h,D}$ and $\mathcal{H}_{h,N}^{\dagger}$ *strong Dirichlet* and *strong Neumann* fields, and the spaces $\mathcal{H}_{h,D}^{\dagger}$ and $\mathcal{H}_{h,N}$ *weak Dirichlet* and *weak Neumann* fields, respectively.

Mixing discrete Dirichlet and Neumann spaces from both discretizations, one immediately obtains a discrete version of Theorem 2.4.1:

Lemma 3.2.19. *It is $\mathcal{H}_{h,D} \cap \mathcal{H}_{h,N}^{\dagger} = \{0\}$.*

Proof. Let $X \in \mathcal{H}_{h,D} \cap \mathcal{H}_{h,N}^{\dagger}$, then $X \in \nabla \mathcal{F}^{\perp} \cap J \nabla \mathcal{F}^{\perp}$. Thus X has vanishing tangential and normal component at each boundary edge, hence it vanishes on triangles adjacent to the boundary, and since X is normally and tangentially continuous across all edges, it follows $X \equiv 0$ everywhere. □

In particular, Lemma 3.2.19 implies that always

$$\mathcal{X}_h = \nabla \mathcal{F} + J \nabla \mathcal{F}.$$

Of course, this sum is never direct. More precisely, the dimension of the intersection space computes as

$$\dim \nabla \mathcal{F} \cap J \nabla \mathcal{F} = 2(n_E - 1) - 2n_F = -2\chi - 2 + 2n_V = 2(h^1 + n_V - 2) > 0,$$

which is always positive and much larger than the dimension of the corresponding space in (3.17). We obtain a second discrete version of the five-term decomposition (2.16).

Theorem 3.2.20. *The space \mathcal{X}_h admits the following five-term decomposition*

$$\mathcal{X}_h = \nabla \mathcal{L}_0 \oplus J\nabla \mathcal{L}_0 \oplus \nabla \mathcal{F} \cap J\nabla \mathcal{F} \oplus (\mathcal{H}_{h,D} + \mathcal{H}_{h,N}^\dagger),$$

where the spaces of strong Dirichlet and Neumann fields form a direct sum.

Proof. By Lemma 3.2.19, the sum $\mathcal{H}_{h,D} + \mathcal{H}_{h,N}^\dagger$ is direct and by the fundamental decompositions Lemma 3.2.6 each of the two summands is orthogonal to $\nabla \mathcal{L}_0$, $J\nabla \mathcal{L}_0$ and either $\nabla \mathcal{F}$ or $J\nabla \mathcal{F}$. \square

Finally, with respect to the heavy use of linear Lagrange elements, we should mention that the spaces of discrete Dirichlet and Neumann fields cannot be derived from a discretization based purely on linear Lagrange ansatz spaces. For instance, although

$$\mathcal{X}_h = \nabla \mathcal{L}_0 \oplus J\nabla \mathcal{L} \oplus (\nabla \mathcal{L}_0 + J\nabla \mathcal{L})^\perp$$

is an orthogonal decomposition, the residue space $(\nabla \mathcal{L}_0 + J\nabla \mathcal{L})^\perp$ has dimension

$$\begin{aligned} \dim(\nabla \mathcal{L}_0 + J\nabla \mathcal{L})^\perp &= 2n_F - n_{iV} - n_V \\ &= 2(n_E - n_V - n_F) + n_F - n_{bE} + n_{bV} \\ &= -2(1 - h^1) + n_F \end{aligned}$$

and is therefore mesh-dependent and has no meaningful topological interpretation any more.

DIV, CURL AND DISCRETE HOLOMORPHIC FUNCTIONS. The intention behind all previous decomposition results is to provide a complete structural understanding of the space \mathcal{X}_h of PCVFs. Central to all these statements are the two spaces of exact vector fields $\nabla \mathcal{L}_{(0)}$ and co-exact vector fields $J\nabla \mathcal{F}_{(0)}$, possibly with boundary conditions applied to the (co-)potentials. All other spaces are derived from these two spaces in the sense that they are subspaces or particular orthogonal complements. In particular, the only remainder from the smooth theory is the discrete (co-)gradient operator, which is, restricted to a single triangle, the smooth surface gradient applied to a linear function. With respect to Green's formula one can also attain a dual point of view by defining a discrete divergence and curl operator acting on PCVFs by those functions forcing Green's formula in the discrete setting to hold true—a paradigm prevalent to mimetic discretization methods. In the context of discrete differential geometry, this was initiated by Polthier and Preuss in [PP03], and later on elaborated on by Wardetzky in [War06]. Following their depiction, one defines implicitly the elements

$$\begin{aligned} \operatorname{div}_{\mathcal{L}_0}(X) &\in \mathcal{L}_0 \text{ such that } \langle \operatorname{div}_{\mathcal{L}_0}(X), \varphi \rangle_{L^2} = -\langle X, \nabla \varphi \rangle_{L^2} \text{ for all } \varphi \in \mathcal{L}_0 \\ \operatorname{curl}_{\mathcal{F}_0}(X) &\in \mathcal{F}_0 \text{ such that } \langle \operatorname{curl}_{\mathcal{F}_0}(X), \psi \rangle_{L^2} = \langle X, J\nabla \psi \rangle_{L^2} \text{ for all } \psi \in \mathcal{F}_0. \end{aligned}$$

for a given PCVF $X \in \mathcal{X}_h$. This gives operators

$$\begin{aligned} \operatorname{div}_{\mathcal{L}_0} : \mathcal{X}_h &\rightarrow \mathcal{L}_0 \\ \operatorname{curl}_{\mathcal{F}_0} : \mathcal{X}_h &\rightarrow \mathcal{F}_0 \end{aligned}$$

which we refer to as *discrete divergence* and *discrete curl*. Then it is by definition

$$\begin{aligned}\ker(\operatorname{div}_{\mathcal{L}_0}) &= \nabla \mathcal{L}_0^\perp \\ \ker(\operatorname{curl}_{\mathcal{F}_0}) &= J\nabla \mathcal{F}_0^\perp\end{aligned}$$

and the decomposition (3.10) becomes

$$\mathcal{X}_h = \nabla \mathcal{L}_0 \oplus (\ker(\operatorname{div}_{\mathcal{L}_0}) \cap \ker(\operatorname{curl}_{\mathcal{F}_0})) \oplus J\nabla \mathcal{F}_0,$$

identifying the space \mathcal{H}_h of discrete harmonic fields as those fields which are discrete divergence- and curl-free. Consequently, the spaces of harmonic Dirichlet and Neumann fields rewrite as

$$\begin{aligned}\mathcal{H}_{h,D} &= \ker(\operatorname{div}_{\mathcal{L}_0}) \cap (J\nabla \mathcal{F}_0^\perp) \\ \mathcal{H}_{h,N} &= \ker(\operatorname{curl}_{\mathcal{F}_0}) \cap (\nabla \mathcal{L}_0^\perp).\end{aligned}$$

Of particular interest are discrete divergence-free gradient fields of Lagrange elements, which are defined by functions $\varphi \in \mathcal{L}$ satisfying $\operatorname{div}_{\mathcal{L}_0}(\nabla \varphi) = 0$. Such fields are frequently used in remeshing and parametrization applications, see e.g. [DKG05, KNP07, SZS08, XZCOX09], mostly due to their regular behaviour in the interior of a domain and the relatively simple implementation of linear Lagrange functions on triangular meshes. These fields are gradients of *discrete harmonic functions*, defined as the elements in the kernel of the stiffness matrix

$$((\nabla \varphi_i, \nabla \varphi_j)_{L^2})_{i=1, \dots, n_{iV}, j=1, \dots, n_{iV}},$$

whose entries can be intrinsically written as cotangent weights, see [PP93]. By adding n_{bV} -many prescribed function values attained at the boundary vertices, there is a unique weak solution to the Laplace problem

$$\Delta f = 0 \text{ subject to } f|_{\partial M} = f_0$$

for a given boundary function f_0 . If M_h is of type $\Sigma_{g,m}$, Lemma 3.2.13 shows that the space $\mathcal{H}_{h,D,\text{ex}}$ captures the $(m-1)$ -many solutions corresponding to discrete boundary functions f_0 which are locally constant on the boundary ∂M_h .

In the construction and theoretical investigation of discrete minimal surfaces and their conjugates, Polthier has set up in [Pol02, Sec. 3.4] a discrete Cauchy-Riemann problem to find a discrete conjugate harmonic function for a given discrete harmonic function $\varphi \in \mathcal{L}$ as

$$\text{Find } \psi \in \mathcal{F} \text{ such that } \nabla \varphi = J\nabla \psi, \quad (3.16)$$

and (3.16) is referred to as the *discrete Cauchy-Riemann equations*. It is shown in [Pol02, Prop. 69]:

Theorem 3.2.21. *Let M_h be simply connected and let $\varphi \in \mathcal{L}$ be discrete harmonic. Then there is—up to a constant—a unique solution $\psi \in \mathcal{F}$ to the discrete Cauchy-Riemann equations.*

Using the decomposition results derived above, this theorem also follows immediately from Theorem 3.2.18: if M_h is simply connected, then $\mathcal{H}_{h,D} = \{0\}$ and therefore every divergence-free gradient field is contained in the *central harmonic component* $\nabla \mathcal{L} \cap J\nabla \mathcal{F}$.

A pair (φ, ψ) satisfying (3.16) constitutes a *discrete holomorphic function* $\varphi + i\psi$, and φ and ψ are *discrete harmonic conjugate* to each other. The full decomposition in Theorem 3.2.18 now shows that the dimension of the space of discrete holomorphic functions on M_h computes as

$$\begin{aligned} \dim \nabla \mathcal{L} \cap J \nabla \mathcal{F} &= 2n_F - n_{iV} - n_{iE} - 2h^1 \\ &= 2n_F - n_V + n_{bV} - 3n_F + n_E - 2h^1 \\ &= -1 + h^1 + n_{bV} - 2h^1 \\ &= n_{bV} - h^1 - 1, \end{aligned} \tag{3.17}$$

and since $h^1 = m - 1$ for a surface of type $\Sigma_{0,m}$, there are, up to the constants, $n_{bV} - m$ linearly independent discrete holomorphic functions. Under the assumption that $\mathcal{H}_{h,D} \cap \mathcal{H}_{h,N} = \{0\}$, this result generalizes as follows:

Lemma 3.2.22. *Let M_h be a surface of type $\Sigma_{g,m}$ and assume that $\mathcal{H}_{h,D} \cap \mathcal{H}_{h,N} = \{0\}$. Then the space of discrete holomorphic functions on M_h has dimension $n_{bV} - 2g - m + 2$.*

Proof. This follows from (3.13) with the same computation as in (3.17), using $h^1 = 2g + m - 1$ and taking constant potentials and copotentials into account. \square

3.3 DECOMPOSITIONS ON SIMPLICIAL SOLIDS

We now apply the same investigation to simplicial solids in \mathbb{R}^3 . This scenario differs in two major aspects from the case of surfaces discussed before: first, vector fields can now represent either 1- or 2-forms and one needs to be careful when it comes to cohomological arguments since in general the spaces $H^k(M)$ and $H^k(M, \partial M)$ are not isomorphic any more. Second, all cohomology is now induced by the cohomology of the boundary, so there is no need for a further splitting of discrete Dirichlet or Neumann fields. As a consequence there is always a complete orthogonal five-term decomposition.

For this section let M_h denote a simplicial solid embedded in \mathbb{R}^3 . Again, we are interested in decomposition results for the space \mathcal{X}_h of piecewise constant vector fields on M_h , which are represented by a constant vector in \mathbb{R}^3 per tetrahedral cell. Let \mathcal{N} and \mathcal{F} denote the spaces of Nédélec elements and Crouzeix-Raviart elements on tetrahedral meshes as defined in Section 3.1, and let $\mathcal{N}_0 \subset \mathcal{N}$ and $\mathcal{F}_0 \subset \mathcal{F}$ denote the subspaces of all elements whose degrees of freedom associated to simplices of the boundary ∂M_h are set to zero.

Lemma 3.3.1. *A PCVF X is in the space $\nabla \mathcal{F}_0^\perp$ if and only if it represents a closed Whitney 2-form, and X is in the space $\nabla \mathcal{F}^\perp$ if and only if it represents a closed Whitney 2-form with vanishing tangential component.*

Proof. The proof is in the same spirit as for Lemma 3.2.1. However, since the involved construction of the Whitney 2-form and the de Rham map differs in this case, we give the details for completeness.

Let $\omega \in \mathcal{W}^2$ be closed, i.e. $d\omega = 0$, then ω is constant over each cell by Lemma 3.1.5. Moreover, since each Whitney form is tangentially continuous, the representing proxy field $X := (\star\omega)^\sharp$ is normally continuous by (2.14), so $X \in \nabla \mathcal{F}_0^\perp$ by Lemma 3.1.2.

Conversely, let $X \in \nabla \mathcal{F}_0^\perp$. Pick an arbitrary, but fixed orientation for each face $f \in M_h^{(2)}$, define $a_f := \int_f \star X^\flat$ and set $\omega := \sum_f a_f \omega_f \in \mathcal{W}^2$. Since X is normally continuous, so is X^\flat

and thus $\mathbf{t}(\star X^\flat)$ is well-defined over f by (2.11). Then for every tetrahedron $t \in M_h^{(3)}$ it is by Stokes' theorem

$$\int_t d\omega = \int_{\partial t} \omega = \sum_{f \in \partial t} a_f \int_f \omega_f = \sum_{f \in \partial t} a_f \epsilon_f$$

where each f now has the boundary orientation induced from the tetrahedron t . Therefore we have to multiply with $\epsilon_f = 1$ if this orientation agrees with the one we have fixed, and $\epsilon_f = -1$ otherwise. Let ν_f denote the outer unit normal of the tetrahedron t at face f . Then by writing this last sum in terms of surface integrals of the vector field X we conclude

$$\sum_{f \in \partial t} a_f \epsilon_f = \sum_{f \in \partial t} \int_f \langle X, \nu_f \rangle dS = \sum_{f \in \partial t} \text{area}(f) \langle X, \nu_f \rangle = \langle X, \sum_{f \in \partial t} \text{area}(f) \cdot \nu_f \rangle = 0$$

since for any tetrahedron the area vectors $\text{area}(f) \cdot \nu_f$ at each face sum up to zero. Hence the assignment $R(d\omega) : t \mapsto \int_t d\omega$ is the zero element in $C^3(M_h)$, and since $R : \mathcal{W}^3 \xrightarrow{\simeq} C^3(M_h)$ is an isomorphism, it follows $d\omega = 0$, i.e. ω is closed.

The addendum follows from the fact that for a boundary face $f \in \partial M_h$ it is $a_f = 0$ if and only if $\mathbf{t}(\star X^\flat) = 0$ if and only if $\mathbf{\bar{n}}(X) = 0$. \square

Lemma 3.3.2. *The following pairs of subspaces are L^2 -orthogonal:*

$$\begin{aligned} \text{curl}(\mathcal{N}) &\perp \nabla \mathcal{F}_0 \\ \text{curl}(\mathcal{N}_0) &\perp \nabla \mathcal{F}. \end{aligned}$$

Proof. With respect to the commutative diagram (3.7) this is now a simple consequence of Lemma 3.3.1: since every exact form is closed, it follows for any $X \in \mathcal{N}$ that $\text{curl}(X)^\flat \in \ker(d_{\mathcal{W}}^2)$, so indeed $\text{curl}(X) \in \nabla \mathcal{F}_0^\perp$.

If in addition $X \in \mathcal{N}_0$, then X^\flat has vanishing tangential component along ∂M_h . Thus by (2.12), dX^\flat has vanishing tangential component, too, which in turn means that $\text{curl}(X)$ has vanishing normal component along ∂M_h , so $\text{curl}(X) \in \nabla \mathcal{F}^\perp$. \square

As in the two-dimensional case, we define the discrete harmonic fields as the L^2 -orthogonal residue space of these two subspace combinations:

Definition 3.3.3 (Discrete Harmonic, Neumann, Dirichlet (3d)). *The L^2 -orthogonal complements of the orthogonal sums $\text{curl}(\mathcal{N}_0) \oplus \nabla \mathcal{F}_0$, $\text{curl}(\mathcal{N}) \oplus \nabla \mathcal{F}_0$ and $\text{curl}(\mathcal{N}_0) \oplus \nabla \mathcal{F}$ within \mathcal{X}_h are the spaces of discrete harmonic fields, discrete Neumann fields and discrete Dirichlet fields, and denoted by \mathcal{H}_h^* , $\mathcal{H}_{h,N}^*$ and $\mathcal{H}_{h,D}^*$, respectively.*

Lemma 3.3.4 (Fundamental Decomposition (3d)). *The space \mathcal{X}_h admits the following L^2 -orthogonal decompositions*

$$\mathcal{X}_h = \text{curl}(\mathcal{N}) \oplus \nabla \mathcal{F}_0 \oplus \mathcal{H}_{h,N}^* \tag{3.18}$$

$$= \text{curl}(\mathcal{N}_0) \oplus \nabla \mathcal{F} \oplus \mathcal{H}_{h,D}^* \tag{3.19}$$

and it is $\dim \mathcal{H}_{h,N}^* = h^2$ and $\dim \mathcal{H}_{h,D}^* = h_r^2$.

Proof. The orthogonality follows directly from Lemma 3.3.2 and the definition of discrete Neumann and Dirichlet fields. Since it is $\nabla \mathcal{F}_0^\perp \cong \{(\star\omega)^\sharp : \omega \in \ker(d_{\mathcal{W}}^2) \subset \mathcal{W}^2\}$ and $\text{curl}(\mathcal{N}) \subseteq \nabla \mathcal{F}_0^\perp$ by Lemma 3.3.1 and Lemma 3.3.2, it follows that

$$\mathcal{H}_{h,N}^\star \cong \nabla \mathcal{F}_0^\perp / \text{curl}(\mathcal{N}) \cong \ker(d_{\mathcal{W}}^2) / \text{im}(d_{\mathcal{W}}^1) \cong Z^2(M_h) / B^2(M_h) = H^2(M_h).$$

Similarly, for the relative version it is

$$\mathcal{H}_{h,D}^\star \cong \nabla \mathcal{F}^\perp / \text{curl}(\mathcal{N}_0) \cong \ker(d_{\mathcal{W}_0}^2) / \text{im}(d_{\mathcal{W}_0}^1) \cong Z^2(M_h, \partial M_h) / B^2(M_h, \partial M_h) = H^2(M_h, \partial M_h).$$

□

Again, we obtain discrete de Rham isomorphisms on the level of cohomology

$$\begin{aligned} \bar{R}_N^\star : \mathcal{H}_{h,N}^\star &\xrightarrow{\cong} H^2(M) \\ \bar{R}_D^\star : \mathcal{H}_{h,D}^\star &\xrightarrow{\cong} H^2(M, \partial M), \end{aligned}$$

this time given by

$$X \mapsto \left[c_X : f \mapsto \int_f \langle X, \nu_f \rangle dS = \langle X, \nu_f \rangle \cdot \text{area}(f) \right]$$

where ν_f is a fixed unit normal to the face $f \in M_h^{(2)}$, cf. the proof of Lemma 3.3.1.

Remark 3.3.5. *In contrast to the definitions of discrete harmonic, Neumann and Dirichlet fields in the two-dimensional case in Definition 3.2.5, in the three-dimensional case the discrete Dirichlet fields have strictly vanishing normal component on each boundary face, and discrete Neumann fields have weakly vanishing tangential component on the boundary. This is because the decompositions Lemma 3.3.4 are in fact decompositions for vector proxies of 2-forms, as becomes clear in the previous proofs: potentials are now vector potentials and the operator curl corresponds to the exterior derivative $d_{\mathcal{W}}^1 : \mathcal{W}^1 \rightarrow \mathcal{W}^2$ on the level of Whitney forms. As a consequence, the corresponding representation isomorphism $\sharp \circ \star : \mathcal{W}^2 \rightarrow \mathcal{X}$, defined piecewise over each cell, swaps boundary conditions by (2.11) and (2.14). The \star -notation in $\mathcal{H}_{h,N}^\star$ and $\mathcal{H}_{h,D}^\star$ should remind the reader of this fact.*

The reason for the interpretation of PCVFs as discrete vector proxies for 2-forms lies in the simplicity of the space \mathcal{F} : each PCVF which is L^2 -orthogonal to all gradients of Crouzeix-Raviart elements is normally continuous across interelement faces, but not tangentially continuous. In contrast, to define a similar decomposition for PCVFs representing 1-forms would require to find an ansatz space \mathcal{V} and a linear operator $T : \mathcal{V} \rightarrow \mathcal{X}$ such that a PCVF is in the orthogonal complement $T(\mathcal{V})^\perp$ if and only if it is tangentially continuous.

A special case of Lemma 3.3.4 was considered by Monk [Mon91]:

Corollary 3.3.6. *Let M_h be a simplicial solid in \mathbb{R}^3 with a connected boundary ∂M_h . Then the space \mathcal{X}_h splits as*

$$\mathcal{X}_h = \text{curl}(\mathcal{N}) \oplus \nabla \mathcal{F}_0.$$

Proof. By Corollary 2.1.3 it is $0 = H^2(M) \cong \mathcal{H}_{h,N}^\star$, and the result follows from Lemma 3.3.4. □

Remark 3.3.7. The article [Mon91] makes the even stronger assumption that M_h must be simply connected. Corollary 3.3.6 shows that this assumption is not necessary for the stated decomposition in [Mon91, Thm. 4.9], though. For instance, it still holds true on a solid torus.

We obtain a discrete version of the Hodge-Morrey-Friedrichs decomposition:

Theorem 3.3.8 (Discrete Hodge-Morrey-Friedrichs Decomposition (3d)). *The space \mathcal{X}_h admits the following L^2 -orthogonal decompositions*

$$\mathcal{X}_h = \text{curl}(\mathcal{N}_0) \oplus \nabla \mathcal{F}_0 \oplus \mathcal{H}_h^* \cap \text{curl}(\mathcal{N}) \oplus \mathcal{H}_{h,N}^* \quad (3.20)$$

$$= \text{curl}(\mathcal{N}_0) \oplus \nabla \mathcal{F}_0 \oplus \mathcal{H}_h^* \cap \nabla \mathcal{F} \oplus \mathcal{H}_{h,D}^*. \quad (3.21)$$

Proof. This is a consequence of Lemma 3.3.4. \square

Let

$$\mathcal{H}_{h,D,\text{ex}}^* := \mathcal{H}_{h,D}^* \cap \text{curl}(\mathcal{N})$$

be the space of exact Dirichlet fields. With respect to the question whether there is a complete decomposition involving both spaces $\mathcal{H}_{h,N}^*$ and $\mathcal{H}_{h,D}^*$ at the same time, we again consider the projection map

$$\text{pr}_N^* : \mathcal{H}_{h,D}^* \rightarrow \mathcal{H}_{h,N}^*, X_D \mapsto X_N$$

where X_N is the Neumann component of the decomposition (3.18):

$$X_D = \text{curl}(\eta) + X_N \in \text{curl}(\mathcal{N}) \oplus \mathcal{H}_{h,N}^*.$$

As in Lemma 3.2.12, we expect that $\ker(\text{pr}_N^*) = \mathcal{H}_{h,D,\text{ex}}^*$. But since M_h is a domain embedded in \mathbb{R}^3 , all Dirichlet fields are in fact exact:

Lemma 3.3.9. *It is $\ker(\text{pr}_N^*) = \mathcal{H}_{h,D,\text{ex}}^* = \mathcal{H}_{h,D}^*$.*

Proof. The argument is analogous to the proof in Lemma 3.2.12. By definition of pr_N^* the diagram

$$\begin{array}{ccc} \mathcal{H}_{h,D}^* & \xrightarrow{\text{pr}_N^*} & \mathcal{H}_{h,N}^* \\ \downarrow \bar{R}_D^* & & \downarrow \bar{R}_N^* \\ H^2(M, \partial M) & \xrightarrow{\pi^*} & H^2(M) \end{array}$$

is commutative, with the vertical arrows being isomorphisms. Therefore $\dim \ker(\text{pr}_N^*) = \dim \ker(\pi^*)$, but because of Lemma 2.1.2 and (2.5), π^* must be the zero map, so that $\ker(\pi^*) = H^2(M, \partial M)$. Since $\mathcal{H}_{h,D}^*$ represent the cohomology classes in $H^2(M, \partial M)$, it is $\pi^*(\bar{R}_D^*(X_D)) = 0 \in H^2(M)$ for every $X_D \in \mathcal{H}_{h,D}^*$, so each X_D is in fact exact and therefore $X_D \in \mathcal{H}_{h,D,\text{ex}}^*$. \square

Here lies a major difference to the general surface case: since M_h is embedded in \mathbb{R}^3 , it follows from the cohomology sequence (2.5) that all maps π^* are zero maps and consequently, all discrete Dirichlet fields are exact. Furthermore, we have seen in Lemma 2.1.2 that the map $\iota^* : H^2(M_h) \rightarrow H^2(\partial M_h)$ is an injection and therefore $\ker(\iota^*) = \{0\}$. Thus there is no need for a discrete analogue for the space of boundary-exact Neumann fields as it would be trivial anyway. We conclude:

Corollary 3.3.10. *It is $\mathcal{X}_h = \text{curl}(\mathcal{N}) + \nabla\mathcal{F}$.*

Proof. By Lemma 3.3.9 it is $\mathcal{H}_{h,D}^* \subset \text{curl}(\mathcal{N})$ and the result follows from (3.21). \square

Corollary 3.3.11. *It is $\mathcal{H}_{h,D}^* \perp \mathcal{H}_{h,N}^*$.*

Proof. This follows from Lemma 3.3.9 and Theorem 3.3.8. \square

Corollary 3.3.12. *It is $\mathcal{H}_{h,N}^* \subset \nabla\mathcal{F}$.*

Proof. It is $\mathcal{H}_{h,N}^* \perp \text{curl}(\mathcal{N}_0)$ and $\mathcal{H}_{h,N}^* \perp \mathcal{H}_{h,D}^*$ by Corollary 3.3.11, so $\mathcal{H}_{h,N}^* \subset \nabla\mathcal{F}$ follows from (3.19). \square

Therefore, for simplicial solids in \mathbb{R}^3 there is a single complete decomposition involving both the spaces $\mathcal{H}_{h,N}^*$ and $\mathcal{H}_{h,D}^*$ as L^2 -orthogonal subspaces:

Theorem 3.3.13 (Complete Decomposition for Simplicial Solids in \mathbb{R}^3). *On a simplicial solid $M_h \subset \mathbb{R}^3$ there is a complete decomposition*

$$\mathcal{X}_h = \text{curl}(\mathcal{N}_0) \oplus \nabla\mathcal{F}_0 \oplus \text{curl}(\mathcal{N}) \cap \nabla\mathcal{F} \oplus \mathcal{H}_{h,N}^* \oplus \mathcal{H}_{h,D}^*. \quad (3.22)$$

Proof. The decomposition follows from Corollary 3.3.11 and Theorem 3.3.8. \square

Again, we refer to the intersection space $\text{curl}(\mathcal{N}) \cap \nabla\mathcal{F}$ as the *central harmonic component*, consisting of all discrete harmonic fields which are exact as well as coexact. In the terminology of [CDG02], these are the *discrete curly gradients* from (2.21). In the smooth situation this space will be infinite-dimensional. For the discrete setting we obtain:

Lemma 3.3.14. *The central harmonic component has dimension*

$$\dim(\text{curl}(\mathcal{N}) \cap \nabla\mathcal{F}) = n_{bF} - h^2 - 1.$$

Proof. By Section 3.1 it is $\dim \text{curl}(\mathcal{N}_0) = n_{iE} - n_{iV} - h_r^1$. Using $h^2 = h_r^1$, $n_{iF} = 4n_T - n_F$ and the formula for the Euler characteristic (3.2), we obtain

$$\begin{aligned} \dim(\text{curl}(\mathcal{N}) \cap \nabla\mathcal{F}) &= 3n_T - (n_{iE} - n_{iV} - h_r^1) - n_{iF} - h^2 - h_r^2 \\ &= 3n_T - n_{iE} + n_{iV} - n_{iF} - h_r^2 \\ &= n_{iV} - n_{iE} + n_{iF} - n_T - h_r^2 + n_{bF} \\ &= n_{bF} - h_r^1 - 1. \end{aligned}$$

\square

Furthermore, the spaces $\nabla\mathcal{F}_0$ and $\text{curl}(\mathcal{N}_0)$ correspond to the spaces of grounded gradients and fluxless knots, respectively. However, in contrast to (2.21), it is now the space $\mathcal{H}_{h,N}^*$ which corresponds to the space HG of harmonic gradients, and similarly, $\mathcal{H}_{h,D}^*$ corresponds to the space HK of harmonic knots. Again, this is due to the fact, that our decomposition interprets vector fields as proxies for 2-forms, as mentioned in Remark 3.3.5. Therefore, the spaces representing absolute and relative cohomology are swapped.

DECOMPOSITION BASED ON LAGRANGE ANSATZ SPACES. In [TLHD03], a three-term decomposition is proposed which is based purely on Lagrange elements as ansatz spaces: let \mathcal{L} denote as usual the space of linear Lagrange elements on M_h , and let

$$\mathcal{L}^3 := \{(\varphi_{x_1}, \varphi_{x_2}, \varphi_{x_3}) : \varphi_{x_i} \in \mathcal{L}\}$$

denote the space of vector Lagrange elements. Again, we have subspaces $\mathcal{L}_0 \subset \mathcal{L}$ and $\mathcal{L}_0^3 \subset \mathcal{L}^3$ spanned by all those elements whose degrees of freedom associated to vertices contained in the boundary ∂M_h are set to zero. The authors then prove the orthogonality $\text{curl}(\mathcal{L}_0^3) \perp \nabla \mathcal{L}_0$ and conclude that there is a decomposition

$$\mathcal{X}_h = \nabla \mathcal{L}_0 \oplus \text{curl}(\mathcal{L}_0^3) \oplus \widetilde{\mathcal{H}}_h^* \quad (3.23)$$

where $\widetilde{\mathcal{H}}_h^*$ is the resulting space of *discrete harmonic fields*, defined as the L^2 -orthogonal complement of the sum of the former two spaces.

In order to compare this decomposition with the decomposition in Theorem 3.3.13, we note that $\mathcal{N} \subset \mathcal{L}^3$. Furthermore, it is shown in [AFW06, Lem. 3.8 and Sec. 5.5] that

$$\text{im}(\text{curl} : \mathcal{L}^3 \rightarrow \mathcal{X}_h) = \text{im}(\text{curl} : \mathcal{N} \rightarrow \mathcal{X}_h).$$

Since $\mathcal{L} \subseteq \mathcal{F}$, it follows from Theorem 3.3.13 that

$$\text{curl}(\mathcal{N}) \cap \nabla \mathcal{F} \oplus \mathcal{H}_{h,N}^* \oplus \mathcal{H}_{h,D}^* \subseteq \widetilde{\mathcal{H}}_h^*,$$

and a computation similar to the one in Lemma 3.3.14 gives

$$\dim \widetilde{\mathcal{H}}_h^* = 3n_T - n_{iV} - (n_{iE} - n_{iV} - h_r^1) = 3n_T - n_{iE} + h_r^1.$$

With respect to Lemma 3.3.2 it is possible to remove the boundary conditions on one of the ansatz spaces in (3.23) and one still obtains an orthogonal decomposition, with a reduced space of discrete harmonic fields as complement. However, as in the two-dimensional case it is not possible to obtain the correct dimensions for the spaces of discrete Dirichlet and Neumann fields by using Lagrange elements only. Indeed, for the corresponding decompositions

$$\begin{aligned} \mathcal{X}_h &= \text{curl}(\mathcal{N}) \oplus \nabla \mathcal{L}_0 \oplus \widetilde{\mathcal{H}}_{h,N}^* \\ &= \text{curl}(\mathcal{N}_0) \oplus \nabla \mathcal{L} \oplus \widetilde{\mathcal{H}}_{h,D}^* \end{aligned}$$

the resulting, “wrong” dimensions

$$\begin{aligned} \dim \widetilde{\mathcal{H}}_{h,N}^* &= h^2 + n_{iF} - n_{iV} \\ \dim \widetilde{\mathcal{H}}_{h,D}^* &= h_r^2 + n_F - n_V \end{aligned}$$

are a simple consequence of Lemma 3.3.4 and the fact that $\dim \mathcal{F}/\mathcal{L} = n_F - n_V$ as well as $\dim \mathcal{F}_0/\mathcal{L}_0 = n_{iF} - n_{iV}$.

3.4 WHEN IS $\mathcal{H}_{h,N} \cap \mathcal{H}_{h,D} = \{0\}$? OBSTRUCTIONS

The discrete analogue $\mathcal{H}_{h,N} \cap \mathcal{H}_{h,D} = \{0\}$ is not always true because of subregions of topological complexity inside a geometry that are poorly connected to the rest of the mesh. This insight can be reduced to a purely combinatorial problem about quasi-harmonic flows on networks which gives a criterion on the mesh discretization to avoid this pathology.

OBSTRUCTIONS. As mentioned in Section 3.2, an important question towards a consistent discretization is whether the discrete version $\mathcal{H}_{h,N} \cap \mathcal{H}_{h,D} = \{0\}$ of Theorem 2.4.1 holds true, too. With respect to the fundamental decompositions in Lemma 3.2.6, this question is equivalent to the equality

$$\mathcal{X}_h = \nabla \mathcal{L} + J \nabla \mathcal{F}. \quad (3.24)$$

But in contrast to the smooth theory, this is not always the case, as a simple calculation shows: computing dimensions, we have $\dim \mathcal{X}_h = 2n_F$, $\dim \nabla \mathcal{L} = n_V - 1$ and $\dim J \nabla \mathcal{F} = n_E - 1$. So even if we assume a direct sum, then by subtracting the relation $3n_F - 2n_E + n_{bE} = 0$ we obtain

$$\begin{aligned} \dim \mathcal{X}_h - \dim(\nabla \mathcal{L} + J \nabla \mathcal{F}) &\geq 2n_F - (n_V - 1) - (n_E - 1) \\ &= 2n_F - n_V - n_E + 2 - (3n_F - 2n_E + n_{bE}) \\ &= -\chi(M_h) + 2 - n_{bE} \\ &= h^1 + 1 - n_{bE}. \end{aligned} \quad (3.25)$$

Therefore, even in the most optimistic case $\nabla \mathcal{L} \cap J \nabla \mathcal{F} = \{0\}$ this difference will be positive whenever $h^1 + 1 > n_{bE}$, i.e. if the discretization of the boundary is too low in comparison to the topological complexity, and the difference is even larger if we do not assume trivial intersection. This already happens on a geometry as simple as a pretzel surface with a single triangle cut out, as shown in Figure 3.6.

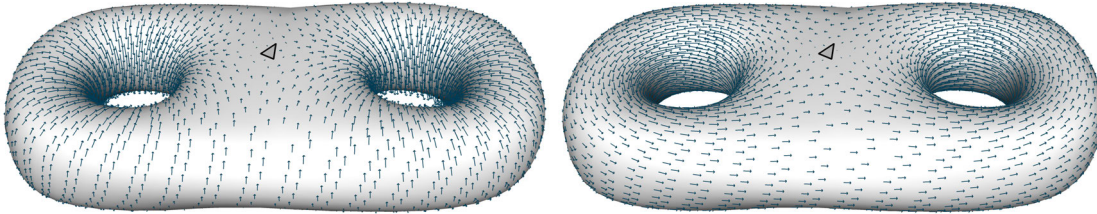


Figure 3.6: Two linearly independent vector fields in the intersection space $\mathcal{H}_{h,N} \cap \mathcal{H}_{h,D}$ on a pretzel surface with a single triangle cut out. For this particular surface it is $3 = n_{bE} < h^1 + 1 = 5$, so $\mathcal{H}_{h,N} \cap \mathcal{H}_{h,D}$ has dimension two, and the shown vector fields form a basis.

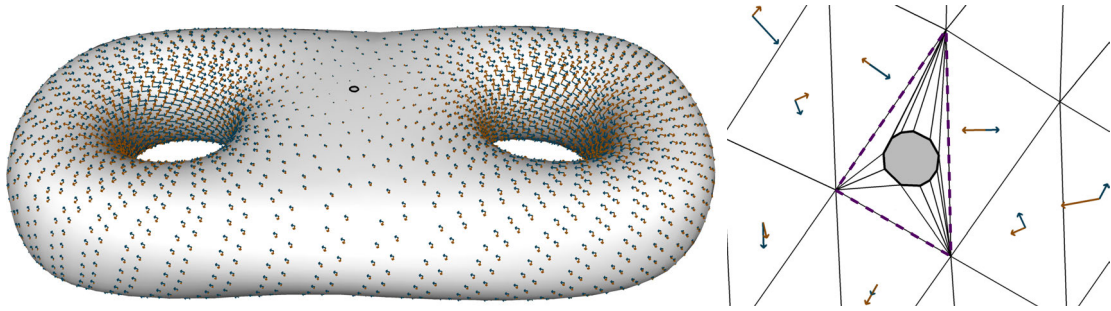


Figure 3.7: A pretzel surface with a hole formed by eleven edges and a close-up of the boundary hole. Still, there are two linearly independent fields in the intersection space $\mathcal{H}_{h,N} \cap \mathcal{H}_{h,D}$, since the hole is surrounded by a triangle (dashed line) constituting an effective boundary of only three edges. This is possible, as for the discrete harmonic fields only tangential continuity is required and thus a vector field which is perpendicular to the edges bounding a subregion can be extended by zero to the interior of that region, which is exactly what happens here.

The situation is even more involved, as depicted in Figure 3.7: even if $n_{bE} \geq h^1 + 1$, it still might be the case that (3.24) does not hold. The reason for this failure are cycles (i.e. closed paths) in M_h that are homologous to boundary cycles (or more generally sums of boundary cycles) and have a substantially smaller number of edges, constituting a virtual boundary with too little edges. However, in general it is not clear how to state precise conditions that are easy to verify for a given surface M_h , as it also depends on the distribution of boundary components across the surface, see Figure 3.8 for a further counterexample.

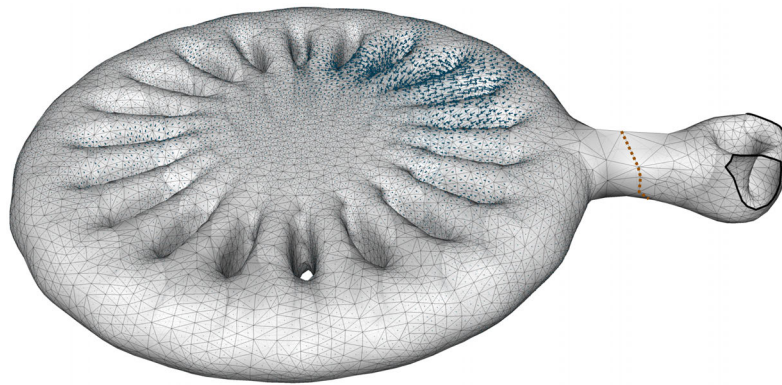


Figure 3.8: On the low-discretized tunnel connecting the high-genus region of a surface of type $\Sigma_{21,2}$ with the boundary region there is an edge cycle homologous not to a single boundary component, but to the sum of both boundary cycles, constituting a boundary cycle with just eight edges acting as a virtual boundary (dashed orange line) of too few edges to compensate the cohomology generated by the high-genus part. As a consequence, a large number of fields in $\mathcal{H}_{h,N} \cap \mathcal{H}_{h,D}$ exist on this geometry.

COMBINATORIAL ANGLE CLASSIFICATION: In the following we derive a combinatorial criterion for the validity of (3.24), based on weightings on directed graphs induced by harmonic fields. This approach is inspired by the work of Lovász and Benjamini on discrete harmonic functions and rotation-free circulations in the context of networks, see [BL03, Lov04], and the determination of a closed surface's genus by observing a random process on a connected subgraph of small size in [BL02b] and [BL02a]. We follow the terminology for the angle classification in directed networks introduced therein.

First we need to generalize the notion of a simplicial surface to include isolated singularities. These are vertices whose link is no longer connected but separates into connected components.

Definition 3.4.1 (Simplicial Surface with Isolated Singularities). *A simplicial surface with isolated singularities is a subset $S_h \subseteq M_h$ triangulated by a subcomplex of a simplicial surface M_h with boundary such that every maximal simplex in S_h is of dimension two.*

We refer to a simplicial surface with isolated singularities as a *singular simplicial surface* for short, keeping in mind that the only singularities allowed are isolated non-manifold vertices.

It follows from the definition of a singular simplicial surface that every edge is adjacent to one or two triangles. Edges that are adjacent to exactly one triangle are called *boundary edges* of S_h , and vertices whose link is disconnected are called *singular*. In particular, a singular simplicial surface does not need to be a topological surface, but it can be thought of as a collection of simplicial subsurfaces $M_{h,i}$ with boundary which are stitched together at individual boundary vertices, becoming the singular vertices. The related, but slightly stronger notion of a *quasi-manifold* requires that in addition any two triangles can be connected by an alternating sequence of triangles and edges, each incident to the next one—a property which is called *strong connectedness*, see [CV91]. See Figure 3.9 for an illustration of the differences. Our more general notion of a singular simplicial surface as defined above has the advantage that it is closed under removal: removing a singular simplicial subsurface S_h from another singular simplicial surface S'_h yields again a (not necessarily connected) singular simplicial surface, which is not true for quasi-manifolds. Of course, the definition of a singular simplicial surface includes quasi-manifolds and simplicial surfaces with boundary.

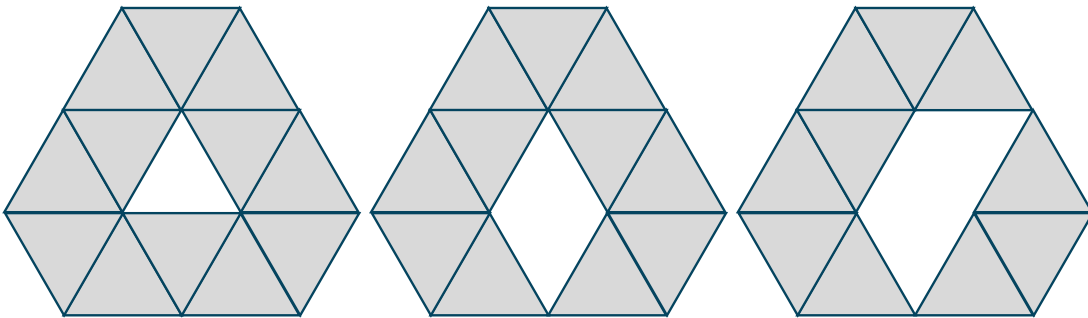


Figure 3.9: Simplicial surface, quasi-manifold and a singular simplicial surface.

In the following we assume that $(M_h, \partial M_h)$ is a simplicial surface with boundary, and $(S_h, \partial S_h)$ always denotes a singular simplicial subsurface of M_h with boundary. We can inherit the orientation on triangles of S_h from M_h . Furthermore we pick an arbitrary, but fixed orientation assigned to each edge $e \in S_h^{(1)}$. For each directed edge e we write $t(e)$ for the tail of e and $h(e)$ for the head of e . An *inner corner* at a vertex v is a quadruple (v, e_1, e_2, f) , where e_1 and e_2 are edges adjacent to v and belong to the face f . An *outer corner* at a boundary vertex v is a triple (v, e_1, e_2) where e_1 and e_2 are both boundary edges (i.e. edges in the subcomplex triangulating ∂S_h) adjacent to v , and, when traversing the adjacent edges to v in a counter-clockwise order, starting at e_1 , there are no further edges between e_1 and e_2 or e_2 and e_1 . This latter condition is necessary to precisely define an outer corner at a singular vertex which could have more than two adjacent boundary edges. For non-singular boundary vertices, this addendum is not needed. Finally, a *corner* is either an inner corner or an outer corner.

Definition 3.4.2 (Weighted Singular Simplicial Surface). A weighted, singular simplicial surface is a singular simplicial surface S_h together with a weighting $w : S_h^{(1)} \rightarrow \mathbb{R}$ which assigns a weight to each directed edge in S_h and satisfies $w(e) = -w(-e)$.

In other words, a weighting is just a simplicial 1-cochain on S_h . In the following it is useful to reorient the edges of S_h such that $w(e) \geq 0$ for a given weighting w . Such an edge orientation is said to be *induced by the weighting* w , see Figure 3.10 for an illustration. Obviously such an induced orientation for a given weighting is not unique, if there are edges e with $w(e) = 0$. These edges are called *0-edges*.

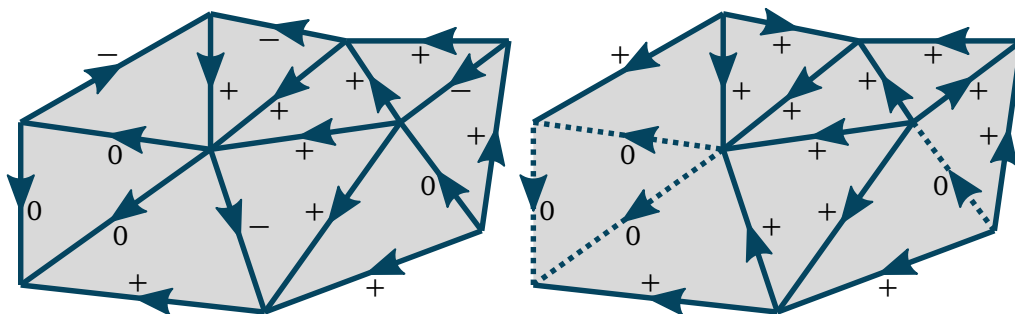


Figure 3.10: Left: a simplicial surface M_h with an arbitrary edge orientation and a weighting defined on it. We have omitted any numerical values but just annotated the edges with the sign of w . Right: the weighting induces a not necessarily unique orientation on M_h by reorienting the edges such that $w(e) \geq 0$ everywhere. The orientation of zero edges can be chosen arbitrarily. Here, their original orientation is preserved (dashed lines).

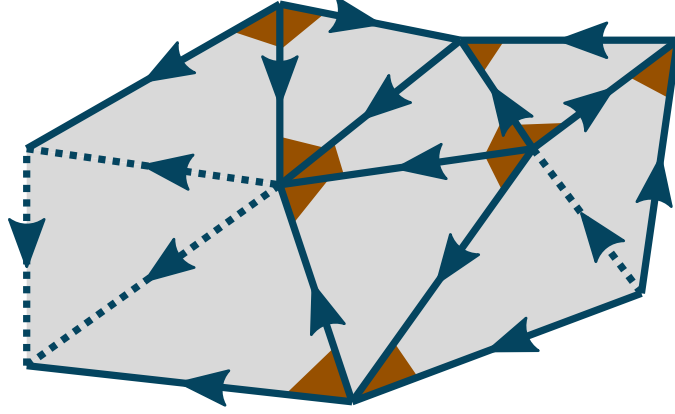


Figure 3.11: Sharp corners (orange) for the weighting depicted in Figure 3.10. All other corners are blunt. Inner corners formed by at least one 0-edge are by definition always blunt, no matter what the edge orientation dictates.

Definition 3.4.3 (Sharp Corner, Blunt Corner). *Let S_h be a weighted, singular simplicial surface with weighting w . An inner corner (v, e_1, e_2, f) is called sharp if*

1. $w(e_1) \neq 0$ and $w(e_2) \neq 0$, and
2. $\text{sgn}(w(e_1)) = \text{sgn}(w(e_2))$ if and only if $t(e_1) = t(e_2)$ or $h(e_1) = h(e_2)$.

All other interior corners are called blunt.

Note that his definition solely depends on the weighting w and not on the orientation we have fixed initially. If we consider the orientation induced by w , then sharp corners are corners at which the two adjacent edges are both either directed towards the common vertex or away from it. In contrast, a blunt corner that does not include a 0-edge is characterized by one of these edges pointing towards the common vertex and the other one away from it. This motivates the naming for these corners, as suggested in [Lov04], and simplifies the visualization of the various corner types, see Figure 3.11. Our notion of blunt corners is slightly more general, as we also include corners formed by 0-edges. Blunt corners in the sense of Lovász [Lov04] are always formed by edges with non-zero weight and thus should be rather called *properly blunt* in our scenario.

We denote the number of sharp corners inside a face f by s_f , the number of blunt inner corners at a vertex v by b_v , and the number of outer corners at v by o_v . Although for a simplicial surface it is always $o_v = 1$, this is not the case any more for singular simplicial surfaces where singular vertices are adjacent to at least four boundary edges. However, it always holds

$$\sum_{v \in S_h^{(0)}} o_v = n_{bE}. \quad (3.26)$$

The following result is an extension of Benjamini's and Lovász' formula in [BL02b, Lov04] to singular surfaces with boundary:

Lemma 3.4.4. *Let S_h be a weighted singular simplicial surface. Then it is*

$$2\chi(S_h) + n_{bE} = \sum_{f \in S_h^{(2)}} (2 - s_f) + \sum_{v \in S_h^{(0)}} (2 - b_v). \quad (3.27)$$

Proof. Let $\deg(v)$ denote the degree of vertex v . Since every corner is either an inner sharp or blunt corner or an outer corner, it is

$$\sum_{v \in S_h^{(0)}} \deg(v) = \sum_{f \in S_h^{(2)}} s_f + \sum_{v \in S_h^{(0)}} b_v + \sum_{v \in S_h^{(0)}} o_v.$$

Furthermore, by the handshake lemma and definition of Euler characteristic it is

$$\sum_{v \in S_h^{(0)}} \deg(v) = 2n_E = 2n_V + 2n_F - 2\chi(S_h).$$

Rearranging these two equations and using (3.26) gives the result. \square

Whereas Lemma 3.4.4 holds for any weighting on S_h , in the following we are mainly interested in weightings that come from harmonic vector fields. The notion of harmonicity can be defined on the level of weightings (or 1-cochains), too: A weighting w on S_h is *rotation-free* or *closed*, if $w(\partial f) = 0$ for each face $f \in S_h^{(2)}$. It is *divergence-free* or a *circulation* if

$$\sum_{e \in S_h^{(1)} : h(e)=v} w(e) - \sum_{e \in S_h^{(1)} : t(e)=v} w(e) = 0.$$

Finally, a weighting, which is both rotation-free and divergence-free is called a *harmonic weighting*.

Note that if w is divergence-free and v is a vertex with at least one adjacent edge e with $w(e) > 0$ pointing towards v , then there must be another edge e' with $w(e') > 0$ pointing away from v . This is a graph-theoretic analogue of the physical understanding that a divergence-free vector field does neither produce nor absorb any flow at any point. In the analysis of electrical networks this is exactly what is expressed by Kirchof's current law. Furthermore, the condition for divergence-freeness appears in various flavours, which usually differ by the choice of weights for the summands $w(e)$. Here we assume constant weights equal to one, but other popular choices include the cotangent weights as in [PP03] or weights based on a dual mesh as described in [Hir03].

It turns out that we can weaken the notions of rotation- and divergence-freeness, since in the following we will merely work with the corner types—the numerical values of the weighting on edges are not even taken into account. In addition, this even becomes a necessity when we consider weightings induced by harmonic PCVFs, since the cochain $R(X)$ coming from the period map applied to a PCVF $X \in \mathcal{H}_{h,N} \cap \mathcal{H}_{h,D}$ does in general not satisfy the divergence-free condition with constant weights, but with the cotangent weights. Therefore we shall consider weightings whose corner types behave similarly to those of harmonic weightings.

Definition 3.4.5. A weighting w on S_h is...

- ...quasi-divergence-free, if every vertex v is either adjacent to 0-edges only, or there are at least two adjacent edges e_1, e_2 with $w(e_i) \neq 0, i = 1, 2$, such that, after reorienting them so that $t(e_1) = t(e_2)$, it is $\text{sgn}(w(e_1)) \neq \text{sgn}(w(e_2))$.
- ...quasi-rotation-free, if every face f is either bounded by 0-edges only, or, after reorienting the bounding edges so that their orientation agrees with the one in ∂f (i.e. so that they form an oriented, closed cycle), there are at least two edges e_1, e_2 with $w(e_i) \neq 0, i = 1, 2$ and $\text{sgn}(w(e_1)) \neq \text{sgn}(w(e_2))$.
- ...quasi-harmonic, if it is both quasi-divergence free and quasi-rotation free.

If we consider an orientation induced by w we can equivalently define w to be quasi-divergence-free if each vertex v which is not adjacent to 0-edges only, has at least two adjacent edges with non-zero weight, one of them pointing towards v and the other away from v . Similarly, quasi-rotation-free implies that each face which is not bounded by 0-edges only is also not bounded by a directed, closed edge cycle. Figure 3.12 illustrates these two notions.

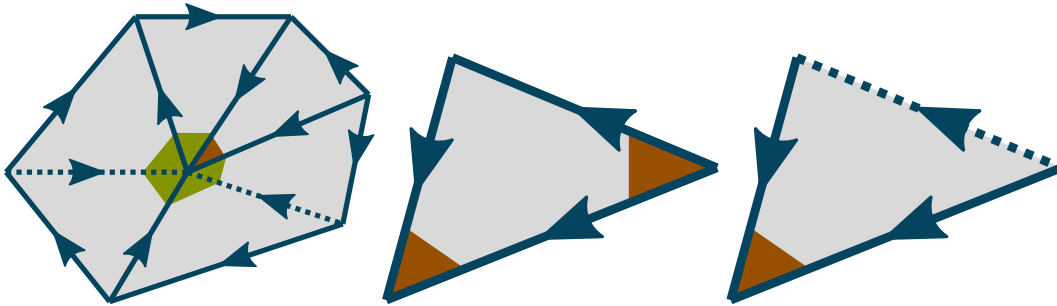


Figure 3.12: Left: A quasi-divergence-free vertex with five adjacent blunt corners (green), one of them being properly blunt and the other four adjacent to 0-edges, as well as one adjacent sharp corner (orange). Middle and right image: two quasi-rotation-free triangles, the first one with $s_f = 2$, the second with $s_f = 1$.

Since these properties merely depend on the sign of a weighting it is enough to restrict attention to weightings $w : S_h^{(1)} \rightarrow \{-1, 0, 1\}$ as already suggested by Figure 3.10.

Theorem 3.4.6. Assume that $n_{bE}(S_h) > -2\chi(S_h)$. Then there is no quasi-harmonic weighting that vanishes on all boundary edges, but is non-zero on all interior edges of S_h .

Proof. We will lead (3.27) to a contradiction. Note that by assumption the left-hand side of the equation is positive. We now show that the right-hand side is non-positive. Assume there is such a weighting w and let the orientation of the edges be induced by w . Since w is quasi-rotation-free, every triangle $f \in S_h$ that does not include a boundary edge, has exactly two sharp angles, so $s_f = 2$ for every such face. For every inner vertex v , the quasi-divergence-free condition requires at least one incident edge to point towards v and another to point away from v , so $b_v \geq 2$. This shows that the right-hand side of (3.27) is non-positive when summing over all interior vertices and all faces not adjacent to boundary edges.

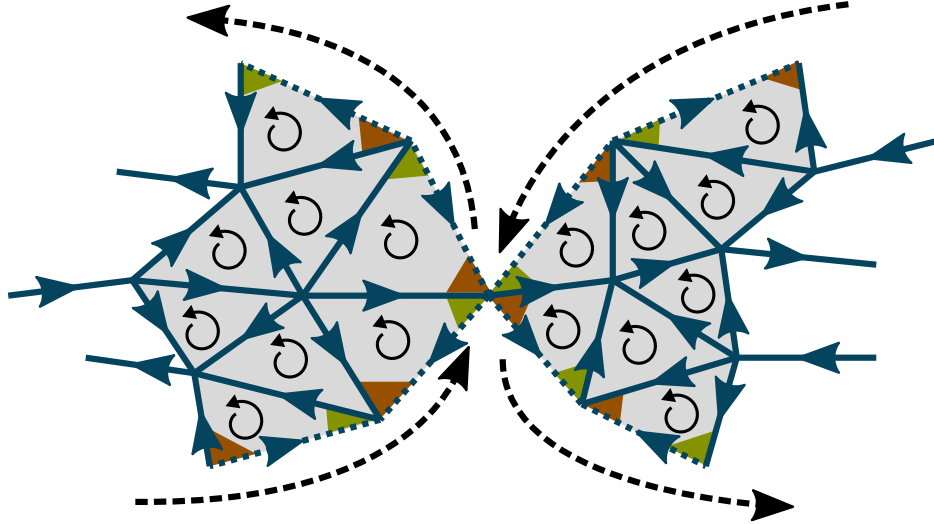


Figure 3.13: Configuration at a singular vertex connecting two simplicial surface patches. Each boundary edge inherits an orientation coming from the oriented triangles according to the global orientation of the simplicial surface M_h , indicated by the black twisted arrows inside the triangles and the dashed black arrows along the boundary components. With respect to this boundary orientation we construct the new weighting \tilde{w} out of w by assigning values $\tilde{w}(e) \in \{-1, +1\}$ at boundary edges $e \in \partial S_h^{(1)}$, such that the corner at $t(e)$ becomes a sharp corner (orange) and the corner $h(e)$ becomes blunt (green). As a result, it is $b_v \geq 2$ and $s_f = 2$ for \tilde{w} , so \tilde{w} is quasi-harmonic, too. The arrow indicators on the boundary edges in the figure already show the values for \tilde{w} .

To include the boundary-adjacent faces and boundary vertices we will construct another quasi-harmonic weighting \tilde{w} out of w with non-positive sums on the right-hand side of (3.27) as follows: for each interior edge $e \in S_h^{(1)}$ set $\tilde{w}(e) := w(e)$. For each non-singular subsurface patch $M_{h,i}$ in S_h , reorient its boundary in the orientation induced from the orientation on $M_{h,i}$. Then, for each boundary edge $e \in \partial M_{h,i}^{(1)}$ adjacent to the face f set $\tilde{w}(e) := a$ with $a \in \{-1, +1\}$ chosen such that the inner corner of f at the vertex $t(e)$ becomes a sharp corner for \tilde{w} . The other corner of f at $h(e)$ then automatically becomes a blunt corner, because the vertex of f opposite to e must be a sharp corner due to the harmonicity of w , cf. Figure 3.13. Thus for \tilde{w} it is $s_f = 2$ for every face adjacent to a boundary edge.

Furthermore, for every boundary vertex which is non-singular it is $b_v \geq 2$: there is exactly one blunt inner corner formed with a boundary edge and at least one other blunt inner corner formed between two interior edges, because w has been quasi-divergence-free at v . Finally, every singular boundary vertex has at least one blunt inner corner per adjacent manifold patch $M_{h,i}$. Figure 3.13 illustrates this situation.

Since w is quasi-harmonic and non-zero on interior edges, \tilde{w} satisfies $b_v \geq 2$ for all vertices $v \in S_h$ and $s_f \geq 2$ for all faces $f \in S_h$, so the right-hand side in (3.27) is indeed non-positive. By assumption the left-hand side is positive, though, which gives the contradiction. □

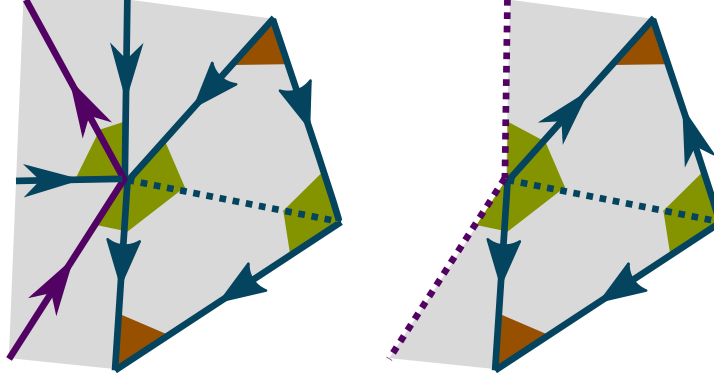


Figure 3.14: Two configurations of isolated 0-edges, together with exemplary continuations of the mesh in a neighbourhood of the left vertex. At each vertex, one of the two blunt corners adjacent to the isolated 0-edge compensates the missing sharp corner in one of the two triangles. Since the weighting is quasi-divergence-free, there is at least another blunt corner formed by non-0-edges (purple edges in the left image) or formed between boundary-0-edges, if the vertex is a boundary vertex and there are no other non-0-edges apart from the ones bounding f_i (purple dashed edges in the right image).

Note that the construction of \tilde{w} in the proof of Theorem 3.4.6 does not alter the total value of the right-hand side; it merely redistributes sharp and blunt angles between the two sums, such that each individual sum becomes non-positive.

Remark 3.4.7. If S_h is a non-singular simplicial surface with boundary, one can directly check that the right-hand side is non-positive for w : for any face f with a boundary 0-edge, it is $s_f = 1$. On the other hand, each boundary vertex must have at least two incident edges with non-zero weights, one of them pointing towards and the other away from it. Adding the two blunt corners at the boundary 0-edges, this gives $b_v \geq 3$ for every boundary vertex. Hence the summand $(2 - b_v) \leq -1$ compensates the positive summand $(2 - s_f) = 1$ for this configuration, and the right-hand side of (3.27) is indeed non-positive.

We now extend Theorem 3.4.6 to include the case that the weighting might have isolated 0-edges in the interior of S_h : these are inner edges e with $w(e) = 0$, which are adjacent to two triangles f_1 and f_2 such that each f_i is bounded by at least one edge e_i with $w(e_i) \neq 0$.

Corollary 3.4.8. Assume that $n_{bE}(S_h) > -2\chi(S_h)$. Then there is no quasi-harmonic weighting on S_h that vanishes on all boundary edges, but is non-zero on all inner edges or has at most isolated inner 0-edges.

Proof. Construct \tilde{w} as in the proof of Theorem 3.4.6. Now if e is an inner isolated 0-edge, then it is $s_{f_i} = 1$ for its two adjacent faces f_1, f_2 . Furthermore, its vertices $v_1 := t(e)$ and $v_2 := h(e)$ each form two blunt corners with e inside f_1 and f_2 . In addition, each v_i must have at least a third blunt inner corner, since the edges of f_1 and f_2 adjacent to v_i are non-zero and \tilde{w} is quasi-divergence free, see Figure 3.14 for an illustration. Therefore $b_{v_i} \geq 3$ for $i = 1, 2$, so $(2 - b_{v_i}) \leq -1$, compensating the positive summands $(2 - s_{f_i}) = 1$ in the sums on

the right-hand side of (3.27). Together with Theorem 3.4.6 this shows that the right-hand side is non-positive. \square

Turning back to the original question whether $\mathcal{H}_{h,N} \cap \mathcal{H}_{h,D} = \{0\}$, the following lemma relates harmonic vector fields in $\mathcal{H}_{h,N} \cap \mathcal{H}_{h,D}$ to quasi-harmonic weightings, provided the surface M_h is triangulated by a *Delaunay triangulation* as characterized in [BS07, Prop. 10]. Therein, an inner edge $e \in M_h^{(1)}$ is said to be *locally Delaunay* if for the angles α, β opposite to e in the two adjacent triangles it holds $\alpha + \beta < \pi$. A *Delaunay triangulation* of M_h then is a triangulation such that every inner edge e is *locally Delaunay*.

Lemma 3.4.9. *Let M_h be Delaunay and let $X \in \mathcal{H}_{h,N} \cap \mathcal{H}_{h,D}$. Then $R(X)$ is a quasi-harmonic weighting which vanishes on all boundary edges.*

Proof. Consider an edge orientation induced by $w := R(X)$. Since $X \in \mathcal{H}_{h,D} \perp J\nabla\mathcal{F}$, the cochain w is closed by Remark 3.2.2. In particular, if the boundary of any face is not formed by 0-edges only, it cannot be a directed edge cycle, so w is quasi-rotation-free. In addition, X is perpendicular to each boundary edge, so w vanishes on the boundary.

Moreover, since $X \in \mathcal{H}_{h,N} \perp \nabla\mathcal{L}$, for each vertex it is

$$0 = \langle X, \nabla\varphi_v \rangle_{L^2} = \frac{1}{2} \left(\sum_{e_i \in M_h^{(1)}:h(e_i)=v} (\cot \alpha_i + \cot \beta_i)w(e_i) - \sum_{e_i \in M_h^{(1)}:t(e_i)=v} (\cot \alpha_i + \cot \beta_i)w(e_i) \right).$$

Since M_h is Delaunay, all weights $(\cot \alpha_i + \cot \beta_i)$ are positive. Therefore, if a vertex v is not adjacent to 0-edges only, there must be at least one edge pointing towards v and another one pointing away from v , both with positive weight, so the weighting is quasi-divergence-free. \square

We would like to apply Theorem 3.4.6 to the quasi-harmonic weighting $w := R(X)$ coming from a vector field $X \in \mathcal{H}_{h,D} \cap \mathcal{H}_{h,N}$. If we knew that w was non-zero or had only isolated 0-edges in the interior of M_h , then Corollary 3.4.8 would immediately imply that $w \equiv 0$ whenever $n_{bE}(M_h) > -2\chi(M_h)$, showing that $\mathcal{H}_{h,D} \cap \mathcal{H}_{h,N}$ is trivial in this case. However, we do not know anything about w on interior edges. In particular there could be whole regions on which w vanishes.

The idea now is to only consider the *support* of X , denoted by $\text{supp}(X)$, i.e. the set of all triangles in M_h on which X is non-zero. These are all triangles which are adjacent to at least one edge e with $w(e) \neq 0$, but since w is quasi-rotation-free, it follows that each such triangle is actually bounded by two or three non-zero edges for w —the case of only one adjacent non-zero edge is not possible.

It is easy to see that the set $S_h := \text{supp}(X)$ is a possibly disconnected singular simplicial subsurface of M_h . The counterexamples in Figures 3.7 and 3.8 suggest that it is not enough to require the inequality $n_{bE}(M_h) > -2\chi(M_h)$ for the fixed surface M_h , but rather for any possibly singular subsurface of M_h . This motivates the *subsurface property*:

(SP) *Every singular simplicial subsurface $S_h \subseteq M_h$ satisfies $n_{bE}(S_h) > -2\chi(S_h)$.*

Theorem 3.4.10. *Let M_h be a simplicial surface with boundary such that*

1. M_h is a Delaunay mesh;
2. M_h satisfies the subsurface property (SP).

Then it is $\mathcal{H}_{h,D} \cap \mathcal{H}_{h,N} = \{0\}$.

Proof. Let $0 \neq X \in \mathcal{H}_{h,D} \cap \mathcal{H}_{h,N}$. Then $S_h := \text{supp}(X) \neq \emptyset$, and because M_h is Delaunay, it follows from Lemma 3.4.9 that $w := R(X)$ is a quasi-harmonic weighting on S_h , vanishing on all boundary edges in ∂S_h , and having at most isolated non-zero edges in the interior, being non-zero everywhere else. Since M_h satisfies property (SP), it is $n_{bE}(S_h) > -2\chi(S_h)$, and by Corollary 3.4.8 we conclude that such a weighting w cannot exist on S_h , a contradiction. Therefore $\mathcal{H}_{h,D} \cap \mathcal{H}_{h,N} = \{0\}$ as claimed. \square

As a consequence of Theorem 3.4.10, discrete Neumann fields are uniquely defined by their tangential projection along the boundary:

Corollary 3.4.11. *Let M_h satisfy the assumptions of Theorem 3.4.10. Then a discrete Neumann field $X \in \mathcal{H}_{h,N}$ is uniquely determined by its tangential projection onto the boundary.*

Proof. Let $X_1, X_2 \in \mathcal{H}_{h,N}$ such that $R(X_1)(e) = R(X_2)(e)$ for all boundary edges $e \in \partial M_h^{(1)}$. Then $X := X_1 - X_2$ satisfies $R(X)(e) = 0$ for all $e \in \partial M_h^{(1)}$, so $X \in \mathcal{H}_{h,N} \cap \mathcal{H}_{h,D}$. By Theorem 3.4.10 it is $X = 0$, so $X_1 = X_2$. \square

The subsurface property which lies at the heart of Theorem 3.4.10 ensures that subregions of topological complexity are well-connected within the mesh and to the boundary, and this is what essentially breaks down in the counterexamples in Figures 3.6 to 3.8. From a practical point of view, though, this ingredient is unsatisfying as it is expensive to check algorithmically. Nevertheless, the question of connectedness of subregions is already present in [BL02b], where the corresponding notion on networks is that of *separability of subgraphs* and it seems unavoidable to pose as a necessary condition.

Moreover, the reduction to weightings with values in $\{-1, 0, 1\}$ appears lossy since it straps off any metric information present on the level of harmonic PCVFs. Hence one could expect that the obtained bound $n_{bE}(S_h) > -2\chi(S_h)$ is too imprecise and could possibly be lowered. That this is not the case is demonstrated in Figure 3.15 on a geometry of type $\Sigma_{2,2}$ (so $\chi(M_h) = -4$), with eight boundary edges in total. This is a surprising result, as in all other considered examples the number of necessary boundary edges is the one computed in (3.25), which is half the size stated in the bound. It seems as if the symmetry of the geometry with respect to the locations of the boundaries plays another role and has an impact on the bound.

Finally, the transformation of a discrete harmonic field into a quasi-harmonic weighting requires the mesh to be Delaunay in order to ensure positivity of the cotangent weights. However, $R(X)$ can still be quasi-harmonic even though some edges are not locally Delaunay, so that this condition can likely be loosened, too. A complete answer to all these questions seems hard, though, and remains for future work.

Many geometries that arise in practice and possess reasonable triangulations satisfy (3.24). Particular care must be taken, though, if M_h has a very high genus in comparison to the number of boundary components (i.e. if $g \gg m$), if the grid discretization around the boundary

holes is particularly coarse, or if M_h can be roughly divided into a region capturing the boundaries and a region of high genus, both connected only by a very coarse discretization as in Figure 3.8, for instance.

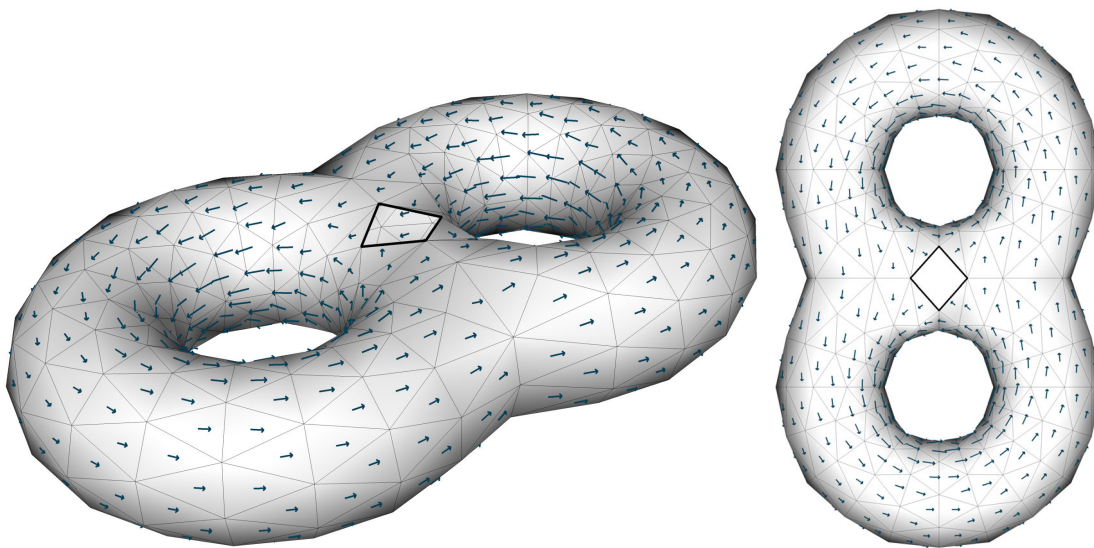


Figure 3.15: A symmetric pretzel surface with two opposite holes cut out. The surface mesh is Delaunay and has eight boundary edges, still there exists a non-trivial field in the intersection space $\mathcal{H}_{h,D} \cap \mathcal{H}_{h,N}$.

CONVERGENCE

We now prove convergence of the discrete decomposition results to their smooth counterparts, following the route suggested by Wardetzky in [War06]. This convergence relies on two approximation errors that need to be controlled: the error that is caused by the approximation of a smooth differential form by a discrete form, and the error that is caused by the approximation of a smooth manifold by a discrete mesh. Consequently, the convergence proof relies on the following ingredients, which are covered in detail in the next chapters:

1. The core ingredient is the convergence result obtained by Dodziuk [Dod76] which states roughly that on a smooth manifold the Whitney interpolants of cochains obtained by applying the de Rham projection to a smooth decomposition converge to the smooth components under refinement of the inscribed smooth triangulation. Dodziuk considers the case of a three-term Hodge-type decomposition into an exact, coexact and harmonic component. This result needs to be generalized to Whitney counterparts of the refined splittings of Neumann and Dirichlet fields into coexact and boundary-exact Neumann as well as exact and boundary-coexact Dirichlet fields.
2. Next, we combine the previous convergence statements with a sequence of metrics \tilde{g}_i converging to the smooth metric g : how does a g -orthogonal decomposition in Whitney spaces compare to decompositions which are orthogonal with respect to the metrics \tilde{g}_i ? This reflects the situation of approximating a smooth manifold by a triangular mesh with a piecewise flat metric, and pulling-back decompositions on the approximating mesh to the smooth manifold.
3. Finally, the corresponding decompositions for PCVFs need to be related to the decompositions of Whitney forms. To this end, we shall compare the projection to \mathcal{X}_h of a Whitney decomposition of a smooth vector field X with the PCVF decomposition of the projection of X to \mathcal{X}_h .

We shall be mainly interested in the refined fundamental decompositions

$$\begin{aligned}\Omega^k &= d\Omega^{k-1} \oplus \mathcal{H}_{N,\text{co}}^k \oplus \mathcal{H}_{N,\partial\text{ex}}^k \oplus \delta\Omega_N^{k+1} \\ &= d\Omega_D^{k-1} \oplus \mathcal{H}_{D,\text{ex}}^k \oplus \mathcal{H}_{D,\partial\text{co}}^k \oplus \delta\Omega^{k+1},\end{aligned}$$

as they contain the topologically relevant spaces. It poses no further problems to apply the same strategy to the other discrete decomposition statements. An analogous argument for the convergence of the corresponding decompositions on simplicial solids goes along the same lines so we shall only mention the few differences in Remark 4.3.4.

SMOOTH ADMISSIBLE TRIANGULATIONS. In the following, let $\{F_i : M \rightarrow M_{h_i}\}_{i \in \mathbb{N}}$ be a family of *smooth triangulations*, i.e. each F_i is a homeomorphism between M and an affine simplicial complex M_{h_i} which is a diffeomorphism when restricted to the preimage of any affine cell in M_{h_i} . The simplicial complex structure K_i on M_{h_i} pulls back to a (curved) simplicial complex structure $\tilde{K}_i := F_i^{-1}(K_{h_i})$ on M .

We will assume that this sequence of triangulations is a subdivision which behaves nicely in the following sense (cf. [Pat75]): define the *mesh size* \tilde{h}_i of \tilde{K}_i as

$$\tilde{h}_i := \sup_{\sigma \in \tilde{K}_i^{(n)}} \text{diam}(\sigma)$$

where $\text{diam}(\sigma)$ denotes the maximum distance of any two points in σ with respect to the Riemannian distance function induced by the metric g . Then this sequence of triangulations shall be such that, first, \tilde{K}_{i+1} is a subdivision of \tilde{K}_i for all i , second, $\tilde{h}_i \rightarrow 0$ for $i \rightarrow \infty$, and third, there is a constant c such that the Riemannian distance between any two vertices of a cell in \tilde{K}_i is bounded from below by $c \cdot \tilde{h}_i$. This latter condition ensures that each triangulation is homogeneous in the sense that all cells are about the same size, and in addition, that no triangles become arbitrarily thin. We will refer to a family of triangulations satisfying these criteria as an *admissible family of triangulations of M* .

4.1 GENERALIZING DODZIUK'S CONVERGENCE RESULT

Dodziuk has proved that the Whitney interpolation of the k -cochain whose values agrees with the integral of a smooth k -form ω on every k -simplex of a triangulation converges to ω in linear order of the mesh size. Furthermore he has defined a three-term Hodge decomposition for Whitney forms and proves convergence of the components to their smooth counterparts. In this section we extend his results to the refined splittings of Neumann and Dirichlet fields.

In this section, we consider the manifold M with its fixed metric g , together with an admissible family $\{F_i : M \rightarrow M_{h_i}\}_{i \in \mathbb{N}}$ of triangulations, inducing simplicial complex structures \tilde{K}_i of mesh size \tilde{h}_i on M . The scalar product and norm without any subscript always denote the L^2 -product and L^2 -norm with respect to the fixed metric g .

Let $\{\lambda_{h_i,j}\}$ denote the piecewise linear barycentric coordinates on M_{h_i} . Then their pullbacks $\{\tilde{\lambda}_{h_i,j} := F_i^* \lambda_{h_i,j}\}$ are barycentric coordinates on M , globally continuous and smooth on the interior of each cell of \tilde{K}_i . A k -form $\omega = d\lambda_{h_i,j_1} \wedge \cdots \wedge d\lambda_{h_i,j_k}$ on a cell of M_{h_i} corresponds to a pullback form $F_i^* \omega = d\tilde{\lambda}_{h_i,j_1} \wedge \cdots \wedge d\tilde{\lambda}_{h_i,j_k}$ on M . Consequently, the space of Whitney k -forms $\mathcal{W}^k(M_{h_i})$ on M_{h_i} pulls back to a space of Whitney k -forms on M , and we denote this space by $\mathcal{W}_i^k := \mathcal{W}_i^k(M)$. Elements in \mathcal{W}_i^k are smooth on every cell in \tilde{K}_i , but not continuous across interelement transitions (except for the case $k = 0$). Still, they have a well-defined tangential trace on facets as was shown in Lemma 3.1.4.

Associated to this family of spaces of Whitney k -forms are projection maps

$$\Phi_i^k := W_i^k \circ R_i^k : \Omega^k(M) \rightarrow \mathcal{W}_i^k,$$

each being the composition of the period map $R_i^k : \Omega^k(M) \rightarrow C^k(\tilde{K}_i)$ onto cochains and the Whitney interpolation map $W_i^k : C^k(\tilde{K}_i) \rightarrow \mathcal{W}_i^k$ to Whitney k -forms on M . For better readability we omit the index k for Φ_i in the following. Note that Φ_i maps exact k -forms to

exact Whitney k -forms, and closed k -forms to closed k -forms, which is a consequence of R_i^k and W_i^k being morphisms of complexes.

The Whitney map is a right-inverse to the period map $R_i^k : \Omega^k(M) \rightarrow C^k(\tilde{K}_i)$, i.e. $R_i^k \circ W_i^k$ is the identity on $C^k(\tilde{K}_i)$. Conversely, Dodziuk has proved that the element $\Phi_i(\omega)$ approximates the smooth form $\omega \in \Omega^k(M)$:

Theorem 4.1.1. *Let $\omega \in \Omega^k(M)$. Then there is a constant c_ω only depending on ω and the initial triangulation \tilde{K}_0 on M such that*

$$\|\omega - \Phi_i(\omega)\| \leq c_\omega \cdot \tilde{h}_i.$$

Proof. [Dod76, Thm. 3.7 and Cor. 3.27] □

FUNDAMENTAL DECOMPOSITIONS IN WHITNEY SPACES. In analogy with the smooth situation we consider the following spaces:

$$\begin{aligned} \mathcal{W}_{i,D}^k &:= \{\omega \in \mathcal{W}_i^k : \mathbf{t}(\omega) = 0 \text{ along } \partial M\} \\ d\mathcal{W}_{i,(D)}^{k-1} &:= \{d\omega : \omega \in \mathcal{W}_{i,(D)}^{k-1}\} \\ \mathcal{X}_i^k &:= \ker(d^k : \mathcal{W}_i^k \rightarrow \mathcal{W}_i^{k+1}) \\ \mathcal{X}_{i,D}^k &:= \ker(d^k|_{\mathcal{W}_{i,D}^k} : \mathcal{W}_{i,D}^k \rightarrow \mathcal{W}_{i,D}^{k+1}) \end{aligned}$$

The spaces of *harmonic Whitney Neumann and Dirichlet fields* are then defined as the L^2 -orthogonal complements

$$\begin{aligned} \mathcal{H}_{\mathcal{W}_{i,N}}^k &:= (d\mathcal{W}_i^{k-1})^{\perp_{\mathcal{X}_i^k}} \\ \mathcal{H}_{\mathcal{W}_{i,D}}^k &:= (d\mathcal{W}_{i,D}^{k-1})^{\perp_{\mathcal{X}_{i,D}^k}} \end{aligned}$$

within the kernel spaces \mathcal{X}_i^k and $\mathcal{X}_{i,D}^k$, respectively. We will need the following slightly modified version of Dodziuk's seminal result [Dod76, Thm. 4.9]:

Theorem 4.1.2 (Convergence of Fundamental Whitney Decompositions). *Let $\omega \in \Omega^k(M)$ and consider the smooth decompositions*

$$\begin{aligned} \omega &= d\alpha + \rho_N + \delta\beta_N \in d\Omega^{k-1} \oplus \mathcal{H}_N^k \oplus \delta\Omega_N^{k+1} \\ &= d\alpha_D + \rho_D + \delta\beta \in d\Omega_D^{k-1} \oplus \mathcal{H}_D^k \oplus \delta\Omega^{k+1} \end{aligned}$$

Let $\Phi_i(\omega) \in \mathcal{W}_i^k$ be the Whitney interpolant and let

$$\begin{aligned} \Phi_i(\omega) &= da_i + r_{i,N} + b_{i,N} \in d\mathcal{W}_i^{k-1} \oplus \mathcal{H}_{\mathcal{W}_{i,N}}^k \oplus (\mathcal{X}_i^k)^\perp \\ &= da_{i,D} + r_{i,D} + b_i \in d\mathcal{W}_{i,D}^{k-1} \oplus \mathcal{H}_{\mathcal{W}_{i,D}}^k \oplus (\mathcal{X}_{i,D}^k)^\perp \end{aligned}$$

be the L^2 -orthogonal decompositions in the space of Whitney k -forms. Then all components converge to their corresponding smooth components in linear order of the mesh size.

Proof. Dodziuk has proved this theorem for the case that the boundary consists of two disjoint closed submanifolds ∂M_1 and ∂M_2 such that ω itself obeys Dirichlet boundary conditions on ∂M_1 and Neumann boundary conditions on ∂M_2 . In our case we do not pose any boundary conditions on ω , but the proof still works the same way. Thus we just give a few comments on the proof, assuming the reader is familiar with the original proof in [Dod76, Thm. 4.9].

Dodziuk first considers the case where ω is harmonic. In our situation the harmonic parts under consideration are either ρ_N or ρ_D , corresponding to either $\partial M_1 = \emptyset$ or $\partial M_2 = \emptyset$ in Dodziuks setting. Therefore this case does not need any modifications.

Second, Dodziuk considers the orthogonal projection $P\Phi_i(\delta\beta_{(N)})$ of the Whitney interpolation of the coexact component onto the space of closed Whitney forms and concludes that this part tends to zero. In our situation we consider elements $w \in \mathcal{X}_i^k = d^*\mathcal{W}_i^{k-1} \oplus \mathcal{H}_{\mathcal{W}_i, N}^k$ and $w_D \in \mathcal{X}_{i, D}^k = d^*\mathcal{W}_{i, D}^{k-1} \oplus \mathcal{H}_{\mathcal{W}_i, D}^k$ and note that

$$\begin{aligned} \langle w, \delta\beta_N \rangle &= \langle dw, \beta_N \rangle - \int_{\partial M} \mathbf{t}(w) \wedge \star \mathbf{n}(\beta_N) = 0 \\ \langle w_D, \delta\beta \rangle &= \langle dw_D, \beta \rangle - \int_{\partial M} \mathbf{t}(w_D) \wedge \star \mathbf{n}(\beta) = 0 \end{aligned}$$

by (3.5), so the analogous estimates

$$\begin{aligned} | \langle P_i\Phi_i(\delta\beta_N), w \rangle | &= | \langle \Phi_i(\delta\beta_N), w \rangle | = | \langle \Phi_i(\delta\beta_N) - \delta\beta_N, w \rangle | \leq \| \Phi_i(\delta\beta_N) - \delta\beta_N \| \| w \| \\ | \langle P_{i, D}\Phi_i(\delta\beta_N), w \rangle | &= | \langle \Phi_i(\delta\beta), w_D \rangle | = | \langle \Phi_i(\delta\beta) - \delta\beta, w_D \rangle | \leq \| \Phi_i(\delta\beta) - \delta\beta \| \| w_D \| \end{aligned}$$

hold true and we conclude that the orthogonal projections $P_{i, D}\Phi_i(\delta\beta)$ and $P_i\Phi_i(\delta\beta_N)$ onto $\mathcal{X}_{i, D}^k$ and \mathcal{X}_i^k tend to zero.

The rest of the proof can be applied literally. In particular a definition for a discrete coderivative is not needed—the space of discrete coexact Whitney forms is replaced by the orthogonal complements of the kernels \mathcal{X}_i^k and $\mathcal{X}_{i, D}^k$. \square

In order to obtain refined decompositions representing inner and boundary cohomology we have to define analogues of (co-)exact and boundary (co-)exact Dirichlet and Neumann fields in the Whitney setting. We start with the Dirichlet fields. All convergence statements of the form $\|x_i - y_i\| \rightarrow 0$ are implicitly understood to hold for $i \rightarrow \infty$.

DIRICHLET SPLITTING. Define the spaces of exact and boundary-coexact Dirichlet Whitney forms by

$$\begin{aligned} \mathcal{H}_{\mathcal{W}_i, D, \text{ex}}^k &:= \mathcal{H}_{\mathcal{W}_i, D}^k \cap d^*\mathcal{W}_i^{k-1} \\ \mathcal{H}_{\mathcal{W}_i, D, \partial \text{co}}^k &:= (\mathcal{H}_{\mathcal{W}_i, D, \text{ex}}^k)^{\perp_{\mathcal{H}_{\mathcal{W}_i, D}^k}} \end{aligned}$$

with the orthogonal complement taken inside $\mathcal{H}_{\mathcal{W}_i, D}^k$. Since Φ_i preserves exactness we obtain as a consequence of Theorem 4.1.2

Lemma 4.1.3. *Let $\rho_D = d\sigma \in \mathcal{H}_{D, \text{ex}}^k$ be an exact Dirichlet k -form and let*

$$\Phi_i(\rho_D) = da_i + ds_i \in d^*\mathcal{W}_{i, D}^{k-1} \oplus \mathcal{H}_{\mathcal{W}_i, D, \text{ex}}^k.$$

Then $\|d\sigma - ds_i\| \rightarrow 0$.

Proof. From Theorem 4.1.2 it follows for the decomposition $\Phi_i(\rho_D) = da_i + ds_i$ that $\|da_i\| \rightarrow 0$, so $\|\rho_D - \Phi_i(\rho_D)\| \rightarrow 0$ implies $\|d\sigma - ds_i\| \rightarrow 0$. \square

We need the following orthogonality result:

Lemma 4.1.4. *Let $\tau \in \mathcal{H}_{D,\partial\text{co}}^k$ be a smooth boundary-coexact Dirichlet k -form and let $da \in d^*\mathcal{W}_i^{k-1}$ with $\mathbf{t}(da) = 0$. Then $\langle da, \tau \rangle = 0$.*

Proof. Since $\delta\tau = 0$, it is

$$\langle da, \tau \rangle = \int_{\partial M} \mathbf{t}(a) \wedge \star \mathbf{n}(\tau).$$

Now, τ is boundary-coexact, so by definition there is an element $\eta \in \Omega^{n-k-1}(\partial M)$ such that $\star \mathbf{n}(\tau) = \iota^*(\star \tau) = d\eta$, and η has a smooth extension to a form $\tilde{\eta} \in \Omega^{n-k-1}(M)$. By repeated use of Green's formula we obtain

$$\begin{aligned} \int_{\partial M} \mathbf{t}(a) \wedge \star \mathbf{n}(\tau) &= \int_{\partial M} \mathbf{t}(a) \wedge \mathbf{t}(d\tilde{\eta}) = \pm \int_{\partial M} \mathbf{t}(a) \wedge \mathbf{t}(\star \star d\tilde{\eta}) = \pm \int_{\partial M} \mathbf{t}(a) \wedge \star \mathbf{n}(\star d\tilde{\eta}) \\ &= \pm (\langle da, \star d\tilde{\eta} \rangle - \langle a, \delta \star d\tilde{\eta} \rangle) \\ &= \pm (\langle da, \delta \star \tilde{\eta} \rangle - \langle a, \delta \delta \star \tilde{\eta} \rangle) \\ &= \pm \langle da, \delta \star \tilde{\eta} \rangle = \pm \int_{\partial M} \mathbf{t}(da) \wedge \star \mathbf{n}(\star \tilde{\eta}) \end{aligned}$$

where the sign \pm depends on the numbers k and n , but obviously does not matter in the proof, because the last boundary integral vanishes as $\mathbf{t}(da) = 0$ by assumption. \square

Theorem 4.1.5 (Convergence of Dirichlet Splitting). *Let $\rho_D = d\sigma + \tau \in \mathcal{H}_{D,\text{ex}}^k \oplus \mathcal{H}_{D,\partial\text{co}}^k$ be a Dirichlet k -form and let*

$$\Phi_i(\rho_D) = da_i + ds_i + t_i \in d^*\mathcal{W}_{i,D}^{k-1} \oplus \mathcal{H}_{\mathcal{W}_{i,D},\text{ex}}^k \oplus \mathcal{H}_{\mathcal{W}_{i,D},\partial\text{co}}^k \quad (4.1)$$

denote its orthogonal decomposition in the space of Whitney forms. Then $\|d\sigma - ds_i\| \rightarrow 0$, $\|\tau - t_i\| \rightarrow 0$ and $\|da_i\| \rightarrow 0$.

Proof. First, let $\Phi_i(d\sigma) = da'_i + ds'_i \in d^*\mathcal{W}_{i,D}^{k-1} \oplus \mathcal{H}_{\mathcal{W}_{i,D},\text{ex}}^k$. From Lemma 4.1.3 we know that $\|da'_i\| \rightarrow 0$ and $\|d\sigma - ds'_i\| \rightarrow 0$. Now let $P_i : \mathcal{W}_i^k \rightarrow d^*\mathcal{W}_{i,D}^{k-1} \oplus \mathcal{H}_{\mathcal{W}_{i,D},\text{ex}}^k$ denote the orthogonal projection. For the second term we estimate as follows: for all $da + ds \in d^*\mathcal{W}_{i,D}^{k-1} \oplus \mathcal{H}_{\mathcal{W}_{i,D},\text{ex}}^k$ it is

$$\begin{aligned} \langle P_i \Phi_i(\tau), da + ds \rangle &= \langle \Phi_i(\tau), da + ds \rangle \\ &= \langle \Phi_i(\tau) - \tau, da + ds \rangle \\ &\leq \|\Phi_i(\tau) - \tau\| \|da + ds\| \end{aligned}$$

where we have used that $\langle \tau, da + ds \rangle = 0$ by Lemma 4.1.4. Thus by Riesz isometry it follows

$$\|P_i \Phi_i(\tau)\| \leq \|\Phi_i(\tau) - \tau\| \rightarrow 0$$

and by writing $P_i\Phi_i(\tau) = da_i'' + ds_i'' \in d\mathcal{W}_{i,D}^{k-1} \oplus \mathcal{H}_{\mathcal{W}_{i,D},\text{ex}}^k$ this implies $\|da_i''\| \rightarrow 0$ and $\|ds_i''\| \rightarrow 0$. Finally let $t_i' := \Phi_i(\tau) - P_i\Phi_i(\tau)$. We rewrite $\Phi_i(\rho_D)$ and reorder terms as follows:

$$\begin{aligned}\Phi_i(\rho_D) &= \Phi_i(d\sigma) + \Phi_i(\tau) \\ &= \Phi_i(d\sigma) + P_i\Phi_i(\tau) + (\Phi_i(\tau) - P_i\Phi_i(\tau)) \\ &= \underbrace{(da_i' + da_i'')}_{=da_i} + \underbrace{(ds_i' + ds_i'')}_{ds_i} + t_i' \in d\mathcal{W}_{i,D}^{k-1} \oplus \mathcal{H}_{\mathcal{W}_{i,D},\text{ex}}^k \oplus \mathcal{H}_{\mathcal{W}_{i,D},\partial\text{co}}^k\end{aligned}$$

Comparing with the decomposition (4.1), it follows $t_i = t_i'$ and we obtain

$$\begin{aligned}\|da_i\| &= \|da_i' + da_i''\| \leq \|da_i'\| + \|da_i''\| \rightarrow 0 \\ \|d\sigma - ds_i\| &= \|d\sigma - ds_i' - ds_i''\| \leq \|d\sigma - ds_i'\| + \|ds_i''\| \rightarrow 0 \\ \|\tau - t_i\| &= \|\tau - (\Phi_i(\tau) - P_i\Phi_i(\tau))\| \leq \|\tau - \Phi_i(\tau)\| + \|P_i\Phi_i(\tau)\| \rightarrow 0.\end{aligned}$$

□

Corollary 4.1.6. *For $\omega \in \Omega^k(M)$ let*

$$\omega = d\alpha_D + (d\sigma + \tau) + \delta\beta \in d\Omega_D^{k-1} \oplus (\mathcal{H}_{D,\text{ex}}^k \oplus \mathcal{H}_{D,\partial\text{co}}^k) \oplus \delta\Omega^{k+1}.$$

Then for the corresponding splitting of the Whitney interpolation

$$\Phi_i(\omega) = da_{i,D} + (ds_i + t_i) + b_i \in d\mathcal{W}_{i,D}^{k-1} \oplus (\mathcal{H}_{\mathcal{W}_{i,D},\text{ex}}^k \oplus \mathcal{H}_{\mathcal{W}_{i,D},\partial\text{co}}^k) \oplus (\mathcal{H}_{i,D}^k)^\perp$$

all components converge to their smooth counterparts.

Proof. Theorem 4.1.2 and Theorem 4.1.5. □

NEUMANN SPLITTING. We now consider the spaces of Whitney boundary-exact and co-exact Neumann fields

$$\begin{aligned}\mathcal{H}_{\mathcal{W}_{i,N},\partial\text{ex}}^k &:= \{w \in \mathcal{H}_{\mathcal{W}_{i,N},\text{co}}^k : \iota^*w = dp \text{ for some } p \in \mathcal{W}_i^{k-1}(\partial M)\} \\ \mathcal{H}_{\mathcal{W}_{i,N},\text{co}}^k &:= (\mathcal{H}_{\mathcal{W}_{i,N},\partial\text{ex}}^k)^\perp_{\mathcal{H}_{\mathcal{W}_{i,N}}^k}\end{aligned}$$

where the orthogonal complement is taken inside $\mathcal{H}_{\mathcal{W}_{i,N}}^k$. We need the following observation:

Lemma 4.1.7. *Let $\omega \in \Omega^k(M)$ be boundary-exact, i.e. there is a $(k-1)$ -form $\varphi \in \Omega^{k-1}(\partial M)$ such that $\iota^*\omega = d\varphi$. Then $\Phi_i(\omega)$ is a boundary-exact Whitney k -form, i.e. there is a Whitney $(k-1)$ -form $p \in \mathcal{W}_i^{k-1}(\partial M)$ such that $dp = \iota^*\Phi_i(\omega)$.*

Proof. The Whitney interpolation W_i^k as well as the period map R_i^k both commute with pull-back to the boundary. For W_i^k this is because barycentric coordinates over a subsimplex are restrictions of barycentric coordinates over the cell. For the period map (or more precisely the period maps R_i^k and $R_i^k|_{\partial M}$ on M and ∂M) it is

$$R_i^k|_{\partial M}(\iota^*\omega)(\tau) = \int_\tau j^*(\iota^*\omega) = \int_\tau \tilde{j}^*\omega = R_i^k(\omega)(\tau)$$

where $j : \tau \hookrightarrow \partial M$ and $\tilde{j} = \iota \circ j : \tau \hookrightarrow M$ denote the inclusions of an arbitrary k -simplex $\tau \in \partial M^{(k)}$ in ∂M and M , and therefore $R_i^k|_{\partial M}(\iota^*\omega) = \iota^*R_i^k(\omega)$. So Φ_i commutes with ι^* , and since both maps also commute with the exterior derivatives on M and ∂M , respectively, it is

$$\iota^*\Phi_i(\omega) = \Phi_i|_{\partial M}(\iota^*\omega) = \Phi_i|_{\partial M}(d\varphi) = d\Phi_i|_{\partial M}(\varphi) =: d\varphi.$$

□

Lemma 4.1.8. *Let $\tau \in \mathcal{H}_{N,\partial\text{ex}}^k$ and let*

$$\Phi_i(\tau) = da_i + s_i + t_i \in d\mathcal{W}_i^{k-1} \oplus \mathcal{H}_{\mathcal{W}_i,N,\text{co}}^k \oplus \mathcal{H}_{\mathcal{W}_i,N,\partial\text{ex}}^k.$$

Then $s_i = 0$, $\|da_i\| \rightarrow 0$ and consequently $\|\tau - t_i\| \rightarrow 0$.

Proof. da_i is boundary-exact and t_i is boundary-exact by definition. By Lemma 4.1.7, $\Phi_i(\tau)$ is boundary-exact, too, and so must be $s_i = \Phi_i(\tau) - da_i - t_i$, i.e. $s_i \in \mathcal{H}_{\mathcal{W}_i,N,\text{co}}^k \cap \mathcal{H}_{\mathcal{W}_i,N,\partial\text{ex}}^k = \{0\}$. From Theorem 4.1.2 it follows $\|da_i\| \rightarrow 0$, which implies $\|\tau - t_i\| \rightarrow 0$. □

Again, we need an orthogonality result between smooth forms and Whitney forms, which is in some sense dual to Lemma 4.1.4:

Lemma 4.1.9. *Let $\delta\sigma \in \mathcal{H}_{N,\text{co}}^k$ be a smooth coexact Neumann field. Let $da \in d\mathcal{W}_i^{k-1}$ be an exact Whitney form and $t \in \mathcal{H}_{\mathcal{W}_i,N,\partial\text{ex}}^k$ a boundary-exact Whitney form. Then*

$$\langle da, \delta\sigma \rangle = \langle t, \delta\sigma \rangle = 0.$$

Proof. The first case is simple:

$$\langle da, \delta\sigma \rangle = \langle a, \delta\delta\sigma \rangle + \int_{\partial M} \mathbf{t}(a) \wedge \star \mathbf{n}(\delta\sigma) = 0$$

since $\mathbf{n}(\delta\sigma) = 0$. For the second case, let $\iota^*t = d\tilde{p}$ for some $p \in \mathcal{W}_i^{k-1}(\partial M)$ and let $\tilde{p} \in \mathcal{W}_i^{k-1}(M)$ be an arbitrary extension of p to M . Again by repeated use of Green's formula we obtain

$$\begin{aligned} \langle t, \delta\sigma \rangle &= \langle dt, \sigma \rangle - \int_{\partial M} \mathbf{t}(t) \wedge \star \mathbf{n}(\delta\sigma) = - \int_{\partial M} \mathbf{t}(d\tilde{p}) \wedge \star \mathbf{n}(\delta\sigma) \\ &= \langle d\tilde{p}, \delta\sigma \rangle - \langle dd\tilde{p}, \sigma \rangle = \langle d\tilde{p}, \delta\sigma \rangle \\ &= \langle \tilde{p}, \delta\delta\sigma \rangle + \int_{\partial M} \mathbf{t}(\tilde{p}) \wedge \star \mathbf{n}(\delta\sigma) = 0. \end{aligned}$$

□

Theorem 4.1.10 (Convergence of Neumann Splitting). *Let $\rho_N = \delta\sigma + \tau \in \mathcal{H}_{N,\text{co}}^k \oplus \mathcal{H}_{N,\partial\text{ex}}^k$ be a Neumann k -form and let*

$$\Phi(\rho_N) = da_i + s_i + t_i \in d\mathcal{W}_i^{k-1} \oplus \mathcal{H}_{\mathcal{W}_i,N,\text{co}}^k \oplus \mathcal{H}_{\mathcal{W}_i,N,\partial\text{ex}}^k \quad (4.2)$$

denote its orthogonal decomposition in the space of Whitney forms. Then $\|\delta\sigma - s_i\| \rightarrow 0$, $\|\tau - t_i\| \rightarrow 0$ and consequently $\|da_i\| \rightarrow 0$.

Proof. The proof is similar to Theorem 4.1.5. First let $\Phi_i(\tau) = da'_i + t'_i$. We know from Lemma 4.1.8 that $\|da'_i\| \rightarrow 0$ and $\|\tau - t'_i\| \rightarrow 0$. Now let $P_i : \mathcal{W}_i^k \rightarrow d^*\mathcal{W}_i^{k-1} \oplus \mathcal{H}_{\mathcal{W}_i, N, \partial \text{ex}}^k$ denote the orthogonal projection. Then for all $da + t \in d^*\mathcal{W}_i^{k-1} \oplus \mathcal{H}_{\mathcal{W}_i, N, \partial \text{ex}}^k$ it is

$$\begin{aligned} \langle P_i \Phi_i(\delta\sigma), da + t \rangle &= \langle \Phi_i(\delta\sigma), da + t \rangle \\ &= \langle \Phi_i(\delta\sigma) - \delta\sigma, da + t \rangle \\ &\leq \|\Phi_i(\delta\sigma) - \delta\sigma\| \|da + t\| \end{aligned}$$

since $\langle \delta\sigma, da + t \rangle = 0$ by Lemma 4.1.9, and again by Riesz isometry we conclude

$$\|P_i \Phi_i(\delta\sigma)\| \leq \|\Phi_i(\delta\sigma) - \delta\sigma\| \rightarrow 0.$$

Writing $P_i \Phi_i(\delta\sigma) = da''_i + t''_i$ this implies $\|da''_i\| \rightarrow 0$ and $\|t''_i\| \rightarrow 0$. Finally, let $s'_i = \Phi_i(\delta\sigma) - P_i \Phi_i(\delta\sigma)$, then

$$\begin{aligned} \Phi_i(\rho_N) &= \Phi_i(\delta\sigma) + \Phi_i(\tau) \\ &= P_i \Phi_i(\delta\sigma) + (\Phi_i(\delta\sigma) - P_i \Phi_i(\delta\sigma)) + \Phi_i(\tau) \\ &= \underbrace{(da'_i + da''_i)}_{=da_i} + s'_i + \underbrace{(t'_i + t''_i)}_{=t_i} \in d^*\mathcal{W}_i^{k-1} \oplus \mathcal{H}_{\mathcal{W}_i, N, \text{co}}^k \oplus \mathcal{H}_{\mathcal{W}_i, N, \partial \text{ex}}^k \end{aligned}$$

and, comparing with (4.2), we obtain $s'_i = s_i$ and

$$\begin{aligned} \|da_i\| &= \|da'_i + da''_i\| \leq \|da'_i\| + \|da''_i\| \rightarrow 0 \\ \|\delta\sigma - s_i\| &= \|\delta\sigma - (\Phi_i(\delta\sigma) - P_i \Phi_i(\delta\sigma))\| \leq \|\delta\sigma - \Phi_i(\delta\sigma)\| + \|P_i \Phi_i(\delta\sigma)\| \rightarrow 0 \\ \|\tau - t_i\| &= \|\tau - t'_i - t''_i\| \leq \|\tau - t'_i\| + \|t''_i\| \rightarrow 0. \end{aligned}$$

□

Corollary 4.1.11. For $\omega \in \Omega^k(M)$ let

$$\omega = da + (\delta\sigma + \tau) + \delta\beta_N \in d\Omega^{k-1} \oplus (\mathcal{H}_{N, \text{co}}^k \oplus \mathcal{H}_{N, \partial \text{ex}}^k) \oplus \delta\Omega_N^{k+1}.$$

Then for the corresponding splitting of the Whitney interpolation

$$\Phi_i(\omega) = da_i + (s_i + t_i) + b_{i, N} \in d^*\mathcal{W}_i^{k-1} \oplus (\mathcal{H}_{\mathcal{W}_i, N, \text{co}}^k \oplus \mathcal{H}_{\mathcal{W}_i, N, \partial \text{ex}}^k) \oplus (\mathcal{X}_i^k)^\perp$$

all components converge to their smooth counterparts.

Proof. Theorem 4.1.2 and Theorem 4.1.10. □

Remark 4.1.12. Crucial to all of these convergence proofs is the reference to the Whitney approximation $\|\omega - \Phi_i(\omega)\|$, and this was shown by Dodziuk to converge linearly in the mesh size \tilde{h}_i , cf. Theorem 4.1.1. As a consequence, the Dirichlet and Neumann splittings converge in linear order of the mesh size, too.

Remark 4.1.13. *Dodziuk's original work [Dod76] involves the definition of a combinatorial coderivative operator $\delta_\Delta : C^{k+1}(M, \partial M) \rightarrow C^k(M, \partial M)$ on the level of cochains, defined as the formal adjoint to the simplicial exterior derivative d_Δ by*

$$\langle d_\Delta c, c' \rangle_\Delta = \langle c, \delta_\Delta c' \rangle_\Delta \quad \text{for all } c \in C^k(M, \partial M), c' \in C^{k+1}(M, \partial M),$$

where the inner product $\langle -, - \rangle_\Delta$ on cochains is defined as the L^2 -product of the respective Whitney interpolants, turning the Whitney interpolation into an isometry. However at the time the article was written it was unclear if this discretization provides a consistent approximation of the smooth coderivative.

More recently, Smits found a positive partial answer to this question for the special case of 1-forms on a triangulated surface under refinement by a regular standard subdivision [Smi91], but the general case (general subdivision schemes, more than two dimensions, k -forms for $k > 1$) remained an open problem.

Only two years ago Arnold et al. [AFGT14] could indeed generalize Smits' result for 1-forms to arbitrary dimensions, provided that the refinement follows a strict subdivision scheme. At the same time they found a counterexample demonstrating that one cannot loosen the assumption on the subdivision scheme, and a numerical experiment shows that there is in general no hope for consistency for arbitrary $1 < k < n$.

Since we are mostly interested in a precise characterization of piecewise constant harmonic fields we did not introduce a combinatorial codifferential, but merely work directly with the kernel spaces $\mathcal{K}_{(D)}^k$ and their orthogonal complements. Moreover, the decompositions in Section 3.3 for PCVFs on simplicial solids correspond to a Whitney approximation by 2-forms for which the experiment in [AFGT14] gives an impressive counterexample to a consistent discrete coderivative, even under a highly regular and uniform refinement rule.

4.2 CONVERGENCE WITH APPROXIMATING METRICS

We now consider the situation of approximating a compact smooth manifold with boundary (M, g) by a sequence of simplicial meshes, each equipped with the piecewise Euclidean metric. These metrics pull back to distorted metrics \tilde{g}_i on M which define a different notion of orthogonality on M . If the distortion induced by the pullback is low, the orthogonal decompositions of Whitney form spaces with respect to g and \tilde{g}_i are close to each other. In particular, for an admissible family of triangulations converging metrically to M , all components converge to each other and by the previous chapter also to the corresponding components of a smooth decomposition.

METRIC DISTORTION. In this chapter we interpret the admissible family of triangulations $\{F_i : M \rightarrow M_{h_i}\}$ as a sequence of piecewise flat meshes approximating a smooth limit mesh. To this end assume that each M_{h_i} is equipped with the locally Euclidean metric g_{h_i} .

The homeomorphisms F_i induce a sequence of pulled-back metrics $\tilde{g}_i := F_i^* g_{h_i}$ on M , which are defined almost everywhere, except for the $(n-1)$ -skeleton of M , and smooth in the interior of every cell. Therefore the induced *metric distortion tensors* Λ_i , implicitly defined almost everywhere by

$$g(\Lambda_i X, Y) := \tilde{g}_i(X, Y) = g_{h_i}(F_* X, F_* Y) \quad \text{for all } X, Y \in \mathcal{X}(M),$$

are smooth, symmetric and positive definite in the interior of every cell of M , too.

The sequence $\{\Lambda_i\}$ of tensor fields measures the deviation of the pulled-back metrics \tilde{g}_i from the smooth metric g . Intuitively, an appropriate approximation should ultimately yield a distortion tensor Λ_i that is close to the identity. At any point p in the interior of a cell, let

$$\|(\Lambda_i)_p\|_p := \sup_{X_p \in T_p M, \|X_p\|_p=1} \|(\Lambda_i)_p X_p\|_p$$

denote its operator norm on $T_p M$, which equals the eigenvalue of Λ_i of maximum magnitude. Let

$$\|\Lambda_i\|_{L^\infty} := \operatorname{ess\,sup}_{p \in M} \|(\Lambda_i)_p\|_p$$

denote the essential supremum of these norms over M . Then $\|\Lambda_i - \operatorname{Id}\|_{L^\infty}$ can be interpreted as the maximal deviation of the distortion tensor Λ_i from the identity, and consequently $\|\Lambda_i - \operatorname{Id}\|_{L^\infty} \rightarrow 0$ is what is meant by *metric convergence*. Equivalently, the essential suprema of all eigenvalues of Λ_i , considered as functions over M , shall tend to 1.

Definition 4.2.1 (Metric Convergence). *The sequence $\{(M_{h_i}, g_{h_i})\}_{i \in \mathbb{N}}$ converges metrically to (M, g) if for the distortion tensors Λ_i it is $\|\Lambda_i - \operatorname{Id}\|_{L^\infty} \rightarrow 0$ for $i \rightarrow \infty$.*

As before, we write $\langle -, - \rangle, \|-\|, \sharp, \oplus$ for the L^2 -product, L^2 -norm and operators depending on the fixed metric g on M without any subscript. In contrast, we write $\langle -, - \rangle_{g_{h_i}}, \|-\|_{g_{h_i}}, \sharp_{h_i}, \oplus_{h_i}$ for the objects on M_{h_i} with respect to the piecewise flat metric g_{h_i} , and $\langle -, - \rangle_{\tilde{g}_i}, \|-\|_{\tilde{g}_i}, \sharp_{\tilde{g}_i}, \oplus_{\tilde{g}_i}$ for the corresponding objects on M with respect to the pulled-back metric \tilde{g}_i . The pulled-back L^2 -product $\langle -, - \rangle_{\tilde{g}_i}$ on $\Omega^k(M)$ then reads as

$$\langle \omega, \eta \rangle_{\tilde{g}_i} = \langle F_{i*} \omega, F_{i*} \eta \rangle_{g_{h_i}},$$

i.e. it is the L^2 -product of the pushforwards on M_{h_i} with respect to g_{h_i} . As a special case, the L^2 -product on $\mathcal{X}_h(M_{h_i})$ pulls back to an L^2 -product on $\mathcal{X}(M)$ given by

$$\langle X, Y \rangle_{\tilde{g}_i} := \int_{M_{h_i}} g_{h_i}(F_*X, F_*Y) \mu_{M_{h_i}} = \int_M g(\Lambda_i X, Y) \sqrt{\det(\Lambda_i)} \mu_M.$$

Furthermore, the isomorphisms \sharp and $\tilde{\sharp}_i$ are related by $\omega^{\tilde{\sharp}_i} = \Lambda_i^{-1} \omega^\sharp$ for $\omega \in \Omega^1(M)$.

In the following we make use of a norm estimate given by Stern in [Ste13]. Therein, he introduces the notion of *singular values of a diffeomorphism* $F : (M, g_M) \rightarrow (N, g_N)$ between smooth manifolds as follows: at each point $p \in M$, pick an oriented g_M -orthonormal basis of $T_p M$, and an oriented g_N -orthonormal basis of $T_{F(p)} N$. With respect to these two bases, the Jacobian DF is represented by an $(n \times n)$ -matrix with singular values $\varsigma_1(p) \geq \varsigma_2(p) \geq \dots \geq \varsigma_n(p) > 0$, which are independent of the choice of the orthonormal bases. These ordered singular values extend to functions $\varsigma_j : M \rightarrow \mathbb{R}$, which are called the singular values of the diffeomorphism. Stern then shows for the L^2 -norms on compact manifolds:

Theorem 4.2.2. *Let $F : (M, g_M) \rightarrow (N, g_N)$ be an orientation-preserving diffeomorphism between compact Riemannian manifolds with singular values $\varsigma_1(p) \geq \dots \geq \varsigma_n(p) > 0$. Then, setting*

$$\begin{aligned} c_\varsigma &:= \left\| (\varsigma_1 \cdots \varsigma_k)^{1/2} (\varsigma_{k+1} \cdots \varsigma_n)^{-1/2} \right\|_\infty^{-1} \\ C_\varsigma &:= \left\| (\varsigma_1 \cdots \varsigma_{n-k})^{1/2} (\varsigma_{n-k+1} \cdots \varsigma_n)^{-1/2} \right\|_\infty, \end{aligned}$$

the following norm equivalence estimate holds for any k -form $\omega \in \Omega^k(M)$:

$$c_\varsigma \|\omega\|_{L^2(M)} \leq \|F_*\omega\|_{L^2(N)} \leq C_\varsigma \|\omega\|_{L^2(M)}. \quad (4.3)$$

Proof. [Ste13, Thm. 5 and Cor. 6] □

Remark 4.2.3. *Although phrased for diffeomorphisms between smooth manifolds, Stern's estimate also applies to our situation where the homeomorphisms $F_i : M \rightarrow M_{h_i}$ are merely piecewise diffeomorphic, because the $(n-1)$ -skeleton is a set of measure zero for the L^2 -product. The sup norm arising in the definition of the constants in Theorem 4.2.2 is then replaced by the essential sup norm.*

The following lemma is an estimate which appears for 1-forms in [War06], albeit with a different bound. Here we generalize it to k -forms.

Lemma 4.2.4. Let $\omega, \eta \in \Omega^k(M)$, and let $c_{\zeta,i}, C_{\zeta,i}$ denote the constants from Theorem 4.2.2 for the piecewise diffeomorphism $F_i : M \rightarrow M_{h_i}$. Then

$$|\langle \omega, \eta \rangle - \langle \omega, \eta \rangle_{\tilde{g}_i}| \leq \frac{1}{2} \cdot \max \left\{ \left| 1 - c_{\zeta,i}^2 \right|, \left| 1 - C_{\zeta,i}^2 \right| \right\} \cdot (\|\omega\|^2 + \|\eta\|^2). \quad (4.4)$$

Proof. The bound is a consequence of the polarization identity for the scalar products:

$$\begin{aligned} |\langle \omega, \eta \rangle - \langle \omega, \eta \rangle_{\tilde{g}_i}| &= \left| \langle \omega, \eta \rangle - \langle F_{i*}\omega, F_{i*}\eta \rangle_{g_{h_i}} \right| \\ &= \frac{1}{4} \left| \|\omega + \eta\|^2 - \|\omega - \eta\|^2 - \|F_{i*}(\omega + \eta)\|_{g_{h_i}}^2 + \|F_{i*}(\omega - \eta)\|_{g_{h_i}}^2 \right| \\ &\leq \frac{1}{4} \left(\left| \|\omega + \eta\|^2 - \|F_{i*}(\omega + \eta)\|_{g_{h_i}}^2 \right| + \left| \|\omega - \eta\|^2 - \|F_{i*}(\omega - \eta)\|_{g_{h_i}}^2 \right| \right) \\ &\leq \frac{1}{4} \cdot \max \left\{ \left| 1 - c_{\zeta,i}^2 \right|, \left| 1 - C_{\zeta,i}^2 \right| \right\} \cdot (\|\omega + \eta\|^2 + \|\omega - \eta\|^2) \\ &= \frac{1}{4} \cdot \max \left\{ \left| 1 - c_{\zeta,i}^2 \right|, \left| 1 - C_{\zeta,i}^2 \right| \right\} \cdot 2(\|\omega\|^2 + \|\eta\|^2) \end{aligned}$$

where the last inequality incorporates the bounds from Theorem 4.2.2. \square

In the following it will be convenient to set

$$\epsilon_i := \max \left\{ \left| 1 - c_{\zeta,i}^2 \right|, \left| 1 - C_{\zeta,i}^2 \right| \right\}.$$

Corollary 4.2.5. For $0 \neq \omega \in \Omega^k(M)$, it is

$$\left| 1 - \frac{\|\omega\|_{\tilde{g}_i}^2}{\|\omega\|^2} \right| \leq \epsilon_i.$$

Proof. Follows immediately from Lemma 4.2.4 with $\eta = \omega$. \square

Corollary 4.2.6. Let $\{M_{h_i}\}$ converge metrically to M . Then for any $\omega, \eta \in \Omega^k(M)$ it is

$$|\langle \omega, \eta \rangle - \langle \omega, \eta \rangle_{\tilde{g}_i}| \rightarrow 0 \quad \text{and} \quad \left| 1 - \frac{\|\omega\|_{\tilde{g}_i}^2}{\|\omega\|^2} \right| \rightarrow 0.$$

Proof. The metric convergence $\|\Lambda_i - \text{Id}\|_{L^\infty} \rightarrow 0$ implies that the essential suprema of the eigenvalues of Λ_i , considered as functions over M , tend to 1. Since these eigenvalues are the squares of the singular values of the Jacobian DF_i for any orthonormal basis, this implies that the essential suprema of all singular values $\{\zeta_j\}$ tend to 1, which in turn implies $c_{\zeta,i} \rightarrow 1$ and $C_{\zeta,i} \rightarrow 1$, so that $\epsilon_i \rightarrow 0$. The result now follows from Lemma 4.2.4 and Corollary 4.2.5. \square

DISTORTED DECOMPOSITIONS IN WHITNEY SPACES. In the following we denote by da , r , $\mathcal{H}_{\mathcal{W}_i, D}^k$ and so on elements and spaces defined by the metric g , and by $d\tilde{a}_i$, \tilde{r}_i , $\widetilde{\mathcal{H}_{\mathcal{W}_i, D}^k}$ and so on elements and spaces defined by the distorted metrics \tilde{g}_i . Note that the spaces of exact forms $d\mathcal{W}_{i, (D)}^{k-1}$ as well as the kernel spaces $\mathcal{K}_{i, (D)}^k$ are not affected by a change of metric, whereas all other spaces—defined as orthogonal complements of certain subspaces—are.

Lemma 4.2.7. *Let $\omega \in \Omega^k(M)$ and let*

$$\Phi_i(\omega) = da_i + r_{i, N} + b_{i, N} \in d\mathcal{W}_i^{k-1} \oplus \mathcal{H}_{\mathcal{W}_i, N}^k \oplus (\mathcal{K}_i^k)^\perp \quad (4.5)$$

$$= d\tilde{a}_i + \tilde{r}_{i, N} + \tilde{b}_{i, N} \in d\mathcal{W}_i^{k-1} \tilde{\Phi}_i \widetilde{\mathcal{H}_{\mathcal{W}_i, N}^k} \tilde{\Phi}_i \widetilde{(\mathcal{K}_i^k)^\perp} \quad (4.6)$$

and

$$\Phi_i(\omega) = da_{i, D} + r_{i, D} + b_i \in d\mathcal{W}_{i, D}^{k-1} \oplus \mathcal{H}_{\mathcal{W}_{i, D}}^k \oplus (\mathcal{K}_{i, D}^k)^\perp \quad (4.7)$$

$$= d\tilde{a}_{i, D} + \tilde{r}_{i, D} + \tilde{b}_i \in d\mathcal{W}_{i, D}^{k-1} \tilde{\Phi}_i \widetilde{\mathcal{H}_{\mathcal{W}_{i, D}}^k} \tilde{\Phi}_i \widetilde{(\mathcal{K}_{i, D}^k)^\perp} \quad (4.8)$$

denote its fundamental decompositions with respect to the metrics g and \tilde{g}_i , respectively. Then, if the sequence $\{M_{h_i}\}$ converges metrically to M , all components converge to each other in the L^2 -norm with respect to g on M .

Proof. This was proved in [War06, Thm. 3.4.6] for the case of 1-forms on a closed surface. The proof applies also to our situation, with a slightly modified argumentation. For instance, for the exact component it is

$$\begin{aligned} \|da_i - d\tilde{a}_i\|^2 &= \langle da_i - d\tilde{a}_i, da_i - d\tilde{a}_i \rangle \\ &= \langle da_i - d\tilde{a}_i, (da_i - \Phi_i(\omega)) + (\Phi_i(\omega) - d\tilde{a}_i) \rangle \\ &= \langle da_i - d\tilde{a}_i, \Phi_i(\omega) - d\tilde{a}_i \rangle \end{aligned}$$

since $(da_i - \Phi_i(\omega))$ is orthogonal to $d\mathcal{W}_i^{k-1}$ for $\langle -, - \rangle$. In contrast, $(\Phi_i(\omega) - d\tilde{a}_i)$ is orthogonal to $d\mathcal{W}_i^{k-1}$ with respect to the product $\langle -, - \rangle_{\tilde{g}_i}$, but not for $\langle -, - \rangle$. Using Lemma 4.2.4, this gives

$$\begin{aligned} \|da_i - d\tilde{a}_i\|^2 &= \left| \langle da_i - d\tilde{a}_i, \Phi_i(\omega) - d\tilde{a}_i \rangle - \langle da_i - d\tilde{a}_i, \Phi_i(\omega) - d\tilde{a}_i \rangle_{\tilde{g}_i} \right| \\ &\leq \frac{1}{2} \epsilon_i \left(\|da_i + \Phi_i(\omega) - 2d\tilde{a}_i\|^2 + \|da_i - \Phi_i(\omega)\|^2 \right). \end{aligned}$$

Metric convergence implies $\epsilon_i \rightarrow 0$. Furthermore, da_i and $\Phi_i(\omega)$ are bounded in the $\|-\|$ -norm, as they converge to the corresponding components of the (bounded) smooth form ω by Theorem 4.1.2, and $\|d\tilde{a}_i\|$ is bounded due to the equivalence of the norms (4.3) and the fact that $\|d\tilde{a}_i\|_{\tilde{g}_i} \leq \|\Phi_i(\omega)\|_{\tilde{g}_i}$ is bounded. Overall, it follows $\|da_i - d\tilde{a}_i\|^2 \rightarrow 0$. A similarly adjusted argument shows the convergence of the other two components in the respective decompositions. \square

To show the convergence of the Dirichlet and Neumann splittings with respect to the distorted metric, we need the following lemma which is tailored to our situation.

Lemma 4.2.8. Let $(X, \langle -, - \rangle)$ be a space with inner product $\langle -, - \rangle$, and let $\{E_i\}$, $\{K_i\}$, $\{Z_i\}$ be sequences of finite-dimensional subspaces of X with $E_i \subseteq K_i \cap Z_i$. Let $\{\langle -, - \rangle_i\}$ denote a sequence of inner products on X such that

$$|\langle x, y \rangle - \langle x, y \rangle_i| \leq \epsilon'_i (\|x\|^2 + \|y\|^2) \quad \text{for all } x, y \in X \quad (4.9)$$

with $\epsilon'_i \rightarrow 0$ for $i \rightarrow \infty$, where $\|-\|$ is the norm induced by $\langle -, - \rangle$. For each $i \in \mathbb{N}$, define H_i and \tilde{H}_i as the orthogonal complements of E_i within K_i with respect to $\langle -, - \rangle$ and $\langle -, - \rangle_i$, i.e.

$$\begin{aligned} E_i \oplus H_i &:= K_i \\ E_i \tilde{\Theta}_i \tilde{H}_i &:= K_i. \end{aligned}$$

Let $U_i := H_i \cap Z_i$ and $\tilde{U}_i := \tilde{H}_i \cap Z_i$, and again define V_i and \tilde{V}_i as orthogonal complements within H_i and \tilde{H}_i by

$$\begin{aligned} U_i \oplus V_i &:= H_i \\ \tilde{U}_i \tilde{\Theta}_i \tilde{V}_i &:= \tilde{H}_i. \end{aligned}$$

Finally, let $\{r_i \in H_i\}$, $\{\tilde{r}_i \in \tilde{H}_i\}$ be sequences such that $\|r_i - \tilde{r}_i\| \rightarrow 0$ and $\|r_i\|$ (or equivalently $\|\tilde{r}_i\|$) stays bounded. Then for the orthogonal decompositions

$$\begin{aligned} r_i &= u_i + v_i \in U_i \oplus V_i \\ \tilde{r}_i &= \tilde{u}_i + \tilde{v}_i \in \tilde{U}_i \tilde{\Theta}_i \tilde{V}_i \end{aligned}$$

it holds $\|u_i - \tilde{u}_i\| \rightarrow 0$ and $\|v_i - \tilde{v}_i\| \rightarrow 0$.

Proof. Let $P_i : K_i \rightarrow K_i \cap Z_i$ and $\tilde{P}_i : K_i \rightarrow K_i \cap Z_i$ denote the orthogonal projections with respect to $\langle -, - \rangle$ and $\langle -, - \rangle_i$, respectively. Since $E_i \subseteq Z_i$, the intersection $K_i \cap Z_i$ has the orthogonal decompositions

$$\begin{aligned} K_i \cap Z_i &= E_i \cap Z_i \oplus H_i \cap Z_i = E_i \oplus U_i \\ &= E_i \cap Z_i \tilde{\Theta}_i \tilde{H}_i \cap Z_i = E_i \tilde{\Theta}_i \tilde{U}_i \end{aligned}$$

and consequently, $P_i r_i = u_i$ and $\tilde{P}_i \tilde{r}_i = \tilde{u}_i$. We then have

$$\begin{aligned} \|u_i - \tilde{u}_i\| &= \|P_i r_i - \tilde{P}_i \tilde{r}_i\| \leq \|P_i r_i - P_i \tilde{r}_i\| + \|P_i \tilde{r}_i - \tilde{P}_i \tilde{r}_i\| \\ &\leq \|P_i\| \|r_i - \tilde{r}_i\| + \|(P_i - \tilde{P}_i) \tilde{r}_i\|. \end{aligned}$$

Since P_i is an orthogonal projection with respect to $\langle -, - \rangle$, it is $\|P_i\| = 1$, and $\|r_i - \tilde{r}_i\| \rightarrow 0$ by assumption. For the second term, note that since u_i and \tilde{u}_i are orthogonal projections to $K_i \cap Z_i$, it is

$$\left. \begin{aligned} \langle u_i, z \rangle &= \langle r_i, z \rangle \\ \langle \tilde{u}_i, z \rangle_i &= \langle \tilde{r}_i, z \rangle_i \end{aligned} \right\} \text{ for all } z \in K_i \cap Z_i.$$

Then with $z_i := P_i \tilde{r}_i$, the convergence assumption (4.9) and Riesz isometry yield over $K_i \cap Z_i$:

$$\begin{aligned}
 \|(P_i - \tilde{P}_i)\tilde{r}_i\| &= \|z_i - \tilde{u}_i\| = \|\langle z_i - \tilde{u}_i, - \rangle\| \\
 &= \sup_{\|z\|=1} \|\langle z_i - \tilde{u}_i, z \rangle\| = \sup_{\|z\|=1} \|\langle z_i, z \rangle - \langle \tilde{u}_i, z \rangle\| \\
 &\leq \sup_{\|z\|=1} \|\langle z_i, z \rangle - \langle \tilde{r}_i, z \rangle_i\| + \sup_{\|z\|=1} \|\langle \tilde{r}_i, z \rangle_i - \langle \tilde{u}_i, z \rangle\| \\
 &= \sup_{\|z\|=1} \|\langle \tilde{r}_i, z \rangle - \langle \tilde{r}_i, z \rangle_i\| + \sup_{\|z\|=1} \|\langle \tilde{r}_i, z \rangle_i - \langle \tilde{u}_i, z \rangle\| \\
 &\leq \sup_{\|z\|=1} \epsilon'_i (\|\tilde{r}_i\|^2 + \|z\|^2) + \epsilon'_i (\|\tilde{u}_i\|^2 + \|z\|^2) \\
 &= \epsilon'_i (\|\tilde{r}_i\|^2 + \|\tilde{u}_i\|^2 + 2).
 \end{aligned}$$

The sequence $\|\tilde{r}_i\|$ is bounded by assumption. For $\|\tilde{u}_i\|$, we first note that

$$\|\tilde{u}_i\|_i^2 \leq \|\tilde{r}_i\|_i^2 + \|\tilde{v}_i\|_i^2 = \|\tilde{r}_i\|_i^2,$$

where the norm is induced by $\langle -, - \rangle_i$. It follows from (4.9) that, first $\|\tilde{r}_i\|_i$ must be bounded, so that $\|\tilde{u}_i\|_i$ is bounded, too, and so, second, that $\|\tilde{u}_i\|$ must also be bounded. The assumption $\epsilon'_i \rightarrow 0$ gives the result. \square

Essential for the proof of Lemma 4.2.8 is the metric independence of the subspaces K_i and Z_i . We obtain the convergence of the distorted Neumann and Dirichlet splittings:

Lemma 4.2.9. *Let $\rho_N \in \mathcal{H}_N^k$ be a harmonic Neumann field and let $r_{i,N}$ and $\tilde{r}_{i,N}$ denote its discrete approximations in the decompositions (4.5) and (4.6). Denote by*

$$\begin{aligned}
 r_{i,N} &= s_{i,N} + t_{i,N} \in \mathcal{H}_{\mathcal{W}_{i,N}, \text{co}}^k \oplus \mathcal{H}_{\mathcal{W}_{i,N}, \partial \text{ex}}^k \\
 \tilde{r}_{i,N} &= \tilde{s}_{i,N} + \tilde{t}_{i,N} \in \mathcal{H}_{\mathcal{W}_{i,N}, \text{co}}^k \tilde{\oplus}_i \mathcal{H}_{\mathcal{W}_{i,N}, \partial \text{ex}}^k
 \end{aligned}$$

their orthogonal decompositions into coexact and boundary-exact Neumann Whitney fields with respect to the metrics g and \tilde{g}_i , respectively. Let $\{M_{h_i}\}$ converge metrically to M . Then it is $\|s_{i,N} - \tilde{s}_{i,N}\| \rightarrow 0$ and $\|t_{i,N} - \tilde{t}_{i,N}\| \rightarrow 0$. In particular, if $\rho_N = \sigma_N + \tau_N$ denotes the smooth decomposition, then both $s_{i,N}$ and $\tilde{s}_{i,N}$ converge to σ_N , and $t_{i,N}$ and $\tilde{t}_{i,N}$ converge to τ_N .

Proof. With the notation of Lemma 4.2.8, set $X := L^2\Omega^k(M)$, the L^2 -closure with respect to g of smooth k -forms on M , and define the spaces $E_i := d\mathcal{W}_i^{k-1}$, $K_i := \mathcal{H}_i^k$ and $Z_i := \{w \in K_i : w \text{ is boundary-exact}\}$. Then $H_i := \mathcal{H}_{\mathcal{W}_{i,N}}^k$, $U_i = \mathcal{H}_{\mathcal{W}_{i,N}, \partial \text{ex}}^k$ and $V_i := \mathcal{H}_{\mathcal{W}_{i,N}, \text{co}}^k$, and similarly for the distorted spaces \tilde{H}_i and so on. The sequences $\{r_i := r_{i,N}\}$ and $\{\tilde{r}_i := \tilde{r}_{i,N}\}$ converge to each other with respect to the metric g on M by Lemma 4.2.7, and also converge to a smooth form on M by Theorem 4.1.2, so they are bounded. Finally, Lemma 4.2.4 ensures the validity of the estimate (4.9). The claim now follows from Lemma 4.2.8. \square

Lemma 4.2.10. Let $\rho_D \in \mathcal{H}_D^k$ be a harmonic Dirichlet field and let $r_{i,D}$ and $\tilde{r}_{i,D}$ denote its discrete approximations in the decompositions (4.7) and (4.8). Denote by

$$\begin{aligned} r_{i,D} &= s_{i,D} + t_{i,D} \in \overline{\mathcal{H}_{\mathcal{W}_{i,D},\text{ex}}^k} \oplus \overline{\mathcal{H}_{\mathcal{W}_{i,D},\partial\text{co}}^k} \\ \tilde{r}_{i,D} &= \tilde{s}_{i,D} + \tilde{t}_{i,D} \in \overline{\mathcal{H}_{\mathcal{W}_{i,D},\text{ex}}^k} \oplus \overline{\mathcal{H}_{\mathcal{W}_{i,D},\partial\text{co}}^k} \end{aligned}$$

their orthogonal decompositions into exact and boundary-coexact Dirichlet Whitney fields with respect to the metrics g and \tilde{g}_i , respectively. Let $\{M_{h_i}\}$ converge metrically to M . Then it is $\|s_{i,D} - \tilde{s}_{i,D}\| \rightarrow 0$ and $\|t_{i,D} - \tilde{t}_{i,D}\| \rightarrow 0$. In particular, if $\rho_D = \sigma_D + \tau_D$ denotes the smooth decomposition, then both $s_{i,D}$ and $\tilde{s}_{i,D}$ converge to σ_D , and $t_{i,D}$ and $\tilde{t}_{i,D}$ converge to τ_D .

Proof. This time, set $X := L^2\Omega^k(M)$, $E_i := d^*\mathcal{W}_{i,D}^{k-1}$, $K_i := \mathcal{H}_{i,D}^k$ and $Z_i := d^*\mathcal{W}_i^{k-1}$. Then $H_i := \mathcal{H}_{\mathcal{W}_{i,D}}^k$, $U_i = \mathcal{H}_{\mathcal{W}_{i,D},\text{ex}}^k$ and $V_i := \mathcal{H}_{\mathcal{W}_{i,D},\partial\text{co}}^k$, and similarly for the distorted spaces \tilde{H}_i and so on, and the claim follows with the same argument as in Lemma 4.2.9. \square

Theorem 4.2.11. Let $\omega \in \Omega^k(M)$ be decomposed as

$$\omega = d\alpha + \sigma_N + \tau_N + \delta\beta_N \in d\Omega^{k-1} \oplus \mathcal{H}_{N,\text{co}}^k \oplus \mathcal{H}_{N,\partial\text{ex}}^k \oplus \delta\Omega_N^{k+1} \quad (4.10)$$

$$= d\alpha_D + \sigma_D + \tau_D + \delta\beta \in d\Omega_D^{k-1} \oplus \mathcal{H}_{D,\text{ex}}^k \oplus \mathcal{H}_{D,\partial\text{co}}^k \oplus \delta\Omega^{k+1} \quad (4.11)$$

and let

$$\Phi_i(\omega) = d\tilde{\alpha}_i + \tilde{s}_{i,N} + \tilde{t}_{i,N} + \tilde{b}_{i,N} \in d^*\mathcal{W}_i^{k-1} \oplus \overline{\tilde{\mathcal{H}}_{\mathcal{W}_{i,N},\text{co}}^k} \oplus \overline{\tilde{\mathcal{H}}_{\mathcal{W}_{i,N},\partial\text{ex}}^k} \oplus \overline{\tilde{\mathcal{H}}_i^k}^\perp \quad (4.12)$$

$$= d\tilde{\alpha}_{i,D} + \tilde{s}_{i,D} + \tilde{t}_{i,D} + \tilde{b}_i \in d^*\mathcal{W}_{i,D}^{k-1} \oplus \overline{\tilde{\mathcal{H}}_{\mathcal{W}_{i,D},\text{ex}}^k} \oplus \overline{\tilde{\mathcal{H}}_{\mathcal{W}_{i,D},\partial\text{co}}^k} \oplus \overline{\tilde{\mathcal{H}}_{i,D}^k}^\perp \quad (4.13)$$

be the decomposition of its Whitney projection with respect to the metrics \tilde{g}_i , and let $\{M_{h_i}\}$ converge metrically to M . Then all components in (4.12) converge to the respective components in (4.10), and all components in (4.13) converge to the respective components in (4.11).

Proof. Corollary 4.1.6 and Corollary 4.1.11 show the convergence of the corresponding decompositions for the smooth metric g , and Lemma 4.2.7 together with Lemma 4.2.9 and Lemma 4.2.10 give the convergence of the distorted Whitney decompositions to the undistorted ones. \square

4.3 APPROXIMATION BY PCVFS

Concluding the approximation proof, this section finally considers the case of approximating a smooth vector X field by a PCVF on a discrete mesh and shows convergence of the discrete decompositions for \mathcal{X}_h to their smooth counterparts. To this end we shall define the approximating vector field as the element $P_{h_i}(X) \in \mathcal{X}_h(M_{h_i})$ that is the L^2 -projection of the piecewise defined pushforward F_*X over M_{h_i} . Its discrete decomposition pulls back to a decomposition on M which is orthogonal with respect to the distorted metric \tilde{g}_i . The proof now compares this decomposition with the distorted Whitney decompositions, and the results from the previous sections and an approximation statement of smooth vector fields by PCVFs in [War06] yield the expected convergence.

Finally it remains to show that approximations by PCVFs and their decompositions according to Section 3.2 and Section 3.3 still converge to their smooth counterparts. For the surface case we will show this explicitly for the following refined fundamental decompositions

$$\begin{aligned}\mathcal{X}_h &= \nabla \mathcal{L} \oplus (\mathcal{H}_{h,N,\text{co}} \oplus \mathcal{H}_{h,N,\partial \text{ex}}) \oplus J \nabla \mathcal{F}_0 \\ &= \nabla \mathcal{L}_0 \oplus (\mathcal{H}_{h,D,\text{ex}} \oplus \mathcal{H}_{h,D,\partial \text{co}}) \oplus J \nabla \mathcal{F}.\end{aligned}$$

For the three-dimensional case we shall only give a remark on how to prove convergence, as this case is not substantially different from the surface case. We shall closely follow the strategy suggested by Wardetzky in [War06, Sec. 3.4.3].

Again, we assume that $\{F_i : M \rightarrow M_{h_i}\}$ is an admissible family of smooth triangulations, where M is now a surface with boundary and M_{h_i} is a sequence of simplicial surfaces. Given a smooth vector field $X \in \mathcal{X}(M)$ on M , its L^2 -best approximation on the simplicial surface M_{h_i} shall be the element $P_{h_i}(X) \in \mathcal{X}_h(M_{h_i})$ satisfying

$$\langle P_{h_i}(X), Y_h \rangle_{g_{h_i}} = \langle F_{i*}X, Y_h \rangle_{g_{h_i}} \quad \text{for all } Y \in \mathcal{X}_h(M_{h_i}),$$

and we denote this projection by $P_{h_i} : L^2 \mathcal{X}(M) \rightarrow \mathcal{X}_h(M_{h_i})$. The pullback $F_i^* P_{h_i}(X)$ is then the L^2 -orthogonal projection of X with respect to $\langle -, - \rangle_{\tilde{g}_i}$ on M onto the space

$$\mathcal{X}_i(M) := F_i^* \mathcal{X}_h(M_{h_i}) = \{F_i^* Y_h : Y_h \in \mathcal{X}_h(M_{h_i})\}$$

which can be considered the space of piecewise constant vector fields with respect to the coordinates $\{\tilde{\lambda}_{h_i,j} = F_i^* \lambda_{h_i,j}\}$ on M : indeed, over any triangle $f \in M_{h_i}^{(2)}$, a constant vector field $X_f = \sum_j a_j \partial \lambda_{h_i,j}$ pulls back to the vector field

$$F^* X_f = \sum_j a_j D F^{-1} \partial \lambda_{h_i,j} = \sum_j a_j \partial \tilde{\lambda}_{h_i,j},$$

having the same constant coefficients as X_f .

If $\tilde{P}_i : L^2 \mathcal{X}(M) \rightarrow \mathcal{X}_i(M)$ denotes the L^2 -orthogonal projection with respect to $\langle -, - \rangle_{\tilde{g}_i}$, then by the above discussion it is $\tilde{P}_i(X) = F^* P_{h_i}(X)$. Hence we can think of this approximation either as the element $\tilde{P}_i(X) \in \mathcal{X}_i(M)$ on M , or as the element $P_{h_i}(X) \in \mathcal{X}_h(M_{h_i})$ on the approximating surface M_{h_i} . Wardetzky has shown that for any vector field $X \in \mathcal{X}(M)$ its projection $\tilde{P}_i(X)$ to $\mathcal{X}_i(M)$ converges to X :

Lemma 4.3.1. *Let $X \in \mathcal{X}(M)$ and let $\{M_{h_i}\}$ converge metrically. Then $\|X - \tilde{P}_i(X)\| \rightarrow 0$.*

Proof. [War06, Lemma 3.4.3] □

Furthermore, for every Whitney form $w \in \mathcal{W}^1(M_{h_i})$ on M_{h_i} with its orthogonal splitting into a closed and coclosed component $w = c + b \in \mathcal{K}^1 \oplus_{h_i} (\mathcal{K}^1)^\perp$ it is

$$P_{h_i}(w^{\sharp h_i}) = P_{h_i}(c^{\sharp h_i}) + P_{h_i}(b^{\sharp h_i}) \in (J\nabla \mathcal{F}_0)^\perp \oplus_{h_i} J\nabla \mathcal{F}_0,$$

and similarly for the splitting $\mathcal{K}_D \oplus_{h_i} \mathcal{K}_D^\perp$, see [War06, Lemma 3.4.5]. Here, by abuse of notation, we denote the orthogonal projection $\mathcal{W}^1(M_{h_i})^{\sharp h_i} \rightarrow \mathcal{X}_h(M_{h_i})$ by P_{h_i} , too. In particular, since c is closed, it follows from Lemma 3.1.5 that $c^{\sharp h_i}$ is already a PCVF on M_{h_i} , i.e. $P_{h_i}(c^{\sharp h_i}) = c^{\sharp h_i}$. We obtain

Corollary 4.3.2. *Let $w \in \mathcal{W}^1(M_{h_i})$ with g_{h_i} -orthogonal decompositions*

$$\begin{aligned} w &= da_i + s_{i,N} + t_{i,N} + b_{i,N} \in d\mathcal{W}_i^0 \oplus_{h_i} \mathcal{H}_{\mathcal{W}_i,N,\text{co}}^1 \oplus_{h_i} \mathcal{H}_{\mathcal{W}_i,N,\partial\text{ex}}^1 \oplus_{h_i} (\mathcal{K}_i^1)^\perp \\ &= da_{i,D} + s_{i,D} + t_{i,D} + b_i \in d\mathcal{W}_{i,D}^0 \oplus_{h_i} \mathcal{H}_{\mathcal{W}_i,D,\text{ex}}^1 \oplus_{h_i} \mathcal{H}_{\mathcal{W}_i,D,\partial\text{co}}^1 \oplus_{h_i} (\mathcal{K}_{i,D}^1)^\perp. \end{aligned}$$

Then its projection $P_{h_i}(w^{\sharp h_i})$ to $\mathcal{X}_h(M_{h_i})$ has the orthogonal decompositions

$$\begin{aligned} (da_i)^{\sharp h_i} + (s_{i,N})^{\sharp h_i} + (t_{i,N})^{\sharp h_i} + P_{h_i}(b_{i,N}^{\sharp h_i}) &\in \nabla \mathcal{L} \oplus_{h_i} (\mathcal{H}_{h_i,N,\text{co}} \oplus_{h_i} \mathcal{H}_{h_i,N,\partial\text{ex}}) \oplus_{h_i} J\nabla \mathcal{F}_0 \\ (da_{i,D})^{\sharp h_i} + (s_{i,D})^{\sharp h_i} + (t_{i,D})^{\sharp h_i} + P_{h_i}(b_i^{\sharp h_i}) &\in \nabla \mathcal{L}_0 \oplus_{h_i} (\mathcal{H}_{h_i,D,\text{ex}} \oplus_{h_i} \mathcal{H}_{h_i,D,\partial\text{co}}) \oplus_{h_i} J\nabla \mathcal{F}. \end{aligned}$$

The previous considerations culminate in the following convergence statements for the refined discrete fundamental decompositions for PCVFs.

Theorem 4.3.3. *Let M be a smooth, compact surface with boundary ∂M , and $\{F_i : M \rightarrow M_{h_i}\}$ be an admissible family of smooth triangulations by simplicial surfaces, converging metrically to M . Let $\omega \in \Omega^1(M)$ be a 1-form with its decompositions*

$$\begin{aligned} \omega &= d\alpha + (\sigma_N + \tau_N) + \delta\beta_N && \in d\mathcal{C}^\infty \oplus (\mathcal{H}_{N,\text{co}}^1 \oplus \mathcal{H}_{N,\partial\text{ex}}^1) \oplus \delta\Omega_N^2 \\ &= d\alpha_D + (\sigma_D + \tau_D) + \delta\beta && \in d\mathcal{C}_D^\infty \oplus (\mathcal{H}_{D,\text{ex}}^1 \oplus \mathcal{H}_{D,\partial\text{co}}^1) \oplus \delta\Omega^2. \end{aligned}$$

Let $X_{h_i} := P_{h_i}(\omega^\#)$ be the projection of $\omega^\#$ to $\mathcal{X}_h(M_{h_i})$ with respect to $\langle -, - \rangle_{g_{h_i}}$, and let

$$\begin{aligned} X_{h_i} &= \nabla\varphi_i + (S_{h_i,N} + T_{h_i,N}) + J\nabla\psi_{i,N} && \in \nabla \mathcal{L} \oplus_{h_i} (\mathcal{H}_{h_i,N,\text{co}} \oplus_{h_i} \mathcal{H}_{h_i,N,\partial\text{ex}}) \oplus_{h_i} J\nabla \mathcal{F}_0 \\ &= \nabla\varphi_{i,D} + (S_{h_i,D} + T_{h_i,D}) + J\nabla\psi_i && \in \nabla \mathcal{L}_0 \oplus_{h_i} (\mathcal{H}_{h_i,D,\text{ex}} \oplus_{h_i} \mathcal{H}_{h_i,D,\partial\text{co}}) \oplus_{h_i} J\nabla \mathcal{F} \end{aligned}$$

Then

$$\begin{aligned} \|(d\alpha)^\# - F_i^* \nabla\varphi_i\| &\rightarrow 0 && \|(d\alpha_D)^\# - F_i^* \nabla\varphi_{i,D}\| &\rightarrow 0 \\ \|\sigma_N^\# - F_i^* S_{h_i,N}\| &\rightarrow 0 && \|(\sigma_D)^\# - F_i^* S_{h_i,D}\| &\rightarrow 0 \\ \|(\tau_N)^\# - F_i^* T_{h_i,N}\| &\rightarrow 0 && \|\tau_D^\# - F_i^* T_{h_i,D}\| &\rightarrow 0 \\ \|(\delta\beta_N)^\# - F_i^* J\nabla\psi_{i,N}\| &\rightarrow 0 && \|(\delta\beta)^\# - F_i^* J\nabla\psi_i\| &\rightarrow 0 \end{aligned}$$

Proof. We show convergence for the first decomposition. The proof for the second is literally the same. First of all, we consider everything on M . Let

$$\begin{aligned} X &:= A + S + T + B \quad := (d\alpha)^\sharp + \sigma_N^\sharp + \tau_N^\sharp + (\delta\beta_N)^\sharp \\ \tilde{P}_i(X) &:= \tilde{A}_i + \tilde{S}_i + \tilde{T}_i + \tilde{B}_i := F^*\nabla\varphi_i + F^*S_{h_i,N} + F^*T_{h_i,N} + F^*J\nabla\psi_{i,N}. \end{aligned}$$

We have to show $\|A - \tilde{A}_i\| \rightarrow 0$ and so on. With respect to Corollary 4.2.6 the convergence to zero with respect to the $\|\cdot\|$ -norm is equivalent to convergence in the $\|\cdot\|_{\tilde{g}_i}$ -norm. Therefore if we do not need to focus on statements for a particular norm we shall write $\|\cdot\|_{(\tilde{g}_i)}$ to indicate that this could either stand for the norm induced by g or the norm induced by \tilde{g}_i . We shall use the following notation

$$\begin{aligned} \Phi_i(\omega) &:= \tilde{a}_{\mathcal{W}_i} + \tilde{s}_{\mathcal{W}_i} + \tilde{t}_{\mathcal{W}_i} + \tilde{b}_{\mathcal{W}_i} \in d\mathcal{W}_i^0 \tilde{\Theta}_i \overline{\mathcal{H}_{\mathcal{W}_i,N,\text{co}}^1} \tilde{\Theta}_i \overline{\mathcal{H}_{\mathcal{W}_i,N,\partial\text{ex}}^1} \tilde{\Theta}_i (\mathcal{X}_i^1)^\perp \\ \tilde{P}_i(\Phi_i(\omega)^{\sharp_i}) &:= \tilde{A}_{\mathcal{W}_i,h} + \tilde{S}_{\mathcal{W}_i,h} + \tilde{T}_{\mathcal{W}_i,h} + \tilde{B}_{\mathcal{W}_i,h} \in F_i^* (\nabla\mathcal{L} \oplus_{h_i} \mathcal{H}_{h_i,N,\text{co}} \oplus_{h_i} \mathcal{H}_{h_i,N,\partial\text{ex}} \oplus_{h_i} J\nabla\mathcal{F}_0) \end{aligned}$$

and conclude as follows:

First, by Corollary 4.1.11 it is $\|d\alpha - \tilde{a}_{\mathcal{W}_i}\|_{(\tilde{g}_i)} \rightarrow 0$, $\|\sigma_N - \tilde{s}_{\mathcal{W}_i}\|_{(\tilde{g}_i)} \rightarrow 0$ and so on. Furthermore, by Lemma 4.3.1, it is $\|\tilde{P}_i(X) - X\|_{(\tilde{g}_i)} \rightarrow 0$.

Second, we claim that $\|\tilde{P}_i(\Phi_i(\omega)^{\sharp_i}) - X\|_{(\tilde{g}_i)} \rightarrow 0$ in both norms. Considering the $\|\cdot\|_{\tilde{g}_i}$ -norm, it is

$$\left\| \tilde{P}_i(\Phi_i(\omega)^{\sharp_i}) - X \right\|_{\tilde{g}_i} \leq \left\| \tilde{P}_i(\Phi_i(\omega)^{\sharp_i}) - \tilde{P}_i(X) \right\|_{\tilde{g}_i} + \left\| \tilde{P}_i(X) - X \right\|_{\tilde{g}_i}$$

The second term tends to zero by Lemma 4.3.1. For the first term we estimate

$$\begin{aligned} \left\| \tilde{P}_i(\Phi_i(\omega)^{\sharp_i}) - X \right\|_{\tilde{g}_i} &\leq \left\| \tilde{P}_i \right\|_{\tilde{g}_i} \left\| \Phi_i(\omega)^{\sharp_i} - X \right\|_{\tilde{g}_i} \\ &\leq \left\| \Phi_i(\omega)^{\sharp_i} - \Phi_i(\omega)^\sharp \right\|_{\tilde{g}_i} + \left\| \Phi_i(\omega)^\sharp - X \right\|_{\tilde{g}_i} \\ &\leq \left\| (\Lambda_i^{-1} - \text{Id})\Phi_i(\omega)^\sharp \right\|_{\tilde{g}_i} + \left\| \Phi_i(\omega)^\sharp - X \right\|_{\tilde{g}_i} \end{aligned}$$

Both terms converge with respect to $\|\cdot\|$ which can be seen as follows:

$$\left\| (\Lambda_i^{-1} - \text{Id})\Phi_i(\omega)^\sharp \right\| \leq \left\| \Lambda_i^{-1} - \text{Id} \right\|_{L^\infty} \left\| \Phi_i(\omega)^\sharp \right\| \rightarrow 0$$

since $\left\| \Lambda_i^{-1} - \text{Id} \right\|_{L^\infty} \rightarrow 0$ and $\left\| \Phi_i(\omega)^\sharp \right\|_{\tilde{g}_i}$ is bounded. Furthermore,

$$\left\| \Phi_i(\omega)^\sharp - X \right\| = \left\| \Phi_i(\omega) - X^b \right\| = \left\| \Phi_i(\omega) - \omega \right\| \rightarrow 0$$

by Theorem 4.1.1. Therefore $\left\| \tilde{P}_i(X) - \tilde{P}_i(\Phi_i(\omega)^{\sharp_i}) \right\|_{(\tilde{g}_i)} \rightarrow 0$, since both terms converge to X . Considering the $\|\cdot\|_{\tilde{g}_i}$ -norm, it follows that all components in the \tilde{g}_i -orthogonal decompositions

$$\begin{aligned} \tilde{P}_i(X) &= \tilde{A}_i + \tilde{S}_i + \tilde{T}_i + \tilde{B}_i \\ \tilde{P}_i(\Phi_i(\omega)^{\sharp_i}) &= \tilde{A}_{\mathcal{W}_i,h} + \tilde{S}_{\mathcal{W}_i,h} + \tilde{T}_{\mathcal{W}_i,h} + \tilde{B}_{\mathcal{W}_i,h} \end{aligned}$$

tend to each other in both norms.

Next, we show that $\tilde{A}_{\mathcal{W}_i, h}$, $\tilde{S}_{\mathcal{W}_i, h}$ and $\tilde{T}_{\mathcal{W}_i, h}$ converge to A , S and T . Note that by Corollary 4.3.2 it is $\tilde{A}_{\mathcal{W}_i, h} = (\tilde{a}_{\mathcal{W}_i})^{\sharp_i}$, $\tilde{S}_{\mathcal{W}_i, h} = (\tilde{s}_{\mathcal{W}_i})^{\sharp_i}$ and $\tilde{T}_{\mathcal{W}_i, h} = (\tilde{t}_{\mathcal{W}_i})^{\sharp_i}$. We obtain

$$\begin{aligned} \|\tilde{A}_{\mathcal{W}_i, h} - A\| &= \left\| (\tilde{a}_{\mathcal{W}_i})^{\sharp_i} - \alpha^{\sharp} \right\| \\ &\leq \left\| (\tilde{a}_{\mathcal{W}_i} - \alpha)^{\sharp_i} \right\| + \left\| \alpha^{\sharp_i} - \alpha^{\sharp} \right\| \\ &= \left\| \Lambda_i^{-1}(\tilde{a}_{\mathcal{W}_i} - \alpha)^{\sharp} \right\| + \left\| \Lambda_i^{-1} \alpha^{\sharp} - \alpha^{\sharp} \right\| \\ &\leq \left\| \Lambda_i^{-1} \right\|_{L^\infty} \left\| (\tilde{a}_{\mathcal{W}_i} - \alpha)^{\sharp} \right\| + \left\| \Lambda_i^{-1} - \text{Id} \right\|_{L^\infty} \left\| \alpha^{\sharp} \right\| \\ &= \left\| \Lambda_i^{-1} \right\|_{L^\infty} \left\| \tilde{a}_{\mathcal{W}_i} - \alpha \right\| + \left\| \Lambda_i^{-1} - \text{Id} \right\|_{L^\infty} \left\| \alpha \right\|. \end{aligned}$$

It is $\left\| \Lambda_i^{-1} \right\|_{L^\infty} \rightarrow 1$ and $\left\| \Lambda_i^{-1} - \text{Id} \right\|_{L^\infty} \rightarrow 0$ by metric convergence, and $\left\| \tilde{a}_{\mathcal{W}_i} - \alpha \right\| \rightarrow 0$ by Corollary 4.1.11. Thus $\left\| \tilde{A}_{\mathcal{W}_i, h} - A \right\| \rightarrow 0$, and the same argument holds for the other two components, too. Finally, since $\tilde{P}_i(X)$, \tilde{A}_i , \tilde{S}_i and \tilde{T}_i converge to X , A , S , and T , it must hold $\left\| \tilde{B}_i - B \right\| \rightarrow 0$, too. □

Remark 4.3.4 (Convergence for Simplicial Solids). *Basically the same line of argument works for the convergence results in the three-dimensional case, keeping the following slight differences in mind. As already mentioned in Remark 3.3.5, the discrete decompositions in Section 3.3 interpret vector fields as vector proxies for 2-forms. Therefore, they need to be compared with the corresponding components in the Whitney decompositions for Whitney 2-forms, too, and not with 1-forms. On the other hand, there is no non-trivial further splitting for the spaces \mathcal{H}_D^* and \mathcal{H}_N^* on three-dimensional domains in \mathbb{R}^3 —all Dirichlet fields are exact and all Neumann fields are coexact. Hence the argumentation following Lemma 4.2.8 is not needed in this case.*

APPLICATIONS

In this last chapter we present applications for the structural decomposition results derived above. In particular, we shall focus on the following aspects:

1. The computation of harmonic fields: harmonic vector fields play a central role in many applications, e.g. in parametrization and remeshing problems in computational geometry or in the numerical treatment of Hodge-Laplace problems, where they arise as non-trivial elements in the kernel. Furthermore, the subspaces of Dirichlet and Neumann fields provide representatives for cohomology classes, with their refined split subspaces of (co-)exact and boundary-(co-)exact fields separating cohomology information induced by the boundary from cohomology coming from the interior of the geometry. In fact they turn out to be useful as a tool for the detection and analysis of topological features. We therefore explain a computational strategy to compute such bases and show a few examples on various test models.
2. The computational decomposition of a given vector field: we have already mentioned several important use cases for Hodge decompositions, ranging from the analysis of vector fields and their singularities to the projection onto particular components of a vector field, e.g. to ensure local integrability. We will present a strategy to compute the refined decompositions derived in Section 3.2 and Section 3.3, based on an iterated L^2 -projection scheme. Finally, we compare our discrete results to smooth fields defined analytically.

5.1 COHOMOLOGY REPRESENTATIVES ON SIMPLICIAL SURFACES

We present a method for computing bases for the spaces of discrete Dirichlet and Neumann fields on simplicial surfaces. In each case, the basis is encoded as a typically low-dimensional null space of an almost-square sparse matrix. For the subspace of exact Dirichlet fields and coexact Neumann fields we obtain a basis of potentials and copotentials in \mathcal{L} and \mathcal{F} , respectively. Several examples demonstrate the practicability of this approach.

As a first application we compute bases for the topologically significant spaces $\mathcal{H}_{h,D}$ and $\mathcal{H}_{h,N}$ and their refined subspaces of (co-)exact and boundary-(co-)exact Dirichlet and Neumann fields on simplicial surfaces. From a combinatorial point of view the computation of (co-)homology generators is a central topic in computational topology, see e.g. [EW05], [Dło12] or [BCC⁺12], just to name a few exemplary articles. For geometric and physical applications, though, it is often desirable not only to compute homology-generating cycles combinatorially, but rather to work with a basis that is formed by harmonic fields which constitute an even flow, being divergence-free and rotation-free at the same time. Since the property of being divergence-free depends on the Riemannian metric, such a basis cannot be constructed by purely combinatorial methods any more, and one has to incorporate an orthogonalization

procedure, see [HKWW10]. In the following we therefore compute orthogonal complements of gradient and cogradient spaces directly to obtain bases for $\mathcal{H}_{h,D}$ and $\mathcal{H}_{h,N}$. Lemma 3.2.6 and Remark 3.2.7 guarantee that these bases will indeed generate the respective cohomology groups.

SETTING UP THE SYSTEM MATRICES. Recall that discrete Dirichlet fields are defined as the orthogonal complement of the sum $\nabla\mathcal{L}_0 \oplus J\nabla\mathcal{F}$. Let $\mathcal{B}_{\mathcal{L}} := \{\varphi_i\}$ be the nodal basis of \mathcal{L} , and $\mathcal{B}_{\mathcal{L}_0} := \{\varphi_{0,i}\} \subset \mathcal{B}_{\mathcal{L}}$ be the subset of basis functions whose degrees of freedom correspond to the inner vertices. Similarly, let $\mathcal{B}_{\mathcal{F}} := \{\psi_i\}$ and $\mathcal{B}_{\mathcal{F}_0}$ be the edge-midpoint bases for \mathcal{F} and \mathcal{F}_0 , respectively, the latter given by all basis functions associated to inner edges. To represent elements in \mathcal{X}_h , we interpret each vector field $X \in \mathcal{X}_h$ as a family of vectors in \mathbb{R}^3 , indexed by the triangles $f \in M_h^{(2)}$. Without the requirement for tangency, a basis is then given by the family $\{E_{f,1}, E_{f,2}, E_{f,3}\}_{f \in M_h^{(2)}}$ with the canonical basis vectors $E_{f,i} = (\delta_{1,i}, \delta_{2,i}, \delta_{3,i}) \in \mathbb{R}^3$, where $\delta_{j,i}$ denotes the Kronecker delta. For simplicity we renumerate these vectors and set $\mathcal{B}_{\mathcal{R}} := \{E_j\}$ for $j = 1, \dots, 3n_F$, and $\mathcal{R} := \mathbb{R}^{3n_F}$. We define the following matrices:

$$\begin{aligned} L_{\nabla\mathcal{L}_0, \mathcal{R}} &:= \left(\langle \nabla\varphi_{0,i}, E_j \rangle_{L^2} \right)_{\substack{i=1, \dots, n_{iV} \\ j=1, \dots, 3n_F}} \\ L_{J\nabla\mathcal{F}, \mathcal{R}} &:= \left(\langle J\nabla\psi_i, E_j \rangle_{L^2} \right)_{\substack{i=1, \dots, n_E-1 \\ j=1, \dots, 3n_F}} \\ L_{N, \mathcal{R}} &:= \left(\langle N_i, E_j \rangle_{L^2} \right)_{\substack{i=1, \dots, n_F \\ j=1, \dots, 3n_F}}, \end{aligned}$$

where N_i is the (constant) normal field of triangle f_i . For an element $X = \sum_i X_i E_i$ in the linear span of $\mathcal{B}_{\mathcal{R}}$ it is $L_{\nabla\mathcal{L}_0, \mathcal{R}} \cdot X = 0$ and $L_{J\nabla\mathcal{F}, \mathcal{R}} \cdot X = 0$ if and only if X is L^2 -orthogonal to all gradient fields of inner Lagrange elements and all cogradient fields of Crouzeix-Raviart elements on M_h , respectively (for the matrix-vector product we identify X with its coefficient vector (X_i) here and in the following). Furthermore, $L_{N, \mathcal{R}} \cdot X = 0$ if and only if X is a tangential vector field to M_h . Stacking these matrices into a single matrix

$$L_{\mathcal{H}_{h,D}} := \begin{pmatrix} L_{\nabla\mathcal{L}_0, \mathcal{R}} \\ L_{J\nabla\mathcal{F}, \mathcal{R}} \\ L_{N, \mathcal{R}} \end{pmatrix} \quad (5.1)$$

of dimension $(n_{iV} + n_E - 1 + n_F) \times 3n_F$, it is

$$\mathcal{H}_{h,D} = \ker(L_{\mathcal{H}_{h,D}}),$$

so finding a basis of $\mathcal{H}_{h,D}$ is equivalent to finding a basis for $\ker(L_{\mathcal{H}_{h,D}})$. We will discuss two approaches to solve for this kernel in Section 5.5. Note that only $n_E - 1$ basis functions of \mathcal{F} are needed, as the constant functions form the kernel of $J\nabla$. Of course, if M_h is embedded in \mathbb{R}^2 , there is no need to enforce tangency and one can perform the computation directly in coordinates of \mathbb{R}^2 , so that the system reduces to a $((n_{iV} + n_E - 1) \times 2n_F)$ -matrix.

The very same strategy can be applied to obtain a basis for $\mathcal{H}_{h,N}$, using the matrices $L_{\nabla\mathcal{L}, \mathcal{R}}$ and $L_{J\nabla\mathcal{F}_0, \mathcal{R}}$ instead of $L_{\nabla\mathcal{L}_0, \mathcal{R}}$ and $L_{J\nabla\mathcal{F}, \mathcal{R}}$ in the stacked system (5.1).

To compute a basis for $\mathcal{H}_{h,D,ex}$, we proceed in a similar fashion. However, since we are seeking gradient fields, a solution X can be written as $X = \nabla\varphi_X := \sum_i X_i \nabla\varphi_i$. This reduces

drastically the system size for two reasons: first, no tangency conditions need to be imposed and second, such gradient fields are automatically orthogonal to $J\nabla\mathcal{F}_0$. In effect, there are just two conditions that need to be satisfied for $\nabla\varphi_X$, namely that $\nabla\varphi_X$ is orthogonal to $\nabla\mathcal{L}_0$, and that it is orthogonal to all $J\nabla\psi_{b,j}$, where $\psi_{b,j} \in \mathcal{F}_b$. Here, \mathcal{F}_b denotes the subspace of \mathcal{F} spanned by all basis functions whose degrees of freedom are associated to boundary edges. A solution is then the gradient field of a discrete harmonic function φ_X which is constant on each boundary component, see Figure 5.13. We set up the matrices

$$L_{\nabla\mathcal{L}_0, \nabla\mathcal{L}} := \left(\langle \nabla\varphi_{0,i}, \nabla\varphi_j \rangle_{L^2} \right)_{\substack{i=1, \dots, n_{iV} \\ j=1, \dots, n_V}}$$

$$L_{J\nabla\mathcal{F}_b, \nabla\mathcal{L}} := \left(\langle J\nabla\psi_{b,i}, \nabla\varphi_j \rangle_{L^2} \right)_{\substack{i=1, \dots, n_{bE} \\ j=1, \dots, n_V}}$$

and stack them to a matrix

$$L_{\mathcal{H}_{h,D,\text{ex}}} := \begin{pmatrix} L_{\nabla\mathcal{L}_0, \nabla\mathcal{L}} \\ L_{J\nabla\mathcal{F}_b, \nabla\mathcal{L}} \\ (1, 0, \dots, 0) \end{pmatrix},$$

where the last row is added to exclude constant functions.

Solving for the $(m-1)$ -dimensional null space of $L_{\mathcal{H}_{h,D,\text{ex}}}$ gives the coefficient vectors for the basis functions $\mathcal{B}_{\mathcal{L}}$, and their gradients form a basis for $\mathcal{H}_{h,D,\text{ex}}$. Once again, a similar procedure can be performed to obtain a basis for $\mathcal{H}_{h,N,\text{co}}$.

Finally, once we have bases $\{Y_1, \dots, Y_{h^1}\}$ for $\mathcal{H}_{h,D}$ and $\{Z_1, \dots, Z_{m-1}\}$ for $\mathcal{H}_{h,D,\text{ex}}$, a basis for $\mathcal{H}_{h,D,\partial\text{co}}$ can be obtained e.g. by solving for the $2g$ -dimensional kernel of the matrix

$$\left(\langle Z_i, Y_j \rangle_{L^2} \right)_{\substack{i=1, \dots, m-1 \\ j=1, \dots, h^1}}$$

and orthonormalize with respect to $\mathcal{H}_{h,D,\text{ex}}$, if necessary.

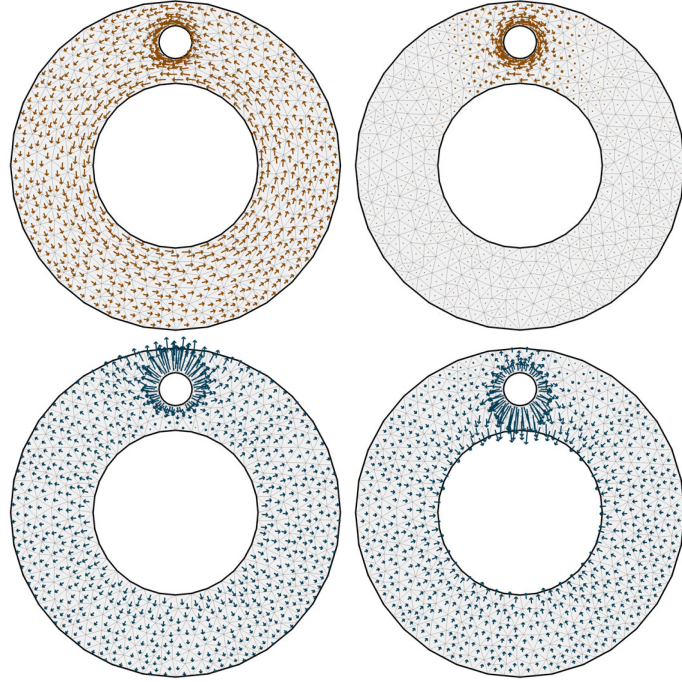


Figure 5.1: Bases for $\mathcal{H}_{h,N}$ and $\mathcal{H}_{h,D}$ on the AwH-model of type $\Sigma_{0,3}$.

EXPERIMENTAL RESULTS. The first example in Figure 5.1 shows bases for $\mathcal{H}_{h,N}$ and $\mathcal{H}_{h,D}$ on a flat annulus geometry with an additional hole cut out (we shall refer to this model by “AwH”), so that $h^1 = 2$. Since this model does not possess any interior cohomology, all Dirichlet fields are exact, and all Neumann fields are coexact. Furthermore, the shown basis for each space is an orthonormal basis, so that all four fields are pairwise orthogonal to each other.

Figure 5.2 shows bases for $\mathcal{H}_{h,N}$ and $\mathcal{H}_{h,D}$ on a torus with an attached cylinder (abbreviated “TwC”), which is topologically a surface of type $\Sigma_{1,2}$. Whereas the spaces $\mathcal{H}_{h,D}$ and $\mathcal{H}_{h,N}$ in the previous example have been L^2 -orthogonal to each other, this is no longer the case for this model due to the presence of non-trivial inner cohomology generators which are shared by both spaces. Although the representing fields are almost orthogonal on the cylindrical region, they concentrate in the same fashion along the longitudinal and latitudinal cycles that reflect homology generated by the torus, and are clearly not orthogonal to each other any more. All fields are non-zero everywhere, even if the small values are not visible in this graphic.

Two pairings of each a Dirichlet and a Neumann field from Figure 5.2 are shown as a close-up on the torus region in Figure 5.3. The first pairing forms mostly acute angles on individual triangles on the torus region, whereas the second pairing forms mostly obtuse angles. In any case, a local non-orthogonality is clearly visible and as these fields concentrate their mass on the torus region, these two pairs are apparently not L^2 -orthogonal.

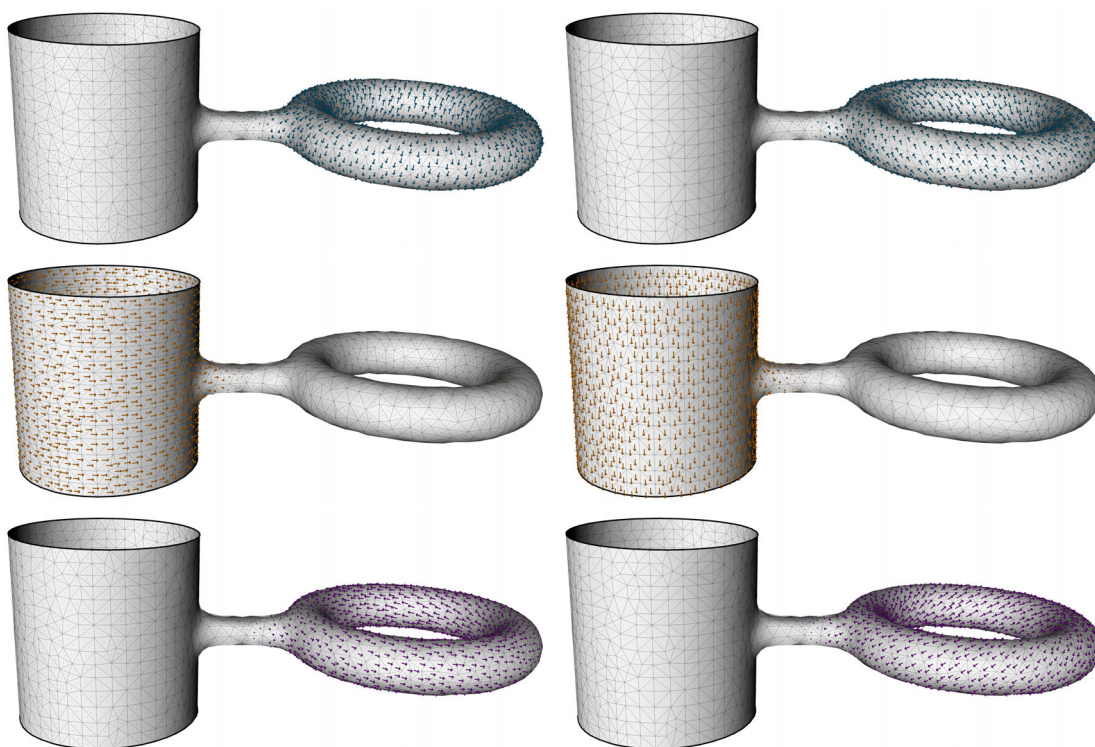


Figure 5.2: Basis fields for $\mathcal{H}_{h,N}$ (left column) and $\mathcal{H}_{h,D}$ (right column) on a torus with a cylinder attached, which is topologically $\Sigma_{1,2}$. The fields in the first and third row all concentrate their mass in the same fashion along the longitudinal and latitudinal cycles that reflect homology generated by the torus, and are clearly not orthogonal to each other any more.

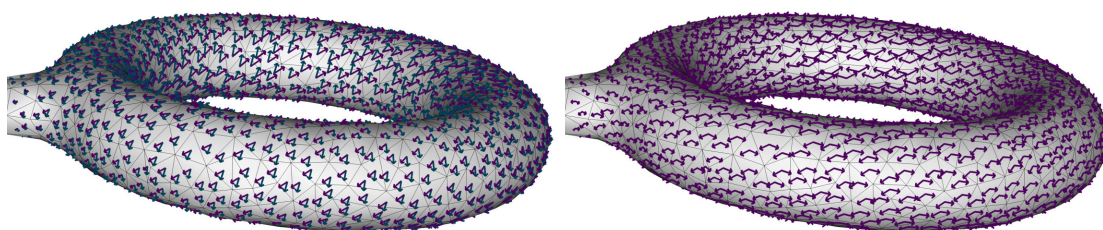


Figure 5.3: Two pairings of Neumann and Dirichlet fields from the bases shown in Figure 5.2. The left image shows the first Neumann field and the third Dirichlet field, forming locally acute angles on each triangle on the torus region. The right image shows the third Neumann field and the third Dirichlet field, forming obtuse angles.

AwH	$\mathcal{H}_{h,D}(a)$	$\mathcal{H}_{h,D}(b)$	TwC	$\mathcal{H}_{h,D}(a)$	$\mathcal{H}_{h,D}(b)$	$\mathcal{H}_{h,D}(c)$
$\mathcal{H}_{h,N}(a)$	1.57	1.57	$\mathcal{H}_{h,N}(a)$	2.30	1.57	0.74
$\mathcal{H}_{h,N}(b)$	1.57	1.57	$\mathcal{H}_{h,N}(b)$	1.62	1.57	1.55
			$\mathcal{H}_{h,N}(c)$	2.41	1.58	2.31

Table 5.1: Angles between the basis fields for $\mathcal{H}_{h,N}$ and $\mathcal{H}_{h,D}$ on the flat AwH-model and the TwC-model in radians. Whereas the angles on the flat AwH-model are all right angles, this is no longer true for the TwC-model, whose toroidal region generates inner cohomology.

This is confirmed by the numerical values for the angles given in Table 5.1. Here, each angle is computed as usual by

$$\cos \alpha = \frac{\langle X, Y \rangle_{L^2}}{\|X\|_{L^2} \|Y\|_{L^2}} \quad \text{for } X \in \mathcal{H}_{h,N}, Y \in \mathcal{H}_{h,D}.$$

Whereas both the second Neumann and Dirichlet field of Figure 5.2 form an angle of almost $\pi/2$ to all other fields, this is not true for the other fields. As the discussion suggested, the first pairing indeed forms an acute L^2 -angle of 0.74 radians, whereas the second pairing forms an obtuse L^2 -angle of 2.31 radians. Note that the angles spanned by the second Neumann and Dirichlet fields which are concentrated on the cylindrical region are only almost right angles. This is because solving for the kernel to compute bases for $\mathcal{H}_{h,N}$ and $\mathcal{H}_{h,D}$ does not take the splitting into the refined subspaces into account a priori. The well-separateness of the solutions is in this example merely coincidence and depends on the numerical solver. In contrast, all angles for the flat AwH-model are truly right angles.

Elaborating on this last aspect, Figure 5.4 shows a basis for the space of Dirichlet fields on the Laurent's hand model ("LH"), where three holes have been cut into the finger tips. Adding the hole at the wrist, this model is of type $\Sigma_{1,4}$, where a toroidal region is formed by the thumb and the index finger. Consequently, $\mathcal{H}_{h,D}$ is five-dimensional. Although the results in the first row of Figure 5.4 already suggest a splitting into $\mathcal{H}_{h,D,\text{ex}}$ (first three images) and $\mathcal{H}_{h,D,\partial\text{co}}$ (last two), this is again merely coincidence and cannot be relied on, as it depends on the solver used to compute the kernel of the system matrix $L_{\mathcal{H}_{h,D}}$. In contrast, the second row shows a true basis for $\mathcal{H}_{h,D,\text{ex}}$ and their corresponding harmonic potential functions. The colouring indicates that the potential is indeed constant on each boundary component.

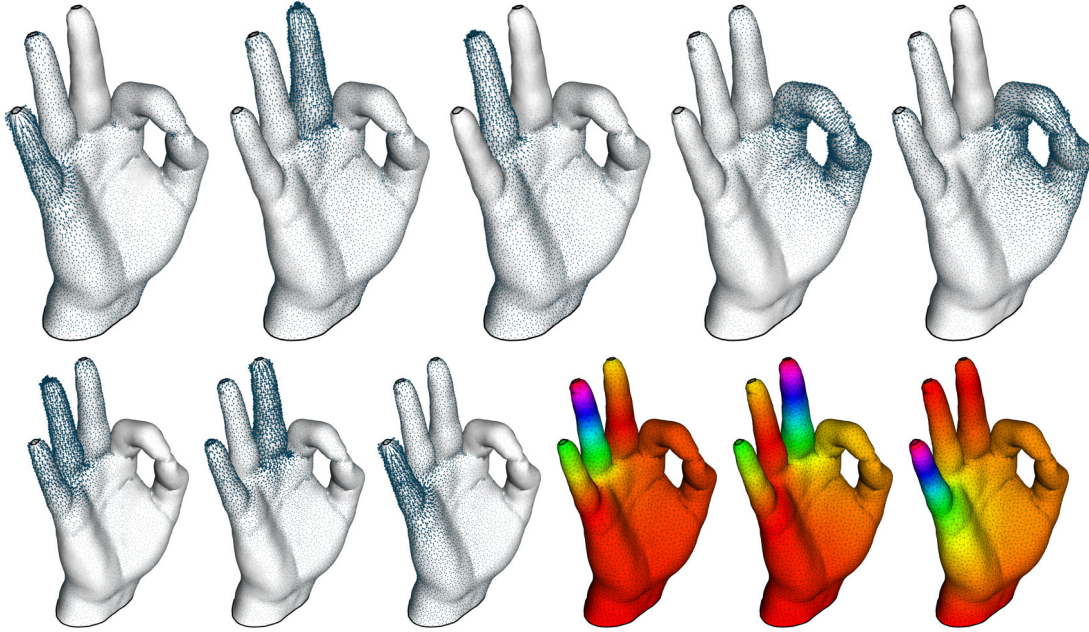


Figure 5.4: First row: Basis for $\mathcal{H}_{h,D}$ on the modified Laurent’s hand model with three holes cut into the finger tips and a fourth hole at the wrist. Second row: Basis for $\mathcal{H}_{h,D,\text{ex}}$ and the corresponding potential functions.

5.2 HODGE DECOMPOSITIONS ON SIMPLICIAL SURFACES

We present an algorithm to compute the decompositions derived in Section 3.2 for a given input vector field. The computation is based on an iterated L^2 -projection on the subspaces of the respective decompositions. The decomposition is tested for discrete interpolations of superpositions of smooth, stereotypical fields. The distinction between boundary and inner cohomology is illustrated in further examples.

Next, we present a computational approach for the decomposition of PCVFs according to the Hodge-type decomposition theorems on simplicial surfaces derived in Section 3.2. The refined decompositions of discrete harmonic Dirichlet and Neumann fields provide a concise distinction between harmonic flows induced from the interior topological features of the geometry and those harmonic flows that reflect the boundary. We assume that we are given a PCVF $X \in \mathcal{X}_h$ which might come from real data or an analytic expression, for instance through interpolation or L^2 -projection onto the space \mathcal{X}_h , representing cell-averages of the original field.

To compute the decomposition, we follow the iterated L^2 -projection approach proposed by [PP03], since it is a conceptually simple and—due to its global nature—robust method: given a vector field $X = X_0 \in \mathcal{X}_h$, compute the L^2 -projection $\text{pr}_{\mathcal{V}_1}(X)$ onto an L^2 -direct summand subspace \mathcal{V}_1 of the orthogonal decomposition of interest, and form the residue $X_1 := X - \text{pr}_{\mathcal{V}_1}(X)$. Now, project X_1 onto the next subspace \mathcal{V}_2 , form the residue X_2 , and iterate until all subspaces are processed. Each projection step amounts to the solution of a linear problem of

the type

$$\text{Find } u \in \mathcal{V}_i \text{ such that } \langle u, v \rangle_{L^2} = \langle X_{i-1}, v \rangle_{L^2} \text{ for all } v \in \mathcal{V}_i. \quad (5.2)$$

Solving these system requires a basis for each subspace \mathcal{V}_i in order to set up the system matrix and the right-hand side. This is easy for the subspaces $\nabla\mathcal{L}_0$, $\nabla\mathcal{L}$, $J\nabla\mathcal{F}_0$ and $J\nabla\mathcal{F}$. For $\nabla\mathcal{L}$ and $J\nabla\mathcal{F}$, one should exclude the constant functions from the kernel, or solve for a least-squares minimum solution instead, for instance.

In order to compute the projection of X onto $\mathcal{H}_{h,D,\text{ex}}$, we first compute a basis $\mathcal{B}_{\mathcal{H}_{h,D,\text{ex}}} = \{Z_1, \dots, Z_{m-1}\}$ for $\mathcal{H}_{h,D,\text{ex}}$ as described in Section 5.1. Each Z_i is of the form

$$Z_i = \sum_{j=1}^{n_V} z_{ij} \nabla\varphi_j \quad \text{with } \varphi_j \in \mathcal{L}$$

with coefficients $z_{ij} \in \mathbb{R}$. Using this basis, we now solve (5.2). The resulting coefficient vector u represents the solution as a linear combination

$$\sum_{i=1}^{m-1} u_i Z_i = \sum_{j=1}^{n_V} \left(\sum_{i=1}^{m-1} u_i z_{ij} \right) \nabla\varphi_j.$$

A pseudocode example for a computational decomposition according to (3.15) is given in Listing 5.1. A computation for the decomposition involving the refined Neumann fields goes along the same lines.

Listing 5.1: Algorithm for the computation of the decomposition (3.15)

```

Input: PCVF  $X \in \mathcal{X}_h$ , integer  $m$  (optional)
 $X_{\nabla\mathcal{L}_0}$    = project( $X$ ,  $\nabla\mathcal{L}_0$ )
 $X_1$       =  $X - X_{\nabla\mathcal{L}_0}$ 
 $X_{J\nabla\mathcal{F}_0}$  = project( $X_1$ ,  $J\nabla\mathcal{F}_0$ )
 $X_2$       =  $X_1 - X_{J\nabla\mathcal{F}_0}$ 
 $X_{\mathcal{H}_h \cap J\nabla\mathcal{F}}$  = project( $X_2$ ,  $J\nabla\mathcal{F}$ )
 $X_3$       =  $X_2 - X_{\mathcal{H}_h \cap J\nabla\mathcal{F}}$ 
 $\mathcal{B}_{\mathcal{H}_{h,D,\text{ex}}}$  = compute_HDex_basis(size= $m-1$ )
 $X_{\mathcal{H}_{h,D,\text{ex}}}$  = project( $X_3$ ,  $\mathcal{B}_{\mathcal{H}_{h,D,\text{ex}}}$ )
 $X_{\mathcal{H}_{h,D,\partial\text{co}}}$  =  $X_3 - X_{\mathcal{H}_{h,D,\text{ex}}}$ 
return  $X_{\nabla\mathcal{L}_0}$ ,  $X_{J\nabla\mathcal{F}_0}$ ,  $X_{\mathcal{H}_h \cap J\nabla\mathcal{F}}$ ,  $X_{\mathcal{H}_{h,D,\text{ex}}}$ ,  $X_{\mathcal{H}_{h,D,\partial\text{co}}}$ 

```

EXPERIMENTAL RESULTS. We present two exemplary computational decompositions. The first one decomposes the L^2 -projection to \mathcal{X}_h of the vector field

$$\begin{aligned}
X_{\text{annulus}} &:= X_{N,\text{co}} + X_{D,\text{ex}} + X_{\text{ex}} + X_{\text{co}} \quad \text{with} \\
X_{N,\text{co}} &:= (x^2 + y^2)^{-1}(-y, x), \\
X_{D,\text{ex}} &:= (x^2 + y^2)^{-1}(x, y), \\
X_{\text{ex}} &:= (2x, 1) = \nabla(x^2 + y), \\
X_{\text{co}} &:= 2(-y, x) = -J\nabla(x^2 + y^2)
\end{aligned}$$

on a flat annulus in \mathbb{R}^2 , centred at the origin. Note that $X_{N,\text{co}}$ and $X_{D,\text{ex}}$ are smooth harmonic fields, i.e. they are curl- and divergence-free. Furthermore, on a perfectly round annulus centred at the origin the rotating field $X_{N,\text{co}}$ is tangential along the boundaries whereas the radial field $X_{D,\text{ex}}$ is orthogonal to the boundaries. Since there is no inner cohomology (the annulus is homeomorphic to $\Sigma_{0,2}$), by Theorem 3.2.18 there is a complete L^2 -orthogonal decomposition involving all the discussed spaces at the same time. The result is shown in Figure 5.5. The exact part X_{ex} contributes predominantly to the central harmonic space $\nabla\mathcal{L} \cap J\nabla\mathcal{F}$ and $\mathcal{H}_{h,D,\text{ex}}$, whereas the harmonic circulation is correctly captured in $\mathcal{H}_{h,N,\text{co}}$.

The parts of the complete decomposition that are not shown correspond to the non-existing inner cohomology and are consequently negligible, with L^2 -norms of magnitude 10^{-12} and lower coming from numerical round-off, see Table 5.2 below. Of course, an additional small discretization error depending on the mesh size is caused by the interpolation step of the smooth field onto \mathcal{X}_h . The harmonic Dirichlet and Neumann components are in fact exact and coexact, respectively, as predicted by Lemma 3.2.17.

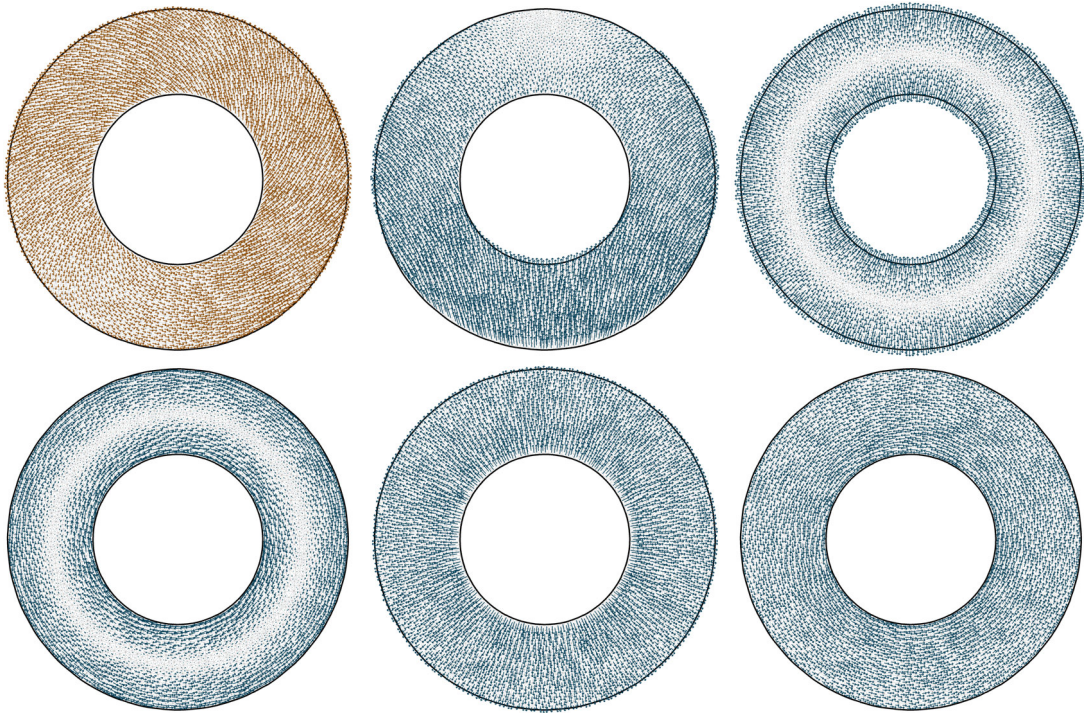


Figure 5.5: Decomposition of the vector field X_{annulus} . Top row: input vector field, central harmonic component in $\nabla\mathcal{L} \cap J\nabla\mathcal{F}$ and exact component in $\nabla\mathcal{L}_0$. Bottom row: coexact component in $J\nabla\mathcal{F}_0$, exact Dirichlet component in $\mathcal{H}_{h,D,\text{ex}}$ and coexact Neumann component in $\mathcal{H}_{h,N,\text{co}}$.

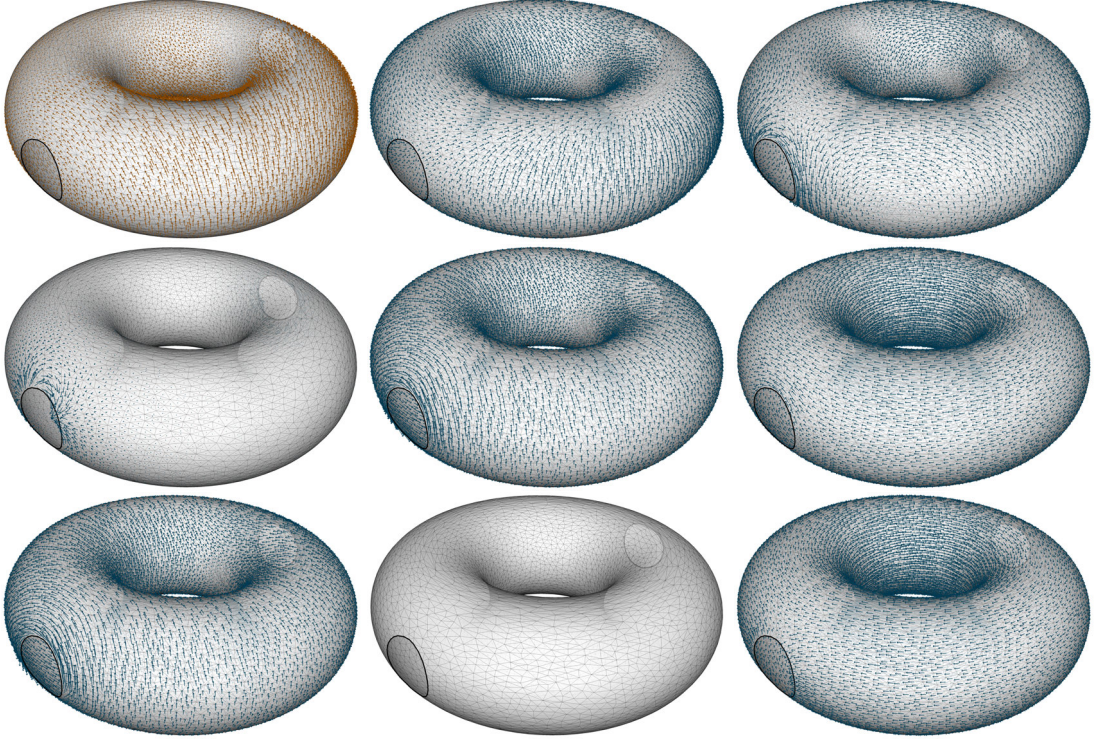


Figure 5.6: First row: input vector field and its components in $\nabla\mathcal{L}_0$ and $J\nabla\mathcal{F}_0$. Second row: components in $\mathcal{H}_h \cap \nabla\mathcal{L}$, $\mathcal{H}_{h,N,\text{co}}$ and $\mathcal{H}_{h,N,\partial\text{ex}}$. Third row: components in $\mathcal{H}_h \cap J\nabla\mathcal{F}$, $\mathcal{H}_{h,D,\text{ex}}$ and $\mathcal{H}_{h,D,\partial\text{co}}$.

The second example, shown in Figure 5.6, compares the decompositions (3.14) and (3.15) for the same input vector field on a torus geometry with two symmetric, opposite holes cut out. The input vector field $X_{\Sigma_{1,2}}$ is the superposition

$$\begin{aligned} X_{\Sigma_{1,2}} &:= X_A + X_B \quad \text{with} \\ X_A &:= (x^2 + y^2)^{-1}(y, -x, 0) \\ X_B &:= (0, z, -y) \end{aligned}$$

of a harmonic flow X_A along the torus and a rotation in the yz -plane around the centre axis through the opposite holes, restricted to the surface mesh and interpolated in \mathcal{X}_h . The boundary-constrained exact and coexact components in $\nabla\mathcal{L}_0$ and $J\nabla\mathcal{F}_0$, respectively, are shared by both decompositions. The harmonic flow X_A is in both cases correctly captured by the corresponding subspace representing inner cohomology, which is $\mathcal{H}_{h,N,\partial\text{ex}}$ in the first case and $\mathcal{H}_{h,D,\partial\text{co}}$ in the second. The harmonic part of the rotation X_B is in the first case captured by $\mathcal{H}_{h,N,\text{co}}$ whereas in the latter it appears in $\mathcal{H}_h \cap J\nabla\mathcal{F}$. In both cases it is a coexact harmonic field. The exact harmonic component which appears as $\mathcal{H}_h \cap \nabla\mathcal{L}$ in the first and as $\mathcal{H}_{h,D,\text{ex}}$ in the second decomposition is in both cases negligible. The boundary behaviour of each component is shown in Figure 5.7.

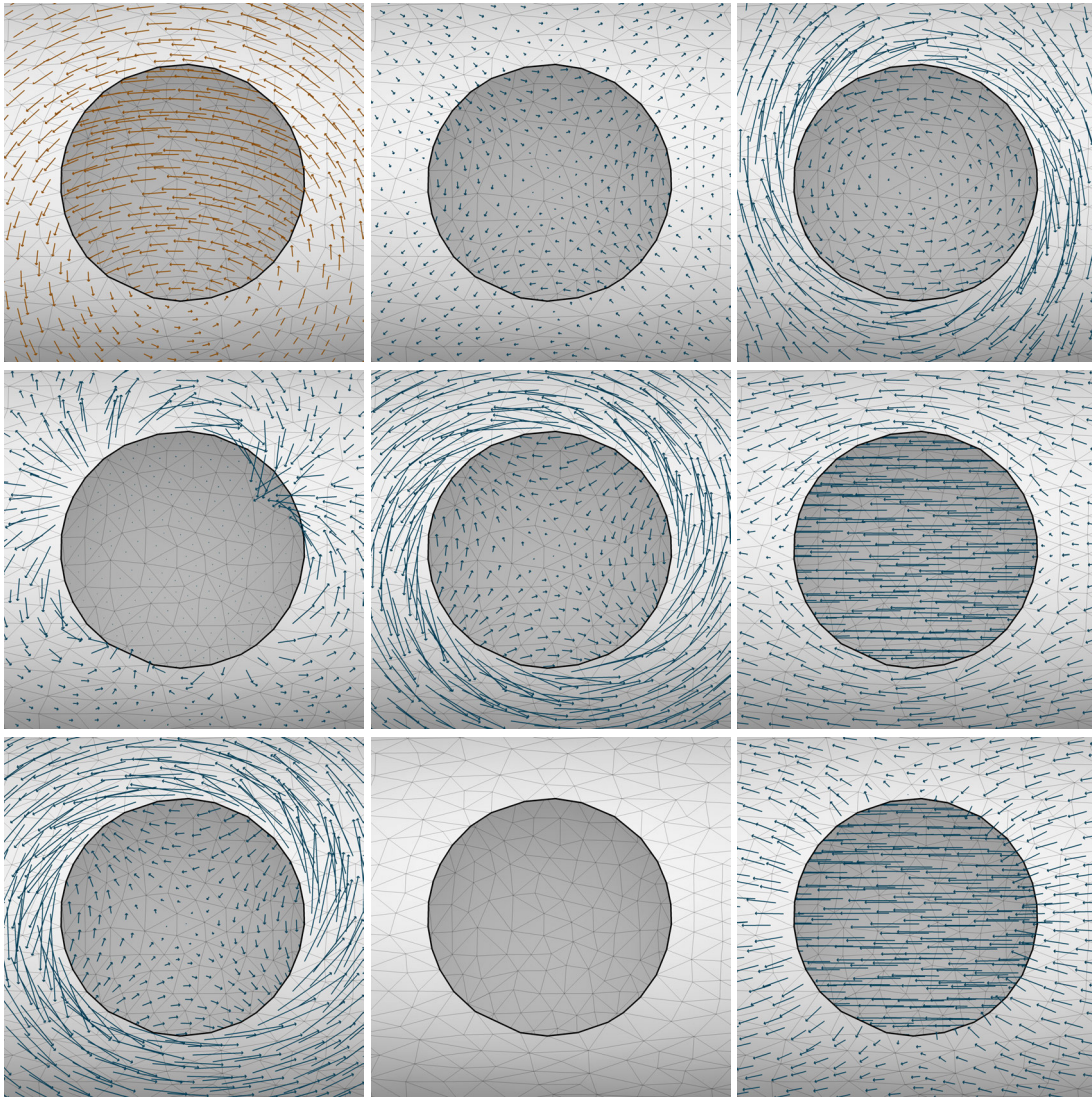


Figure 5.7: Boundary close-ups for the components shown in Figure 5.6. The boundary-exactness of the component in $\mathcal{H}_{h,N,\partial_{\text{ex}}}$ is clearly visible (second row, third image). The rotation induced by the field X_B is mostly captured by the coexact components (pictures on the main skew diagonal).

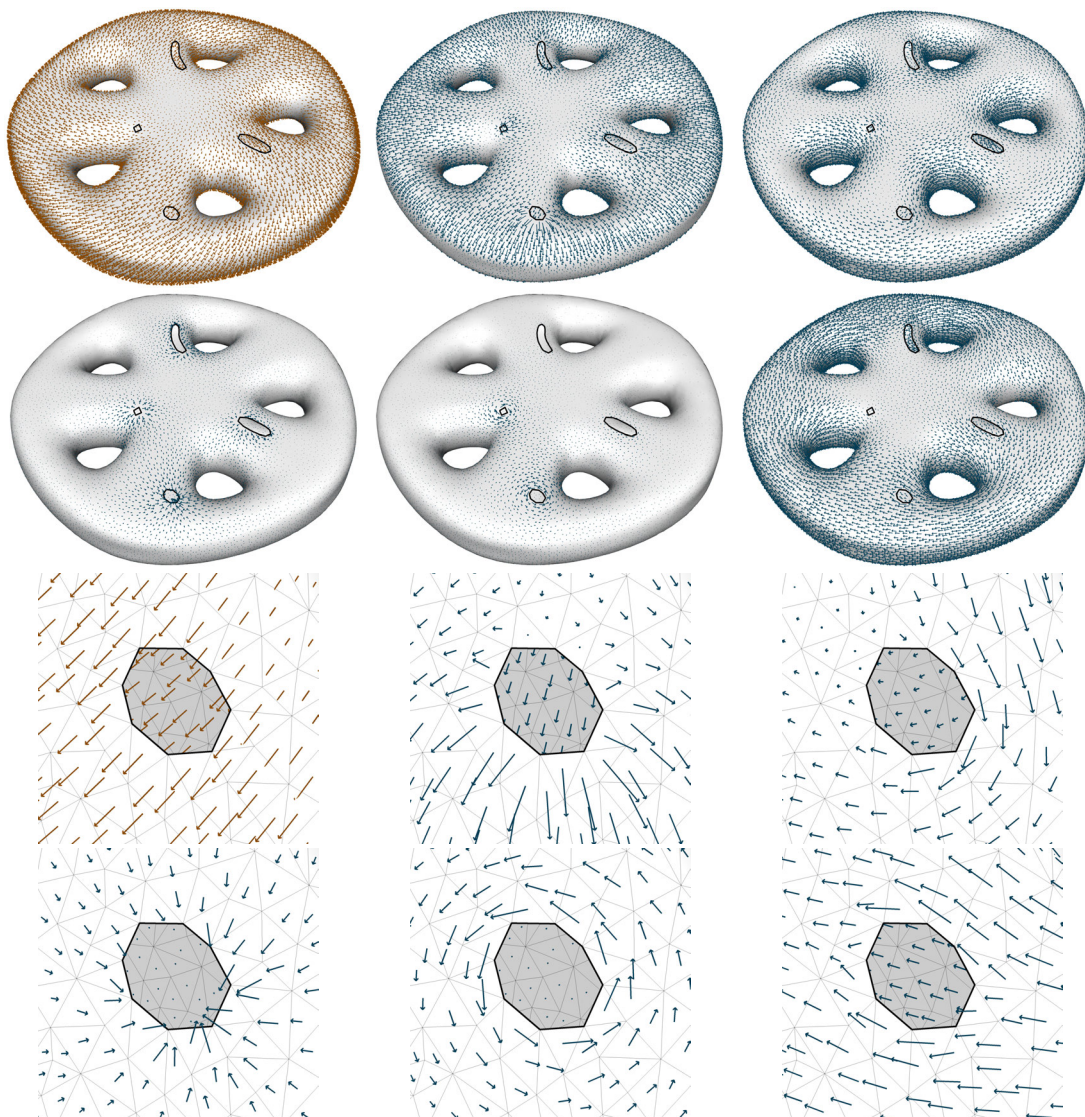


Figure 5.8: Decomposition of the vector field $X_{\Sigma_{5,4}}$ on a surface of type $\Sigma_{5,4}$. Top row: input vector field, exact component in $\nabla\mathcal{L}_0$ and coexact component in $J\nabla\mathcal{F}_0$. Second row: harmonic exact component in $\mathcal{H}_h \cap \nabla\mathcal{L}$, coexact Neumann component in $\mathcal{H}_{h,N,\text{co}}$ and boundary-exact Neumann component in $\mathcal{H}_{h,N,\partial\text{ex}}$. Third and fourth row: close-ups of the boundary behaviour around the lower left boundary hole for each component, following the same order as above. The exact component in $\nabla\mathcal{L}_0$ is perpendicular to the boundary, whereas the components of the harmonic Neumann part as well as the coexact component in $J\nabla\mathcal{F}_0$ are mostly tangential. The harmonic exact component in $\mathcal{H}_h \cap \nabla\mathcal{L}$ does not obey any particular boundary behaviour.

The last example is a decomposition according to (3.14) on a more complicated geometry of type $\Sigma_{5,4}$, see Figure 5.8. The field $X_{\Sigma_{5,4}}$ to be decomposed is once again a superposi-

tion of several elementary fields: a harmonic circulation component around the right-most handle, a rotational global component and a divergence component in the centre of the geometry, defined on the ambient space and restricted and interpolated in \mathcal{X}_h . We mainly find contributions in the subspaces $\nabla \mathcal{L}_0$, $J\nabla \mathcal{F}_0$ and $\mathcal{H}_{h,N,\partial \text{co}}$, the latter reflecting the global harmonic flow around the “inner geometry” (the handles). See Table 5.2 for the L^2 -norms for the components.

Space	X_{annulus}	$X_{\Sigma_{5,4}}$	Space	X_{annulus}	$X_{\Sigma_{5,4}}$
Input	5.82	2.80			
$\nabla \mathcal{L}_0$	0.44	1.61	$\mathcal{H}_{h,D,\text{ex}}$	3.21	-
$\nabla \mathcal{F}_0$	0.89	1.08	$\mathcal{H}_{h,D,\partial \text{co}}$	10^{-12}	-
$\mathcal{H}_h \cap \nabla \mathcal{L}$	-	0.33	$\mathcal{H}_{h,N,\text{co}}$	4.33	0.06
$\nabla \mathcal{L} \cap J\nabla \mathcal{F}$	1.95	-	$\mathcal{H}_{h,N,\partial \text{ex}}$	10^{-14}	1.48

Table 5.2: L^2 -norms of the components of the decomposed vector fields. Entries with a hyphen do not exist in the computed decompositions.

5.3 COHOMOLOGY REPRESENTATIVES ON SIMPLICIAL SOLIDS

We compute bases for the spaces $\mathcal{H}_{h,D}^*$ and $\mathcal{H}_{h,N}^*$ on simplicial solids. The basis for discrete Neumann fields can be directly computed in the ansatz space \mathcal{F} , which reduces the size of the matrix whose kernel has to be solved for. For discrete Dirichlet fields we obtain a basis in the ansatz space \mathcal{X}_h . Still one can obtain a vector potential by projecting the solution onto the space $\text{curl}(\mathcal{N})$. Two examples on geometries exhibiting both cavities and solid handles are shown.

We now demonstrate how to compute representatives for cohomology classes on simplicial solids in \mathbb{R}^3 . These representatives reveal the non-trivial topology of the domain—for domains embedded in \mathbb{R}^3 topological features come from solid handle bodies or from cavities in the interior. Although the strategy is in the same spirit as in Section 5.1, there are a few differences.

SETTING UP THE SYSTEM MATRICES. In virtue of Theorem 3.3.8, a basis for the space of Dirichlet fields $\mathcal{H}_{h,D}^*$ is given by a basis for the orthogonal complement of $\text{curl}(\mathcal{N}_0) \oplus \nabla \mathcal{F}$.

Let $\mathcal{B}_{\mathcal{N}} := \{\eta_i\}$ be the edge basis for the Nédélec elements \mathcal{N} , and let $\mathcal{B}_{\mathcal{N}_0} := \{\eta_{0,i}\} \subset \mathcal{B}_{\mathcal{N}}$ be the subset of basis functions whose degrees of freedom correspond to the inner edges. Similarly, let $\mathcal{B}_{\mathcal{F}} := \{\psi_i\}$ and $\mathcal{B}_{\mathcal{F}_0}$ be the face-midpoint bases for \mathcal{F} and \mathcal{F}_0 , respectively, the latter containing all basis functions associated to inner faces. A basis for \mathcal{X}_h is given by the family $\{E_{t,1}, E_{t,2}, E_{t,3}\}_{t \in M_h^{(3)}}$ indexed by the cells, where $E_{t,i} = (\delta_{1,i}, \delta_{2,i}, \delta_{3,i}) \in \mathbb{R}^3$ are the canonical basis vectors. Again, for simplicity we renumerate these vectors and set $\mathcal{B}_{\mathcal{R}} := \{E_j\}$ for $j = 1, \dots, 3n_T$, and $\mathcal{R} := \mathbb{R}^{3n_T}$. We define the following matrices:

$$L_{\text{curl}(\mathcal{N}_0), \mathcal{R}} := \left(\langle \text{curl}(\eta_{0,i}), E_j \rangle_{L^2} \right)_{\substack{i=1, \dots, n_{iE} \\ j=1, \dots, 3n_T}}$$

$$L_{\nabla \mathcal{F}, \mathcal{R}} := \left(\langle \nabla \psi_i, E_j \rangle_{L^2} \right)_{\substack{i=1, \dots, n_F-1 \\ j=1, \dots, 3n_T}}$$

Then for an element $X = \sum_i X_i E_i$ in the linear span of $\mathcal{B}_{\mathcal{R}}$ it is $L_{\text{curl}(\mathcal{N}_0), \mathcal{R}} \cdot X = 0$ and $L_{\nabla \mathcal{F}, \mathcal{R}} \cdot X = 0$ if and only if X is L^2 -orthogonal to all curl fields of inner Nédélec elements

and all cogradient fields of Crouzeix-Raviart elements, respectively. Stacking these matrices into a single matrix

$$L_{\mathcal{H}_{h,D}^*} := \begin{pmatrix} L_{\text{curl}(\mathcal{N}_0), \mathcal{R}} \\ L_{\nabla \mathcal{F}, \mathcal{R}} \end{pmatrix} \quad (5.3)$$

of dimension $(n_{iE} + n_F - 1) \times 3n_T$, it is

$$\mathcal{H}_{h,D}^* = \ker(L_{\mathcal{H}_{h,D}^*})$$

which needs to be solved for. Only $n_F - 1$ basis functions of \mathcal{F} are needed, since the constants are in the kernel of the gradient. Furthermore, the rows in the matrix $L_{\text{curl}(\mathcal{N}_0), \mathcal{R}}$ are linearly dependent, since curl has a large kernel of dimension $n_{iV} + h_r^1 = n_{iV} + h^2$, which follows from Section 3.1. However, since the computation of a coimage basis for curl would itself require the computation of a harmonic basis representing h_r^1 , we keep redundant rows, as this does not have an apparent effect on the numerical solution.

Again, the same strategy can be applied to obtain a basis for $\mathcal{H}_{h,N}^*$, using the stacked matrix

$$L_{\mathcal{H}_{h,N}^*} := \begin{pmatrix} L_{\text{curl}(\mathcal{N}), \mathcal{R}} \\ L_{\nabla \mathcal{F}_0, \mathcal{R}} \end{pmatrix},$$

which is now of dimension $(n_E + n_{iF}) \times 3n_T$, and solve for its kernel.

Both these methods provide us with a basis for $\mathcal{H}_{h,D}^*$ and $\mathcal{H}_{h,N}^*$, respectively, expressed in the basis $\{E_j\}$ of \mathcal{X}_h . But because of Lemma 3.3.9 and Corollary 3.3.12, Dirichlet fields are exact and Neumann fields are coexact. Thus in order to compute Neumann fields, we can actually span the kernel of $L_{\mathcal{H}_{h,N}^*}$ by elements in $\nabla \mathcal{F}$, leading to the matrices

$$\begin{aligned} L_{\text{curl}(\mathcal{N}_b), \nabla \mathcal{F}} &:= (\langle \text{curl}(\eta_i), \nabla \psi_j \rangle_{L^2})_{\substack{i=1, \dots, n_{bE} \\ j=1, \dots, n_F}} \\ L_{\nabla \mathcal{F}_0, \nabla \mathcal{F}} &:= (\langle \nabla \psi_{0,i}, \nabla \psi_j \rangle_{L^2})_{\substack{i=1, \dots, n_{iF} \\ j=1, \dots, n_F}} \\ L_{\mathcal{H}_{h,N}^*} &:= \begin{pmatrix} L_{\text{curl}(\mathcal{N}_b), \nabla \mathcal{F}} \\ L_{\nabla \mathcal{F}_0, \nabla \mathcal{F}} \\ (1, 0, \dots, 0) \end{pmatrix} \end{aligned}$$

As in the computation for $\mathcal{H}_{h,D,\text{ex}}^*$ in the surface case, it is sufficient to ensure orthogonality of the gradient to elements $\text{curl}(\mathcal{N}_b)$ whose degrees of freedom are associated to boundary edges only. The additional row $(1, 0, \dots, 0)$ excludes the kernel of ∇ on \mathcal{F} .

Given that n_F is usually significantly smaller than $3n_T$ —see e.g. [Gum00, Sec. 9] which gives a ratio estimate of $n_V : n_E : n_F : n_T = 1 : 6.5 : 11 : 5.5$ for tetrahedral meshes with small Euler characteristic and boundary, or the data for our test meshes in Table 5.3—this reduces the system size roughly to two thirds of its original size. Moreover, a solution does not only provide a vector field, but also its copotential function, up to a constant.

However, in contrast to the two-dimensional case, this strategy does not work out for the space $\mathcal{H}_{h,D}^* = \mathcal{H}_{h,D,\text{ex}}^*$, because of the non-trivial kernel of curl which cannot be ruled out as easily as for the ansatz space $\nabla \mathcal{F}$. The best one can do with this approach is to first solve for the kernel of (5.3) and then compute an L^2 -projection onto $\text{curl}(\mathcal{N})$ in order to obtain a potential field for each basis element of $\mathcal{H}_{h,D}^*$.

Model	n_V	n_E	n_F	n_T	$n_V : n_E : n_F : n_T$
SUS	1813	11792	10312	9332	1.00 : 6.50 : 10.65 : 5.15
ST	1255	6466	9398	4187	1.00 : 5.15 : 7.49 : 3.34
SwC	1888	12246	19993	9633	1.00 : 6.49 : 10.59 : 5.10
DTwC	6575	36701	56030	25904	1.00 : 5.58 : 8.52 : 3.94
G3C2	8902	53482	83304	38724	1.00 : 6.01 : 9.36 : 4.35

Table 5.3: Mesh data for three-dimensional solid meshes used in the experiments.

EXPERIMENTAL RESULTS. In the following experiments we have computed streamlines instead of plotting the vector glyphs directly in order to improve the visual perception of the three-dimensional fields in the solid. The colouring encodes the velocity of the flow, i.e. the length of the vectors at each point—orange indicates a higher velocity relative to blue regions.

Figure 5.9 shows a basis for the spaces $\mathcal{H}_{h,N}^*$ and $\mathcal{H}_{h,D}^*$ on a solid double-torus geometry with a cavity around the origin (“DTwC”). The high velocity around the cavity stems from the fact that this boundary component has a much smaller area than the outer boundary of the geometry and that the total integrated in- and outflow of a divergence-free field has to sum up to zero. The Dirichlet fields correspond to the two handles of the geometry.

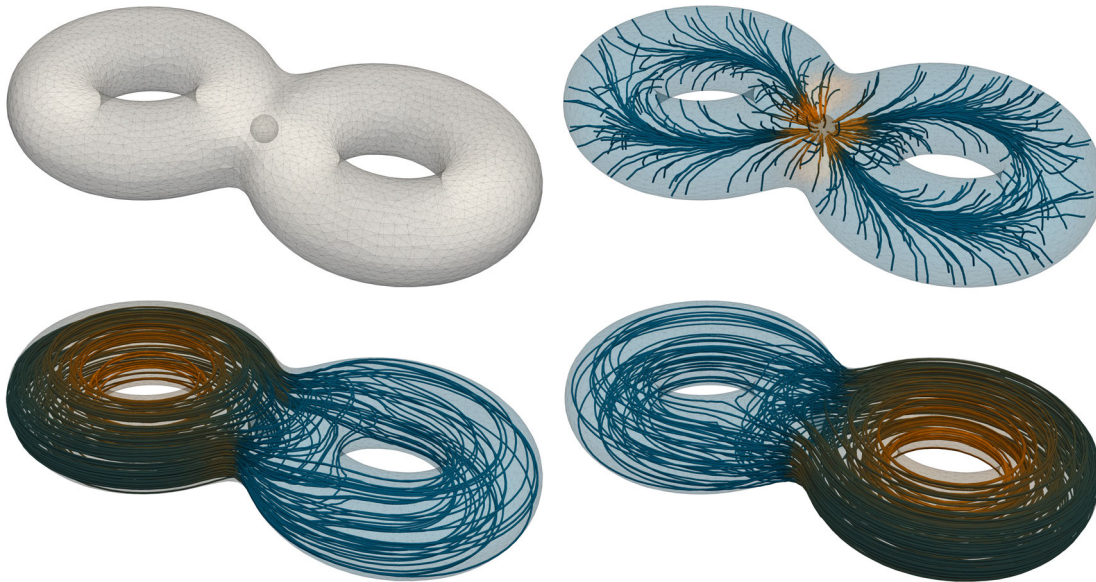


Figure 5.9: Cohomology bases on the double-torus with a cavity. First row: model and discrete Neumann basis. Second row: discrete Dirichlet basis.

As a second example, we compute the Dirichlet and Neumann basis on a geometry with $h^1 = 3$ and $h^2 = 2$, see Figure 5.10 which we refer to as “G3C2”. Again, the two cavities, which are generators for the second cohomology space, are nicely separated by the two Neumann basis fields, but for a higher cohomological dimension this is not necessarily the case as the computed Dirichlet basis shows.

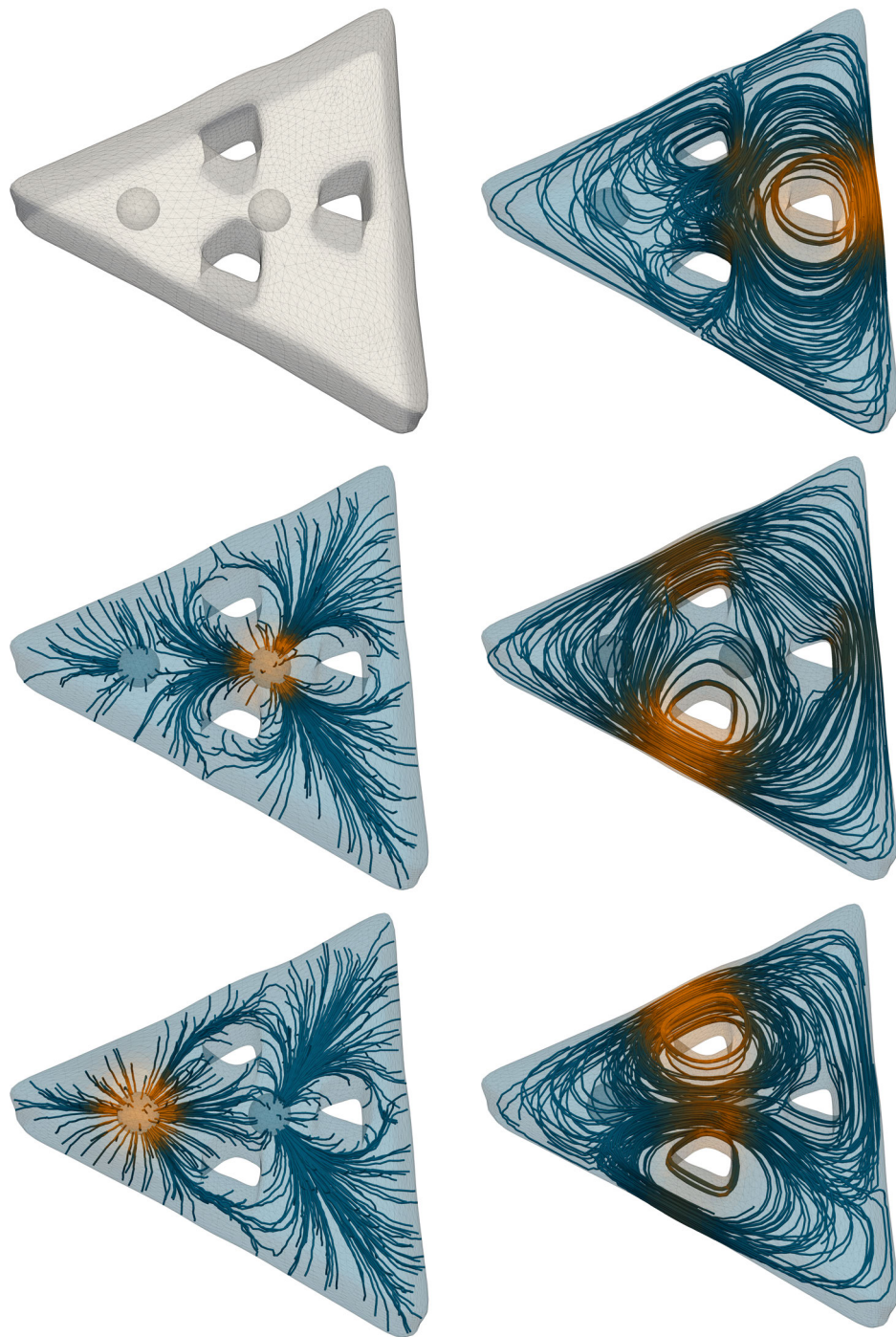


Figure 5.10: Cohomology bases on the model “G3C2” with three handles and two cavities and therefore $h^1 = 3$ and $h^2 = 2$. First column: model and discrete Neumann basis. Second column: discrete Dirichlet basis.

5.4 HODGE DECOMPOSITIONS ON SIMPLICIAL SOLIDS

We compute the complete Hodge decomposition on simplicial solids and evaluate our algorithm by computing decompositions for interpolants of stereotypical fields which are contained in exactly one subspace of the smooth decomposition.

Finally, we discuss computational decompositions of PCVFs on simplicial solids. With respect to Theorem 3.3.13 we shall only care for the complete decomposition

$$\mathcal{X}_h = \text{curl}(\mathcal{N}_0) \oplus \nabla \mathcal{F}_0 \oplus \text{curl}(\mathcal{N}) \cap \nabla \mathcal{F} \oplus \mathcal{H}_{h,N}^* \oplus \mathcal{H}_{h,D}^*. \quad (5.4)$$

Following the iterated L^2 -projection algorithm in Section 5.2, we compute the decomposition as described in Listing 5.2. Note that the projection of $X_{\mathcal{H}_h \cap \nabla \mathcal{F}}$ onto $\text{curl}(\mathcal{N})$ is still an element in $\mathcal{H}_h \cap \nabla \mathcal{F}$, since the sum $\text{curl}(\mathcal{N}_0) \oplus \mathcal{H}_{h,D}^* \subset \text{curl}(\mathcal{N})$ is orthogonal to $\mathcal{H}_h \cap \nabla \mathcal{F}$. The projection is therefore indeed an element in the harmonic centre $\text{curl}(\mathcal{N}) \cap \nabla \mathcal{F}$.

Listing 5.2: Algorithm for the computation of the decomposition (5.4)

```

Input: PCVF  $X \in \mathcal{X}_h$ 
 $X_{\text{curl}(\mathcal{N}_0)}$  = project( $X$ ,  $\text{curl}(\mathcal{N}_0)$ )
 $X_1$  =  $X - X_{\text{curl}(\mathcal{N}_0)}$ 
 $X_{\nabla \mathcal{F}_0}$  = project( $X_1$ ,  $\nabla \mathcal{F}_0$ )
 $X_2$  =  $X_1 - X_{\nabla \mathcal{F}_0}$ 
 $X_{\mathcal{H}_h \cap \nabla \mathcal{F}}$  = project( $X_2$ ,  $\nabla \mathcal{F}$ )
 $X_{\mathcal{H}_{h,D}^*}$  =  $X_2 - X_{\mathcal{H}_h \cap \nabla \mathcal{F}}$ 
 $X_{\text{curl}(\mathcal{N}) \cap \nabla \mathcal{F}}$  = project( $X_{\mathcal{H}_h \cap \nabla \mathcal{F}}$ ,  $\text{curl}(\mathcal{N})$ )
 $X_{\mathcal{H}_{h,N}^*}$  =  $X_{\mathcal{H}_h \cap \nabla \mathcal{F}} - X_{\text{curl}(\mathcal{N}) \cap \nabla \mathcal{F}}$ 
return  $X_{\text{curl}(\mathcal{N}_0)}$ ,  $X_{\nabla \mathcal{F}_0}$ ,  $X_{\text{curl}(\mathcal{N}) \cap \nabla \mathcal{F}}$ ,  $X_{\mathcal{H}_{h,N}^*}$ ,  $X_{\mathcal{H}_{h,D}^*}$ 
    
```

EXPERIMENTAL RESULTS. As a first example, we consider the following stereotypical vector fields and compare them with the components of their discrete decompositions:

$$\begin{aligned}
 X_{\text{ex}_0^*} &:= (y, -x, 0) = \text{curl}(-zx, -zy, -z^2) \\
 X_{\text{co}_0^*} &:= (x, y, z) = \frac{1}{2} \nabla(x^2 + y^2 + z^2 - 1) \\
 X_C &:= -\frac{1}{2} \cdot (1, 1, 1) \\
 X_{N^*} &= \frac{1}{(x^2 + y^2 + z^2)^{3/2}} (x, y, z) \\
 X_{D^*} &= \frac{1}{x^2 + y^2} (y, -x, 0).
 \end{aligned} \quad (5.5)$$

Each of these fields represents one subspace of the smooth five-term decomposition (2.21), provided they are defined on the correct domain. For the first three fields this will be a solid unit sphere (“SUS”) centred at the origin. The last two fields become singular at the origin, but they are harmonic at all non-zero points. X_{N^*} is a radial field and therefore normal to the boundary of a solid sphere with a concentric cavity (“SwC”), whereas X_{D^*} is tangential to the boundary of a solid torus (“ST”) centred at the origin. Figure 5.11 illustrates these three types of domains.

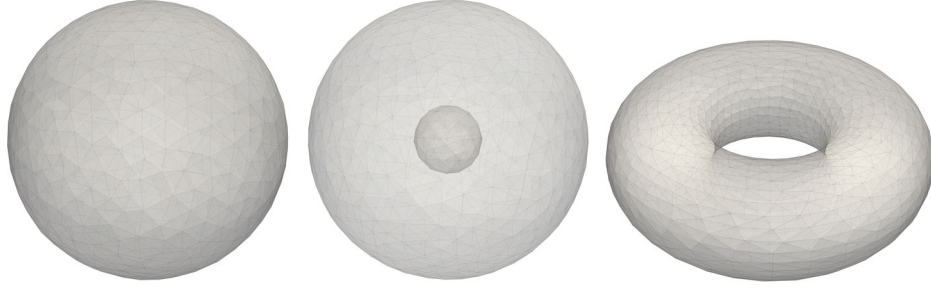


Figure 5.11: A solid unit sphere, a solid sphere with a cavity centred at the origin and a solid torus are the prototypes of domains for representative fields in the five-term decomposition on simplicial solids.

The field $X_{\text{ex}_0^*}$ is the curl field of a vector field which is normal to the boundary of the solid unit sphere, which can be seen as follows: at each point on the boundary, the unit normal is given by the direction vector (x, y, z) . Since it is

$$(zx, zy, z^2) \times (x, y, z) = 0,$$

(zx, zy, z^2) has no tangential component on the boundary. We therefore expect $X_{\text{ex}_0^*}$ to be reflected in the space $\text{curl}(\mathcal{N}_0)$.

The field $X_{\text{co}_0^*}$ is the gradient of a function which vanishes on the boundary of the solid unit sphere, so we expect this field to be represented in $\nabla\mathcal{F}_0$.

Note that since we decompose vector proxies for 2-forms, the curl field is in fact the exact component with its corresponding 2-form being in the image of the exterior derivative, whereas the gradient field is coexact. Following the same convention as for Dirichlet and Neumann fields in the three-dimensional case, the asterisk in the subscript should remind the reader of this fact.

The constant field X_C is both the gradient of a potential and the curl of a rotation around a centre axis through the sphere passing through the origin and the point $(0.5, 0.5, 0.5)$. Since it is harmonic, it is a candidate for the harmonic centre space $\text{curl}(\mathcal{N}) \cap \nabla\mathcal{F}$.

The last two vector fields X_{N^*} and X_{D^*} are both divergence- and curl-free, i.e. harmonic. X_{D^*} is tangential to the boundary of a solid torus, whereas X_{N^*} is normal to any sphere of arbitrary radius, centred at the origin. So we expect X_{D^*} to be reflected by a field in $X_{\mathcal{H}_{h,D}^*} \in \mathcal{H}_{h,D}^*$ on a solid torus, whereas X_{N^*} should be reflected by an element $X_{\mathcal{H}_{h,N}^*} \in \mathcal{H}_{h,N}^*$ on a sphere with a concentric cavity in the interior, cutting out a neighbourhood of the origin, which is a singularity for the vector field.

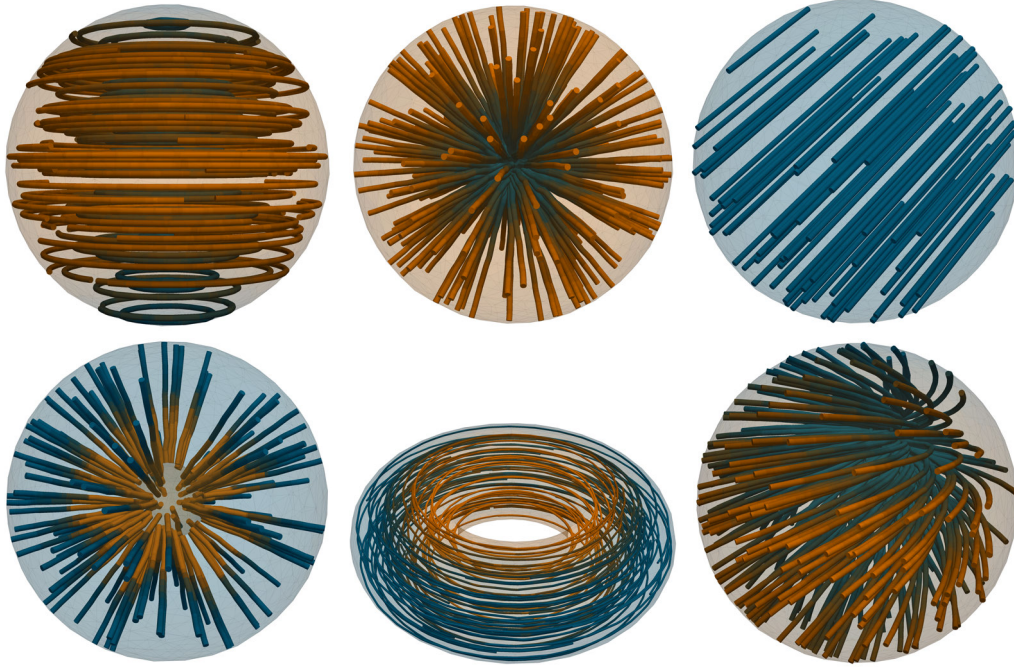


Figure 5.12: Discrete interpolants of stereotypical vector fields for the five-term decomposition from (5.5) and the superposition field (5.6). First row: Interpolants of the fields $X_{\text{ex}_0^*}$, $X_{\text{co}_0^*}$ and X_C on a solid sphere. Second row: The fields X_{N^*} , X_{D^*} and the superposition $X_{\text{ex}_0^* + \text{co}_0^* + C}$ on a sphere with a cavity, a solid torus and a solid sphere, respectively. For the five stereotypes, their reproductions in the respective subspaces of the decomposition are visually identical with the input fields. The decomposed parts of the superposition agree visually with the fields in the first row. See Table 5.4 for a quantitative evaluation.

In addition, we consider the superposition

$$X_{\text{ex}_0^* + \text{co}_0^* + C} := X_{\text{ex}_0^*} + X_{\text{co}_0^*} + X_C \quad (5.6)$$

and compute its discrete decomposition. Ideally, the three components are recovered in the corresponding discrete spaces. The discrete interpolants of these vector fields on the respective geometries are shown in Figure 5.12.

Table 5.4 lists the L^2 -norms of each vector field and each of its components in the decomposition. As expected, the dominant components in each decomposition are reflected in the correct subspaces. Of course, the components in the other subspaces, albeit magnitudes smaller, usually do not vanish due to discretization errors caused by the approximation of the smooth mesh, the interpolation of the smooth field and the numerical solver.

	$X_{\text{ex}_0^*}$	$X_{\text{co}_0^*}$	X_C	X_{N^*}	X_{D^*}	$X_{\text{ex}_0^*+\text{co}_0^*+C}$
\mathcal{X}_h	1.27	1.55	1.75	6.14	3.17	2.66
$\text{curl}(\mathcal{N})$	1.26	10^{-13}	10^{-12}	0.03	10^{-3}	1.27
$\nabla \mathcal{F}_0$	0.03	1.55	10^{-13}	1.00	0.17	1.55
$\text{curl}(\mathcal{N}) \cap \nabla \mathcal{F}$	0.02	0.01	1.75	0.08	0.05	1.75
$\mathcal{H}_{h,N}^*$	10^{-13}	10^{-12}	10^{-10}	6.05	10^{-11}	10^{-10}
$\mathcal{H}_{h,D}^*$	10^{-12}	10^{-13}	10^{-12}	10^{-12}	3.16	10^{-12}

Table 5.4: L^2 -norms of the components of the decomposed vector fields from (5.5) and (5.6).

5.5 NUMERICAL ASPECTS

We elaborate on a few computational aspects for the above-mentioned algorithms. This includes the numerical approach we have taken for the null space computation of a matrix as well as the numerical representation of the smooth fields in the decomposition experiments.

INTRINSIC REPRESENTATION OF PCVFs. Given a simplicial surface mesh M_h , PCVFs can be intrinsically represented by picking two directed edges $e_{f,1}, e_{f,2}$ of each triangle f , and writing X_f as a linear combination $\sum_i a_{f,i} e_{f,i}$. Assuming that no triangle is degenerated, these edges form a basis for the tangent plane to f when interpreted as vectors in \mathbb{R}^3 . Alternatively, these vector fields can be defined in Euclidean coordinates of the ambient space, where each vector X_f is specified as a vector in Euclidean coordinates of \mathbb{R}^3 , and we have used this formulation in our computations. It has the advantage that their definition is intuitive and computations can often be easily performed as operations on \mathbb{R}^3 without any need of coordinate transformations. On the other hand, the property of being tangential to M_h usually needs to be enforced explicitly and added as a linear constraint as was done in (5.1).

To compute the surface gradient $\nabla \varphi$ of a function $\varphi \in \mathcal{L}$ or the cogradient $J\nabla \psi$ for $\psi \in \mathcal{F}$, there are again two options: by representing these vector fields as intrinsic quantities expressed in terms of the weighted and rotated edges of M_h , see (3.3), or via pullback to a reference element as was done e.g. in [RHCM13].

INTERPOLATION AND PROJECTION. In the computational decompositions in Section 5.2 and Section 5.4, the smooth fields that have been analytically defined in the coordinates of the ambient space were represented by discrete fields approximating the smooth fields on a mesh approximation of a smooth shape, say a smooth annulus or a smooth sphere. To perform this approximation, there are two natural choices: the first option is the computation of an L^2 -best approximation of the restriction of a smooth field X to the mesh, which is a linear system of the type

$$\text{Find } X_h \in \mathcal{X}_h \text{ such that } \langle X_h, Y_h \rangle_{L^2} = \langle X|_{M_h}, Y_h \rangle_{L^2} \text{ for all } Y_h \in \mathcal{X}_h,$$

involving a quadrature to approximate the integral on the right hand side.

The second option is the interpolation of the smooth field in the function space \mathcal{X}_h . For PCVFs, this is achieved by point evaluation inside a cell t , say at the barycentre b_t , leading to a discrete version X_h whose representing vector over t is given by $X(b_t)$. In the above experiments we have used this approach for simplicity. This choice does not destroy the

convergence and approximation results from Chapter 4, since this interpolation is of the same linear approximation order as a perfect L^2 -best approximation of X , see the proof of [War06, Lemma 3.4.3].

SOLVING FOR THE NULL SPACE. The matrices $L_{\mathcal{H}_{h,D}^{(*)}}$ and $L_{\mathcal{H}_{h,N}^{(*)}}$ constructed in Sections 5.1 and 5.3 are fairly large, almost-square, sparse matrices, whose kernel dimension equals the dimension of some cohomology space and is therefore usually very small in comparison to the matrix size. To compute a null space basis for such a matrix, we have employed two different approaches—a sparse, rank-revealing QR-decomposition as a direct solver and an iterative eigensolver for a partial eigenspectrum on a transformed system—, both leading to comparable results.

On the direct side, methods based on *rank-revealing QR-decompositions* (RRQR) and the *singular value decomposition* (SVD) are common strategies for the numerical computation of the rank and null space for a given matrix L , see e.g. [GVL13, FD13] or the `null` and `rank` methods provided by *MATLAB* [TM16]. The SVD decomposes an $(m \times n)$ -matrix L as

$$L = U^t \cdot \text{diag}(\zeta_1, \dots, \zeta_q) \cdot V, \quad (5.7)$$

where U is an orthogonal $(m \times m)$ -matrix, V is an orthogonal $(n \times n)$ -matrix and the matrix $\text{diag}(\zeta_1, \dots, \zeta_q)$ is a rectangular diagonal $(m \times n)$ -matrix with the singular values ζ_i on its diagonal, and $q = \min(m, n)$. Assuming that the singular values are ordered as

$$\zeta_1 \geq \zeta_2 \geq \dots \geq \zeta_k > \zeta_{k+1} = \dots = \zeta_q = 0$$

for some $1 \leq k \leq q$, an orthonormal basis for the kernel of L is then given by the last $(n - k)$ columns of the transpose V^t .

A rank-revealing QR-decomposition decomposes L as

$$L \cdot P = Q \cdot R$$

with an orthogonal $(m \times m)$ -matrix Q , an upper trapezoidal $(m \times n)$ -matrix R and a column permutation matrix P , such that the first k columns of Q form a basis for $\text{range}(L)$, where k denotes the rank of L . Consequently, the last $(m - k)$ columns of Q form an orthonormal basis for the orthogonal complement of $\text{range}(L)$ within \mathbb{R}^m . Since $\ker(L)$ is the orthonormal complement of $\text{range}(L^t)$, we therefore compute the RRQR for the matrix L^t to obtain an orthonormal $(n \times n)$ -matrix Q , whose last $(n - k)$ columns are a basis for the null space of L .

However, this approach has two drawbacks: for one thing, the resulting orthogonal matrices are in general not sparse any more. This can be overcome by a sparse QR-decomposition (SPQR) algorithm which tries to reduce the fill-in of Q and R . We have chosen the `spqr` implementation provided by the *SuiteSparse* library [Dav11] which gives reliable results, even for large models. However, although still as sparse as possible, the density of the Q -matrix is considerably higher as in the iterated approach presented below, resulting in much higher memory consumption and computation time. Here, an alternative approach could be the algorithm suggested by Gotsman [GT08] based on a sparse LU-decomposition. See also Table 5.5 for a comparison of the number of non-zero entries in the direct and iterative approach.

Second, the singular values are almost always never zero in numerical computations due to round-off errors, so that L is usually never rank-deficient. This can be solved by providing

Example	nnz(L)	nnz($L^t L$)	nnz(Q)	nnz(R)	$m \times n$
$\mathcal{H}_{h,D}/\text{AwH}$	0.009	0.04	0.19	0.03	1608×1610
$\mathcal{H}_{h,N}/\text{AwH}$	0.009	0.04	0.2	0.03	1608×1610
$\mathcal{H}_{h,D}/\text{TwC}$	0.06	0.34	2.73	0.18	8997×9000
$\mathcal{H}_{h,N}/\text{TwC}$	0.06	0.35	2.73	0.19	8997×9000
$\mathcal{H}_{h,D}/\text{LH}$	0.21	1.20	17.25	0.83	29656×29661
$\mathcal{H}_{h,N}/\text{LH}$	0.21	1.20	17.13	0.84	29656×29661
$\mathcal{H}_{h,D}^*/\text{ST}$	0.10	0.57	11.65	1.14	12791×12561
$\mathcal{H}_{h,N}^*/\text{SwC}$	0.29	1.62	73.54	9.23	30784×28899
$\mathcal{H}_{h,D}^*/\text{G3C2}$	0.29	1.52	75.62	4.77	34456×33594
$\mathcal{H}_{h,N}^*/\text{G3C2}$	0.32	1.56	58.62	5.72	36588×33594

Table 5.5: Number of non-zero (nnz) entries in millions for the system matrices and its SPQR-factors in various examples. The horizontal line separates simplicial surfaces (top part) from simplicial solids (bottom part).

a tolerance value ϵ and treating all columns with L^2 -norm smaller than ϵ as zero. In our experiments we have chosen a value close to machine precision, say $\epsilon = 10^{-14}$. The work by Foster and Davis [FD13] might provide a further solution to circumvent this problem.

In contrast to the use of a direct solver, the second approach is an ad hoc strategy motivated by the fact that the kernel is usually very small in comparison to the matrix size. From the SVD (5.7) it follows that the $(n \times n)$ square matrix

$$M := L^t \cdot L = V^t \cdot \text{diag}(\zeta_1, \dots, \zeta_q, \underbrace{0, \dots, 0}_{n-q})^2 \cdot V$$

has the same kernel as L . A basis for $\ker(L)$ is therefore given by the eigenvectors corresponding to the zero-eigenvalues of the symmetric matrix M . These can be efficiently computed with iterative solvers that provide an option for a partial computation of the eigenspectrum. But again, there are errors due to round-off and the numerical rank of M might differ from its pure rank. Here, there are two options: if we know the dimension d of the cohomology space in question in advance, we can provide this number to the solver to solve for the eigenvectors corresponding to the d smallest eigenvalues. On the contrary, if we do not know this number, it still seems possible to deduce the correct value for d , for we always observed a clear gap in the order of magnitude of the eigenvalues found when solving for the smallest ones in our experiments. Hence, one can stop the iteration once this gap exceeds a certain threshold, often of magnitude 10^5 or higher, as can be seen in Table 5.6. The resulting eigenvectors for the d smallest eigenvalues then constitute a basis for $\ker(L)$.

Example	μ_1	μ_2	μ_3	μ_4	μ_5	μ_6	μ_7	μ_8	μ_9	μ_{10}
$\mathcal{H}_{h,D}/\text{AwH}$	20	19	6	6	5	5	5	5	5	5
$\mathcal{H}_{h,N}/\text{AwH}$	20	19	6	5	5	5	5	4	4	4
$\mathcal{H}_{h,D}/\text{TwC}$	19	18	18	6	6	6	6	6	6	6
$\mathcal{H}_{h,N}/\text{TwC}$	19	18	18	7	6	6	6	6	6	5
$\mathcal{H}_{h,D}/\text{LH}$	16	16	16	16	16	7	6	3	3	3
$\mathcal{H}_{h,N}/\text{LH}$	16	16	16	16	15	10	4	3	3	3
$\mathcal{H}_{h,D}^*/\text{ST}$	21	7	6	5	5	5	5	5	5	5
$\mathcal{H}_{h,N}^*/\text{SwC}$	19	6	6	6	6	6	6	6	6	6
$\mathcal{H}_{h,D}^*/\text{G3C2}$	18	18	18	10	7	7	7	7	6	6
$\mathcal{H}_{h,N}^*/\text{G3C2}$	19	19	6	5	5	5	5	5	5	5

Table 5.6: Order of magnitude of the first ten eigenvalues μ_i for various experiments, encoded by the exponent k for the order 10^{-k} . Thus, the larger the numbers, the smaller the magnitude of the eigenvalue. In each row, the number of bold entries correspond to the correct number of expected solutions, given by the dimension of the respective cohomology space. In each case there is a clear gap in the spectrum between the smallest eigenvalues and the following eigenvalues.

Surprisingly, solutions to eigenvalues which are larger than the d smallest ones can still exhibit a very structured behaviour, too, as shown in Figure 5.13. This is, however, unpredictable behaviour and depends solely on the solver.



Figure 5.13: Eigenvectors for the next five smallest eigenvalues. These eigenvalues are of orders 10^{-7} to 10^{-3} , whereas the five correct solutions in Figure 5.4 correspond to eigenvalues of order 10^{-16} , so there is a clear gap of magnitude in the eigenspectrum, cf. Table 5.6. Whereas some of these eigenvectors are obviously nonsense (first two images), others can give surprisingly well-structured vector fields, depending on the solver.

In the experiments in the previous sections this approach outperforms the direct solver in terms of computation time, but it does not come without drawbacks. For one thing, the formation of the product $L^t \cdot L$ squares the singular values. As a consequence this can have an influence on the gap in the eigenspectrum, since very small, but non-zero singular values

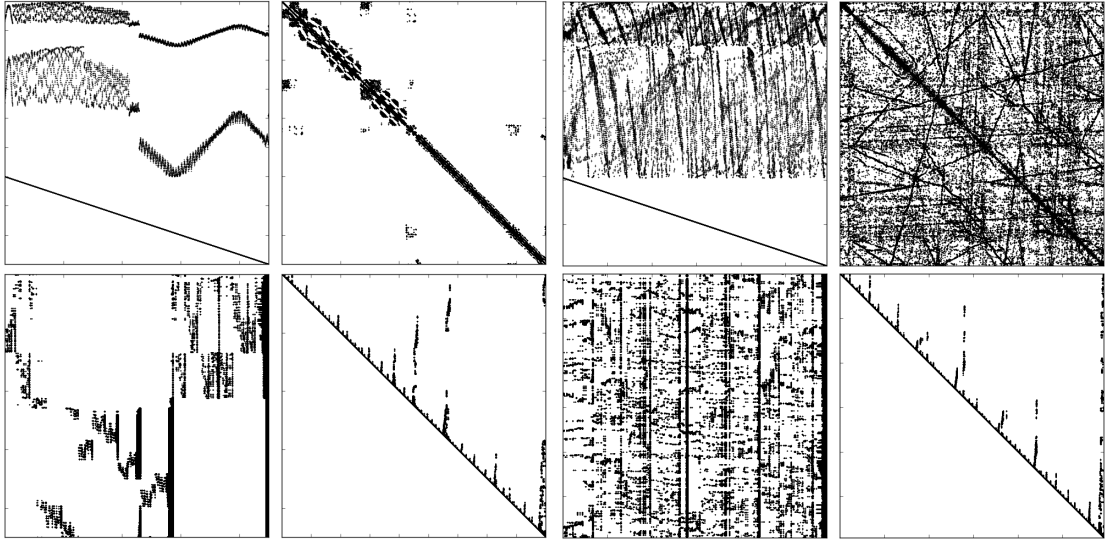


Figure 5.14: Fill patterns of the system matrices L , $L^t L$ and the QR-factors of L . Top row: the matrices L_1 , $L_1^t L_1$, L_2 and $L_2^t L_2$ with $L_1 := L_{\mathcal{H}_{h,N}}$ on the TwC-model, and $L_2 := L_{\mathcal{H}_{h,D}}$ on the LH-model. Bottom row: The matrices Q_1 , R_1 , Q_2 and R_2 from the SPQR-decompositions $L_1 P_1 = Q_1 R_1$ and $L_2 P_2 = Q_2 R_2$.

can become indistinguishable from the true zero eigenvalues up to machine precision. In our examples this did not cause any problems, but from a theoretical point of view this problem cannot be neglected and there are surely example meshes on which the eigenspectrum of M does not exhibit a visible gap in the order of magnitudes to tell apart the correct solutions from the non-correct ones. In addition, the fill-in of M is usually much higher than the fill-in of L , so the good sparsity property of L is partially lost. Still, it is much lower than the fill-in of the Q matrix in the SPQR-decomposition, see Table 5.5 and Figure 5.14 for a visualization of two fill patterns in our experiments.

Summarizing, whereas the SPQR-decomposition is from a theoretical point of view the preferred approach, the solution based on an iterative solver provides in practice a reliable and more efficient method with respect to both memory consumption and computation time. Of course, for complex geometries one has to be very careful in the choice of an appropriate solving strategy.

SOFTWARE AND DATA. The assembly of the system matrices as well as the projections and interpolations on certain function spaces was carried out with the *FEniCS* library [ABH⁺15], [LMW12], version 2016.1.0. It provides a domain specific language for the formulation of variational problems and assembly of matrices, and implements a variety of commonly used FEM families. For the iterative eigensolvers we use the *ARPACK* package as wrapped by the Python library *SciPy* [JOP⁺], version 0.18.0, which implements an implicitly restarted Lanczos method, and the eigensolver provided by the *SLEPc* library [HRV05], wrapped by *FEniCS*' *SLEPcEigensolver* class, which implements a Krylov-Schur method by default [HRTV07]. Both solvers compute comparable solutions, but the *SLEPc* eigensolver was usually faster.

For the sparse QR-decomposition we used the `spqr` algorithm [Dav11] from the *SuiteSparse* library [D⁺], version 4.4.1. The visualization was done with the *JavaView* library [PKPR02], version 4.60, and *ParaView/VTK* [Aya15, SML06], version 5.1.2.

The modified hand model in Figures 5.4 and 5.13 is based on the *Laurent's hand* model which is provided courtesy of INRIA by the *AIM@SHAPE-VISIONAIR* shape repository.

BIBLIOGRAPHY

- [ABH⁺15] Martin Alnæs, Jan Blechta, Johan Hake, August Johansson, Benjamin Kehlet, Anders Logg, Chris Richardson, Johannes Ring, Marie Rognes, and Garth Wells. The FEniCS project version 1.5. *Archive of Numerical Software*, 3(100), 2015.
- [AFGT14] Douglas N. Arnold, Richard Falk, Johnny Guzmán, and Gantumur Tsogtgerel. On the consistency of the combinatorial codifferential. *Transactions of the American Mathematical Society*, 366(10):5487–5502, 2014.
- [AFW06] Douglas N. Arnold, Richard Falk, and Ragnar Winther. Finite element exterior calculus, homological techniques, and applications. *Acta Numer.*, 15:1–155, 2006.
- [AFW10] Douglas N. Arnold, Richard Falk, and Ragnar Winther. Finite element exterior calculus: from Hodge theory to numerical stability. *Bulletin of the American mathematical society*, 47(2):281–354, 2010.
- [AMR88] Ralph Abraham, Jerrold E. Marsden, and Tudor S. Ratiu. *Manifolds, Tensor Analysis, and Applications*. Number Bd. 75 in Applied Mathematical Sciences. Springer New York, 1988.
- [AOCBC15] Omri Azencot, Maks Ovsjanikov, Frédéric Chazal, and Mirela Ben-Chen. Discrete derivatives of vector fields on surfaces—an operator approach. *ACM Transactions on Graphics (TOG)*, 34(3):29, 2015.
- [Aya15] Utkarsh Ayachit. *The Paraview Guide: A Parallel Visualization Application*. Kitware, Incorporated, 2015.
- [BCC⁺12] Oleksiy Busaryev, Sergio Cabello, Chao Chen, Tamal K. Dey, and Yusu Wang. *Algorithm Theory – SWAT 2012: 13th Scandinavian Symposium and Workshops, Helsinki, Finland, July 4-6, 2012. Proceedings*, chapter Annotating Simplices with a Homology Basis and Its Applications, pages 189–200. Springer Berlin Heidelberg, 2012.
- [BH06] Pavel B. Bochev and James M. Hyman. Principles of Mimetic Discretizations of Differential Operators. In Douglas N. Arnold, Pavel B. Bochev, Richard B. Lehoucq, Roy A. Nicolaides, and Mikhail Shashkov, editors, *Compatible Spatial Discretizations*, number 142 in The IMA Volumes in Mathematics and its Applications, pages 89–119. Springer New York, January 2006.
- [BL02a] Itai Benjamini and László Lovász. Determining the genus of a map by local observation of a simple random process. *arXiv preprint math/0202127*, 2002.

- [BL02b] Itai Benjamini and László Lovász. Global information from local observation. In *Annual Symposium on Foundations of Computer Science - Proceedings*, pages 701–710. IEEE Comput. Soc, 2002.
- [BL03] Itai Benjamini and László Lovász. Harmonic and analytic functions on graphs. *Journal of Geometry*, 76(1-2):3–15, 2003.
- [BNPB13] Harsh Bhatia, Gregory Norgard, Valerio Pascucci, and Peer-Timo Bremer. The Helmholtz-Hodge decomposition - a survey. *IEEE Transactions on Visualization and Computer Graphics*, 19(8):1386–1404, 2013.
- [Bos88] Alain Bossavit. Whitney forms: A class of finite elements for three-dimensional computations in electromagnetism. *IEE Proceedings A-Physical Science, Measurement and Instrumentation, Management and Education-Reviews*, 135(8):493–500, 1988.
- [Bre93] Glen E. Bredon. *Topology and Geometry*. Graduate Texts in Mathematics. Springer, 1993.
- [BS07] Alexander I. Bobenko and Boris A. Springborn. A discrete Laplace-Beltrami operator for simplicial surfaces. *Discrete & Computational Geometry*, 38(4):740–756, December 2007.
- [CDG02] Jason Cantarella, Dennis DeTurck, and Herman Gluck. Vector calculus and the topology of domains in 3-space. *The American Mathematical Monthly*, 109(5):409–442, 2002.
- [CV91] Antonio F. Costa and Alba Valverde. On folded coverings of quasi-manifolds with boundary. *Annali dell'Università di Ferrara*, 37(1):13–26, 1991.
- [D⁺] Timothy A. Davis et al. SuiteSparse : A suite of sparse matrix software, 2014–. [Online; accessed 2016-09-15].
- [Dav11] Timothy A. Davis. Algorithm 915, SuiteSparseQR: Multifrontal multithreaded rank-revealing sparse QR factorization. *ACM Transactions on Mathematical Software (TOMS)*, 38(1):8, 2011.
- [DKG05] Shen Dong, Scott Kircher, and Michael Garland. Harmonic functions for quadrilateral remeshing of arbitrary manifolds. *Comput. Aided Geom. Des.*, 22(5):392–423, July 2005.
- [Dło12] Paweł Dłotko. A fast algorithm to compute cohomology group generators of orientable 2-manifolds. *Pattern Recognition Letters*, 33(11):1468 – 1476, 2012. Computational Topology in Image Context.
- [Dod76] Jozef Dodziuk. Finite-difference approach to the Hodge theory of harmonic forms. *American Journal of Mathematics*, pages 79–104, 1976.
- [EW05] Jeff Erickson and Kim Whittlesey. Greedy optimal homotopy and homology generators. In *Proceedings of the Sixteenth Annual ACM-SIAM Symposium on Discrete Algorithms*. Society for Industrial and Applied Mathematics, 2005.

- [FD13] Leslie V. Foster and Timothy A. Davis. Algorithm 933: Reliable calculation of numerical rank, null space bases, pseudoinverse solutions, and basic solutions using SuiteSparseQR. *ACM Trans. Math. Softw.*, 40(1):7:1–7:23, October 2013.
- [Fri55] Kurt Otto Friedrichs. Differential forms on Riemannian manifolds. *Communications on Pure and Applied Mathematics*, 8(4):551–590, 1955.
- [GT08] Craig Gotsman and Sivan Toledo. On the computation of null spaces of sparse rectangular matrices. *SIAM Journal on Matrix Analysis and Applications*, 30(2):445–463, 2008.
- [Gum00] Stefan Gumhold. *Mesh Compression*. PhD thesis, Eberhard-Karls-Universität zu Tübingen, 2000.
- [GVL13] Gene H. Golub and Charles F. Van Loan. *Matrix computations*, 2013.
- [Hat02] Allen Hatcher. *Algebraic Topology*. Cambridge University Press, 2002.
- [Hir03] Anil N. Hirani. *Discrete exterior calculus*. PhD thesis, California Institute of Technology, 2003.
- [HKWW10] Anil N. Hirani, Kaushik Kalyanaraman, Han Wang, and Seth Watts. Cohomologous harmonic cochains. *arXiv preprint arXiv:1012.2835*, 2010.
- [HRTV07] Vicente Hernández, Jose E. Román, Andrés Tomás, and Vicente Vidal. Krylov-schur methods in SLEPc. *Universitat Politecnica de Valencia, Tech. Rep. STR-7*, 2007.
- [HRV05] Vicente Hernández, Jose E. Román, and Vicente Vidal. SLEPc: A scalable and flexible toolkit for the solution of eigenvalue problems. *ACM Trans. Math. Software*, 31(3):351–362, 2005.
- [HS12] Michael Holst and Ari Stern. Geometric variational crimes: Hilbert complexes, finite element exterior calculus, and problems on hypersurfaces. *Foundations of Computational Mathematics*, 12(3):263–293, 2012.
- [JOP⁺] Eric Jones, Travis Oliphant, Pearu Peterson, et al. SciPy: Open source scientific tools for Python, 2001–. [Online; accessed 2016-09-13].
- [Kin97] L.C. Kinsey. *Topology of Surfaces*. Undergraduate Texts in Mathematics. Springer New York, 1997.
- [KNP07] Felix Kälberer, Matthias Nieser, and Konrad Polthier. QuadCover – Surface parameterization using branched coverings. *Comput. Graph. Forum*, 26(3):375–384, 2007.
- [KNP14] Niklas Krauth, Matthias Nieser, and Konrad Polthier. Differential-based geometry and texture editing with brushes. *Journal of mathematical imaging and vision*, 48(2):359–368, 2014.
- [Lee03] John M. Lee. *Introduction to Smooth Manifolds*. Graduate Texts in Mathematics. Springer, 2003.

- [LMW12] Anders Logg, Kent-Andre Mardal, and Garth Wells, editors. *Automated Solution of Differential Equations by the Finite Element Method*, volume 84 of *Lecture Notes in Computational Science and Engineering*. Springer, 2012.
- [Lov04] László Lovász. Discrete analytic functions: an exposition. *Surveys in differential geometry*, 9:241–273, 2004.
- [Man14] Ciprian Manolescu. Triangulations of manifolds. *ICCM Not*, 2(2):21–23, 2014.
- [Mon91] Peter B. Monk. A mixed method for approximating Maxwell’s equations. *SIAM J. Numer. Anal.*, 28(6):1610–1634, December 1991.
- [Mun84] James R. Munkres. *Elements of Algebraic Topology*. Advanced book classics. Perseus Books, 1984.
- [Né80] Jean-Claude Nédélec. Mixed finite elements in R^3 . *Numerische Mathematik*, 35:315–341, 1980.
- [Pat75] Vijay K. Patodi. Riemannian structures and triangulations of manifolds. In *International Congress of Mathematicians*, page 39, 1975.
- [PKPRO2] Konrad Polthier, Samy Khadem, Eike Preuss, and Ulrich Reitebuch. Publication of interactive visualizations with JavaView. In *Multimedia Tools for Communicating Mathematics*, pages 241–264. Springer Berlin Heidelberg, 2002.
- [Pol02] Konrad Polthier. Polyhedral surfaces of constant mean curvature. Habilitationsschrift, Technische Universität Berlin, 2002.
- [PP93] Ulrich Pinkall and Konrad Polthier. Computing discrete minimal surfaces and their conjugates. *Experimental mathematics*, 2(1):15–36, 1993.
- [PP03] Konrad Polthier and Eike Preuss. Identifying vector field singularities using a discrete Hodge decomposition. In Hans-Christian Hege and Konrad Polthier, editors, *Visualization and Mathematics III*, pages 113–134. Springer Verlag, 2003.
- [PPL⁺10] Fabiano Petronetto, Afonso Paiva, Marcos Lage, Geovan Tavares, Helio Lopes, and Thomas Lewiner. Meshless Helmholtz-Hodge decomposition. *IEEE transactions on visualization and computer graphics*, 16(2):338–349, 2010.
- [RHCM13] Marie E. Rognes, David A. Ham, Colin J. Cotter, and Andrew T. T. McRae. Automating the solution of PDEs on the sphere and other manifolds in FEniCS 1.2. *Geoscientific Model Development*, 6(6):2099–2119, 2013.
- [RHS16] Wieland Reich, Mario Hlawitschka, and Gerik Scheuermann. Decomposition of vector fields beyond problems of first order and their applications. In *Topological Methods in Data Analysis and Visualization IV: Theory, Algorithms, and Applications*. Springer, 2016.
- [RT77] Pierre-Arnaud Raviart and Jean-Marie Thomas. A mixed finite element method for 2-nd order elliptic problems. In *Mathematical aspects of finite element methods*, pages 292–315. Springer, 1977.

- [Sch95] Günter Schwarz. *Hodge decomposition: a method for solving boundary value problems*. Lecture notes in mathematics. Springer, 1995.
- [Sho09] Clayton Shonkwiler. *Poincaré Duality Angles on Riemannian Manifolds with Boundary*. PhD thesis, University of Pennsylvania, 2009.
- [Sho13] Clayton Shonkwiler. Poincaré duality angles and the Dirichlet-to-Neumann operator. *Inverse Problems*, 29(4), 2013.
- [Smi91] Lieven Smits. Combinatorial approximation to the divergence of one-forms on surfaces. *Israel Journal of Mathematics*, 75(2-3):257–271, 1991.
- [SML06] Will Schroeder, Ken Martin, and Bill Lorensen. *The Visualization Toolkit: An Object-oriented Approach to 3D Graphics*. Kitware, 2006.
- [Ste13] Ari Stern. L^p change of variables inequalities on manifolds. *Math. Inequal. Appl.*, 16(1):55–67, 2013.
- [SZ12] Andrzej Szymczak and Eugene Zhang. Robust morse decompositions of piecewise constant vector fields. *IEEE Transactions on Visualization and Computer Graphics*, 18(6):938–951, 2012.
- [SZS08] Oliver Schall, Rhaleb Zayer, and Hans-Peter Seidel. Controlled field generation for quad-remeshing. In *Proceedings of the 2008 ACM Symposium on Solid and Physical Modeling, SPM '08*, pages 295–300. ACM, 2008.
- [TLHD03] Yiyong Tong, Santiago Lombeyda, Anil N. Hirani, and Mathieu Desbrun. Discrete multiscale vector field decomposition. In *ACM SIGGRAPH 2003 Papers, SIGGRAPH '03*, pages 445–452. ACM, 2003.
- [TM16] Inc. The MathWorks. Matlab r2016a, 2016. [Online; accessed 2016-09-14].
- [War06] Max Wardetzky. *Discrete Differential Operators on Polyhedral Surfaces - Convergence and Approximation*. PhD thesis, Freie Universität Berlin, 2006.
- [Whi12] Hassler Whitney. *Geometric Integration Theory*. Princeton mathematical series. Dover Publications, 2012.
- [XZCOX09] Kai Xu, Hao Zhang, Daniel Cohen-Or, and Yueshan Xiong. Dynamic harmonic fields for surface processing. *Computers & Graphics*, 33(3):391–398, 2009.

INDEX

- 0-edge, 50
 - isolated, 55
- L^2 -product on $\Omega^k(M)$, 11
- Boundaries, 8
- Boundary edge, 49
- Boundary operator, 7
- Bounded domain, 9
- Cell, 21
- Central harmonic component
 - 2d, 40
 - 3d, 45
- Circulation, 52
- Coboundaries, 8
- Coboundary operator, 8
- Cocycles, 8
- Coderivative, 12
- Coexact k -form, 14
- Cogradient space, 24
- Cohomology, 8
 - long exact sequence, 8
 - relative, 8
- Corner, 50
 - blunt, 51
 - inner, 50
 - outer, 50
 - properly blunt, 51
 - sharp, 51
- Crouzeix-Raviart elements, 23
- Curly gradient, 20
- Cycles, 8
- De Rham complex, 12
- De Rham map, 16
- Degrees of freedom, 23
- Delaunay
 - locally, 56
 - triangulation, 56
- Differential form
 - normal component, 13
 - tangential component, 13
- Dirichlet boundary condition, 15
- Dirichlet field, 15
- Discrete curl, 40
- Discrete divergence, 40
- Discrete holomorphic function, 41
- Elementary form, 26
- Euler characteristic, 21
- Exact k -form, 14
- Exterior derivative, 12
- Facet, 21
- Fluxless knot, 20
- Fundamental decomposition (2d), 32
- Fundamental decomposition (3d), 43
- Generalized Barycentric coordinates, 23
- Gradient, 24
- Green's formula, 12
- Grounded gradient, 20
- Harmonic k -form, 14
- Harmonic gradient, 20
- Harmonic knot, 20
- Hodge star operator, 11
- Hodge-Morrey-Friedrichs
 - discrete (2d), 33
 - discrete (3d), 44
 - smooth decomposition, 15
- Homology, 8
 - long exact sequence, 8
 - relative, 8
- Interpolation, 99

- Lefschetz-Poincaré duality, 8
- Leibniz rule, 12
- Linear Lagrange elements, 23
- Mayer-Vietoris sequence, 8
- Mesh size, 60
- Metric convergence, 68
- Metric distortion tensor, 68
- Musical isomorphisms, 13
- Neumann boundary condition, 15
- Neumann field, 15
- Normal jump, 22
- Normally continuous, 23
- Nédélec elements, 28
- Orientation
 - induced by weighting, 50
- Outer unit normal, 12
- PCVF, 22
- Period map, 16
- Piecewise Constant Vector Field, 22
- Poincaré duality, 8
- Quasi-manifold, 49
- Relative cochains, 8
- Riemannian volume form, 11
- RRQR, 99
- Simplicial chains, 7
- Simplicial cochains, 8
- Simplicial manifold with boundary, 21
- Simplicial solid, 21
- Simplicial surface, 21
 - singular, 49
 - with isolated singularities, 49
- Singular value of a diffeomorphism, 69
- Singular vertex, 49
- Smooth triangulation, 60
 - admissible family, 60
- SPQR, 99
- Stokes' theorem, 12
- Subsurface property, 56
- Support, 56
- Surface of type $\Sigma_{g,m}$, 9
- SVD, 99
- Tangential jump, 22
- Tangentially continuous, 23
- Vector field
 - normal component, 12
 - proxy, 14
 - tangential component, 12
- Wedge product, 11
- Weighting, 50
 - closed, 52
 - divergence-free, 52
 - harmonic, 52
 - quasi-divergence-free, 53
 - quasi-harmonic, 53
 - quasi-rotation-free, 53
 - rotation-free, 52
- Whitney form, 26
- Whitney map, 27

SELBSTSTÄNDIGKEITSERKLÄRUNG

Hiermit versichere ich, dass ich alle Hilfsmittel und Hilfen angegeben und die vorliegende Arbeit auf dieser Grundlage selbstständig verfasst habe. Ich habe die Arbeit nicht in einem früheren Promotionsverfahren eingereicht.

Berlin, 2016

Konstantin Poelke

ZUSAMMENFASSUNG

Die vorliegende Arbeit entwickelt eine diskrete Theorie von Hodge-artigen Zerlegungssätzen für den Raum der stückweise konstanten Vektorfelder auf orientierten, simplizialen Flächen mit Rand und simplizialen dreidimensionalen Gebieten in \mathbb{R}^3 . Ein besonderer Schwerpunkt liegt dabei auf einer konsistenten Diskretisierung sowohl bezüglich geometrischer als auch bezüglich topologischer Eigenschaften, die sich in Teilräumen konkreter Repräsentanten für Kohomologiegruppen manifestieren.

Dazu werden zunächst die differentialgeometrischen und topologischen Grundlagen der glatten Theorie für n -dimensionale berandete Mannigfaltigkeiten zusammengefasst. Neben den klassischen Hodge-Zerlegungssätzen wird insbesondere auf ein aktuelles Resultat von Shonkwiler eingegangen, das harmonische Felder klassifiziert, welche es erlauben, nicht-triviale Kohomologie induziert durch die Randkomponenten von der „inneren Kohomologie“ der Mannigfaltigkeit zu unterscheiden.

Basierend auf linearen Lagrange- und Crouzeix-Raviart-Ansatzräumen sowie kantenbasierten Nédélec-Elementen wird dann zunächst die Diskretisierung für den Flächenfall entwickelt. Dabei fällt den Definitionen der Räume der diskret-harmonischen Neumann- und Dirichlet-Felder $\mathcal{H}_{h,N}$ und $\mathcal{H}_{h,D}$ besondere Bedeutung zu. Für allgemeine Flächen von Genus $g > 0$ mit m Randkomponenten erhält man diskrete Analoga der Hodge-Morrey-Friedrichs-Zerlegungen, die um die Differenzierung von Shonkwiler erweitert werden. Speziell für $g = 0$ erhält man eine vollständige Fünf-Term-Zerlegung, da solche Flächen keine innere Kohomologie besitzen – hier sind die Räume $\mathcal{H}_{h,N}$ und $\mathcal{H}_{h,D}$ orthogonal zueinander, was für $g > 0$ nicht der Fall ist. Vergleichbare Resultate werden für den Fall dreidimensionaler, simplizialer, eingebetteter Gebiete in \mathbb{R}^3 erzielt. In beiden Fällen spielt das orthogonale Komplement des Gradientenraumes der Crouzeix-Raviart-Elemente eine besondere Rolle, da dieser Raum den Zusammenhang zu geschlossenen Whitney-Formen und damit zur simplizialen Kohomologie herstellt.

Ein tiefes Resultat im Glatten besagt, dass der Schnitt der Räume der Neumann- und Dirichlet-Formen stets trivial ist. Die vergleichbare Aussage $\mathcal{H}_{h,N} \cap \mathcal{H}_{h,D} = \{0\}$ gilt im Diskreten jedoch im Allgemeinen für Flächen mit $g > 0$ nicht. Vielmehr spielt hier auf erstaunliche Weise die Kombinatorik des Gitters eine entscheidende Rolle, die topologisch reichhaltige Teilregionen der Geometrie mit der Gitterkonnektivität zum Rest der Geometrie in Verbindung setzt. Dazu wird ein Kriterium an das Gitter aufgestellt, dass die Gültigkeit der diskreten Aussage garantiert.

Nach der Entwicklung der konsistenten Diskretisierung wird nun die Konvergenz der diskreten Zerlegungen bewiesen. Dafür wird zunächst ein fundamentales Resultat von Dodziuk zur Konvergenz von Whitney-Formen auf einer glatten Referenz-Triangulierung auf die erweiterten Zerlegungen verallgemeinert. Anschließend werden die verfeinerten Zerlegungen bezüglich einer Folge approximierender Metriken $\{\tilde{g}_i\}$ untersucht. Setzt man Konvergenz der Metriken gegen die Metrik der glatten Referenzgeometrie voraus, konvergieren auch die Zerlegungen, die orthogonal bezüglich der Metriken \tilde{g}_i sind. Schließlich erhält man die Konvergenz der Rückzüge der diskreten Zerlegungen gegen die glatten Zerlegungen.

Die Arbeit schließt ab mit zwei zentralen Anwendungen der diskreten Hodge-Theorie in der modernen Geometrieverarbeitung: Zum einen werden Algorithmen zur Berechnung orthogonaler, harmonischer Basen für die topologisch relevanten Teilräume vorgestellt. Zum anderen wird ein Verfahren zur numerischen Berechnung von Zerlegungen für ein gegebenes stückweise konstantes Vektorfeld beschrieben und evaluiert. Dazu werden Stereotypen von repräsentativen glatten Feldern auf simplizialen Geometrien interpoliert und die Komponenten der Zerlegung mit den Komponenten der glatten Zerlegung verglichen.